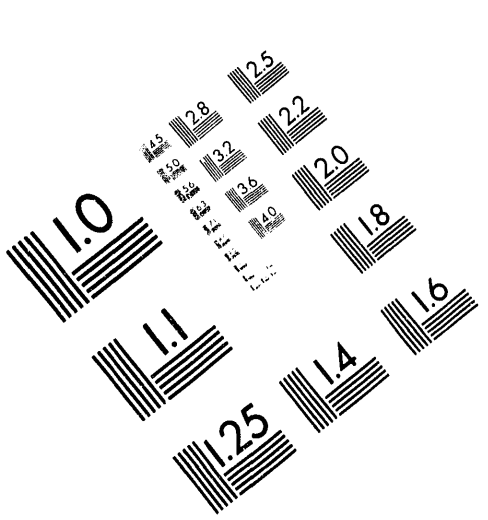

Association for Information and Image Management

1100 Wayne Avenue, Suite 1100
Silver Spring, Maryland 20910

301/587-8202

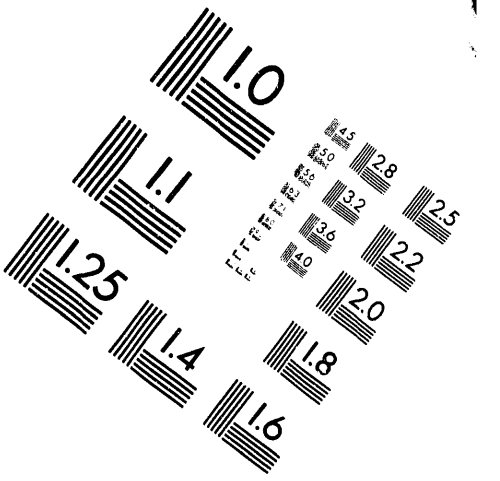

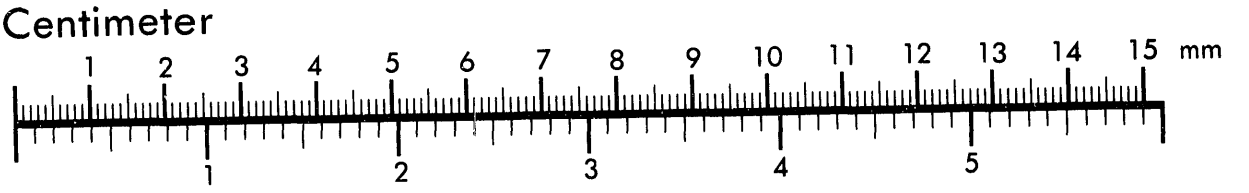

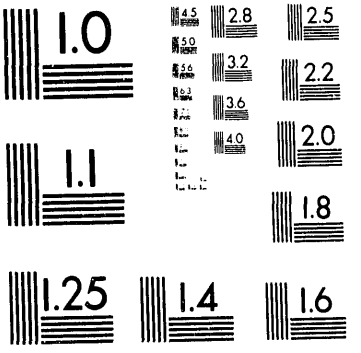

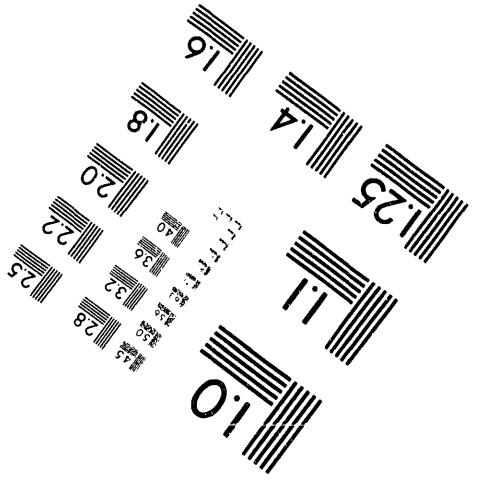

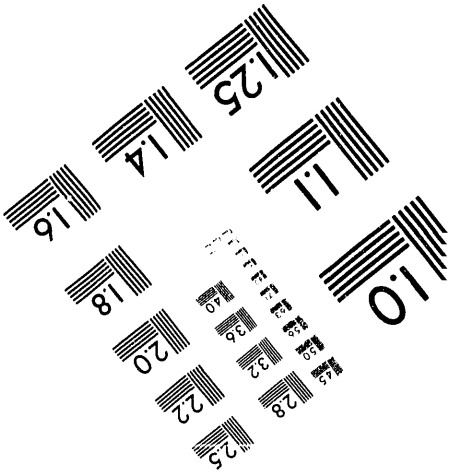

1 of 2

CONF-9106235
PNL-SA-21596
UC-607

ELEVENTH DOE WORKSHOP ON PERSONNEL NEUTRON DOSIMETRY

June 3-7, 1991
Las Vegas, Nevada

Prepared for the:
U.S. Department of Energy
Assistant Secretary for
Environment, Safety and Health
Office of Health

FOREWORD

Since its formation, the Office of Health (EH-40) has stressed the importance of the exchange of information related to and improvements in neutron dosimetry. This Workshop was the eleventh in the series sponsored by the Department of Energy (DOE). It provided a forum for operational personnel at DOE facilities to discuss current issues related to neutron dosimetry and for leading investigators in the field to discuss promising approaches for future research.

A total of 26 papers were presented including the keynote address by Dr. Warren K. Sinclair, who spoke on, "The 1990 Recommendations of the ICRP and their Biological Background." The first several papers discussed difficulties in measuring neutrons of different energies and ways of compensating or deriving correction factors at individual facilities. Presentations were also given by the U.S. Navy and Air Force. Current research in neutron dosimeter development was the subject of the largest number of papers. These included a number on the development of neutron spectrometers.

Because of the complexity of the subject and the need for better neutron dosimetry, continuation of this series of workshops is planned for the future.

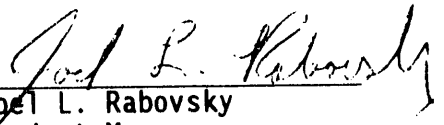

Joel L. Rabovsky
Project Manager
Health Physics Programs
Division
Office of Health Physics
and Industrial Hygiene

C. Rick Jones
Director
Office of Health Physics
and Industrial Hygiene

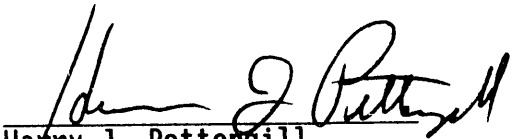

Harry J. Pettengill
Deputy Assistant Secretary
for Health

TABLE OF CONTENTS

ELEVENTH DEPARTMENT OF ENERGY WORKSHOP ON PERSONNEL NEUTRON DOSIMETRY

WORKSHOP ORGANIZING COMMITTEE

J. L. Rabovsky, U.S. Department of Energy
L. G. Faust, Pacific Northwest Laboratory
J. A. Leonowich, Pacific Northwest Laboratory

TECHNICAL SECRETARY

J. A. Leonowich, Pacific Northwest Laboratory

PROGRAM COORDINATORS

L. C. Stacy, Pacific Northwest Laboratory
L. M. Stoetzel, Pacific Northwest Laboratory

WORD PROCESSOR

M. Cross, Pacific Northwest Laboratory

ACKNOWLEDGMENTS

The organizers of this Workshop would like to extend their appreciation to all of the participants for their contribution to a successful meeting. Special thanks are extended to L. S. Sygitowicz, Reynolds Electrical & Engineering Co., Inc., Las Vegas, Nevada, for his assistance with local arrangements and tours. We would also like to extend our appreciation to Marianna Cross, the word processor for the proceedings, as well as to Lisa Stoetzel and Linda Stacy for their help in coordinating the multitude of details associated with the Workshop.

INTRODUCTION

The United States Department of Energy (DOE) has a number of unique problems in the area of neutron dosimetry. There is the *potential* for some DOE personnel and their contractors to be exposed to significant, measurable levels of neutron radiation. While the doses received are kept below current limits, there are a number of regulatory and scientific aspects in this area that are rapidly changing. The general limits for exposure and the radiation weighting factors (quality factors) for neutron effective dose are the subject of active discussion and recent recommendations of the International Commission on Radiological Protection (ICRP). The three recommendations that are likely to have the greatest impact are: (1) the reduction of the annual dose limit averaged over 5 years from 50 to 20 mSv, (2) the development of the weighting factor, W_R, to replace the quality factor, Q, and (3) the assignment of increased values to W_R, particularly in the range from 100 keV to 2 MeV. Additionally, for individual monitoring, it will also be necessary to revise ICRP Publication 51 so that the new radiation weighting factors are incorporated into the fluence to equivalent dose conversion factors. In addition, the revision should also: (1) address the confusion about the interrelationship between Q, W_R, LET, and RBE, and (2) clarify the relationship between the ICRU operational quantities and effective dose. These changes potentially have profound consequences on how we do neutron dosimetry in the DOE complex. It is quite clear that we will have to be more accurate in our future monitoring.

Since the last DOE-sponsored neutron workshop in 1983, there has been little change in the character and quality of personnel neutron dosimetry systems. The primary detectors in use today are TLD albedo dosimeters, track etch detectors using CR-39, and NTA film. There is, however, a slow movement away from NTA film and also increased use of CR-39. There are also a number of new techniques for individual neutron monitoring, including track etch detectors using (n,α) boron radiators, electronic dosimeters using small tissue equivalent proportional counters, bubble detectors, and finally optically stimulated luminescence (OSL). All of these exciting new areas are discussed in these proceedings.

The following papers formed the basis of the Eleventh Department of Energy Workshop on Personnel Neutron Dosimetry held in Las Vegas, Nevada, June 4-7, 1991. In addition to the papers there were several panel discussions and forums where the present state and future direction of personnel neutron dosimetry in the DOE were discussed at length. This venue provided an excellent opportunity for operational DOE health physicists to communicate their needs and frustrations with the present state of neutron dosimetry to the researchers present at the meeting. This interaction should prove invaluable in steering the future course of DOE-sponsored neutron dosimetry research towards solutions that are "field workable." Unfortunately, these discussions could not be included in the proceedings. It was clear, however, that neutron dosimetry is an area of great interest and continuing concern to the participants of the workshop. The reader is, therefore, encouraged to review the papers in this volume and to make use of the references given by the authors.

KEYNOTE ADDRESS

THE 1990 RECOMMENDATIONS OF THE ICRP AND THEIR BIOLOGICAL BACKGROUND

Presented by

Dr. Warren K. Sinclair

President
National Council on Radiation Protection and Measurements

ABSTRACT

In its Publication No. 60, the International Commission on Radiological Protection (ICRP) has introduced the new quantity equivalent dose in tissue T by the definition

$$H_T = \sum W_R \cdot D_{T,R}$$

where $D_{T,R}$ is the absorbed dose averaged over the tissue or organ T and W_R is the radiation weighting factor. The latter depends on the incident radiation, i.e. type and energy, but is independent of the tissue.

On the other hand, the customarily defined quantity dose equivalent is maintained — in particular the operational dose equivalent quantities introduced in ICRU Report No. 39 — but the relationship between the quality factor Q(L) and the linear energy transfer L has been redefined. In the case of neutrons, this gives rise to an increase in the corresponding fluence-to-dose equivalent conversion factors.

The biological background for introducing these changes will be discussed in this presentation.

NEUTRON DOSIMETRY AT LLNL

D. E. Hankins

Lawrence Livermore National Laboratory
Livermore, California, USA

INTRODUCTION

At the Lawrence Livermore National Laboratory (LLNL), only a small number of our personnel receive neutron exposures. With a few exceptions, these personnel work in our plutonium facility. The exposures are primarily to neutrons from (1) the spontaneous fissioning of fissile material and (2) oxides of fissile material. The neutron energies range from a fission spectrum, due to work with plutonium without any shielding, down to lightly moderated spectrum, due to work in shielded glove boxes. Personnel who work in the plutonium vaults are exposed to neutron spectrum containing a large component of room scattered neutron and thermal-energy neutrons.

ALBEDO NEUTRON DOSIMETERS

The differences in the neutron spectra make the use of albedo neutron dosimeters at LLNL difficult. We used albedo neutron dosimeters at LLNL from 1975 to 1985. Their use requires that a calibration factor be determined at each exposure area of facility. Extensive measurements were made to determine these calibration factors by using the 9- to 3-in. sphere ratio that I developed while at Los Alamos National Laboratory. These measurements indicated that in some facilities the variation in calibration factors was small and the albedo neutron dosimeter could be used with an accuracy of ± 30 to 50 percent. A "facility calibration factor" was applied to the thermoluminescent dosimeters (TLD) readings from the albedo dosimeters worn by the personnel working in those areas. At other facilities, however, the calibration factors varied widely and a single factor could not be used. The person wearing the albedo dosimeter would be contacted each month and questioned about the type of neutron exposure he/she received during the preceding month. Based on this discussion, a calibration factor was selected and applied to the TLD readings to obtain his/her neutron exposure.

The albedo neutron dosimeter used at LLNL was the "Hankins type" dosimeter.[1] This dosimeter was designed following an extensive study of the effect that differences in the size, shape, internal moderator, and cadmium thickness have on the dosimeter response.[2] The advantage of the Hankins type dosimeter over other albedo dosimeters is that it can be worn backwards and allowed to pull away from the body. One of the important, and unfortunate, conclusions from the study in Ref. 2 was that changing the design of albedo dosimeters has little effect on their neutron energy response. Therefore, the neutron energy or the calibration factor cannot be determined from the readings of multiple TLDs in a dosimeter or from a combination of several types of albedo neutron dosimeters.

CR-39 DOSIMETERS

The development of CR-39 as a personnel neutron dosimeter took a major step forward when in 1984 Tommasino, et al., found that electrochemically etched CR-39 foils had a relatively flat energy response for neutron energies between 100 keV and 5 MeV.[3] The development of CR-39 for personnel dosimetry application was funded by the U.S. Department of Energy, with the research being done by the Special Projects Division of the Hazards Control Department at LLNL. When this work reached the point where a CR-39 dosimeter could be used with reasonable accuracy, LLNL immediately dropped albedo dosimeters and switched to the CR-39 dosimeter. Continued research a LLNL resulted in improvements in the accuracy of the dosimeter and development of improved techniques in the etching and reading procedures. An automatic reading technique for the CR-39 foils was in the final stages of development when funding was dropped in 1990.

A four-stage etching procedure is used at LLNL to electrochemically etch CR-39 foils. The foils are read using an image analyzer specifically designed for reading CR-39 foils. The dosimetry system in use at LLNL has a lower limit of detection at 10 mrem and has a nearly flat energy dependence from 150 keV to 5.0 MeV. It has an accuracy of ± 10 mrem between 10 and 100 mrem and ± 10 percent between 100 mrem and 5.0 rem. Its directional response follows closely the directional dose dependence curve. It has a linear dose response from 10 to about 400 mrem and is correctable to 5.0 rem. A complete description of the dosimetry system is given in Ref. 4.

At LLNL there are about 70 personnel wearing the CR-39 neutron dosimeters, which are exchanged monthly. The neutron doses received by personnel seldom exceed 100 mrem. About 4 days of effort are required each month to read and evaluate the exposures, although about a third of this time is used for quality assurance of the dosimeter system.

FIELD SURVEYS

Surveys of neutron dose rates in radiation areas are made using rem-meters (9-in. spheres or modified Andersen-Braun). Occasionally, the multisphere neutron spectrometer is used and the results unfolded using either iterative or multiple random perturbation computer programs. Agreement between dosimeter and survey results will never be good because the survey instruments respond to neutrons in a 4-pi geometry, but the personnel dosimeters are responding closer to a 2-pi geometry. This is especially important for exposures occurring in the vaults where the neutrons impinge approximately isotropically.

CONCLUSION

Etching and reading of CR-39 is more labor intensive than reading of the TLDs in albedo neutron dosimeters, but the accuracy of the results obtained with CR-39 is much better than can be obtained using an albedo dosimeter. At LLNL, we consider the improved accuracy to far outweigh the small increase

in the cost of the CR-39 dosimetry system and have been using the CR-39 dosimetry system successfully for over 5 years.

REFERENCES

1. D.E. HANKINS, "A Small, Inexpensive Albedo-Neutron Dosimeter," Los Alamos National Laboratory, Los Alamos, NM, LA-5261 (1973).

2. D.E. HANKINS, "Factors Affecting the Design of Albedo-Neutron Dosimeters Containing Lithium Fluoride Thermoluminescent Dosimeters," Los Alamos National Laboratory, Los Alamos, NM, LA-4832 (1972).

3. L. TOMMASINO, G. ZAPPOROLI, P. SPEIZIO, R.V. GRIFFITH, and G. ESPINOSA, "Different Etching Processes of Damage-Track Detectors for Personnel Neutron Dosimetry," Proc. 12th Intern. Conf. Solid State Nuclear Track Detectors; also published in Nuclear Tracks and Radiation Measurements, 8(1-4), 335-3399 (1984).

4. D.E. HANKINS, S.G. HOMANN, and B. BUDDEMEIER, "Personnel Neutron Dosimetry Using Electrochemically Etched CR-39 Foils," Lawrence Livermore National Laboratory, Livermore, CA, UCRL-53833, Rev. 1 (1989).

NEVADA TEST SITE NEUTRON DOSIMETRY-PROBLEMS/SOLUTIONS [a]

L. S. Sygitowicz, C. T. Bastian, I. J. Wells, and P. N. Koch

Reynolds Electrical and Engineering Company
P.O. Box 98521
Las Vegas, Nevada 89193-8951

Historically, neutron dosimetry at the NTS was done using NTA film and albedo LiF TLD's. In 1987 the dosimeter type was changed from the albedo TLD based system to a CR-39 track etch based system modeled after the program developed by D. Hankins at LLNL.

Routine issue and return is performed quarterly for selected personnel using bar-code readers at permanent locations. The capability exists for work site issue as-needed. Issue data are transmitted by telephone to a central computer where it is stored until the dosimeter is returned, processed and read, and the dose calculation is performed. Dose equivalent calculations are performed using LOTUS 123 and the results are printed as a hard copy record. The issue and dose information are hand-entered into the Dosimetry database. An application is currently being developed to automate this sequence.

The CR-39 is etched in chambers made of Lucite (methyl methacrylate). Hankins and Budemier found that some LLNL chambers were warping with age, affecting dosimeter results. Experience at the NTS has confirmed this. Track density per unit dose equivalent would vary from column to column in the chamber. An unsuccessful attempt was made to remedy this problem by adding a heavy aluminum bar across the chamber top and using a torque wrench to assure uniform tightening of the bolts.

A newly designed chamber has been fabricated. The KOH reservoir was partitioned into four sections each of just sufficient size to accommodate openings to wet six foils. This left walls around each section to support the assembly top. Wall penetrations allow fluid levels to equalize. More bolts were added in an attempt to assure uniform clamping pressures. These chambers are being tested.

Reading the foils is accomplished with a TV camera coupled to a microscope. The original method was to illuminate the foil from beneath, using transmitted light. An Artek bacterial colony counter is used to recognize, mark and count the tracks. Using transmitted light produced dark shadows on a bright field, and tracks could not be distinguished from surface defects. Therefore, to avoid background counts, only the best CR-39 was used.

(a) Work supported by the Department of Energy, under Contract DE-AC08-89NV10630.

P. Koch (REECo) found that low reflection-angle lighting from above the foils produced bright track images on a dark field enabling the colony counter to reject most surface defects.[a] He performed the studies and developed the equipment necessary for optimum application of this technique. The result was reduction of foil background and a decrease in the CR-39 rejection rate.

During reading, the foils were mounted individually on the microscope stage which was moved manually to allow six areas per foil to be read. To reduce the read time, an automated programmable microscope stage was constructed and implemented. The stage holds 24 foils and performs the movements necessary to count six areas per foil.

REECo has acquired the "frame grabber" hardware and software needed to digitize the TV image and use the track size distribution and dose calculation software written by S Homann (LLNL). Use of this system will eliminate much of the manual data transfer that is currently done. The track size distribution software is expected to be useful in the further reduction of background.

As track densities rise an increasing number of tracks are nearly coincident and the ability of the colony counter to resolve and mark them for counting steadily deteriorates. A study showed that the effect was due to orientation of track pairs as well as their proximity. Calibration data was used to define a second order equation that can be used for dose calculations up to 6 rem.

An experience at the NTS indicates that dose equivalents in the range of 20 rem are measurable. A dosimeter used for environmental monitoring was exposed to a low level source for 2304 hrs at the waste storage area. The Artek counter yielded 16411 tracks/cm^2 and a linearity corrected dose equivalent of 23.85 rem. Visual counting yielded a density of 49700 tracks/cm^2 and a dose equivalent of 20.29 rem. A dosimeter exposed for 96 hr in the same neutron field produced a density of 2800 tracks/cm^2 and a linearity corrected dose equivalent of 0.96 rem. This equates to a dose equivalent of 23.02 rem in 2304 hr.

A study was conducted to document the neutron dosimeter background at the NTS. Information used for the study was compiled from records of background foils in each batch. The average background at Mercury is 7.5 mrem/yr. As is evident from the graph, the data are highly variable from sheet to sheet. There is some question whether this background in from neutrons, physical defects in the plastic, or alpha tracks originating from Rn daughter contamination acquired during some stage of manufacturing.

Calibration is performed at the Dosimetry Calibration Facility on the NTS. The dosimeters are mounted on a phantom, and the source is transferred to the outdoor range manually. This system does not conform to the ALARA concept, although the doses received are low. A new calibration range has been designed for retrofit into the existing building.

(a) P.N. Koch and L.S. Sygitowicz. An Improved Technique for Reading CR-39 Track Etch Neutron Dosimeters. Health Phys. 58, Sup. 1:S64;1991.

Foil etch quality control accounts for a large fraction of the program cost. At lease 6 of each 24-foil batch are for QC. An additional 2 or 3 foils per batch are used in the blind audit program. Almost 50% of the dosimeters processed are for quality control. As is evident from the background dosimeter results, this amount of QC is necessary.

After adopting the system from LLNL, REECo personnel have made some contributions to progress in the field, but there continue to be some unsolved problems. A major one is evidenced by marked variations in calibration foil track densities. This may be caused by an unequal power application to all foils in the same chamber.

Though the system is very labor intensive with expensive QC requirements, it is attractive for NTS operations where exposures, of small magnitude to be a small number of people, come mostly from high energy neutrons from PuBe or AmBe sources.

To use CR-39 in a facility where a large number of personnel are monitored, all aspects of the program need to be automated. Steps have been taken in the issue/return, reading, and dose processing areas to automate processing. These consist of developing computer applications to control equipment, and record and manipulate the information collected during these operations. Most of these are currently in progress and in varying stages of completion.

Dosimeter assembly and disassembly, foil preparation and chamber loading and unloading are still manual operations. There appears to be little hope for anything but invention of mechanical aids that produce small increments in efficiency.

The number of QC dosimeters required to maintain the reliability of the system is high, and must remain so until etch chambers of improved reliability can be made.

NEUTRON DOSIMETRY PROGRAM AT MOUND - PROBLEMS AND SOLUTIONS

M. K. Winegardner

EG&G Mound Applied Technologies, Inc.
P.O. Box 3000
Miamisburg, OH 45343

NEUTRON DOSIMETRY PROGRAM

The Mound personnel neutron dosimetry program utilizes TLD albedo technology. The neutron dosimeter design incorporates a two-element spectrometer for site-specific neutron quality determination and empirical application of field neutron calibration factors. Design elements feature two Li(6)F (TLD-600) chips for neutron detection and one Li(7)F (TLD-700) chip for gamma compensation of the TLD-600 chips. One TLD-600 chip is Cadmium shielded on the front side of the dosimeter, the other is Cadmium shielded from the back side. Tin filters are placed opposite of the Cadmium shield on each of the TLD-600 chips and on both sides of the TLD-700 chip for symmetrically equivalent gamma absorption characteristics. Neutron quality determination is accomplished by the albedo neutron-to-incident thermal neutron response ratio above the Cadmium cutoff. This front Cadmium shielded-to-back Cadmium shielded response ratio, compensated for the presence of gamma radiation, provides the basis for neutron energy calibration via the albedo response curve.

Neutron calibration source energies vary over the range of 1 to 4 MeV inclusive of the following in order of increasing energy: Polyethylene spherically moderated Pu(238)O(18), Pu(238)F, Pu(238)O(18), Cf(252), and Pu(239)Be. Data from the various neutron spectra follow the typical albedo response curve thus providing for the empirical relationship which establishes the algorithm for neutron dose equivalent.[1]

PROBLEMS

General problems that occur with field application of the neutron dosimetry program at Mound include improper use of the dosimeter by the dosimeter wearer, field neutron source configuration changes, and problems associated with TLD readout/process equipment. One aspect of the design of this neutron dosimeter is an asymmetrical response geometry. Also, albedo neutron response is dependent on close proximity of the dosimeter to the body in the torso region of the dosimeter wearer. Neutron source configuration changes can result from a variety of factors including building or facility modifications, project scaling up/down, and neutron source strength. These factors can all result in neutron spectral variations that must be anticipated in dosimeter design and field use applications. Additionally, problems associated with the direct contact heating TLD readout/process result in non-uniform TL chip heating due to mechanically stressed TL materials and encapsulating media (generally

PTFE teflon). Unreliable readout system performance will encroach without frequent large-scale TL chip inventory replacement.

SOLUTIONS

Direct solutions to the TLD related neutron dosimetry problems at Mound have included increasing employee awareness of proper dosimeter use and care through instructional training, brochures, etc., and changeover to new hot gas, non-contact TLD readout technology via the Harshaw Model 8800 TLD reader. The new Harshaw Model 8800 reader system's non-contact, positive temperature control, hot nitrogen gas readout process allows an approximate 10-fold increase in TL chip life and a substantial increase in reliability as related to individual TL chip sensitivity tracking and utilization. The concept of the Time Temperature Profile (TTP) allows for a wide variety of TL chip size and phosphor types as well as encapsulation materials, if desired, to be used concurrently in a particular dosimetry system.

Neutron field spectra characterization of the Radioisotopic Thermoelectric Generator (RTG) Production and Testing Facility and the former hydrogenous imaging via Californium Multiplication (CFX) Facility was an important aspect of establishing current neutron spectral and dosimetric conditions.[2] This provides for an applied, long term solution by application of a standard against which future facility and/or neutron source type modifications can be evaluated.

Additional, more comprehensive solutions include adaptation of a combined TLD/TED (Electrochemical Track Etch Dosimeter) with an appropriate algorithm for neutron dose equivalent determination. It is suggested that the TLD component be used as a qualitative indicator of neutron dose, while the TED component be used as a qualitative indicator of neutron dose, while the TED component be used in the actual quantitative evaluation of the neutron dose equivalent due to its apparent sensitivity and greater flexibility as a neutron spectrometer. Application of electrochemical TED technology was attempted at Mound during the 1986-88 U.S. Department of Energy (DOE) field test evaluation and preliminary implementation program, however, achievement of applied TED capability did not materialize. Although technical interest in TED has been very good (electrochemical TED's good energy response range and minimum detectible neutron dose capabilities) throughout the DOE community, an overall lack of support of technical programs at the managerial/administrative levels has resulted in lack of available programmatic funding. Issues such as cost of automation and increased technical staffing requirements have become more important than the apparent technological solution of vastly improved neutron dosimetry via electrochemical TED. A greater emphasis is now being placed on achieving compliance with sub-state-of-the-art technology such that emphasis on development and production of new viable technological solutions is becoming less and less due to cost effectiveness issues alone. Worker health, safety, and protection issues such as the ability to measure defined quantities to smaller degrees and As Low As Reasonably Achievable (ALARA) principles are not being adequately addressed.

Currently, personnel neutron dosimetry in the United States is undergoing a technological applications stalemate of similar proportions to that seen in the overall economic sector. It is this author's suggestion that in this current climate of greater emphasis on compliance and lesser emphasis on new viable solutions, that technological directive and guidance will be mandatory before allocation of

resources will occur in the field. In order to implement technologies such as electrochemical TED past the research and development bench and into small, medium, and large-scaled applied personnel dosimetry systems, adequate lead time of at least two budget cycles must be given these directives in order for programmatic impact to occur.

1. Mound's Thermoluminescent Personnel Dosimeter for Neutron and Photon Monitoring, M. Edward Anderson and Sue L. Crain, MLM-2808, June 25, 1981.

2. Neutron Measurements in Californium Multiplier (CFX) and Radioisotope Thermoelectric Generator (RTG) Facilities at Mound Laboratories, M. K. Murphy, G. W. R. Endres, and D. L. Haggard, May, 1990.

NEUTRON DOSIMETRY AT THE SAVANNAH RIVER SITE[a]

K. W. Crase and R. M. Hall

Health Protection Department
Westinghouse Savannah River Company
P.O. Box 616
Aiken, SC 29802

ABSTRACT

The Savannah River Site is operated by Westinghouse Savannah River Company for the U.S. Department of Energy. It is located adjacent to the Savannah River and occupies approximately 300 square miles in portions of three South Carolina counties. Several site facilities involve neutron exposures to radiation workers. Neutron exposures currently contribute about 20 percent of the site collective annual dose. The Hoy type albedo dosimeter is used for neutron dose determination.

In this paper, the nature and extent of neutron exposures at the Savannah River Site are described, including details about the range of exposure conditions, numbers of personnel monitored, and collective dose. The current status of the neutron dosimetry program is discussed. Areas which are the current focus for improvement are discussed. These include: energy dependence of neutron dosimeters, methods for determining effective dose equivalent from external neutron exposures, and methods of determining effective dose equivalent from partial body neutron exposures.

(a) Work supported by the U.S. Department of Energy through contract with the Westinghouse Savannah River Company, under Contract No. DE-AC09-89-SR18035.

THE MARTIN MARIETTA ENERGY SYSTEMS PERSONNEL NEUTRON DOSIMETRY PROGRAM

K. L. McMahan

Oak Ridge National Laboratory
P.O. Box 2008, Building 2652-A
Oak Ridge, TN 37830-6290

INTRODUCTION

Martin Marietta Energy Systems, Inc. (Energy Systems), manages five sites for the U.S. Department of Energy. Personnel dosimetry for four of the five sites is coordinated through a Centralized External Dosimetry System (CEDS). These four sites are the Oak Ridge National Laboratory (ORNL), the Oak Ridge Y-12 Plant (Y-12), the Oak Ridge K-25 Site (K-25), and the Paducah Gaseous Diffusion Plant (PGDP). The fifth Energy Systems site, Portsmouth Gaseous Diffusion Plant, has an independent personnel dosimetry program. The current CEDS personnel neutron dosimeter was first issued in January 1989, after an evaluation and characterization of the dosimeters' response in the workplaces was performed.

For the workplace characterization, Energy Systems contracted with Pacific Northwest Laboratory (PNL) to perform neutron measurements at selected locations at ORNL and Y-12. K-25 and PGDP were not included because their neutron radiation fields were similar to others already planned for characterization at ORNL and Y-12. Since the initial characterization, PNL has returned to Oak Ridge twice to perform follow up measurements, and another visit is planned in the near future.

CEDS NEUTRON DOSIMETER DESIGN

The CEDS personnel neutron dosimeter, shown in Figure 1, is the standard Harshaw 8806B neutron dosimeter[1] manufactured by Solon Technologies, Inc. The dosimeter card contains four thermoluminescent chips, and can be processed in the Harshaw 8800 automatic reader. This dosimeter has two 0.015 inch thick lithium-6 fluoride (^{6}LiF) chips (elements 1 and 4) and two 0.015 inch thick ^{7}LiF chips (elements 2 and 3). When assembled in the holder, one ^{6}LiF - ^{7}LiF pair is positioned behind a 0.018 inch thick cadmium (Cd) filter. The other pair is covered only by the plastic of the holder. The back of the holder has two loops across its width through which the wearer's belt is threaded. The plastic is colored red to easily distinguish it as the neutron dosimeter; the beta-gamma dosimeter is blue in color.

The dosimeter's design has two distinct advantages. First, the pairing of ^{6}LiF and ^{7}LiF chips makes the gamma signal subtraction relatively simple. The symmetrical design ensures that photons are detected by the ^{6}LiF and ^{7}LiF chips with essentially the same sensitivity. The second advantage is that

the holder's belt loop design ensures that the device that is calibrated as an albedo dosimeter is actually used as an albedo dosimeter.

FIELD CHARACTERIZATION OF DOSIMETERS

Energy Systems and PNL personnel performed neutron measurements at over twenty locations in ORNL and Y-12.[2] The ORNL locations included isotopic neutron source make up and fabrication facilities, accelerator facilities, the High Flux Isotope Reactor (HFIR), calibration facilities, and a TRU waste storage facility. The Y-12 locations included a neutron source storage area and a uranium fluoride (UF_4) storage area.

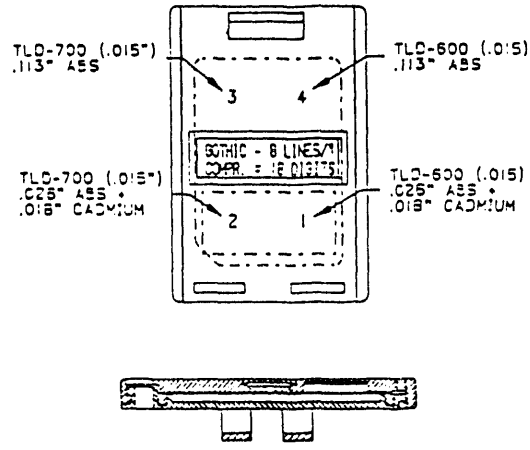

FIGURE 1. Harshaw 8806B Neutron Dosimeter

PNL used several types of neutron field characterization instruments for the measurements, including tissue equivalent proportional counters (TEPCs), Bonner spheres, a helium-3 detector, and an NE213 spectrometer. For personnel dosimetry purposes, the neutron dose equivalents obtained from the TEPCs were used as the reference measurements for the neutron dosimeter characterization. At each location, detectors were set up near a phantom on which neutron TLDs were mounted.

To analyze the results, the net neutron responses of the cadmium and plastic covered elements are each divided into the delivered neutron dose equivalent reported from the TEPCs. Where two TEPCs were used, the average of the reported results was used. The resulting ratios are TL-response-to-dose-equivalent correction factors, named CFCD and CFPL for the cadmium filtered and plastic covered elements, respectively. These ratios are presented for selected fields in Table 1.

TABLE 1. TLD Response to Neutron Dose Equivalent Correction Factors for the CEDS Personnel Neutron Dosimeter

	CFCD	CFPL	CFPL/CFCD
Bare Cf-252	1.432	1.117	0.78
15 cm D_2O moderated Cf-252	0.131	0.102	0.78
REDC TURF glove box	0.635	0.456	0.72
REDC Room 111 glove box	0.363	0.241	0.66
REDC TDF	0.205	0.106	0.52
SWSA waste cask	0.113	0.059	0.52
REDC waste cask	0.068	0.037	0.54
ORELA	0.027	0.015	0.56
HFIR	0.0057	0.0021	0.37

TECHNICAL PROBLEMS AND SOLUTIONS

Even a quick analysis of the correction factors shows that the dosimeter design is not capable of providing enough information from which to empirically derive the delivered neutron dose equivalent. This is perhaps most obvious in observing the correction factors for both bare and D_2O-moderated californium-252 (Cf-252) in a low scatter facility. The ratio of the net neutron response of the cadmium filtered elements to that of the plastic covered elements for each of these spectra is essentially the same, but the ratio of the delivered dose equivalent to net TL response differs by approximately a factor of ten for similarly filtered elements.

Other observations of the data show that the ratio of CFPL to CFCD is not a very sensitive indicator of the spectrum in which the dosimeter was irradiated, varying only between about 0.45 for fields with a high thermal component, and 0.7 for relatively hard spectra, while the magnitude of CFCD and CFPL vary by more than a factor of fifty. The obvious conclusion is that the neutron dosimeter is not capable of reporting the neutron dose equivalent without a prior knowledge of the dosimeter's response in the spectrum of interest.

These limitations are overcome by analyzing the possible spectra to which different groups of personnel may be exposed, and administratively ensuring that the appropriate correction factors are applied to the TLD results. Since workers do not always work exclusively in a single neutron spectrum, and because there are a variety of spectra present at Energy Systems sites (particularly ORNL), types of work were analyzed and workers are now placed into one of nineteen standing categories of neutron work. Each category has a somewhat unique CFCD and CFPL which are applied to the workers' dosimeter processing results. For work categories which mix two or more types of spectra, CFCD and CFPL are weighted conservatively by an occupancy factor and a dose rate using a standard two parameter weighting technique supplied by Los Alamos National Laboratory.

ADMINISTRATIVE PROBLEMS AND SOLUTIONS

The need to associate workers with the type of work they perform presents an administrative challenge. CEDS monitors approximately 350 "permanent" neutron workers, and approximately 300 visitors per quarter. When workers switch job assignments, a switch in the category of assignment is triggered by the area radiation protection supervisor. Currently, these changes are tracked on a personal computer database at ORNL. The dose calculation programs are also executed from this computer. Neutron dose equivalent results are transferred in a batch process to the personnel dosimetry records minicomputer (a VAX 6320) once per quarter. A project is underway to upgrade and transfer all neutron data processing and storage operations to the minicomputer.

Special jobs and facility upgrades also pose an administrative problem, since PNL is not and cannot realistically be "on call" to characterize the fields. To solve this problem, ORNL's operational and research dosimetry groups are teaming up to provide an on site capability for the necessary measurements. Several approaches are being considered in parallel, including on site TEPC measurement capability, adapting Piesch and Burgkhardt's single sphere albedo technique[3] to area neutron measurements, and area bubble dosimeter spectrometer measurements.

REFERENCES

1. Harshaw Product Specification, Solon Technologies, Inc., Solon, Ohio.

2. "Neutron Dose Equivalent and Energy Spectra Measurements at the Oak Ridge National Laboratory and Y-12 Plant," private correspondence, K.L. Soldat, et al., May 1990.

3. "Measurement of Neutron Field Quantities Using the Single Sphere Albedo Technique," E. Piesch and B. Burgkhardt, Proceedings of the Fifth Symposium on Neutron Dosimetry, Munich/Neuherberg, FRG, September 1984, pp. 403-413.

IMPROVING PERSONNEL NEUTRON DOSIMETRY AT THE INEL

F. M. Cummings, F. L. Kalbeitzer, and R. D. Carlson

Department of Energy, Idaho Operations Office
785 DOE Place
Idaho Falls, ID 83402-4149

ABSTRACT

The personnel neutron dosimeter used at the Idaho National Engineering Laboratory (INEL) was modelled after the Hankins style albedo dosimeter and uses six thermoluminescence dosimeter (TLD) chips encased in a cadmium box. Personnel neutron dosimeters are assembled, disassembled and analyzed manually and the neutron dose equivalent is determined by dividing the difference of the average signals from the irradiated ^{6}LiF chips and the irradiated ^{7}LiF chips by a calibration factor. The neutron dose equivalent result is adjusted to account for differences between the field neutron energy spectrum and the calibration neutron energy spectrum using a Field Neutron Correction Factor (FNCF). The FNCF's have been determined for approximately 15 locations at the INEL by applying the ratio of responses from 9" and 3" spheres to the calibration curve determined by Hankins. The application of small FNCF's has resulted in a significant number of false positive neutron dose equivalent results. The Radiological Sciences Branch intends to perform a variety of neutron dose and energy spectral measurements at the previously identified locations to improve the assessment of personnel neutron dose equivalent. Using the results of those measurements, (1) new FNCF's will be developed, (2) a practical field technique will be developed to verify the FNCF's and to identify new areas of concern and (3) the lower limit of detection for neutron dose equivalent will be determined as a function of the neutron energy spectrum.

INTRODUCTION

The Radiological Sciences Branch (RSB), part of DOE's federally staffed Radiological and Environmental Sciences Laboratory (RESL), conducts applied research to improve and develop techniques used to assess neutron personnel dose equivalent at the INEL. Prior to January, 1989, the Dosimetry Branch of the RESL was responsible both for operating the personnel dosimetry program at the INEL and for conducting research in support of that program. In January, 1989, the INEL personnel dosimetry program was restructured. The operational part of the dosimetry program was contracted to EG&G Idaho, Inc. The Dosimetry Branch which was renamed the RSB is responsible for the oversight of the operational dosimetry program and also conducts research to support the operational dosimetry program. This study to characterize the neutron fields at the INEL and recommend improvements is part of the RSB support function.

INEL NEUTRON DOSIMETER

The INEL neutron dosimeter was modelled after the Hankins style albedo dosimeter. It uses six thermoluminescence dosimeter (TLD) chips encased in a cadmium box. The six chips include three ^{7}LiF (Harshaw TLD-700) chips and three ^{7}LiF (Harshaw TLD-600) chips. Four to six days prior to issuing the dosimeters, the chips are annealed for 1.5 hours at 405°C and 16 hours at 85°C and the dosimeters are assembled. {The oven loading is such that the mass of the chips in the oven has an insignificant effect on the temperature variability.} Some of the dosimeters are issued as area background dosimeters from which the background signal is determined.

After the dosimeters are collected from the field, the chips are analyzed manually in a Harshaw Model 2000 TLD reader. The signals from the ^{6}LiF chips and ^{7}LiF chips are averaged in both the irradiated dosimeters and the area background dosimeters. The net signal for the two types of chips in an irradiated dosimeter is the difference between the average signal due to irradiation and the average signal due to background. The neutron dose equivalent is determined by dividing the difference of the average signals from the irradiated ^{6}LiF chips and the irradiated ^{7}LiF chips by a field neutron calibration factor (FNCF). The FNCF accounts for differences in the energy response of the dosimeter between the field neutron energy spectrum and the calibration neutron energy spectrum.

DETERMINATION OF FNCF'S

FNCF's have been determined for approximately 15 locations at the INEL by applying the ratio of responses from 9" and 3" spheres to the empirically determined calibration curve from Hankins[1]. At the inception of the program roughly fifteen years ago, the 9"/3" measurements were verified by comparing the neutron dose equivalents determined using the TLD results with neutron dose equivalents determined using the 9" remball at several locations. Since the initial verifications were performed, new locations have been added without verifying that the FNCF's are still valid.

The 9"/3" sphere response technique has not been rigorously tested and verified in the literature. On the contrary, a statistical analysis of results of measurements obtained in nuclear power plants revealed a weak correlation of 9"/3" sphere response ratios to the Hankins calibration factor when compared to neutron dose equivalents obtained using multispheres and the tissue equivalent proportional counter (TEPC)[2] . Another report suggests that while the 9"/3" sphere response ratio method may be used for ratios above 0.2, that when those ratios fall below 0.2, the calibration curve reported by Hankins[3] is not applicable. Finally, Swaja and Yeh published results which raise potential problems with the technique based on differences in the construction of the 9" remballs[4].

If it is determined that the 9"/3" sphere response technique is not the best method of determining field calibrations for albedo neutron dosimetry provided at the INEL to radiation workers in reactor environments and if the neutron dose equivalent determined using the 9" remball is not the best conventionally true dose equivalent, then it is important to characterize all the neutron fields at the INEL to: (1) determine FNCF's which reflect a more conventionally true neutron dose equivalent, (2) identify

those neutron fields that have changed due to modification of equipment and facility design and (3) characterize neutron fields arising from new experiments.

LOWER LIMIT OF DETECTION

Because the lower limit of detection (LLD) for the Hankins dosimeter depends strongly on the energy spectrum of the neutron field, a significant number of false positive personnel neutron dose equivalent results have arisen. For more weakly interacting neutron fields (those fields with higher energy neutrons), the lack of precision from the decreased signal in the TLD tends to raise the lower limit of detection. A greater LLD together with a small FNCF (both resulting from higher neutron energy spectra) impacts the operational program by increasing the number of false positive personnel neutron dose equivalent results. This condition diverts resources into determining causes of the false positive results instead of improving the current system of dose assessment.

PROPOSED SOLUTION

To determine the more conventionally true FNCF's it is planned that measurements be performed at each location using: (1) the INEL dosimeter to determine the response of the dosimeter, (2) CR-39 to determine the applicability of this technique at the INEL (3), a TEPC to determine the reference neutron dose equivalent, (3) a ^{3}He spectrometer to determine the neutron energy spectrum below 1 MeV, (4) 9"/3" sphere response ratios to provide information for indexing the FNCF'S, (5) a 9" remball to determine the response of the remball and (6) multispheres to determine the neutron energy spectrum, primarily in fields with higher energy neutrons.

A phantom stand has been constructed which will allow dosimeter irradiations and the TEPC and ^{3}He measurements to be performed simultaneously. The neutron dose and spectrometer system shown was assembled at the Pacific Northwest Laboratory for RESL. The system includes a 2.25" TEPC manufactured by Far West Technology, a 1"-diameter 11"-long cylindrical ^{3}He neutron detector, ORTEC Spectroscopy Amplifiers, a Model FS105 four input field spectrometer manufactured by Paulus Engineering Company and a GrID portable computer. The analysis and control software was developed at PNL and is being modified at RESL to allow for uninterrupted data collection.

A study is already underway at RESL to evaluate the feasibility and desirability of incorporating CR-39 into the INEL personnel neutron dosimeter. CR-39 films will be irradiated at the previously mentioned locations and these data will be used to further evaluate that option.

OBJECTIVES

The objective of our performing these measurements is to determine new FNCF's based on results which better represent the conventionally true dose equivalent or to verify the existing FNCF'S.

Simultaneously, the applicability of using CR-39 at INEL will be evaluated.

At the same time, the LLD's will be determined for each location and for each energy spectrum. Once the LLD's have been determined, we will determine the advisability of using a single value for a neutron dose equivalent reporting cut-off, or area specific values.

Finally, a procedure will be implemented by which health physics technicians will annually verify the 9"/3" ratios at the locations for which they are responsible. It is hoped that the annual verification of 9"/3" sphere response ratios will alert personnel in the field to the need for identifying changing and new conditions which could impact the FNCF'S.

REFERENCES

(1) Hankins, D.E., 1977. "Energy Dependence Measurements of Remmeters and Albedo Neutron Dosimeters at Neutron Energies of Thermal and Between 2 key and 5.67 MeV", in: Proceedings of the International Radiation Protection Association IVth International Congress, Paris p. 553.

(2) Eisenhauer, C.M. and R.B. Schwartz, 1983. "Analysis of Measurements with Personnel Dosimeters and Portable Instruments for Determining Neutron Dose Equivalent at Nuclear Power Plants." U.S. Nuclear Regulatory Commission report NUREG/CR-3400, Washington, D.C. 20555.

(3) Rathbun, L.A. and G.W.R. Endres, 1983. "Correlation of Neutron Data Taken at Commercial Nuclear Sites." U.S. Nuclear Regulatory Commission report NUREG/CR-2893, Washington, D.C. 20555.

(4) Swaja, R.E. and S.H. Yeh, 1987. "Potential Problems with Using Sphere Ratios to Determine Neutron Albedo Dosimetry Correction Factors," in Radiation Protection Management, Volume 4, No. 3, May/June 1987.

NEUTRON DOSIMETRY PROGRAM: PROBLEMS AND SOLUTIONS RELATED TO THE SUPERCONDUCTING SUPER COLLIDER

J. S. Bull and L. V. Coulson

Superconducting Super Collider Laboratory
2550 Beckleymeade Ave., Suite 125, MS-1071
Dallas, Texas 75237

The Superconducting Super Collider (SSC) is the latest in the line of record-setting particle accelerators used for high energy physics research. When completed, the SSC will be 54 miles circumference and capable of accelerating protons to 20 TeV. Neutron dosimetry at high energy particle accelerators has always provided a unique challenge to health physicists. Neutron fluence and spectra outside accelerator enclosures are determined by many factors, such as particle type and energy, beam loss conditions, and shielding design. Experimental data on particle production and spectra do not exist at these energies; thus reliance is placed on production models and physical processes which are based on information obtained from lower energy machines.

Currently, the focus of work regarding radiation protection at the SSC Laboratory is in shielding design. The SSCL has pledged that the dose rate at the site boundary will be less than 10 mrem/yr. To meet this goal, the main accelerator will lie between 45 and 300 feet below the ground surface. In addition, a set of design guidelines, listed in Table 1, have been developed for use in the shielding design. Two beam loss conditions are considered during the shielding design: the expected highest beam losses during normal operations, and the losses due to a beam accident. For the non-superconducting magnet accelerators, a beam accident has been defined as the total loss of beam for one hour, concentrated at one point. For the superconducting accelerators, the maximum beam accident is limited to the loss of one beam pulse, since such a loss would quench the magnets and disable the accelerator. The SSC plans to minimize the use of fences by providing enough passive shielding for each accelerator to reduce the above ground dose to less than 20 mrem/yr.

Diverse radiation fields are produced by high energy particle interactions. When a high energy particle hits a target, a cascade of particles, consisting mainly of protons, neutrons, kaons, and muons is produced. Initially, this shower is concentrated in the forward direction, but as the energy is spread among more particles, the particle fluence becomes more isotropic. In addition, as the average particle energy decreases, charged particles are stopped by ionization, leaving neutrons to dominate the particle spectra emerging from a lateral shield. The amount of material needed to reduce the neutron fluence to tolerable levels depends on the beam loss parameters. For the SSC, several meters of material such as concrete or earth is required to reduce the dose equivalent to 10 mrem per accident. However, in the forward direction and beyond a few meters of shielding, muons dominate the radiation field. Since

TABLE 1. Design Guidelines for Radiation Protection at the SSCL

Area	Design Limits	Remarks
Site Boundary	≤ 10 mrem/yr	Dose from all sources of radiation at the SSC
Uncontrolled Area	≤ 20 mrem/yr ≤ 10 mrem/accident	Unrestricted public access
Controlled Area-Minimal Occupancy	≤ 2 mrem/hr ≤ 20 mrem/accident	Public access restricted by signs and fences
Radiation Area-Continuous Occupancy	≤ 0.25 mrem/hr ≤ 100 mrem/accident	Occupied by radiation workers for at least 2 hr/day

muons interact weakly with matter, several kilometers of earth are required to stop them. For example, the muon vector lengths for the SSC beam backstops are in excess of 5 km.[a]

To aid in shielding design, several Monte-Carlo computer codes have been developed to calculate the dose equivalent due to accelerator beams. One such program, CASIM[b], uses a hadronic production model and weighted averaging to determine the star density for a user-supplied shielding configuration. From the star density, dose equivalent and activation concentrations can be estimated. Figure 1 shows the dose per accident (4×10^{14} protons) for a 20 TeV beam in the collider, calculated with CASIM. As can be seen, 22 feet of earth is required to reduce the dose equivalent to 10 mrem. As the shielding thickness is increased, the dose equivalent decreases approximately a factor of 10 per three feet of shielding, thus at 45 feet, the dose equivalent will be less than 10^{-6} mrem per accident.

The absorbed dose due to neutron leakage through penetrations in the bulk shielding is another concern at the SSC. Several large shafts, up to 30 feet in diameter, are necessary for equipment delivery and personnel access into the accelerator. Neutron attenuation through accelerator labyrinths is complicated by the high energy neutrons produced by the beam interaction. Figure 2 shows a typical

(a) J.D. Jackson, "SSC Environmental Radiation Shielding," SSC Task Force Report, SSC-SR-1026, July 1987.

(b) A. Van Ginneken and M. Awschalom, High Energy Particle Interactions in Large Targets, Volume 1, Fermi National Accelerator Laboratory Report, 1975.

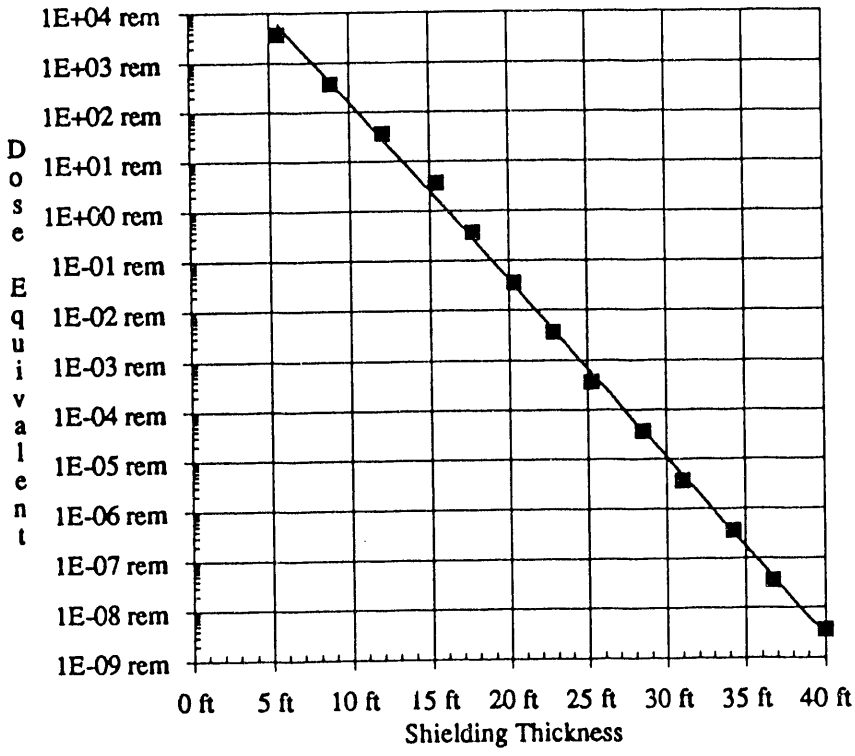

FIGURE 1. Dose Equivalent vs Shield Thickness (density = 2.3 g/cm^3) for an accidental loss of 20 TeV beam (4 x 10^{14} protons)

neutron spectrum measured in the accelerator enclosure at Fermilab.[a] This graph shows a 1/E distribution plus a peak in the spectrum around 1 MeV. Preliminary calculations of the neutron spectra in the SSC utility shafts (18 feet diameter) have been performed,[b] and are shown in Figure 3, along with the schematic drawing of the shaft. This graph plots the neutron spectra at distances of 10 m, 30 m, and 60 m from the base of the vertical shaft. The 1 MeV peak is eliminated by the 90 degree bend in the labyrinth, and, as the length of the shaft increases, the neutron spectra soften. However, the dose equivalent at the surface exceeds the design guidelines, even for a 250 feet deep shaft. Additional shielding in the utility shaft or above the opening will be required during machine operations.

(a) Freeman, W.S., et al. 1987. "Measurements of Neutron Spectra and Doses in the Tevatron Tunnel for Up to 800 GeV Circulating Proton Beams," in Health Physics of Radiation Generating Machines, Proceedings of the Twentieth Midyear Topical Symposium of the Health Physics Society, edited by W.P. Swanson and D.D. Busick, CONF-8602106, National Technical Information Service, U.S. Department of Commerce, Springfield, VA.

(b) Buishev, I.S., N.V. Mokhov, and T.E. Toohig. "The SSC Shafts Calculational Study." To be published as a SSC note, 1991.

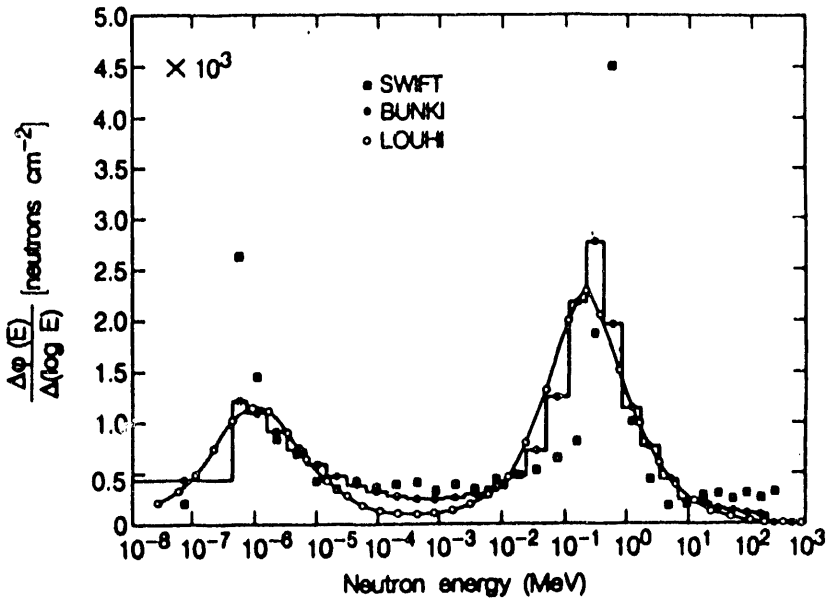

FIGURE 2. Neutron spectra measured during 800 GeV beam operation in the accelerator enclosure at Fermilab with a multisphere neutron spectrometer. The different curves are derived from different unfolding codes. From (Reference 3).

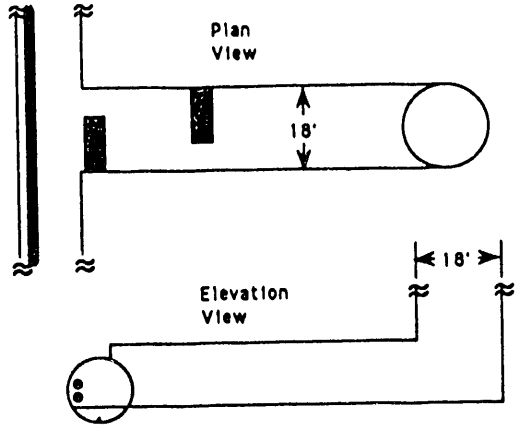

a) SSC Utility Shaft.

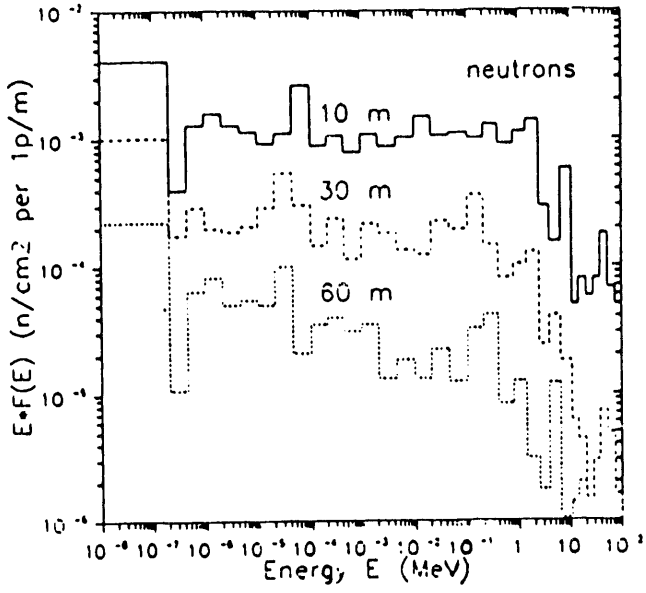

b) Calculated neutron spectra in the vertical leg of the SSC utility shaft at 10 m, 30 m, and 60 m, measured from the base of the shaft. From (Reference 4).

FIGURE 3.

Since none of the accelerators at the SSCL are expected to start commissioning until the end of 1994, the SSC has not yet established a neutron dosimetry program. A survey of eleven DOE accelerator facilities conducted in 1989 revealed that TLD systems are used for neutron dosimetry at seven laboratories, while the rest use NTA film badges.[a] This report also indicated several fields of accelerator neutron dosimetry in need of more research, including personnel dosimetry options, shielding techniques, and neutron production cross sections and spectra from particle bombardment of various target materials. This type of research would be best conducted by the establishment of a facility, such as a beam line, dedicated to accelerator health physics research. Such a facility would be instrumental in addressing the problems associated with accelerator neutron dosimetry.

This work is supported by Superconducting Super Collider Laboratory under Department of Energy contract number DE-8C02-89ER40486.

(a) Coulson, L.V., et al. 1989. "Accelerator Health Physics at DOE Laboratories: A Characterization." Fermi National Accelerator Laboratory Report, FN-510.

HANFORD PERSONNEL NEUTRON DOSIMETRY PROBLEMS AND SOLUTIONS[a]

J. J. Fix, W. V. Baumgartner, L. W. Brackenbush,
L. L. Nichols, T. J. Paul, and A. W. Endres

Pacific Northwest Laboratory
Richland, Washington 99352

INTRODUCTION

The response of albedo personnel neutron dosimeters to neutron radiation is significantly dependent on energy (Brackenbush et al. 1980). Typically dosimeters are calibrated to the neutron spectra expected in the work environment to improve the accuracy of recorded personnel dose. Often, the field environment providing the most significant personnel neutron dose is selected as the basis for calculating personnel neutron dose. At Hanford, the "fluorinator" hood at the Hanford Plutonium Finishing Plant (PFP) was selected as the work environment providing the greatest potential for neutron dose to Hanford personnel. This work environment has been characterized on numerous occasions to ensure that personnel doses determined with the Hanford albedo dosimeter, using the Hanford site-specific calibration, correctly determines the actual neutron dose for this location.

For routine calibration, Hanford dosimeters are exposed to unmoderated ^{252}Cf. The exposure time is increased, by a factor of 1.73, so that the dosimeter response is similar between the field and calibration exposures. As such, fast neutron doses calculated with the Hanford dose algorithm and site-specific calibration are, on average, a factor of 1.73 less than the given dose for exposures with a bare ^{252}Cf source. For comparison, the calculated fast neutron dose, using the Hanford site-specific calibration, is a factor of about 6 greater than the dose for a cadmium-covered, 15-cm-diameter D_2O moderated ^{252}Cf source exposure. These factors illustrate the significant dependence of the albedo dosimeter response on the neutron spectrum.

HANFORD DOSE ASSESSMENT METHODOLOGY

Since introducing the Hanford albedo thermoluminescent dosimeter in 1972, the same algorithm was used until October 1989, with some minor procedural changes, to calculate dose for Hanford personnel. Detailed discussion of the changes made over the years is discussed in Wilson et al. (1990). The general form of the fast neutron dose equation follows:

$$FN_h = C_1(^6LiF_{Cd} - {}^7LiF_{Sn}) - C_2[^6LiF_{Sn} - {}^6LiF_{Cd}] \quad (1)$$

(a) Work supported by the U.S. Department of Energy under Contract DE-AC06-76RLO 1830.

where, FN_h refers to the fast neutron dose calculated using the historical algorithm, and C_1 and C_2 are calibration factors determined from exposures to a bare ^{252}Cf source and in the middle stringer of the Hanford Sigma Pile, respectively. $^6LiF_{Sn}$ and $^7LiF_{Sn}$ refer to the response of thermoluminescent phosphors with tin filters on the front and back (i.e., facing body) side. The ^6LiF is enriched to at least 95% in the ^6Li isotope, whereas the ^7LiF has less than 0.01% of the ^6LiF isotope. $^6LiF_{Cd}$ refers to the phosphor position which has a cadmium and a tin filter on the front and back of the dosimeter, respectively. An illustration of the Hanford albedo dosimeter, used by all radiation worker personnel, and prototype track etch neutron dosimeter component is shown in Figure 1. This figure shows the existing design of the Hanford albedo dosimeter in which positions #1 and #2 primarily are used for shallow and deep dose. Positions #3, #4, and #5 are used in neutron dosimetry. Table 1 provides a summary of the filtration used for each dosimeter position. In this design, cadmium filtration is used on the front side of the ^6LiF phosphor in position #4 to eliminate any response to incident thermal neutron (i.e., energy less than about 0.4 eV) radiation. The response of the ^7LiF phosphor in position #5 is used to photon compensate the neutron sensitive phosphors in positions #3 and #4. Each of these phosphors has a nearly equivalent response to 16 keV photons.

Although numerous field measurements indicate that this dose calculation methodology provides reasonable dose estimates for Hanford work environments, the performance of the algorithm did not meet the requirements of the DOE Laboratory Accreditation Program (DOE 1986). The average dose calculated from 15 dosimeters, as used in the performance testing, was very close to the given exposures. However, the variance was too large to pass the criteria. The algorithm performance was able to meet the performance requirements of the "American National Standard for dosimetry - Personnel Dosimetry Performance Criteria for Testing" (ANSI 1983) as used in the National Voluntary Laboratory Accreditation Program (NVLAP).

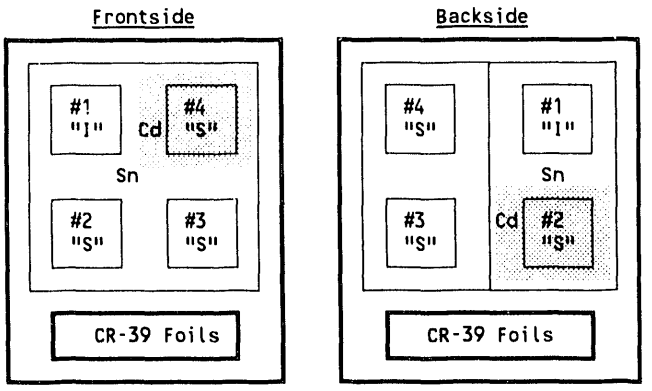

FIGURE 1. Illustration of Prototype Hanford Combination Personnel Neutron Dosimeter Showing Filter and Phosphor Placement for Existing Dosimeter Design and Placement of Two CR-39 Foils

TABLE 1. Filtration used with Hanford Albedo Dosimeter

Position	Phosphor	Filtration	
		Frontside	Backside
#1	^{7}LiF	(a)	(a)
#2	^{7}LiF	Al	Al
#3	^{6}LiF	Sn	Sn
#4	^{6}LiF	Cd/Sn[(b)]	Sn
#5	^{7}LiF	Sn	Sn

(a) Plastic filtration on front and back of phosphor.
(b) Cadmium filter on outside of tin filter. Positions #3, #4, and #5 have the equivalent response to 16 keV photon radiation.

A simplified neutron dose algorithm was developed and implemented for routine use at Hanford effective with the October 1989 dose results. The use of this algorithm was determined following several months of evaluation. It was recognized that the historical algorithm likely provided the best average dose estimate for Hanford personnel. However, there were instances when the algorithm would produce a larger than expected variance, which provided inadequate performance, in dosimeter performance testing. Evaluations were conducted to determine the causes for these failures. The historical algorithm resulted in greater error propagation because of the number of terms involved. It was recommended that until the performance of this algorithm could be improved to assuredly pass the DOE accreditation performance criteria, the following simplified algorithm be used:

$$FN_s = C_8(^{6}LiF_{Cd} - ^{7}LiF_{Sn}) \quad (2)$$

where FN_s is the calculated fast neutron dose using the simplified algorithm and C_8 is the spectrum dependent calibration factor. This equation is currently being used in place of Equation (1). This algorithm meets the DOELAP performance criteria and was formally accredited effective January 1990. A further change in the reporting of neutron dose became effective with the January 1990 dose report in which a total neutron dose only was reported. This is determined as follows:

$$TN = FN_s + SN \quad (3)$$

where TN is the total neutron dose, FN_s is the fast neutron dose component using Equation (2) and SN is the slow neutron dose component determined from formulation as follows:

$$SN = C_4[^{6}LiF_{Sn} - ^{6}LiF_{Cd}] \quad (4)$$

where C_4 is determined from a Sigma Pile calibration exposure.

For the majority of Hanford work environments, there is little contribution from thermal neutron exposure. It was recognized, at the beginning, that Equation (3) will result in an overestimation of neutron doses for work environments in which the neutron spectra are thermalized to a greater extent than the field spectra used to determine the Hanford site-specific calibration factor. To minimize this occurrence, quality control criteria were incorporated into the algorithm based on the following formulation:

$$[{}^{6}LiF_{Sn} / {}^{6}LiF_{Cd}] > 1.38 \qquad (5)$$

Whenever Equation (5) is true, then the fast neutron dose is calculated using Equation (1).

COMPARATIVE MEASUREMENTS FROM SELECTED NEUTRON SOURCES

During the past year, measurements have been conducted from selected neutron sources to further evaluate the best alternative currently available for conducting personnel neutron dosimetry at Hanford. These measurements complement the measurements conducted in the work environment during the past several years (Fix et al. 1981, Fix et al. 1982).[(a)(b)(c)] Measurements were taken at PFP from three plutonium neutron sources. In addition, measurements were taken of a National Institute of Standards and Technology (NIST) traceable neutron source. Hanford albedo neutron and CR-39 track etch dosimeters were used in all of these measurements. Multisphere spectrometers and Tissue Equivalent Proportional Counters (TEPC) were used to determine the actual neutron dose rate.

Selected plutonium neutron sources used at PFP included plutonium tetrafluoride, plutonium metal and plutonium oxide. Measurements were taken using the bare sources as well as, for certain sources, selected thicknesses of plexiglass shielding to simulate glovebox shielding in the work environment. Measurements were also taken of the NIST traceable ^{252}Cf source in the 318 building using no shielding as well as with selected thicknesses of plexiglass (Pmma) shielding.

The following field conditions were experienced during the measurements:

- Significant background neutron radiation was present for the plutonium metal and oxide measurements.

- Placement of dosimeters and instruments at 50 cm from the different sources resulted in some perturbation of the neutron fluence.

(a) Nichols, L. L., 1988. "Neutron Dose and Spectral Measurements at 234-5 Building." Letter to W. A. Decker, dated May 17, 1988.

(b) Cummings, F. M. and L. L. Nichols, 1986. "Neutron Field Measurements at the 234-5 Building." Internal Report dated October, 1986.

(c) Roberson, P. L., F. M. Cummings and J. J. Fix, 1985. "Neutron and Gamma Field Measurements at the 234-5 Facility." Internal Report dated September 20, 1985.

- Dose rates from the sources varied by more than 4 orders of magnitude which resulted in pulse pile-up problems at the high dose rates and long count times for the low doses.

The data collected are summarized in Table 2. The Hanford albedo dosimeter generally overestimated the measured dose in exposure situations with large amounts of moderator to produce low-energy neutrons. This is particularly true for the simplified algorithm [Equation (2)] without any criteria to correct for the effect of scattered neutrons [Equation (5)]. The degree of overestimation is strongly dependent upon the degree of neutron scattering. The CR-39 dosimeter results were generally within 25% of the measured dose for all exposure geometries. Efforts are underway to finalize this information in a PNL technical report.

TABLE 2. Comparison of Selected Source Measurements

	Dose Results in mrem				
Source	Measured	CR-39	FN_h	FN_s	FN_s[(a)]
^{252}Cf Bare	500	460	333	333	333
^{252}Cf + 1.26 cm Pmma	1017	961	1036	979	979
^{252}Cf + 2.54 cm Pmma	996	898	1308	1351	1351
^{252}Cf + 5.08 cm Pmma	529	473	716	1161	716
^{252}Cf + 10.16 cm Pmma	996	428	816	1178	816
^{252}Cf + 15.24 cm Pmma	774	587	1883	2745	1883
^{252}Cf D_2O Mod.	1000	952	5688	5000	5000
PuF_4	1683	1670	1178	189	1178
PuF_4 + 2.54 cm Pmma	1108	1238	1801	1812	1801
PuF_4 + 5.08 cm Pmma	693	1006	829	2712	829
PuO_2	96	74	51	51	51
Pu Metal	146	137	69	97	97

(a) Recorded dose calculated using Equation (2) and, alternatively when Equation (5) is true, using Equation (1).

PARALLEL MEASUREMENT OF PERSONNEL DOSE USING HANFORD ALBEDO AND TRACK ETCH DOSIMETER COMPONENTS

During a 4-month period in 1988, approximately 40 Hanford personnel were provided with the prototype Hanford combination albedo and CR-39 track etch dosimeter shown in Figure 1. The results of this study indicated that the CR-39 dosimeter component could perform as well as the Hanford albedo dosimeter with proper calibration. However, there were several instances in which the two CR-39 foils differed from one another significantly. This difference was attributed to a material quality control problem, which required investigation prior to continuing the evaluation. Beginning with the December 1990 monthly dosimeter exchange, the study was continued with approximately 10 Hanford neutron workers being monitored with the combination dosimeter each month. As expected, the dose results using the CR-39 dosimeter are lower than observed with the albedo dosimeter using either the simplified [i.e., Equation (2) without the quality control criteria of Equation (5)] or the historical [i.e., Equation (1)] algorithms. This is illustrated in Table 3 for four months of data.

The results with the CR-39 dosimeter are consistently lower than results with the Hanford albedo dosimeter using either the simplified or historical algorithms. There is a strong likelihood that the actual dose is greater than determined with the CR-39 dosimeter and less than determined with the albedo dosimeter. The CR-39 dosimeter is anticipated to underestimate the actual neutron dose because of the large angular response of the CR-39 material and because the work environment in which the dosimeters are worn is anticipated to have a significant neutron scatter component. A significant fraction of the scatter component is anticipated to be less than the CR-39 energy threshold of approximately 100 keV. Methods to better determine the personnel dose using the combination dosimeter are continuing to be evaluated.

TABLE 3. Observed Dose Comparisons with Combination Dosimeter

Month	No. of Dosimeters	Hanford Albedo[a]		CR-39
		Simplified	Historical	
December	7	184 mrem	89 mrem	37 mrem
January	7	148	67	21
February	7	81	29	21
March	7	144	71	22

(a) Reported doses equal to historical column using Equation (2) plus Equation (5) quality control criteria.

EFFORTS TO IMPROVE DOSE RESPONSE OF HANFORD ALBEDO DOSIMETER

Efforts are underway to evaluate options for improving the dose interpretation using the albedo dosimeter. Preliminary statistical models such as linear regression and non-linear regression of selected dosimeter response variables failed to establish a functional relationship for the neutron sources of interest. Several functional relationships could be used to determine the best value of the calibration factors shown in Equation (1). The factor could be based on the observed dosimeter response for dosimeter positions 3 and 4. In this manner, the existing dose formulation [i.e., Equation (2)], which has DOELAP accreditation, could continue to be used. To illustrate, the determination of the calibration factor was changed to include the capability of modifying the calibration factor as a function of neutron energy. The relationship being evaluated follows:

$$C_n = C_x [(^6LiF_{Cd} - {}^7LiF_{Sn})/(^6LiF_{Sn} - {}^7LiF_{Sn})] \quad (6)$$

where C_x is a spectrum-dependent calibration factor. Plans are to choose a factor appropriate for bare ^{252}Cf for DOELAP performance testing and a Hanford site-specific factor for Hanford work environments. With the use of this formulation, the calibration factor is adjusted depending upon the degree of thermalization measured by the ratio of the net neutron response (i.e., gamma response subtracted by $^7LiF_{Sn}$) for dosimeter positions #3 and #4.

PLANNED IMPLEMENTATION OF A COMBINATION ALBEDO AND CR-39 TRACK ETCH DOSIMETER

Hanford is currently scheduled to implement a combination albedo and CR-39 dosimeter effective January 1, 1993. The design of this dosimeter is shown in Figure 2. All four positions of the dosimeter will be photon equivalent. One position contains a $^7LiF_{Sn}$ phosphor (i.e., tin on both sides) to photon compensate the three ^6LiF phosphors. The filtration on the three ^6LiF phosphors follows:

- one position with only tin filtration on the front and back
- one position with cadmium filtration on the front and tin on the back
- one position with tin filtration on the front and cadmium on the back.

The additional ^6LiF phosphor, compared to the existing Hanford albedo dosimeter, is anticipated to provide greater capability to determine the correction necessary to compensate for the neutron energy spectrum incident upon the dosimeter. This information would be used in choosing a calibration factor. Two CR-39 foils would be used in this dosimeter. Methods to be used for routine dose evaluation are currently being evaluated.

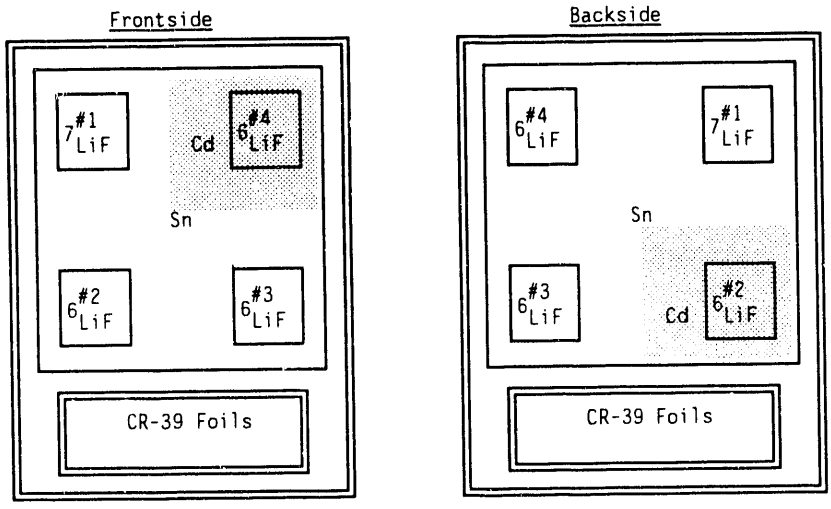

FIGURE 2. Illustration of Planned Hanford Combination Personnel Neutron Dosimeter.

CONCLUSIONS

Neutron dosimetry has been extensively studied at Hanford from the inception of operations in the mid-1940s (Wilson et al. 1990). Numerous studies have been conducted during the past 45 years to better ensure the accuracy of recorded dose for Hanford personnel. Until a personnel dosimeter is available that incorporates a direct measure of neutron dose to the person, technical uncertainties in the accuracy of the recorded dose will continue. At Hanford, studies are continuing to evaluate methods for reducing the uncertainty. Strong reliance is placed on parallel dosimeter and instrument measurements in the work environment. Field measurements in Hanford facilities have been and continue to be a critical element to ensuring the credibility of routine dosimeter results.

REFERENCES

American National Standard Institute. 1983. American National Standard for Dosimetry - Personnel Dosimetry Performance-Criteria for Testing. ANSI N13.11, New York, New York.

Brackenbush, L. W., G. W. R. Endres, J. M. Selby, and E. J. Vallario. 1980. Personnel Neutron Dosimetry at Department of Energy Facilities. PNL-3213, Pacific Northwest Laboratory, Richland, Washington.

Fix, J. J., G. W. R. Endres, F. M. Cummings, J. M. Aldrich, M. R. Thorson, and R. L. Kathren. 1981. Hanford Personnel Dosimeter Supporting Studies FY-1980. PNL-3536, Pacific Northwest Laboratory, Richland, Washington.

Fix, J. J., J. M. Hobbs, P. L. Roberson, D. L. Haggard, K. L. Holbrook, M. R. Thorson, and F. M. Cummings. 1982. Hanford Personnel Dosimeter Supporting Studies FY-1981. PNL-3736, Pacific Northwest Laboratory, Richland, Washington.

U.S. Department of Energy. 1986. Department of Energy Standard for the Performance Testing of Personnel Dosimetry Systems. DOE/EH-0027, U.S. Department of Energy, Washington, D.C.

Wilson, R. H., J. J. Fix, W. V. Baumgartner, and L. L. Nichols. 1990. Description and Evaluation of the Hanford Personnel Dosimeter Program From 1944 Through 1989. PNL-7447, Pacific Northwest Laboratory, Richland, Washington.

U.S. NAVY'S PERSONNEL NEUTRON DOSIMETRY PROGRAM

J. E. DeCicco, and S. W. Doremus

Naval Dosimetry Center
National Navel Medical Center
Bethesda, MD 20889

Since 1964 the Navy has been monitoring personnel for exposure to neutrons. With nuclear reactors, special nuclear materials, neutron calibration sources, and high energy linear accelerators, the Navy has cognizance over more neutron sources than any other single organization in the world. Personnel neutron monitoring in the Navy was first accomplished using NTA film from 1964 through 1980. In 1975 the Navy instituted albedo neutron dosimetry, which would completely replace NTA film in 1981. The Navy's first albedo neutron dosimeter, the DT-583 (Harshaw NG-67), contained a pair of LiF-600/LiF-700 thermoluminescent phosphors situated behind a cadmium filter. These phosphors were processed using contact heat, to 300°C, with a Harshaw Model 2271 TLD reader. Since 1989 the Navy has been using the DT-648 (STI/Harshaw 8800) albedo neutron dosimeter, containing a pair of thinner LiF-600/LiF-700 thermoluminescent phosphors, without cadmium filtration, processed using hot gas to 300°C with a Harshaw Model 8800 TLD reader system.

Albedo neutron dosimetry has many advantages over NTA film, but also one considerable disadvantage: energy dependence. Initially in April 1973 the DT-583 dosimeter was calibrated on a 5 gallon water-filled Lucite phantom with a bare Cf-252 source at a distance of 35 cm. A neutron fluence-to-rem conversion factor of 6.57 cm^{-2} s^{-1} = 1 mrem hr^{-1} was used to calculate delivered neutron doses for calibrations. In December 1977 the neutron fluence-to-rem conversion factor was changed to 8.0 cm^{-2} s^{-1} = 1 mrem hr^{-1}. Other calibration changes instituted at that time included the use of a slightly thicker water-filled Lucite phantom and an increase in the source to phantom distance to 50 cm. Overall, these changes resulted in a reduction in personnel neutron doses by 25%.

From 1975 through 1982 the Navy directed considerable efforts toward assessing the complexity of its field neutron spectra, evaluating techniques to correct the neutron response of its albedo dosimeter, and developing methods to perform neutron area monitoring.

As a result of investigating field neutron spectra, the Navy again modified its calibration procedure in September 1979, by changing its calibration source to Cf-252 moderated with two inches of polyethylene. This source's spectrum more closely represented spectra found aboard ships, and as a result, shipboard personnel neutron doses were reduced 45%. However, this single source's spectrum did not adequately represent all the different spectra encountered in the Navy. Therefore, a method for establishing neutron energy correction factors for the DT-583 was established using Hankins' 9-to-3 ratio method. However, since the Eberline radiac was not readily available throughout the Navy, a similar procedure was established using the AN/PDR-70 (the Snoopy remmeter) with its probe in different configurations. Implementing the AN/PDR-70 protocol, the Navy envisioned having only one neutron

energy correction factor for each type radiation worker (i.e., nuclear, weapons, radiographer & medical, where applicable), at each facility. Thus, at each facility, surveys were taken at locations were a typical radiation worker received most of his/her exposure, weighted by an occupancy time at each location. In September 1982 the Navy established the first neutron energy correction factor for the DT-583 using the AN/PDR-70 protocol.

The Navy's newest albedo dosimeter is calibrated on an ANSI standard PMMA phantom using a D_2O moderated Cf-252 source at 50 cm. Despite physical and calibration dissimilarities between the DT-583 and DT-648, it was anticipated that the neutron energy correction factors developed for the DT-583 could be modified for the DT-648. Simultaneously exposing both dosimeters to Naval Research Laboratory spectra, it was demonstrated that DT-583 neutron energy correction factors could be modified by a single number to generate corresponding correction factors for the DT-648. Presently, sufficient laboratory and field data have been collected to fully characterize the energy response of the DT-648 using the AN/PDR-70 protocol. Analysis of the data shows that the ratio of the count rates from the AN/PDR-70 partially assembled to fully assembled can predict a neutron energy correction factor for the DT-648.

Neutron area monitoring was first accomplished using a DT-583 dosimeter mounted on a 15x15x7.5 cm rectangular polyethylene block. During 1976 and 1977 it became apparent that the response characteristics of this method were less than desirable and work began on an "ideal" dose equivalent area monitor. Several designs were tested before ultimately selecting one which utilized a modified AN/PDR-70 remmeter. The remmeter's BF_3 tube was replaced with a card holder that held two DT-583 LiF cards. The rest of the tube cavity was filled with polyethylene. The modified moderator was housed in a 0.6 cm thick aluminum mounting bracket. This area monitor proved to be essentially energy independent for both neutron and photon exposures. The area monitor was adopted for use by the Navy in May 1978 and continues to be used today (upgraded for use with the newer DT-648 card in 1989).

Currently the Naval Dosimetry Center provides dosimetry to over 550 user commands. Of these, 255 commands monitor personnel (over 20,000 at any one time) for exposure to neutrons.

AIR FORCE NEUTRON DOSIMETRY PROGRAM[a]

E. H. Maher and R. M. Thurlow

United Stated Air Force
Armstrong Laboratory
AL/OEBS, Brooks ABF, TX 78235-5000

ABSTRACT

Approximately 1000 Air Force personnel are monitored for neutron radiation resulting from various sources at more than thirty worldwide locations. Neutron radiation spanning several orders of magnitude in energy is encountered. The Air Force currently uses albedo thermoluminescent neutron dosimeters for personnel monitoring. The energy dependence of the albedo neutron dosimeter is a current problem and the development of site specific correction factors is ongoing. A summary of data on the energy dependence is presented as well as efforts to develop algorithms for the dosimeter. An overview of current Air Force neutron dosimetry users and needs is also presented.

(a) Submission of full paper was waived.

INDIVIDUAL MONITORING DOSIMETRY IN EUROPE[a]

H. G. Menzel

Commission of the European Communities
Brussels, Belgium

ABSTRACT

This report discusses the various types of individual monitoring systems presently in use within the European community and neutron dosimetry research being coordinated by the EURADOS working group. Research is currently being conducted on nuclear track dosimeters, primarily with CR-39 (TM), and TLD-albedo dosimeters. Studies are being conducted on the energy and angular response of each type of dosimeter.

Because the response of dosimeters depends on the energy of the neutrons, it is necessary to have spectral information to accurately assess the dose. Neutron energy spectrum measurements are being performed in typical work place environments. Work is also progressing on development of calibration sources which will be representative of the neutron energy spectrum found in typical neutron exposure situations. This work utilizes 14 MeV neutrons incident on a uranium block with various other filters.

Research is also continuing on neutron dosimetry using tissue equivalent proportional counters and microdosimetric techniques. The results of intercomparisons between several different instruments are discussed. In addition to personnel dosimetry, these systems are being used to record the dose to passengers and flight crews aboard commercial aircraft.

(a) Submission of full paper was waived.

SUMMARY OF PERSONNEL NEUTRON DOSIMETER PERFORMANCE AND THE IMPACT OF RECENT CHANGES TO DOE'S LABORATORY ACCREDITATION PROGRAM

R. M. Loesch

DOELAP HQ Administrator
U.S. Department of Energy
Washington, D.C.

ABSTRACT

The Department of Energy (DOE) has been testing neutron personnel dosimeters as part of its Laboratory Accreditation Program (DOELAP) since 1985. A ^{252}Cf neutron source is used unmoderated and moderated by 15 cm of D_2O covered by 0.05 cm of cadmium. Mixtures of neutrons and photons are also provided. This paper summaries the performance of DOE personnel neutron dosimeters.

Recent and proposed changes in the administration of the DOELAP program that have impacts on the accreditated facilities are also presented.

NEUTRON PERSONNEL DOSIMETRY INTERCOMPARISON STUDIES[a]

C. S. Sims

Oak Ridge National Laboratory
Oak Ridge, TN 37831-6379

INTRODUCTION

The Dosimetry Applications Research (DOSAR) Group at the Oak Ridge National Laboratory (ORNL) has conducted sixteen Neutron Personnel Dosimetry Intercomparison Studies (PDIS) since 1974. During these studies, dosimeters are mailed to DOSAR, exposed to low-level (typically in the 0.3 - 5.0 mSv range) neutron dose equivalents in a variety of mixed neutron-gamma radiation fields, and then returned to the participants for evaluation. The Health Physics Research Reactor (HPRR) was used as the primary radiation source in PDIS 1-12 and radioisotopic neutron sources at DOESAR's Radiation Calibration Laboratory (RADCAL) were mainly used, along with sources and accelerators at cooperating institutions, in PDIS 13-16. Conclusions based on 13,560 measurements made by 146 different participating organizations (102 - U.S.) are presented.

GENERAL CONCLUSIONS

The PDIS are more popular than ever. The 1991 study, PDIS 16, was the largest of the studies. A total of 67 participant organizations submitted 1,787 dosimeters for testing in seven different radiation fields.

The type of neutron dosimeter used most in the PDIS is TLD albedo. It is followed by direct interaction TLD, track, film, and combination (TLD albedo-track) dosimeters. The use of track dosimeters is increasing, the use of film neutron dosimeters is decreasing, and the use of combination dosimeters is holding steady. It is obvious that the best dosimeter to use depends on the energy spectrum where the dose equivalent measurement is made.

Considering all dosimeter types in all PDIS, 67% of the measurements yielded results within $\pm 50\%$ of reference values. It should be noted that the measurements were made under ideal conditions and that field measurements can't be expected to be this good. It should also be noted that accuracy is not increasing with time. The most accurate PDIS was PDIS 3 conducted in 1977.

(a) Work sponsored by the U.S. Department of Energy under contract DE-AC05-84OR21400 with Martin Marietta Energy Systems, Inc.

CONCLUSIONS BASED ON TESTS WITH THE HPRR

These tests were conducted in a variety of spectra using the HPRR unshielded as well as with concrete, steel, and Lucite shields. The average energy ranged from about 0.6 MeV to 1.3 MeV.

The PDIS tests with the HPRR show that, overall the TLD albedo neutron dosimeter is the most accurate type. The second most accurate type in the PDIS is the combination dosimeter. These types also exhibited the best sensitivity in the PDIS. At neutron dose equivalents (H) of about 0.5 mSv, 96% of TLD albedo dosimeters yielded a non-zero response. A non-zero response was obtained from 91% of combination dosimeters, 83% of direct interaction TLD, 75% of film dosimeters, and only 53% of track dosimeters.

Neutron dosimeter accuracy is much better at $H > 1.5$ mSv than it is at about 0.5 mSv. Considering all HPRR tests, 60% of neutron dosimeters gave results within $\pm 50\%$ of reference values. If H is limited to > 1.5 mSv, this is improved to 77%. If H is limited to about 0.5 mSv, this is reduced to 38%.

CONCLUSIONS BASED ON ACCELERATOR TESTS

A total of 550 measurements of accelerator neutrons by 48 participating organizations was made in PDIS 8 (1982). More measurements were made during PDIS 16, but the results are not yet available. Two values of H (0.60 and 10.0 mSv) and four different neutron energies (0.57, 1.2, 5.3, and 15 MeV) were used during PDIS 8.

Overall, 50% of the measurements were within $\pm 50\%$ of reference values. TLD albedo dosimeters were the most accurate type for the 0.57 and 1.2 MeV exposures as well as being the most accurate overall. Film neutron dosimeters were the least accurate overall, but were the most accurate type for the 5.3 MeV measurements. Combination dosimeters were second in overall accuracy. Track dosimeters were the most accurate type for the 15 MeV exposures.

CONCLUSIONS BASED ON TESTS WITH RADIOISOTOPIC SOURCES

Radioisotopic sources (primarily ^{238}PuBe and ^{252}Cf unmoderated and moderated by D_2O and polyethylene) were used in PDIS 13-16. Since PDIS 16 results are not yet available, the conclusions are based on PDIS 13-15 measurements.

Overall, 74% of measurements yielded results within $\pm 50\%$ of reference values. Track dosimeters were the most accurate; they were followed by TLD albedo and then direct interaction TLD.

The familiar type sources (i.e., those used in mandatory national performance tests) were measured most accurately. For example, 80% of the measurements made of $^{252}Cf(D_2O)$ sources were within $\pm 50\%$ of reference values. This percentage fell to 66% for ^{238}PuBe and to 64% for ^{252}Cf moderated with 15-cm of polyethylene.

Angular dependence studies were performed with a $^{252}Cf(D_2O)$ source in PDIS 14-15 at 45° and at 60°. At 60°, the average response is about 72% of that at perpendicular incidence for TLD albedo neutron dosimeters, 68% for direct interaction TLD, and 55% for track neutron dosimeters.

COMBINATION TLD/TED TASK PROGRESS

M. A. Parkhurst

Pacific Northwest Laboratory
Richland, Washington 99352

The Department of Energy initiated the study of track detectors based on a polymer known as CR-39 through its program entitled Personnel Neutron Dosimetry Evaluation and Upgrade. The task evaluating CR-39 for neutron dosimetry was named the Combination TLD/TED Task denoting the use of thermoluminescence and track etch detectors in a combined system. The initial efforts originating in the late 1970s and early 1980s were conducted by Dick Griffith of Livermore National Laboratory (LLNL) with the assistance of Luigi Tomassino of ENEA in Italy on summer assignment to LLNL. The usefulness of CR-39 in neutron detection had been discovered previously but was inconsistent in its response and difficult to read accurately when processed by chemical etching. The first major improvement Griffith and Tomassino made to the process was to use electrochemical etching after a short chemical etch. This vastly enhanced the size of the tracks and improved their readout enormously. With the larger tracks, through-the-microscope manual track counting was no longer necessary. Off-the-shelf biological colony counters were able to read the image from the microscope through a TV camera and count the tracks with ease.

Detector Material

At the 1983 Neutron Workshop, CR-39 used at LLNL and PNL was obtained through a French source because it proved to be superior to the American sources for our application. The material was cast by American Acrylics and cut by laser. Because it was becoming increasingly difficult to obtain the French monomer, a U.S. supplier was desired. This prompted several efforts to reevaluate American monomer samples and identify ways to improve the material. The University of Berkeley physics laboratory through the efforts of Doctors Greg Tarle, Buford Price, and Michael Salamon provided considerable expertise in the study of the material in conjunction with their study of cosmic particles. The University of Connecticut, through the direction of Doctors Julian Johnson and Samuel Huang, provided graduate students to examine the various monomer products and ways to purify them. The groups discovered that PPG Industries, Inc., operating out of Pittsburgh, was producing a purified CR-39 monomer that was nominally 93% pure, a significant improvement over their 85% industrial grade material.

The use of the 93% monomer and improvements in the casting procedures provided a more consistent polymer with an acceptable background. Attempts to reduce the background further by purifying the monomer even more was highly successful on a small scale. However, efforts to produce better products on a large scale were hampered by poor starting material and were not particularly successful.

In an effort to enhance the neutron responsiveness of CR-39 to neutron interaction or reduce process time, additional materials were copolymerized with the CR-39 to provide more potential damage sites. Chemicals such as maleic anhydride were introduced to determine their compatibility in a CR-39 polymer chain. Copolymerization proved unsucessful with most chemicals tried. The maleic anhydride

successfully polymerized with the CR-39 and the product formed was more easily etched than the CR-39 alone. However, the neutron responsiveness of this product was inconsistent and its evaluation was discontinued. The study was useful in identifying the carbonate linkages of the CR-39 polymer as being highly susceptible to radiation.

Currently, American Acrylics continues to cast the 93% PPG monomer for our use. British, Japanese, Italian, and French products are also available to those in the CR-39 detector business. In most cases, the CR-39 or equivalent product is much better than what was available in the early 1980s, but differences between material batches even from the same manufacturer continue to require characterization of each batch. Thickness differences between sheets of the same batch and within the sheets themselves are greater than desired for consistent response using electrochemical etch but seldom prevent the use of the material.

Processing

Following the transition to electrochemical etch in the early 1980s, the track detectors were processed first by chemical etching in a 60°C solution of about 6 N KOH for 3 hours followed by electrochemical etching at ambient temperatures using a series of single cell chambers. The exposed side of the detector was placed next to the part of the chamber holding the KOH etchant. The backside was placed against a solution of NaCl, functioning as an electrolyte. The samples were etched for 5 hours. Power was supplied through an audio-oscillator and step-up transformer to obtain 2000 V and 2000 Hz.

In the mid-1980s, L. Tomassino reported favorable results using electrochemical etching at 60°C without the chemical etching step. He had experimented with processing parameters and obtained his best results when etching for several hours at a high voltage and low frequency and then increasing the frequency during the last step of the etch.

Concurrently, Steve Homann of LLNL and Homann-Bell Enterprises, developed a power supply specifically tailored to the needs of electrochemical etching and a process chamber design that was more useful than others evaluated in processing many samples at once. These two developments were extremely useful in progressing with CR-39 because they helped reduce many of the variables plaguing sample processing. Now up to 24 samples per chamber could be run under essentially identical environments of temperature and electric field strength. Once Homann and Dale Hankins, who had taken over LLNL's track etch efforts, had the opportunity to perfect the chamber design, making it more convenient and nearly leak-free, electrochemical etching was ready for parameter optimization.

Optimization of the processing parameters has been reviewed periodically with different desired end points. Maximum neutron response with minimum background can be obtained using parameters like 5 h etch at 2500 or higher voltage and 60 hz followed by a "blow up" period of 23 or so minutes with the frequency raised to 2000 hz. Optimum track size discrimination may work best using a regime like 3 h at high voltage and low frequency followed by a 45 minute or so blow up period. Actual parameters used depend on material and its thickness as well as the processing and readout equipment used.

Readout

Electrochemically etched tracks are large enough that they may be counted using the magnification of a microfiche reader. In fact, several developmental laboratories use these readers to manually count tracks. LLNL and PNL had been using Biotran Colony Counters to automatically count the numbers of tracks from the samples since 1983. This counting method, along with the new processing equipment, allowed much faster progress and each laboratory could process up to 48 samples a day. More capacity could easily be added with larger oven/incubators.

PNL initiated a study of the neutron interaction response mechanism by studying proton exposures over a variety of monoenergetic beam energies and angles. Beams of deuterons and carbon nuclei were also used to expose CR-39. One interesting result of this study was the difference in track size from these particles. Knowing there was a relationship between track size and LET, it was more a conformation than a discovery, but it led to the desire for greater neutron track-size discrimination capability than was available with the colony counter. A commercial image analysis program was ordered along with the computer peripherals to run it and a programmable stage that would allow readout of numerous samples without human intervention. The program operated very well for counting tracks in samples with at least several tracks per viewing area. It did not work well on background samples where tracks were absent and the autofocus unit had nothing to focus on. For this readon, periodic interaction in the readout remained necessary. The track size histogram program provided a first automated viewing of the variation in track areas versus the neutron source or monoenergetic beam energy. This capability provided PNL with a way to further evaluate the possibility of relating track size with quality factor and analyze anomolous results.

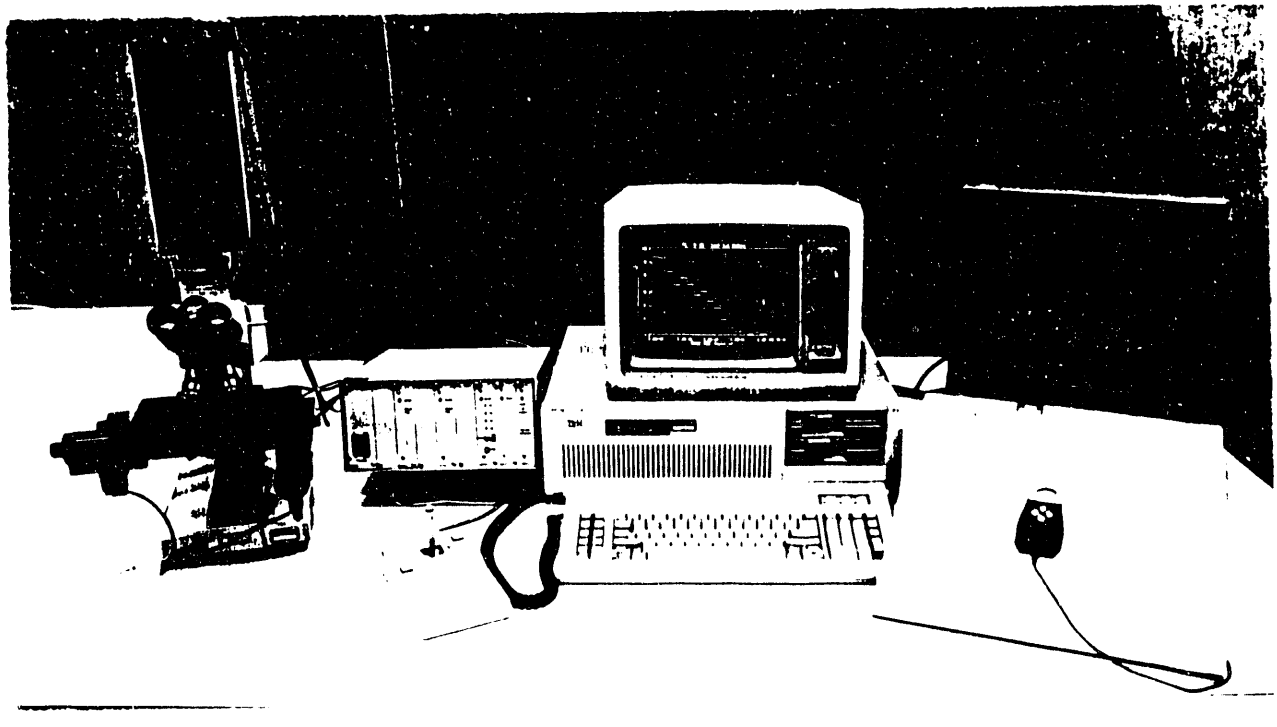

Automated track counting and size analysis equipment
(reverse image shown on TV monitor)

LLNL took a separate approach to image programming and the track size distributions. They decided to develop a program that would eventually be available to DOE laboratories (without commercial image fees) and would base sample readout on track size distribution as well as track density for each sample. As image program technology progressed, they were able to include into the program a background (of the viewing area) subtraction to remove most artifacts. The program now helps identify those samples that are beyond normal track distributions for further study.

Other Developments

The minimum energy detection of CR-39 is around 100 keV using electrochemical etching, nearly 300 keV using conventional chemical etching. In many ways the 100 keV minimum is valuable in dose assessment, especially when trying to identify the fast neutron component of a field. Sometimes, however, detection of lower energy neutrons by CR-39 is desired and can be accomplished using filters or radiators that convert in incoming neutron below the energy threshold to particles that are detectable. One such method is the use of boron in the radiator material to interact with neutrons and produce alpha particles which are detected with great efficiency by the CR-39. Studies demonstrated that boron/poly vinyl alcohol radiator was successful in creating the (n,α) interaction with CR-39 from the low and intermediate energy neutrons without interfering with the (n,p) response from high energy neutrons. Because alpha tracks tend to be larger than protron tracks, discrimination between the fast and slower neutrons can be evaluated using track size.

The high energy maximum usefulness of CR-39 has been pondered but not well defined. Although the program has not specifically addressed high energy neutron detection, a number of small studies have addressed the ability of CR-39 to detect neutron energies above 20 MeV. A maximum threshold has not been attempted, but observations show an increase in the number of large particle interactions at high energies. The use of specific radiators to moderate the neutrons should be useful in expanding the maximum range of the material.

A variation in readout has been useful by REECo at the Nevada Test Site to reduce the difficulties in track counting caused by surface defects and artifacts. They observed that the contrast provided by reflected light is useful in more accurate track counting, particularly where material or optics are less than the best in quality.

Several types of sample loading devices have been designed to move CR-39 into and out of position for readout. Some of these devices were purchased commercially and others were designed and fabricated by the track detector lab and support personnel. Some of these devices are completely programmable and require no interaction once readout sequence is programmed. Others require manual interface with the computer or readout stage to move samples into place. These devices have proved successful but could stand improvment.

Conclusions

CR-39 dosimetry remains labor intensive. Samples must be identified either through expensive laser numbering systems, bar code application, or engraving using primitive or sophisticated means. The samples are hand loaded into the etch chamber and carefully sealed to prevent leakage of the KOH etchant. Following sample removal and cleaning, they must be loaded for readout. Manual involvment beyond this point depends on the sophistication of the counting equipment. Programmable auto loading

of the samples may reduce supervision during readout as long as focusing can be satisfactorily controlled. Exact focusing is especially critical for track size analysis.

Because the process and readout of CR-39 track detectors is labor intensive, its use is usually limited to situations where neutron exposure is expected or may be received. Some facilities may choose to read out only those CR-39 detectors for samples where the TLD neutron element showed a neutron response above a certain threshold of perhaps 20 or 50 mrem.

In spite of its shortcomings, the use of CR-39 to detect fast neutrons has many advantages. Used in conjunction the TLDs and/or NTA film (for high accelerator energies), it provides superior readout of fast neutron fields in most occupational settings.

Future plans include experimenting with laser readout procedures to identify potential techniques that allow deading of CR-39 damage istes with little or no chemical processing. In an ongoing task at PNL, a track recognition program written to determine the statistical probability of an unknown exposure being from one of several standard sources or monoenergetic beams, is being prepared for translation to Pascal (LLNL's program language) to take the input from LLNL's readout program and analyze the track size distribution by the track recognition pattern program. And periodic endeavors to reduce process time and labor through changes in processing parameters will continue as new theories for such improvements are devised. All in all, CR-39 has found a useful place in dosimetry as part of a combination TLD/TED system that quantifies the portion of the overall neutron response due to fast neutrons, allowing more accurate application quality factors to calculate dose equivalent.

CR-39 PERSONNEL NEUTRON DOSIMETERS: ENHANCED SENSITIVITY VIA BORON-DOPING[a]

M. F. Koenig, J. A. Feldman[b], J .F. Johnson, and S. J. Huang

Institute of Materials Science
University of Connecticut
Storrs, CT 06269

M. A. Parkhurst

Pacific Northwest Laboratory
P.O. Box 999
Richland, WA 99352

ABSTRACT

An improved CR-39 neutron dosimeter has been designed and tested. This dosimeter has a thin (roughly 20 μm) boron-containing layer between the poly(ethylene-co-vinyl acetate) radiator and the CR-39 substrate, which increases its sensitivity to low energy (50 keV) neutrons by an order of magnitude and to thermal neutrons by nearly two orders of magnitude. This layer consists of sodium borate dispersed in a poly(vinyl alcohol) matrix. The response of the improved dosimeter was measured with monoenergetic neutron beams from thermal energies to 15 MeV, and boron contents from zero to 52 μg cm^{-2} (saturated solution). Maximum sensitivity occurs at a boron content of about 35 μg cm^{-2}, but a significant improvement in sensitivity was observed for even a boron content of 11 μg cm^{-2}. By incorporating just a small amount of boron (less than 1 μg cm^{-2}), it is possible that a dosimeter with a nearly flat response over the neutron energies tested could be achieved.

INTRODUCTION

CR-39 is a thermosetting allyl carbonate resin which is used as a solid state nuclear track detector (SSNTD), a type of personnel neutron dosimeter (Cartwright et al. 1978; Mahesh and Vij 1985). It is generally used with a 0.5 to 2 mm thick polyethylene (PE) radiator, which also helps protect the CR-39 from abrasion (Benton et al. 1981; Ipe 1984). The radiator, being rich in hydrogen, increases the sensitivity of the CR-39 substrate to medium and high energy neutron bombardment via the proton-recoil effect. After neutron exposure and subsequent removal of the radiator, the latent tracks are developed

---

(a) Accepted for publication in the HPS Journal.
(b) Current address: W.R. Grace & Co., Washington Research Center, 7379 Rte. 32, Columbia, MD 21044.

into etch pits by chemical or electrochemical etching in basic solution for several hours at temperatures between 40°C and 70°C (Mahesh and Vij 1985; Tommasino 1987).

This type of dosimeter is most useful for neutron energies between 200 keV and 20 MeV (Benton et al. 1981); its response has been calculated to be flat to within ±30% from 70 keV to 6 MeV (Cross 1986). For lower energy neutrons, other types of personnel dosimeters are often used, such as thermoluminescent dosimeters (TLDs), which are quite sensitive to thermal neutrons (Douglas and Marshall 1978; Griffith et al. 1979). Several researchers have tried to increase the sensitivity of the CR-39 dosimeter to low energy neutrons by the incorporation of boron into the radiator (Oda et al. 1987; Matiullah and Durrani 1988), or the CR-39 substrate (Tsuruta and Juto 1984; Harvey and Weeks 1986). Boron is an obvious choice due to its high cross section for thermal and low-energy neutrons (3837 barns cm^{-2}). Boron interacts with neutrons mainly by the $^{10}B(n,\alpha)^{7}Li$ reaction (Condon and Odishaw 1967).

This paper describes a new approach to the incorporation of boron into the CR-39 dosimeter. The new dosimeter design places a thin (about 20 μm) layer of sodium borate ($Na_2B_4O_7$) dispersed in a poly(vinyl alcohol) (PVA) matrix between the polyethylene radiator and the CR-39 substrate. This design is important for two reasons. First, the alpha particles generated by the $^{10}B(n,\alpha)^{7}Li$ interaction have a shorter mean free path than the recoil protons from the PE radiator, and are therefore placed closer to the CR-39 surface. Secondly, since the boron-containing layer is thin, it should not significantly attenuate the flux of recoil protons from the PE radiator. Therefore, both radiator layers should act independently, and the CR-39 substrate should see the combined effect of the two radiator layers. This new dosimeter design was tested by neutron irradiation over energies ranging from thermal to 15 MeV. The optimum boron content was also determined for maximum sensitivity to low energy neutrons.

DOSIMETER FABRICATION PROCEDURES

A schematic drawing of the improved CR-39 dosimeter is shown in Figure 1. The poly(vinyl alcohol)/borate layer (labelled B in the figure) was the only part of the dosimeter which was varied. Determining the optimum concentration of boron in this layer was the goal of this work.

Poly(ethylene-co-vinyl acetate) film

This film is the outermost layer of the dosimeter (layer A in Figure 1). It was made from a poly(ethylene-vinyl acetate) copolymer from DuPont[a], 82/18 mole percent of ethylene/vinyl acetate, M_w = 40,000 g $mole^{-1}$ (melt index = 55,000). It was received in pellet form and used as received. A Teflon®[b] mold was used to press the polymer into films. This mold consisted of three 230 x 230 x 0.25 mm (9 x 9 x 0.010 inch) Teflon® sheets stacked together, the center sheet having a 18 mm x 18 mm

---

(a) Elvax, grade 410, from E.I. duPont de Nemours & Co., 1007 Market St., Wilmington, DE 19898.

(b) Teflon is a registered trademark of E.I. duPont de Nemours & Co.

(7 x 7 inch) square section removed from the middle to provide room for the copolymer film to be pressed. No release agent was used during this process. About 9.5 g of copolymer pellets were placed in the center of the mold and the assembly then heated to 150°C under about 2.8 MPa (400 psi) pressure. Upon melting of the copolymer, a pressure of 17.2 MPa (2500 psi) was applied for 5 minutes, after which the copolymer was cooled under pressure to about 50°C. Cooling took roughly five minutes for these films. Nearly sixty dosimeter radiators could be made from one copolymer film since each dosimeter has dimensions of 30 x 15 x 0.76 mm (1.2 x 0.6 x 0.03 inches). A separate film was pressed for each different boron concentration that was used.

Poly(vinyl alcohol)/borate layer

This film, labelled B in Figure 1, was made by roll-coating the boron-containing solutions upon the pressed poly(ethylene-co-vinyl acetate) films discussed above (layer A), with subsequent evaporation of the solvent. A separate pressed film was used as a substrate for each different boron concentration.

To simplify the preparation of the boron-containing solutions, two other solutions were first prepared. A stock solution was made by dissolving 12.5009 g $\pm$ 0.0002 g of PVA in 250 ml of distilled water in a volumetric flask. The PVA used was a poly(vinyl alcohol-co-vinyl acetate), 75% hydrolyzed, M_w = 3000 g mole^{-1}, obtained from Polysciences.[a] This solution was somewhat viscous, but its concentration of 50 g l^{-1} PVA is well below the critical concentration to gel (100 g l^{-1}) for this polymer at room temperature. A saturated solution was made by mixing 125 ml of the stock solution with about 10 g of sodium borate ($Na_2B_4O_7$, anhydrous, 99% purity, obtained from Aldrich[b]). The solution was then placed in an oven set at 46°C for 12 hours to aid dissolution of the sodium borate. Excess sodium borate still remained in the bottom of the flask (roughly 2 g). The solution was then allowed to cool for 12 hours to reach room temperature (26°C).

Boron-containing solutions of various concentrations were then made by diluting the saturated solution with the stock solution. To make the boron-containing layers, the pressed films were placed on the backs of non-stick coated baking pans, and 64 μm (2.5 mils) thick adhesive tape was placed around the perimeter of the pressed films to secure them to the pans and to determine the thickness of the surface coverage. Approximately 3 ml of solution was then placed on the pressed film, and a straight glass rod was then rolled across the entire film to remove the excess solution. This left a surface coverage of boron-containing solution, which was then placed in an oven for one week to dry at 40°C. The final layer thickness after drying was estimated to be about 20 μm.

Poly(vinyl acetate) layer

This film, labelled C in Figure 1, was placed on the surface to make a tacky layer for better adhesion to the CR-39 dosimeter. Approximately 1.4 g of a low molecular weight poly(vinyl acetate) (PVAc) obtained from Aldrich was placed in 50 ml of dioxane. The same procedure as was used to make

---

(a) Polysciences, Inc., 400 Valley Rd., Warrington, PA 18976.
(b) Aldrich Chemical Company, Inc., 1001 West Saint Paul Avenue, Milwaukee, WI 53233.

the boron-containing layer was then followed in making this layer from the PVAc/dioxane solution. The films were placed back in the ovens to dry at 40°C for 3 days. The resulting film thickness was estimated to be 20 μm. It was later found that 2 or 3 times this amount of PVAc in dioxane (0.1 g ml^{-1}) would have performed better as an adhesive layer.

Replacement of the radiators on the CR-39 dosimeters

The polyethylene-coated CR-39 used in this study was manufactured by American Acrylics[a] and laser cut into smaller samples at Applied Fusion.[b] Each sample measured 30 x 15 x 0.76 mm (1.2 x 0.6 x 0.03 inches). These samples were labelled with a scribe to denote the boron concentration and batch number. The PE radiator was then removed from the CR-39 sample and the sample placed on the boron-containing film. Equal numbers of each batch number were used. After the CR-39 samples had been placed on the boron-containing films, the samples were clamped between two glass plates using metal spring clips. The assemblies were then placed in an oven overnight at 40°C, after which the film was cut and the individual dosimeters separated.

TESTING PROCEDURES

The testing of this boron-containing dosimeter was performed in two stages. The preliminary stage (Feldman 1988) consisted of determining the performance of the dosimeter over a wide range of boron content and at several different neutron energies. The second stage consisted of finding the optimum concentration of boron for this radiator thickness and configuration, and of extending the range of neutron energies examined.

Range of boron concentrations

For the preliminary neutron exposures, concentrations of zero, 25, 50, 75, and 100 percent of saturation of borax ($Na_2B_4O_7$) in the poly(vinyl alcohol)/water solution were used. It was found that the dosimeters made using the 75% solution had the most favorable response, with the 25% solution anomalously high. In light of these results, it was decided to use six different concentrations, namely zero, 25, 60, 70, 80, and 90 percent of saturation, to better define the shape of the response curve in the vicinity of the expected maximum near 75%. The zero percent solution was made in the same manner as the boron-containing specimens, merely omitting boron, to serve as an internal calibration standard.

Neutron exposures

The boron-containing dosimeters were all irradiated at the Battelle Pacific Northwest Laboratories' Van de Graaff Accelerator Facility. The first set of dosimeters were exposed to neutron energies of < 0.1 keV (thermal), 30 keV, 60 keV, and 120 keV. Four samples of each boron concentration were

---

(a) American Acrylics and Plastics, Inc., 300 Benton Street, Stratford, CT 06497.
(b) Applied Fusion, 1915 Republic, San Leandro, CA 94577.

irradiated. The second set of dosimeters were exposed to neutron energies of 50 keV, 75 keV, 100 keV, 150 keV, 500 keV, 1 MeV and 15 MeV. Two samples of each boron concentration were irradiated. Exposures of 150 to 200 mrem were used for both sets of dosimeters. The dosimeters were placed in four stacks of six within a circle of 6 cm diameter for these exposures. The arrangement of the dosimeters was varied in each stack to try to minimize any dependence on sample position.

Electrochemical etching was used to develop the tracks (i.e., etch pits) in the CR-39 after neutron exposure. This etching was performed at Battelle Pacific Northwest Laboratories. The dosimeters and a 6.25 N KOH solution were warmed separately overnight to 60°C. The electrochemical etching was carried out at 60°C in two cycles: Five hours at an AC voltage and frequency of 2500 V and 60 Hz followed by 23 minutes at 2500 V and 2000 Hz. The dosimeters were rinsed in acetic acid and then in distilled water to remove any KOH residue.

Analysis of the track density and track size distributions were performed at the University of Connecticut using a Cambridge[a] Quantimet 900 Image Analysis System for the first set of dosimeters and for selected dosimeters from the second set of exposures. A NIKON[b] BIOPHOT microscope equipped with a motorized stage was used in transmission mode at 100 X magnification. A total of 32 fields were averaged for the track measurements on each dosimeter, which covered an area of approximately 30 mm^2. Image analysis of the second set of dosimeters was performed at Battelle using similar conditions. Track size distributions of selected dosimeters from the second set were also analyzed at the University of Connecticut.

Quantification of the boron content

The absolute amount of the boron in the dosimeters was expected to be small because of the thinness of the boron-containing layer (about 20 μm). This made quantitative analysis with spectroscopic techniques such as Infrared Spectroscopy difficult because of the weak signal detected from such small amounts of boron. For these reasons, it was decided to quantify the amount of boron present in the solutions used to make the boron-containing layer of the dosimeters, and to then calculate the amount of boron in the dosimeters. This was accomplished by the following method. The boron-containing solutions were placed in a water bath set to 26°C and equilibrated. Four milliliters of each solution were then removed with a volumetric pipet, placed into pre-weighed polystyrene evaporation dishes, and dried in a vacuum oven set to 40°C. The vacuum oven was evacuated using a rotary pump with ultimate pressure of about 0.1 Pa (1 x 10^{-3} Torr). The residues were then weighed to $\pm$0.0001 g on a Cahn[c] model 10141 laboratory balance. Two repetitions were performed: one group was dried for 36 hours and a second group for three weeks.

(a) Cambridge Instruments Ltd., Restat Road, Cambridge CB1 3QH England.
(b) Nikon, Inc., Instrument Division, 623 Stewart Ave., Garden City, NY 11530.
(c) Cahn Instruments, Inc., 16207 S. Carmenita Rd., Cerritos, CA 90701.

Thermogravimetric analysis was performed on a few of the residue samples to determine the percentage water remaining after the vacuum drying using a DuPont system.[a] Approximately 35 to 50 mg of material was used for each analysis, and the sample oven was purged with nitrogen gas. The temperature reading was calibrated using Curie points of alumel (163°C) and nickel (354°C). A heating rate of 10°C min^{-1} was used to heat the samples from 50°C to 400°C, with isothermal pauses of 15 minutes duration at 120°C, 180°C, and 350°C. An isothermal pause of 25 minutes at 120°C was used for the two sodium borate samples obtained from solution. This heating schedule was chosen after consulting the Merck Index (Windholz et al. 1976), which gave the chemical formula for hydrated sodium borate as $Na_2B_4O_7 \cdot 10\ H_2O$ and stated that 5 moles of water are lost at 100°C, 9 moles of water at 150°C, and it becomes anhydrous at 320°C. Therefore, the ratio of 5:4:1 moles of water lost at each temperature is expected for the fully hydrated material.

RESULTS AND DISCUSSION

Dosimeter response

Photomicrographs and track-size distributions for dosimeters with boron-doped and standard PE radiators are shown in Figures 2 through 7. These results were obtained with the Quantimet 900 system at the University of Connecticut, after neutron irradiation and electrochemical etching of the dosimeters. Figure 2 shows photomicrographs of two specimens after 100 keV neutron irradiation. It is evident that there are both large and small etch pits on both specimens, but there are more etch pits on the boron-doped specimen, and also more large etch pits. From Figure 3, which shows the size distribution of etch pits on each of these two specimens, it can be seen that the specimen with only a PE radiator has a large maximum at a track diameter of about 10 μm. The specimen with a boron-doped radiator has the same maximum at 10 μm with about the same intensity as the PE sample, but superimposed over this track size distribution is another distribution with a maximum just above 80 μm. From these graphs, we can assign the small track size distribution as being due to the recoil protons from the PE radiator and the large track size distribution to the alpha particles from the $^{10}B(n,\alpha)^7Li$ nuclear reaction. Also, since the small track size distributions on both samples have comparable intensities, most of the increased sensitivity of the boron-containing dosimeter is due to the $^{10}B(n,\alpha)^7Li$ reaction. Furthermore, it can be concluded that the boron-containing layer is thin enough to prevent attenuation of the recoil protons from the PE/PVAc layer above it. Therefore, both of these layers work independently, so there are essentially two radiator layers. At 50 keV, Figure 4 shows much higher sensitivity for the boron-containing dosimeter, and many large etch pits. The etch pit size distributions in Figure 5 again show two size distributions for the boron-containing dosimeter and only one for the PE. The y-axis scales show about an order of magnitude higher sensitivity for the boron-containing specimen, again due to the alpha particles from the $^{10}B(n,\alpha)^7Li$ reaction. Figures 6 and 7 show comparable responses for both dosimeters at 15 MeV.

(a) TGA model 951, E.I. duPont de Nemours & Co.

Track-size distributions for thermal neutron bombardment from the first set of dosimeters shows the same trends. Two sets of distributions were seen, one between 10 and 40 μm and the other between 50 and 80 μm. The relative intensities of these two distributions differ by about two orders of magnitude, as reflected in Table 1.

A summary of the results from the first set of neutron exposures for the boron-containing dosimeters are shown in Table 1. In this table, the response of the dosimeter is given by the number of tracks (i.e., etch pits) per square centimeter per mrem and the boron concentration given as the percent of saturation, with a saturated borax ($Na_2B_4O_7$)/PVA solution equal to 100%. These numbers have been corrected for an average background count of 70 tracks cm^{-2}. From this table it can be seen that the 0% boron dosimeter has a consistently higher response than the standard polyethylene dosimeter. This is because the radiator thickness used for the boron dosimeters is about twice as thick as that of the PE dosimeter. It has been shown (Ipe 1984) that the (n,p) response increases with increasing PE radiator thickness up to a thickness of about 4.5 mm. Also evident from this table is the well-known decrease in sensitivity for the PE radiator below 100 keV (Benton et al. 1981; Cross 1986). The data in Table 1 also show several other trends with variation in neutron energy. Compared to the 0% boron dosimeters, the boron-containing dosimeters show a two-fold increase in sensitivity at 120 keV, an order of magnitude increase at 30 keV and 60 keV, and about a forty-fold increase at thermal energies. This corresponds to even larger increases over the PE dosimeter due to the combined influences of the boron content and thicker poly(ethylene-co-vinyl acetate) radiator. Furthermore, another factor of five increase in sensitivity should be possible by using sodium borate that has been enriched in the ^{10}B isotope.

The results of the neutron irradiations for the second set of boron-doped dosimeters are shown in Table 2. These values are calculated as the number of tracks $cm^{-2} \cdot mrem^{-1}$, and are corrected for a background of 35 tracks cm^{-2}. This data is shown graphically in Figure 8, with the response of the dosimeters plotted as a function of neutron energy. The same general conclusions obtained from the first set of exposures, listed in Table 1, are also reflected in this data set. From this data, a 3 X gain in sensitivity is seen at 150 keV and an order of magnitude gain at 50 keV over the PE radiator. Also evident is the decline in sensitivity of the PE radiator dosimeter below about 100 keV.

Quantification of the boron content

As was described on the Testing Procedures section, 4 ml portions of the boron-containing solutions were dried and weighed to determine the actual amount of PVA and boron in the dosimeters. Two separate determinations were made. The solutions were left in the vacuum oven for times of 36 hours and 3 weeks, with similar results. The results of these two determinations of the residue weights and concentrations of sodium borate are shown in Tables 3 and 4.

To calculate the correct weight of sodium borate in the residues, it was necessary first to determine the amount of residual water left after this vacuum treatment. Since the weights of the residues from the zero percent boron solution (which contained only PVA) were within 1% to 2% of the expected weights, it was evident that any residual water was absorbed by the sodium borate. Therefore, a saturated solution of sodium borate in water was made and 4 ml samples of this solution were dried in

the vacuum oven and weighed. One sample was weighed after 3 days and again after 2 weeks; the difference between these two weighings was only 0.4%, so the conditions appear stable over this length of time and the sample appears to have reached equilibrium. Another sample was placed with the second set of residue samples (results are given in Table 4), so this sample was dried under exactly the same conditions as the second set of residue samples. Thermogravimetric analysis (TGA) was performed on each of these two sodium borate samples to determine the percentage water remaining; also analyzed was a sodium borate sample from the starting material (as received from Aldrich). As mentioned previously, the ratio of moles of water lost at each isothermal pause in the TGA thermog was expected to be 5:4:1 for the fully hydrated material. The measured ratios were much less than expected for all three samples, but water was still lost at each of the temperatures. Thus the water content and distribution within the solid sodium borate are difficult to predict, and are best determined experimentally for the particular conditions used. The total water content for these samples was measured to be 1.2%, 15.5%, and 20.1% for the as received, dried two weeks, and dried three weeks sodium borate samples. Therefore, the starting material was nearly anhydrous, the water content of the second set of samples (Table 4) was 20.1%, and the value for the first set of samples was taken as the average between these two determinations, namely 17.8%.

Using these corrections, the concentration of sodium borate ($Na_2B_4O_7$) in the boron-containing solutions was calculated as shown in Tables 3 and 4. If each of these concentrations is used to calculate the concentration of the original saturated PVA/sodium borate solution, all of the values fall between 36 and 39.5 g l^{-1} except for the 25% solution. Therefore, averaging these values (omitting the 25% solution) gives a concentration of 37.7 $\pm$ 1.3 g l^{-1} of $Na_2B_4O_7$ for the saturated solution, whereas the 25% solution contains slightly less sodium borate than expected, probably due to error in measuring when the 25% solution was made. The best estimates of the concentration of sodium borate in each of the boron-containing solutions is shown in Table 5. Using these concentrations and the thickness of the liquid roll-coated films (2.5 mils = 0.00635 cm thick), the amounts of sodium borate and of boron per square centimeter in the films have been calculated in Table 5. These values of course assume a homogeneous distribution of sodium borate in the film, which is valid only for the low boron concentrations (25% solution). The other films showed heterogeneity in the dried residue, with some sodium borate crystallizing separately from the PVA, evident as a white powder.

The main disadvantage in using this method of measuring the boron content is that the borate complexed with the poly(vinyl alcohol) is not differentiable from the borate dissolved in the water and not complexed. However, since neutron interaction can be viewed as primarily an atomic event to a first approximation, complexation should not have a significant effect on the sensitivity of the dosimeter, but should only help to disperse the borate and help to make a more uniform distribution of borate throughout the film.

Optimum boron content

From Figure 9 and Table 2, it can be seen that the optimum boron content is at about 70% of saturation, which is a boron content of about 35 μg cm^{-2}, as determined from the data in Table 5. Similarly, the data from Table 1 shows that 75% boron content gave consistently high sensitivity.

Two other conclusions can also be made by referring to the data in Tables 1 and 2. At boron contents above 70%, the sensitivity of the dosimeter decreases. This is probably due to a "shielding" effect of the boron, i.e. absorption of protons and alpha particles such that the flux of charged particles to the CR-39 surface is decreased. This means that the boron-containing layer should be kept thin and that good contact with the CR-39 surface is important because of the short penetration depth of the alpha particles. At boron contents below 70%, the sensitivity falls off, but even at 25% of saturation the sensitivity is much increased over the PE radiator. Since the boron-containing solutions above 50% of saturation gave residues that were two phase when the solutions were dried in the evaporation dishes, which would lead to streaking and possibly an inhomogeneous distribution of boron throughout the PVA/borate layer, it would seem that a boron content of 25 to 50% of saturation would give more consistent results for use with the dosimeters. Using a 25% boron content would also be more economical for the manufacturers than 70%.

Since the standard PE radiator dosimeters fall off in sensitivity below about 100 keV, while boron-containing dosimeters increase in sensitivity at low neutron energies, it might also be possible to manufacture a boron-containing dosimeter which would have a flat response (constant sensitivity) over the entire energy range from thermal energies to 15 MeV. This could be accomplished by incorporating just a small amount of boron (0.1 to 2% of saturation, 0.05 to 1.0 $\mu g\ cm^{-2}$) in the boron layer, which would just compensate the decline in sensitivity of the PE radiator. This could be very useful for two reasons: (a) the limited dose range of the CR-39 dosimeter, which decreases as the sensitivity increases, and (b) the dosimeter then becomes direct reading, i.e. one track equals a given number of neutrons, independent of energy. The difference in track sizes between the recoil protons and alpha particles would still give an indication of neutron energy distribution, or an "average energy" depending on the large track/small track ratio.

CONCLUSIONS

These experiments show that the addition of boron to the dosimeter in a thin enriched layer between the PE radiator and the CR-39 substrate increases the sensitivity of the CR-39 dosimeter. With this design, the alpha particles from the $^{10}B(n,\alpha)^{7}Li$ reaction and the recoil protons from the PE layer can both reach the surface of the CR-39 to create damaged areas resulting in a dosimeter with essentially two independent radiators. The relative contributions from the two radiator layers can be determined due to the difference in track sizes between the alpha particles (70 to 80 μm diameter) and the recoil protons (10-μm diameter). Maximum sensitivity was reached at about 70% of saturation (35 to 40 $\mu g\ cm^{-2}$ of boron), although even 25% (10 $\mu g\ cm^{-2}$) gave greatly improved sensitivity. These boron-containing dosimeters gave an order of magnitude increase in sensitivity below 100 keV, and two orders of magnitude increase at thermal energies. Another factor of five increase in sensitivity is expected for dosimeters made using sodium borate that is enriched in ^{10}B. Too high a boron content or too thick a layer decreases sensitivity of the dosimeters, apparently due to a shielding of the CR-39 substrate by the boron. A dosimeter which contains only a small amount of boron (0.1 to 2%) would give a fairly constant sensitivity over the entire neutron energy range from thermal to 15 MeV, by just compensating for the decrease in sensitivity of the proton recoil effect in the PE layer at low neutron energies. Perhaps a high-sensitivity boron-doped dosimeter and a flat response boron-doped dosimeter could be used in

tandem to measure neutron exposure. This would be advantageous because both dosimeters could be processed under the same conditions and both would give a permanent record of the exposure.

Acknowledgment -- This work was performed under contract DE-AC06-76RLO-1830 for the U.S. Department of Energy.

REFERENCES

Benton, E. V., R. A. Oswald, A. L. Frank, and R. V. Wheeler. 1981. Proton-Recoil Neutron Dosimeter for Personnel Monitoring. *Health Phys.* 40:801-809.

Cartwright, B. G., E. K. Shirk, and P. B. Price. 1978. A Nuclear-Track-Recording Polymer of Unique Sensitivity and Resolution. *Nucl. Instr. Meth.* 153:457-460.

Condon, E. U. and H. Odishaw. 1967. *Handbook of Physics*, 2nd edition. McGraw-Hill, New York.

Cross, W. G. 1986. Characteristics of Track Detectors for Personnel Neutron Dosimetry. *Nucl. Tracks* 12:533-542.

Douglas, J. A. and M. Marshall. 1978. The Responses of Some TL Albedo Neutron Dosimeters. *Health Phys.* 35:315-324.

Feldman, J. A. 1988. Polymer Network Formation and Behavior. Ph.D. dissertation, University of Connecticut.

Griffith, R. V., D. E. Hankins, R. B. Gammage, L. Tommasino, and R. V. Wheeler, R. V. 1979. Recent Developments in Personnel Neutron Dosimeters- A Review. *Health Phys.* 36:235-260.

Harvey, J. R. and A. R. Weeks. 1986. A Neutron Dosimetry System Based on the Chemical Etch of CR39. *Nucl. Tracks* 12:629-632.

Ipe, N. E. P. 1984. Factors Affecting Track Registration Characteristics of CR-39 Polymer When Used as a Fast Neutron Detector. Ph.D. dissertation, Purdue University.

Mahesh, K. and D. R. Vij. 1985. Techniques of Radiation Dosimetry. Holsted Press, New Delhi.

Matiullah, and S. A. Durrani. 1988. A Mathematical Model for Thermal-Neutron Dosimetry Using Electrochemically Etched CR-39 Detectors with (n,p) and (n,a) Converters. *Nucl. Tracks Radiat. Meas.* 15:511-514.

Oda, K., M. Michijima, and H. Miyake. 1987. CR39-BN Detector for Thermal-Neutron Dosimetry. *J. Nucl. Sci. Technol.* 24:129-134.

Tommasino, L. 1987. Recent Trends in Radioprotection Dosimetry: Promising Solutions for Personal Neutron Dosimetry. *Nucl. Instr. Meth.* A255:293-297.

Tsuruta, T. and N. Juto. 1984. Neutron Dosimetry with Boron-Doped CR-39 Plastic. *J. Nucl. Sci. Technol.* 21:871-876.

Windholz, M., S. Budavari, L. Y. Stroumtsos, and M. N. Fertig. 1976. *Merck Index*, 9th edition. Merck and Co., Inc., Rahway, N.J.

TABLE 1. Results from the first set of neutron exposures (Feldman 1988), showing the response of the modified dosimeter (tracks $cm^{-2} \cdot mrem^{-1}$) at several neutron energies and boron concentrations.

Boron content (% of saturation)	Neutron Energies			
	Thermal	30 keV	60 keV	120 keV
0	1.68	0.45	0.32	3.34
25	64.25	3.54	8.39	4.87
50	41.89	1.88	3.53	4.14
75	77.35	13.18	11.88	6.22
100	37.93	7.61	3.18	3.98
PE	0.34	0.19	0.15	1.82

TABLE 2. Results for the second set of neutron exposures, showing the response (tracks $cm^{-2} \cdot mrem^{-1}$) at several neutron energies and boron concentrations.

Boron content (% of sat.)	Neutron Energies						
	50 keV	75 keV	100 keV	150 keV	500 keV	1 MeV	15 MeV
0	3.4	7.4	10.0	9.2	7.9	7.3	2.4
25	10.1	15.1	18.7	17.6	9.3	8.6	2.5
60	25.4	17.2	19.0	18.7	9.8	8.2	2.6
70	42.0	20.6	20.0	21.7	11.5	10.1	2.5
80	13.5	18.9	12.7	15.3	9.5	9.8	2.3
90	18.0	26.0	28.6	14.2	10.9	8.7	2.4
PE	1.0	2.2	6.8	7.8	7.0	6.1	2.2

TABLE 3. Weights of pans, residues, and calculated concentrations of sodium borate in the boron--containing solutions; determination #1, after 36 hours in the vacuum oven.

Boron content (% of sat.)	Weight of pan (g)	Weight after drying (g)	Weight of residue (g)	Weight of $Na_2B_4O_7 \cdot nH_2O$ (g)	Weight -20.1% H_2O (g)	Conc. of $Na_2B_4O_7$ ($g\ L^{-1}$)	
						this solution	100% solution
0	1.4330	1.6278	0.1948	0	0	0	0
25	1.4244	1.6579	0.2335	0.0387	0.0309	7.7	30.4
60	1.4423	1.7478	0.3055	0.1107	0.0885	22.1	36.9
70	1.4594	1.7802	0.3208	0.1260	0.1007	25.2	36.0
80	1.4198	1.7641	0.3443	0.1495	0.1195	29.9	37.3
90	1.4354	1.7931	0.3577	0.1629	0.1302	32.6	36.2

TABLE 4. Weights of pans, residues, and calculated concentrations of sodium borate in the boron-containing solutions; determination #2, after three weeks in the vacuum oven.

Boron content (% of sat.)	Weight of pan (g)	Weight after drying (g)	Weight of residue (g)	Weight of $Na_2B_4O_7 .nH_2O$ (g)	Weight -17.8% H_2O (g)	Conc. of $Na_2B_4O_7$ ($g\ L^{-1}$) this solution	100% solution
0	1.4828	1.6802	0.1974	0	0	0	0
25	1.4563	1.6939	0.2376	0.0402	0.0330	8.3	33.0
60	1.4608	1.7729	0.3121	0.1147	0.0943	23.6	39.3
70	1.4658	1.7955	0.3297	0.1323	0.1088	27.2	38.9
80	1.4607	1.8095	0.3488	0.1514	0.1245	31.1	38.9
90	1.4650	1.8307	0.3657	0.1683	0.1383	34.6	38.4

TABLE 5. Calculated values for the concentration of $Na_2B_4O_7$ in each of the boron-containing solutions, in the films made from these solutions, and the boron content in the films.

Boron content (% of sat.)	$Na_2B_4O_7$ in solution ($g\ L^{-1}$)	$Na_2B_4O_7$ in film ($g\ cm^{-2}$) x 10^4	Boron in film ($g\ cm^{-2}$) x 10^5	($\mu g\ cm^{-2}$)[a]
0	0	0	0	0
25	8.0	0.51	1.09	11
60	22.6	1.44	3.09	31
70	26.4	1.68	3.60	36
80	30.2	1.92	4.12	41
90	33.9	2.15	4.63	46

[a]Values ± 4%

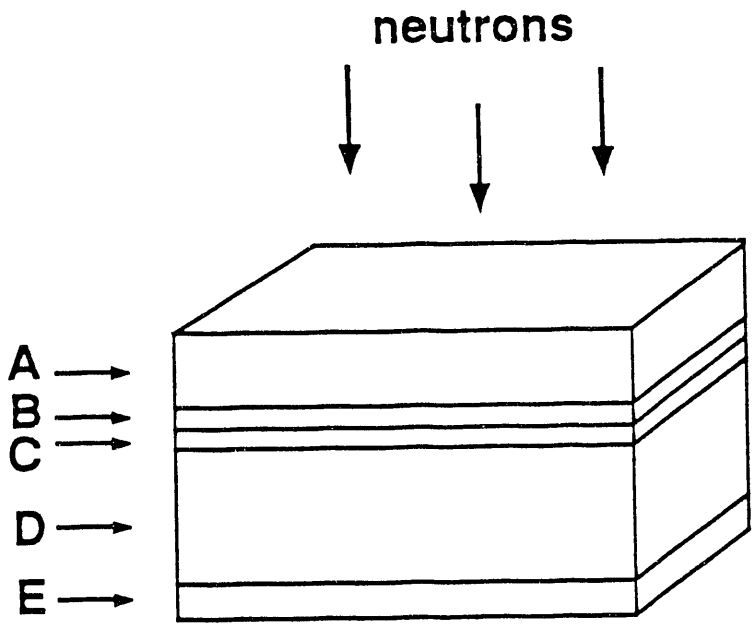

Thickness (mm)	
250	A = POLY(ETHYLENE-CO-VINYL ACETATE) PRESSED FILM
20	B = POLY(VINYL ALCOHOL) / SODIUM BORATE
20	C = POLY(VINYL ACETATE)
640	D = CR-39
130	E = POLY(ETHYLENE) / POLY(VINYL ACETATE) COEXTRUDED FILM

FIGURE 1. Schematic of the CR-39 dosimeter with a boron-doped radiator layer.

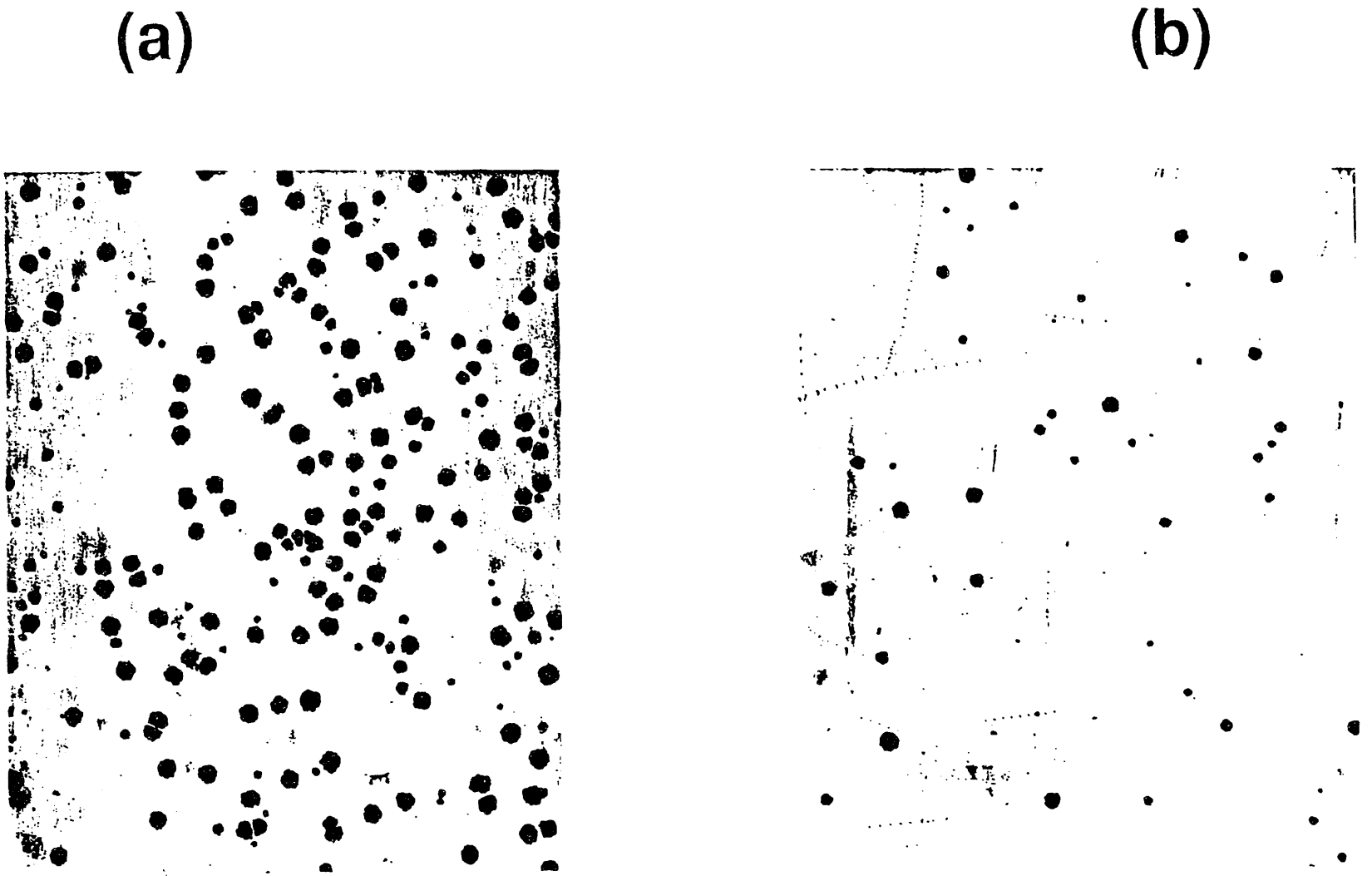

FIGURE 2. Photomicrographs of two specimens after exposure to 100 keV neutrons and electrochemical etching: (a) boron-doped radiator made from 70% solution, and (b) PE radiator.

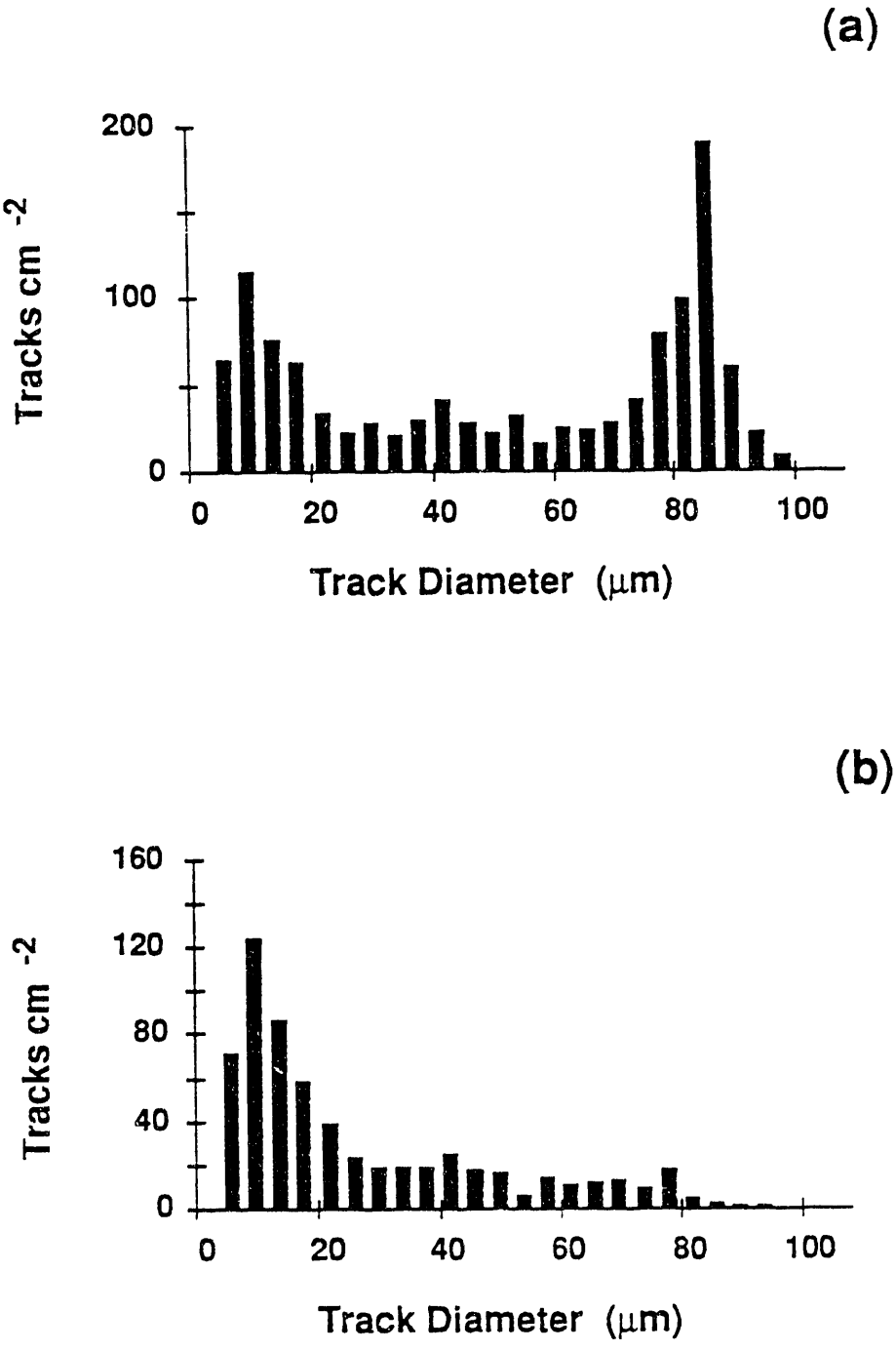

FIGURE 3. Etch pit size distributions for the two specimens in Figure 2, which were irradiated with 100 keV neutrons.

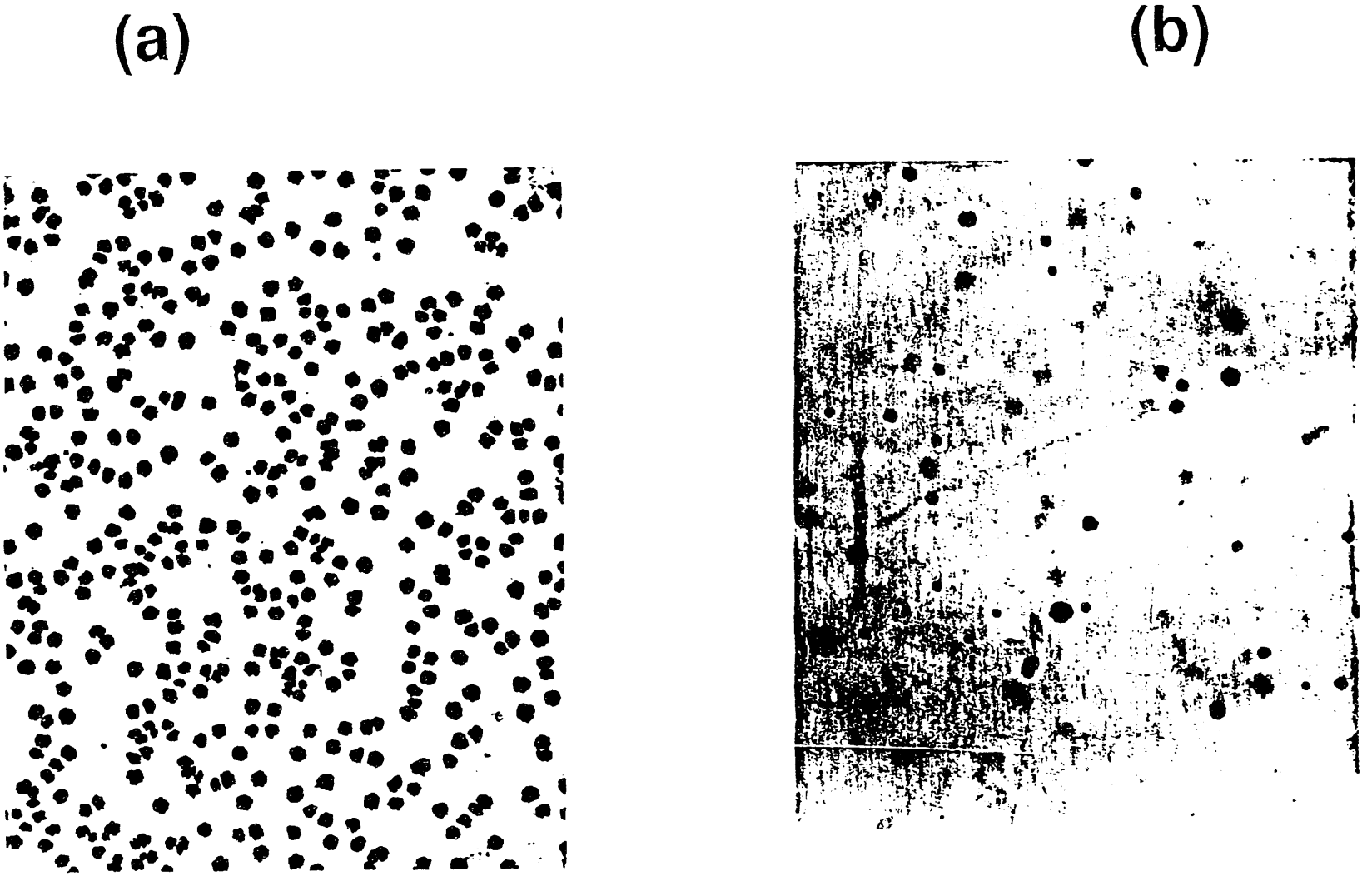

FIGURE 4. Photomicrographs of two specimens after exposure to 50 keV neutrons and electrochemical etching: (a) boron-doped radiator made from 70% solution, and (b) PE radiator.

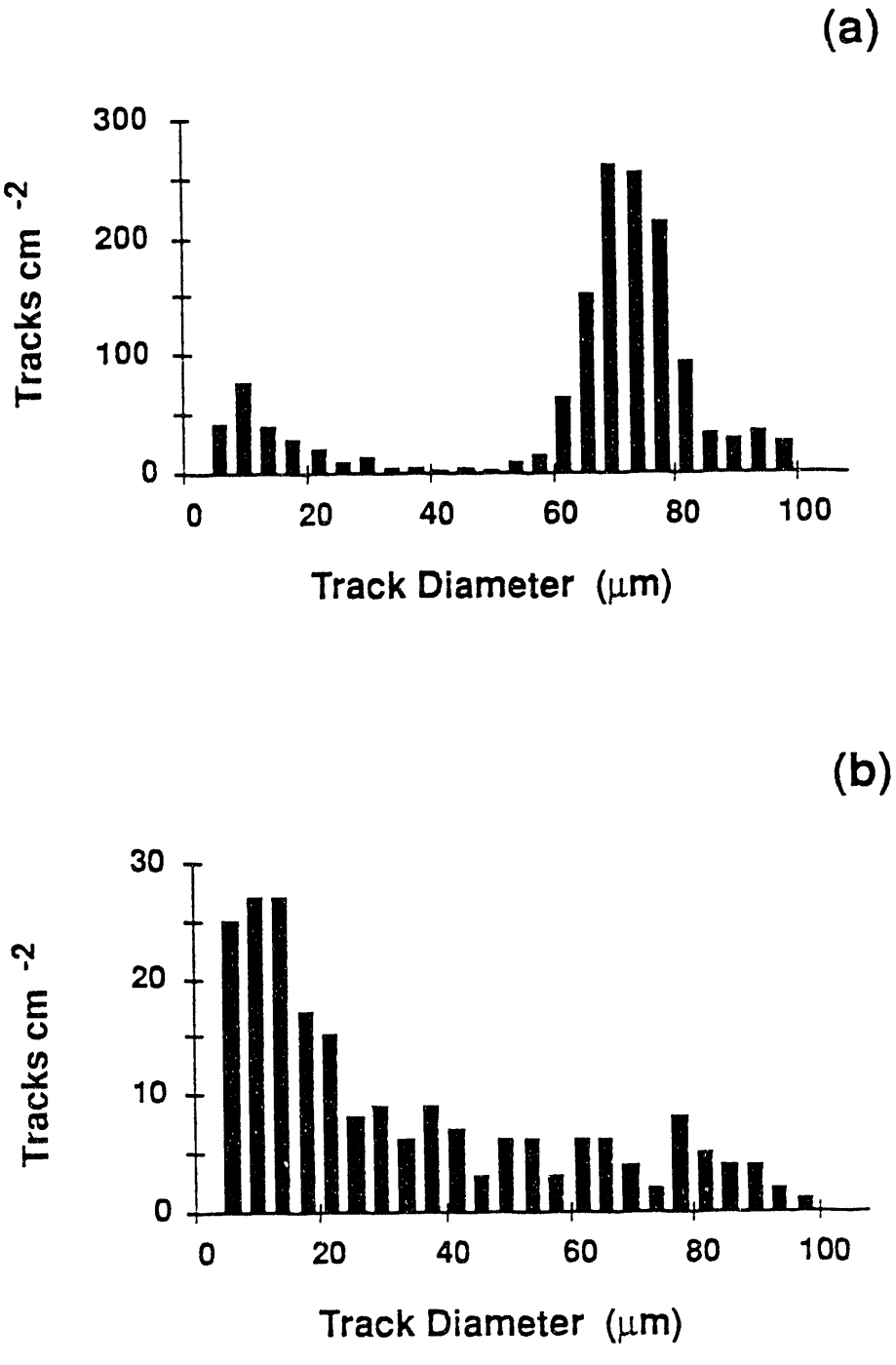

FIGURE 5. Etch pit size distributions for the two specimens in Figure 4, which were irradiated with 50 keV neutrons.

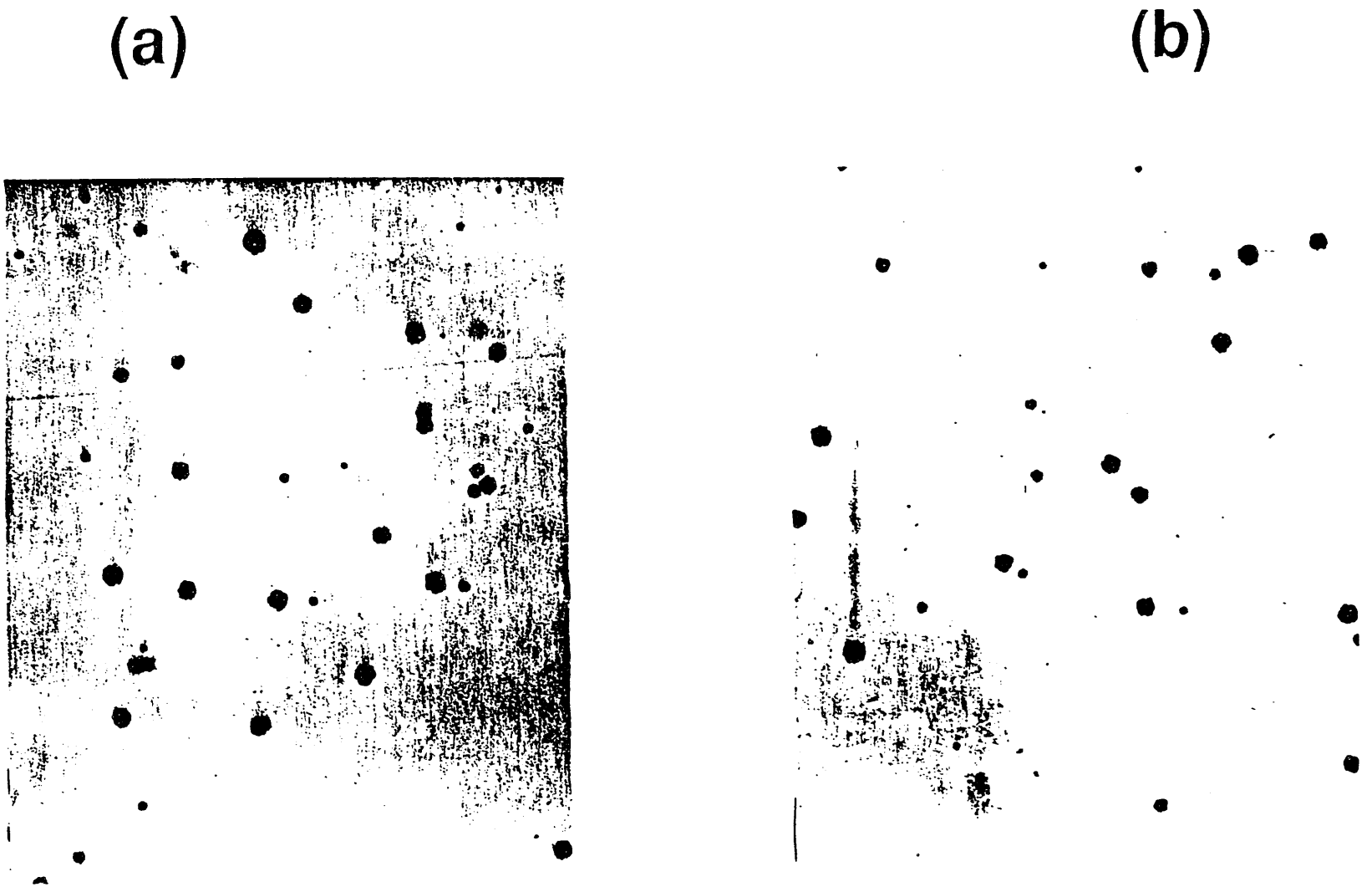

FIGURE 6. Photomicrographs of two specimens after exposure to 15 MeV neutrons and electrochemical etching: (a) boron-doped radiator made from 70% solution, and (b) PE radiator.

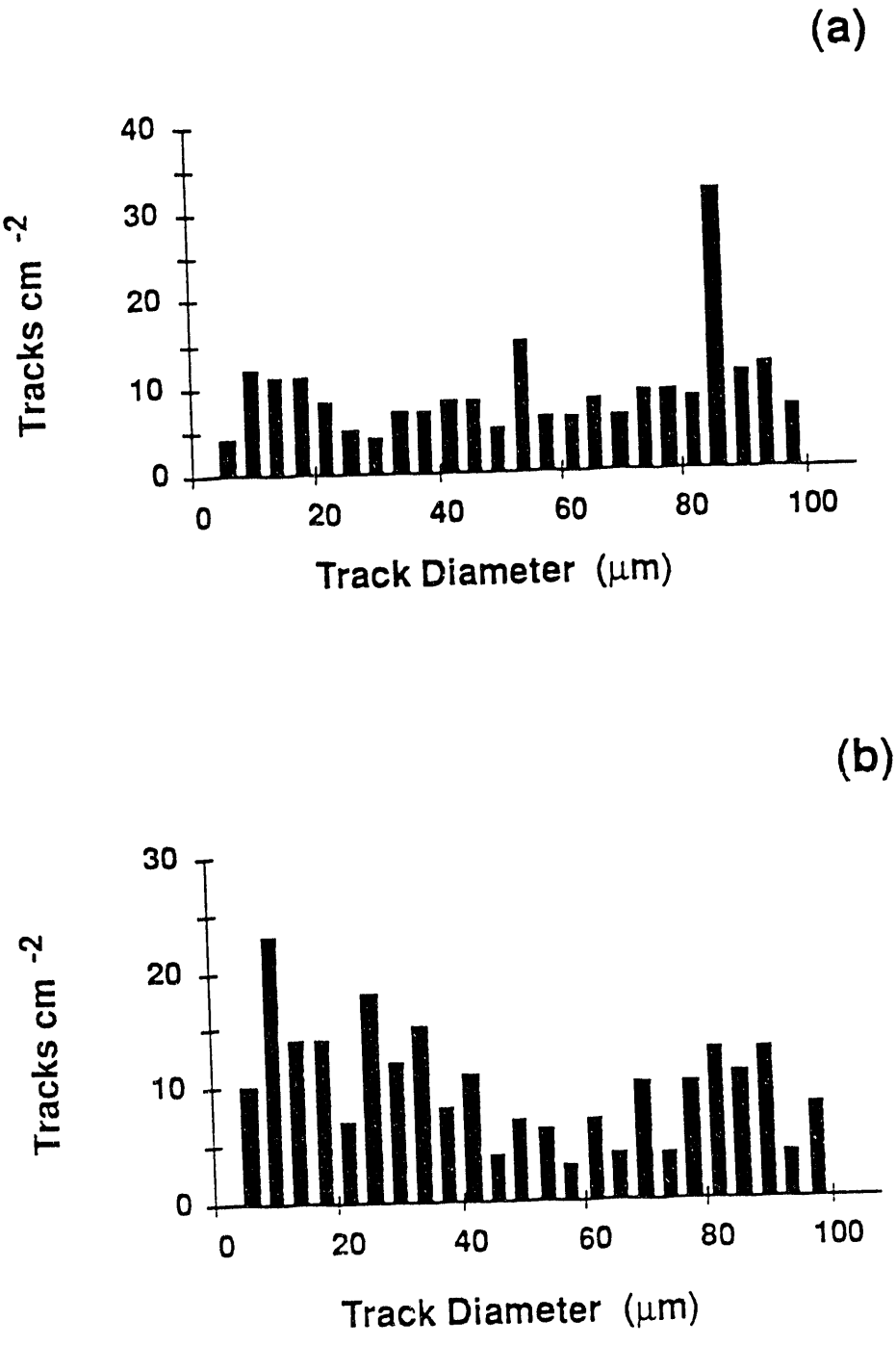

FIGURE 7. Etch pit size distributions for the two specimens in Figure 6, which were irradiated with 15 MeV neutrons.

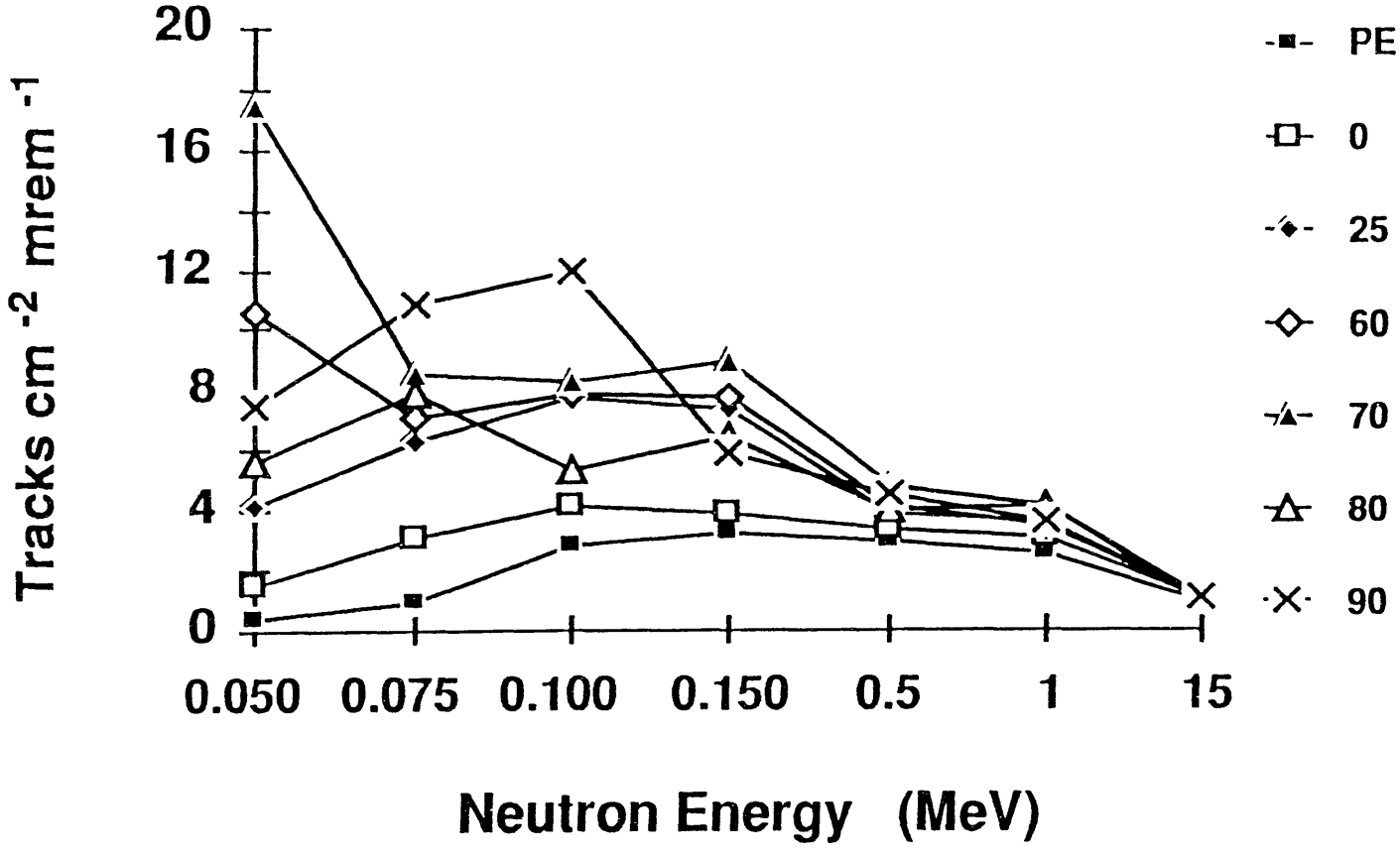

FIGURE 8. Data from Table 1, showing the variation in response of the dosimeters with neutron energy.

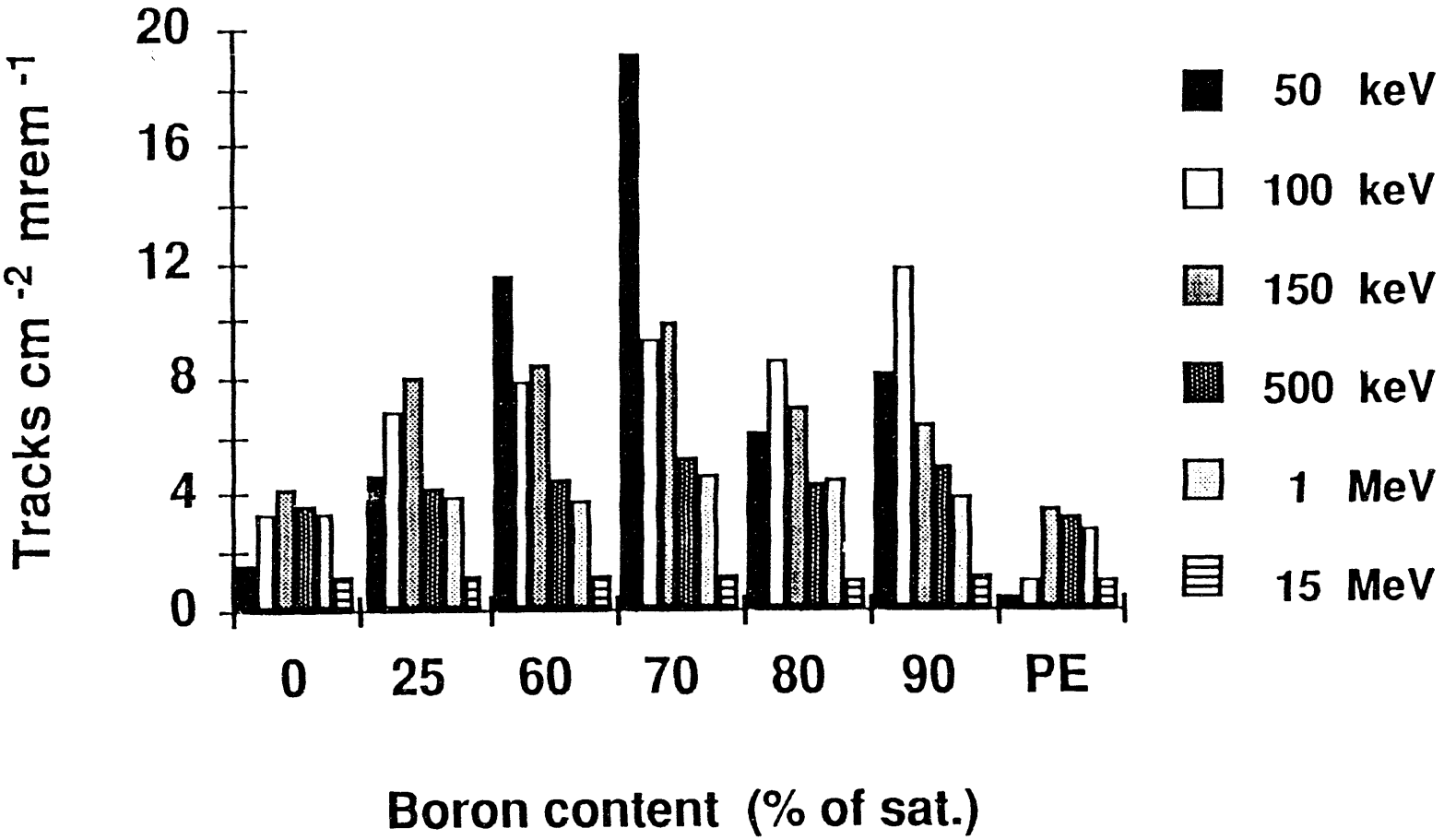

FIGURE 9. Bar graph of data from Table 2, showing the variation in response of the dosimeters with baron concentration.

NEUTRON DOSIMETRY USING OPTICALLY STIMULATED LUMINESCENCE[a]

S. D. Miller and P. A. Eschbach

Pacific Northwest Laboratory
P.O. Box 999, K3-57
Richland, WA 99352

INTRODUCTION

The addition of thermoluminescent (TL) materials within hydrogenous matrices to detect neutron-induced proton recoils for radiation dosimetry is a well-known concept. Previous attempts to implement this technique have met with limited success, primarily due to the high temperatures required for TL readout and the low melting temperatures of hydrogen-rich plastics. Research in recent years at Pacific Northwest Laboratories (PNL) has produced a new Optically Stimulated Luminescence (OSL) technique known as the Cooled Optically Stimulated Luminescence (COSL) that offers, for the first time, the capability of performing extremely sensitive radiation dosimetry at low temperatures. In addition to its extreme sensitivity, the COSL technique offers multiple readout capability, limited fading in a one-year period, and the capability of analyzing single grains within a hydrogenous matrix.

Bulk neutron detection of fine-grained COSL material within a hydrogenous matrix is incapable of adequately separating gamma and neutron dose. The technique of individual readout of fine grains within a hydrogenous matrix can separate neutron and gamma dose due to the large differences in the radiation's linear energy transfer values. Proton recoils, produced through knock-on-collisions with hydrogen, deposit nearly all of their energy within very small grains (0.1-100 microns), while gamma rays are only capable of very small energy depositions. The scintillation analog of the individual grain readout technique was demonstrated over 30 years ago and was known as the Hornyak button. Hornyak demonstrated in 1952 that neutrons and gamma rays could be separated on the basis of pulse height a using fine-grained ZnS scintillator in a plastic matrix (1). A COSL laser scanning reader, capable of analyzing the energy depositions within individual grains, based on the newly developed COSL technology, is currently under construction and will provide the capability of measuring pulse height spectra.

A number of advantages of an all solid-state plastic matrix OSL dosimeter make it worthwhile to investigate (2). The dosimeter is tissue-equivalent to neutrons, nearly angular independent due to the spherical symmetry of the active volumes, inexpensive to produce, simple to use, and of a size and shape suitable for fast neutron personnel monitoring. The data generated from the plastic matrix COSL dosimeter will resemble track-etch data, but will not require any chemical or electrochemical processing. Automation and acceptance of the technology may therefore be more easily accomplished. The simple design of the plastic-matrix COSL dosimeter will not be temperature, pressure, or humidity dependent.

(a) Work supported by the U.S. Department of Energy under Contract DE-AC06-76RLO 1830.

These properties make the plastic matrix OSL dosimeter favorable when compared with bubble technology. Additionally, COSL readout is non-destructive and therefore lends itself to application as a lifetime dosimeter as well as a dosimetry technique for pregnant female radiation workers.

ASPECTS OF COSL DOSIMETRY

The COSL readout process, diagramed in Figure 1, consists of three readout steps (3). After annealing either by conventional TL annealing (400 C° for 30 minutes) or by an optical erasure method developed at PNL (4), the dosimeters are ready for room temperature radiation exposure. After exposure at room temperature, the dosimeters are analyzed with the three-step process. First, the dosimeters are cooled (in a few seconds), to liquid nitrogen temperature (77 K). Then, secondly, the dosimeters are subjected to optical stimulation. The third step, occurring 10 seconds after the optical stimulation, is warming the dosimeter back to room temperature. As the dosimeter warms, light proportional to the radiation exposure is emitted and collected by a phototube. The entire three-step process takes well under one minute to complete.

The most sensitive COSL material is presently TL dosimeter (TLD) grade CaF_2:Mn. While CaF_2:Mn is not the only material that exhibits COSL properties, it is the material that has shown the most potential to date. An optical annealing process has been developed for CaF_2:Mn, involving room temperature ultraviolet treatment using 326-nm laser light. The development of this annealing procedure, the data of which are plotted in Figure 2, has enabled the optical annealing of fine-grained COSL material within a hydrogenous matrix at room temperature. COSL readout, as a function of 326-nm light energy, is shown in Figure 3. The most sensitive mode is achieved by illuminating the material at about 35 mJ and is also an area of the response curve that is slowly varying. Reading the COSL dosimeters in this region permits more tolerance on the amount of optical energy required. COSL dosimeters are not totally erased after one readout, unlike TLDs which lose all of their signal after the first readout. It is possible to perform multiple readout (Figure 4), in which as little as 10% of the original reading is lost. In its most sensitive mode, a loss of about 50% of the original reading is observed. The multiple readout capability could be potentially very important in a lifetime dosimeter and also for use with pregnant female radiation workers. Sensitivity of the COSL process was measured and the results are found in Figure 5. A gamma exposure of 100 micro-R is easily measurable with much lower minimum detectable amounts possible in the future. The final characteristic of importance to the plastic-matrix COSL reader was the long-term fading properties. Ten dosimeters per month were analyzed for a period of over one year to measure the COSL fading curve in CaF_2:Mn. The results of the fade study are provided in Figure 6. The solid lines represent the 95% confidence interval. A line of slope zero can be drawn within the 95% confidence interval. Therefore, the data are consistent with zero fading in one year. A linear regression of the data yielded approximately a 5% fade during the one-year test period.

COSL LASER SCANNING READER

An artist's conception of the COSL laser scanning reader is displayed in Figure 7. The readout process proceeds in the following way. The plastic matrix containing the COSL material is initially cooled to liquid nitrogen temperature. The optical excitation is carried out in one of two ways. The first technique is to excite only a small area with the excitation beam. The second technique involves exciting the entire dosimeter area with the excitation beam. Exciting only a very small area will be advantageous if a large interfering background signal needs to be reduced. The excitation of the entire dosimeter area is advantageous because the entire area can be excited at the same time. After excitation is complete, the dosimeter is translated through an intense CO_2 laser beam and readout of individual grains is accomplished. The COSL emission is recorded using the photon counting method in the multichannel scaling mode.

The physical basis for neutron and gamma discrimination is best explained by observing the way in which the two types of radiation deposit energy within small volumes. Figure 8 shows the energy deposited by a gamma ray and a proton recoil. The gamma ray energy is spread over a volume much larger than the COSL grain, while the proton recoil is capable of depositing its total energy within the grain diameter. The linear energy transfer characteristics therefore permit separation of the two types of radiation based only on the size of the pulse produced. It will be PNL's goal to demonstrate this type of data using realistic neutron and gamma sources. The initial data will be taken using a proton shooter that can deposit a large number of protons within a small area. The first data will therefore demonstrate the principle of detecting large energy depositions that are larger than will ultimately be required for the measurement of single proton events. Using these data, the reader will be refined and made more sensitive as the goal of reading individual proton recoil events is approached. The top and side views of the COSL laser scanning reader are found in Figures 9 and 10.

CONCLUSION

A new technology has been developed that is capable, in principle, of producing a new solid-state neutron dosimeter. The new dosimetry system will be all solid-state, will not require chemical processing, and will be insensitive to normal temperatures, humidities, and pressures. In addition to improving CaF_2:Mn COSL sensitivity, a number of other OSL and COSL materials are currently being examined that may provide 10 to 100 times more sensitive results. Future research will concentrate on the reading of individual grains and the measurement of pulse height spectra in order to measure fast neutrons in the presence of gamma radiation, as well as the development of better OSL/COSL techniques in existing and new materials.

REFERENCES

1. Hornyak, W. F. (1952). A Fast Neutron Detector. Rev. Sci. Inst. **23**, 264-267.

2. Miller, S. D., Stahl, K. A., Endres, G. W. R., and McDonald, J. C. (1989). Optical Annealing of CaF_2:Mn for Cooled Optically Stimulated Luminescence. Radiat. Prot. Dosim. **29**(3), 195-198.

3. Lakshmanan, A. R. (1989). Cooled Optically Stimulated Luminescence - A New Development in Thermoluminescence Dosimetry. Radiat. Prot. Dosim. **27**(2), 71-72.

4. Miller, S. D., Endres, G. W. R., McDonald, J. C., and Swinth, K. L. (1988). Cooled Optically Stimulated Luminescence in CaF_2:Mn. Radiat. Prot. Dosim. **25**(3), 201-206.

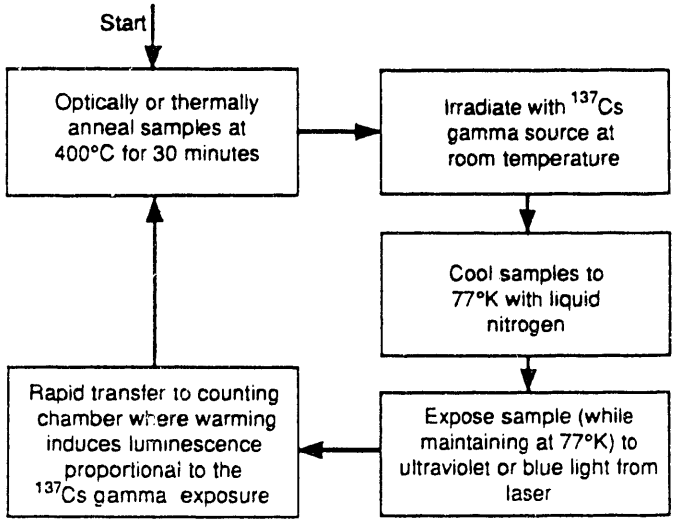

Step-by-Step COSL Readout Procedure

S9105080.3R

FIGURE 1. The readout procedure used to interrogate dosimeters with the COSL process.

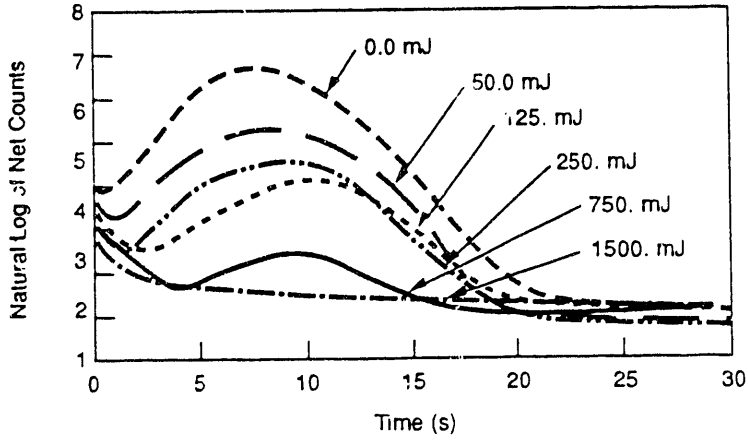

10-mR CaF_2 :Mn COSL Readouts versus 326-nm Laser Annealing

S9105080.17r

FIGURE 2. Optical annealing of the COSL response with increasing exposure to 326-nm ultraviolet light.

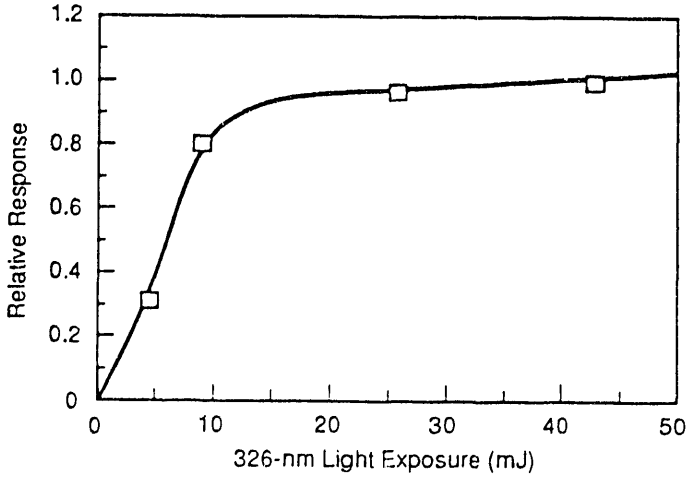

FIGURE 3. COSL response as a function of 326-nm ultraviolet laser exposure.

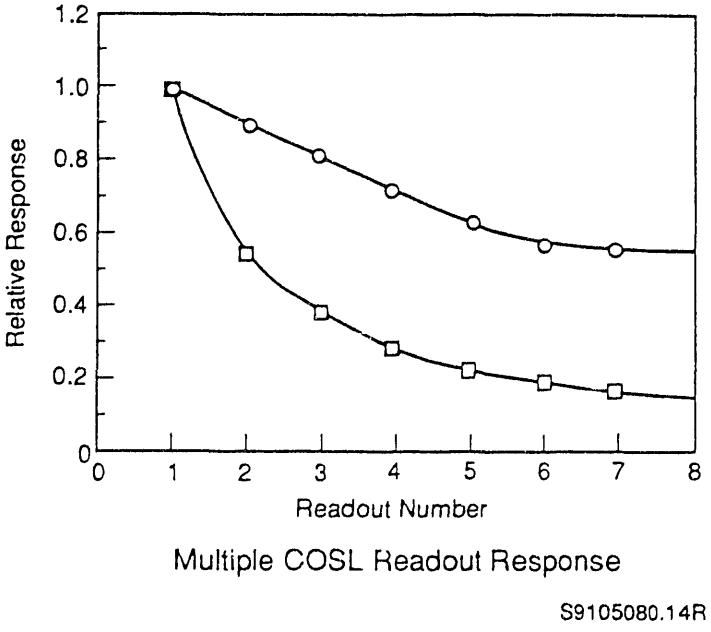

FIGURE 4. Individual dosimeters were interrogated multiple times. The data represented with the squares were acquired at the optimum laser exposure (most sensitive). The data represented with the circles were acquired at a sub-optimal laser exposure (less sensitive). The sub-optimal readout does not diminish the signal as rapidly.

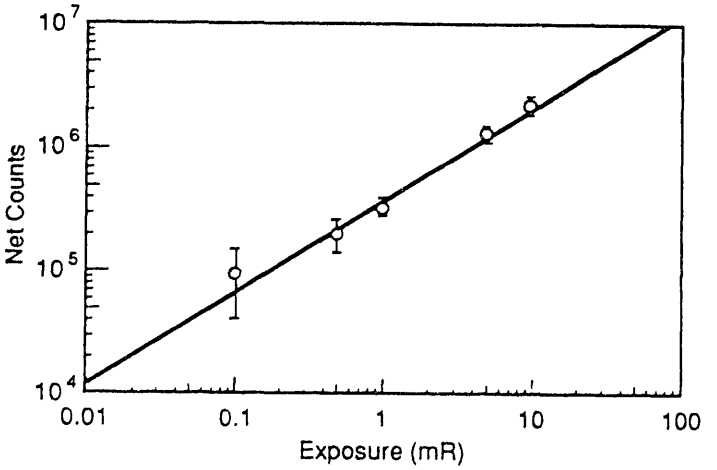

FIGURE 5. Net COSL counts from CaF_2:Mn dosimeters exposed to various exposure levels from gamma radiation. The line is a least squares fit to the data. Five data points were averaged to arrive at each point on the graph, the error bars represent the standard deveiation of each particular data set.

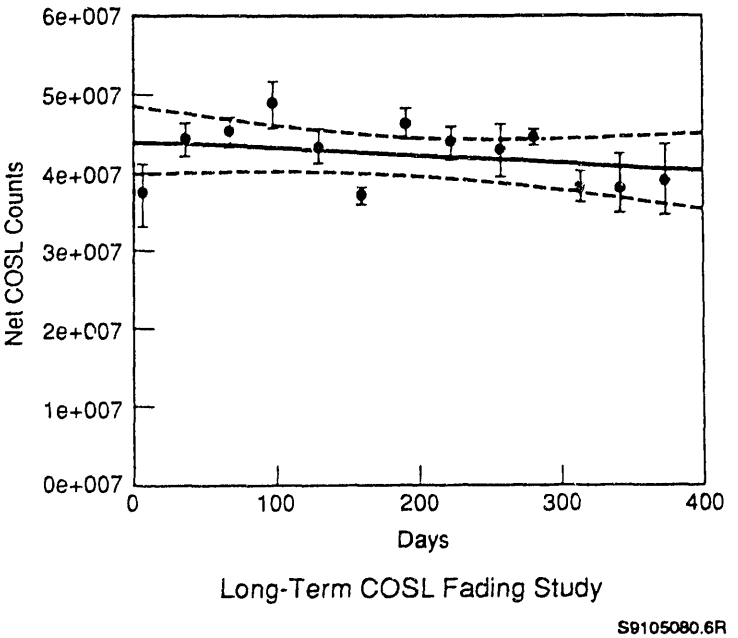

FIGURE 6. A group of CaF_2:Mn dosimeters were exposed to gamma radiation on day zero. Every month, for approximately a one year period, the dosimeters were interrogated with the COSL process. The average of the thirteen interrogations is plotted with the solid line. The dashed lines represent a 95% confidence level.

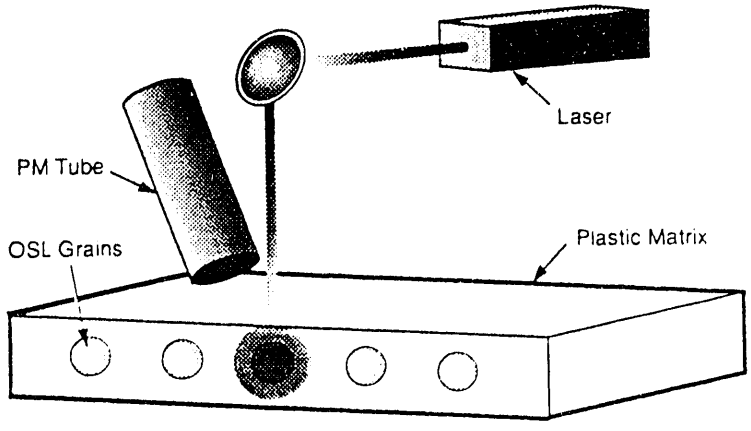

OSL Single Grain Readout

S9105080.1r

FIGURE 7. A conceptual figure showing the interrogation of a single grain of CaF_2:Mn within the plastic matrix.

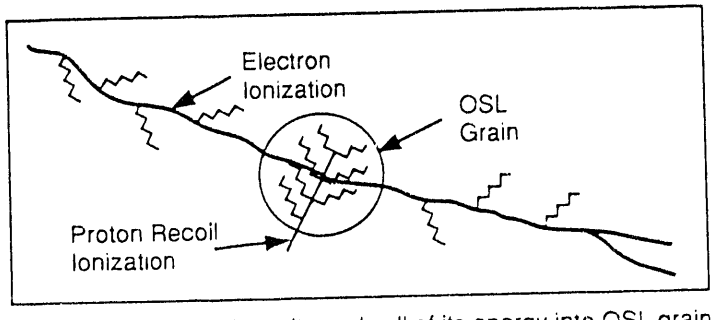

- Proton recoil can deposit nearly all of its energy into OSL grain
- Electron can only deposit a small fraction of its energy

Pulse Height Discrimination Between Neutron and Gamma Radiations

S9105080.7R

FIGURE 8. A conceptual figure displaying the tendency of proton-recoils to deposit energy in a very localized area.

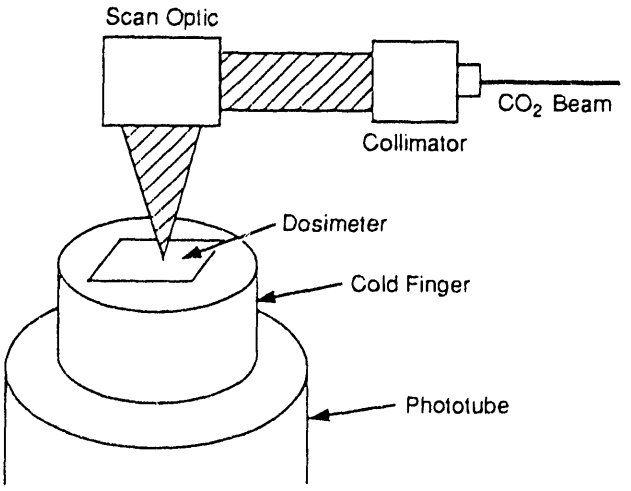

Laser Scanning Reader (Side View)

S9105080.10R

FIGURE 9. The plastic dosimeters are cooled on the cold finger, exposed to visible light, and then small spots are warmed to room temperature with the CO_2 laser beam.

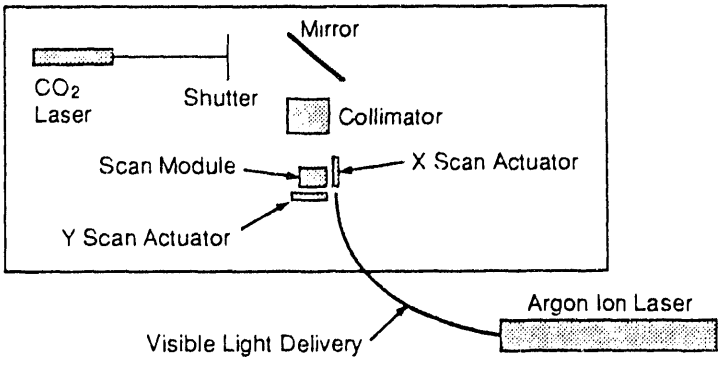

Laser Scanning Reader (Top View)

S9105080.9R

FIGURE 10. The optical layout used to deliver both visible (stimulating light) and invisible (warming radiation) to the plastic CaF_2:Mn dosimeter.

LASER-HEATED THERMOLUMINESCENCE NEUTRON DOSIMETRY[a]

P. Braunlich

International Sensor Technology, Inc.
WSU Research and Development Park
N.E. 1425 Terre View Drive
Pullman, WA 99163

INTRODUCTION

Since we first discussed laser-heated TLD at this workshop in 1982 (1), a family of instruments has been developed that is based on efficient, fast and reproducible heating of special thin-layer dosimeter configurations with microprocessor-controlled laser beams of uniform intensity profile. Applications include personnel dosimetry in mixed beta, photon and neutron fields, two-dimensional dose mapping, and remote fiber-optic dosimetry. The development effort was driven by the possibility of very rapid energy transfer from a laser beam to a small, thin dosimeter element and the associated dramatic increase in the signal-to-noise ratio. Potential improvements in the dosimetry of non-penetrating radiation and fast neutrons were immediately obvious as a result of this capability.

Significant advances in the development of low cost lasers, beam shaping optics, and control techniques were required for laser TLD to become practical. Completely new dosimeter elements and fabrication technology had to be developed as none of the dosimeters available from any manufacturer are suitable for this heating method.

In the following sections we will first briefly describe three different types of laser-based thermoluminescence dosimetry systems. All have neutron dose measurement capabilities. Thereafter, some preliminary results will be presented that were obtained with LiF and $Mg_2B_4O_7$:Tm laser-heated albedo dosimeters, both of which can be incorporated in the IST personnel TLD badge. Finally, the present status of the laser knock-on proton detector for direct fast neutron dosimetry will be discussed.

LASER-HEATED DESKTOP TLD SYSTEM

The reader for personnel and environmental dosimetry is available in two versions: (a) a semi-automated one of approximately 60 cm width, 40 cm height, and 43 cm depth, capable of reading the eight dosimeter elements of the hand-inserted badge in about 35 seconds, and (b) a fully automated reader which processes up to 200 eight-element badges per hour (Fig. 1). Both are based on the same electro-optic technology and similar digital systems control, signal processing, and data file management (2). The beam from a nominal 10 W CO_2 laser is guided through a Ge window into a light-tight compartment (Fig. 2). A small portion of it is split off with a ZnSe plate and directed to a power detector for closed-loop power control. The main beam is shaped into a 3.5 mm x 3.5 mm square of

uniform intensity profile in the plane of the dosimeter. The TL emission is collected by a highly reflective ellipsoidal reflector and measured by a temperature-stabilized bialkali photomultiplier tube. Single photon counting is replaced by current integration of the PMT signal above approximately 100 mrem ^{137}Cs gamma dose as measured by the standard $CaSO_4$:Tm element. The laser heating power delivery is "time-shaped" for optimal heating and annealing cycles, including pre-anneal and post-anneal treatments, that can exceed 400°C. The dosimeter is immediately re-useable with residual signals less than 0.1% after doses up to 10 rem. Significantly higher doses may require the elements to undergo two or more additional heating cycles for sufficient zeroing.

The dosimeter badge (Fig. 3) consists of a round plastic disc (38 mm diameter) which accepts eight 2.9 mm x 2.9 mm dosimeter elements on a 3.4 x 3.4 mm^2 aluminum oxide substrate. It contains provisions for thin beta windows and energy correction filters and can be configured to include a special "knock-on proton counter" element for fast neutron dosimetry. Two elements are reserved for albedo dosimetry and four $CaSO_4$:Tm elements are employed for energy-independent deep and shallow photon dose measurement in the ranges from 17 keV x-rays to ^{60}Co gammas. Energy-independent beta doses (down to ^{147}Pm beta energies) are measured using two $Mg_2B_4O_7$:Tm elements. This disc features six bayonet tabs and is placed into the cavity of the back housing. A ring is rotated, locking the assembly in and achieving a watertight seal. During the reading process inside both versions of the laser TLD reader, opening of the badge, positioning the elements sequentially into the laser beam and resealing are performed automatically. The back of the dosimeter disc is equipped with a "smart chip" (EEPROM) which is interrogated and updated during the read cycle. It contains information on the badge ID, the heating cycles required for optimal trap emptying, calibration constants, background signals, and history of use for each of the eight different dosimeter elements. A special snap-on cover prevents collection of dirt and provides convenient means for fixing the badge to clothing by a belt loop and a clip.

Conventional 0.4 mm thick LiF chips may be used. However, in order to achieve total insensitivity to humidity and guarantee over 1000 re-uses, IST dosimeter elements should be mounted in the badge. They consist of an approximately 50 micrometer thick layer of TLD powder (all commercially available TLD materials except LiF may be specified) that is fired onto the 125 micrometer thick substrate. A thin overcoat of a special glass seals the element. It is fabricated entirely from inorganic materials to avoid problems with light sensitivity and non-radiation induced signals that are typically associated with TLDs on organic substrates or made with organic binder agents. Some preliminary performance data of the system are given in Tables 1.

LASER-HEATED TL DOSE MAPPING SYSTEM

Thermoluminescence imaging of dose distributions has been reported first by Yasuno and coworkers (3), but has not yet been developed into a commercial product (a special version of a TL dose imaging device having better than 50 micrometer spatial resolution is the proton counter for fast neutron dosimetry discussed below). For a number of interesting applications, high spatial resolution is not required (4), and the associated very long reading times (3) of the stored image can be considerably reduced by sampling the image on a coarser grid (typically 3 mm x 3 mm).

Some of the areas in which the measurement of these two-dimensional "dose maps" have generated considerable interest are quality control of radiation treatment beams (beam profiles, dose deposition in water and humanoid phantoms), experimental treatment planning, and assessment of dose distributions caused by very intense short x-ray flashes used in radiation hardness testing of electronic components and circuits. The electro-optics employed in IST's dose mapping system are essentially identical to those of the laser-TLD readers with the exception of the size of the square uniform beam which is typically reduced to 1.5 mm x 1.5 mm. The dosimeter of Fig. 1 is replaced by a polyimide sheet onto which either an array of discrete spots or a thin continuous layer of TLD powder is deposited. The size of the sheet can be chosen up to 30 cm x 40 cm. An x-y translation stage moves it under computer control in the laser beam. Image processing software is provided which permits, with simple commands from a keyboard, zooming in on areas where higher resolution is required or to allow reduction of the resolution for increasing the reading speed. Other features include digital filtering, dose contour selection, three-dimensional display of the dose vs. x,y position, etc. Examples of dose maps obtained with radiation treatment beams from an accelerator are shown in Figs. 4 and 5. Although we have not yet investigated the performance of these sheets in measuring neutron dose distributions, we anticipate no principle problems for monitoring, for example, high energy neutron beams for cancer treatment by using CaF_2:Tm powder similar to the experiment we performed with the fiber-optic probe (see Fig. 6 below).

REMOTE FIBER-OPTIC TLD

From the outset, one of the most intriguing dosimeter configurations suitable for laser-heating has been the fiber-optic TLD probe. Early versions have been based on CO_2 (5) and Nd:YAG (6) lasers, but were abandoned because of the lack of a suitable fiber for 10.6 micrometer CO_2 laser beam and the cost and instability of cw solid state lasers. Significant progress in the development of a remote fiber-optic TLD system has been made in the last year after semiconductor lasers with sufficient beam power became available at steadily decreasing costs. A prototype system with four of a possible five probes attached is shown in Fig. 6. The construction of the TLD probe tips was described in REF. 6. Anticipated fields of application are radiation oncology and monitoring radioactive waste sites. Examples of remotely measured glow curves due to doses deposited in PMMA by high energy neutron beams for cancer treatment are shown in Fig. 7.

LASER NEUTRON TLD

The most obvious application of laser heating in neutron TLD is albedo dosimetry which is readily implemented using 0.4 mm thick isotope-separated LiF chips. Some results we have obtained are listed in Table 2. With the goal of eliminating the sensitivity of the badge to humidity, maintaining complete laser anneal capability and assuring re-use of at least 1000 times, we are developing albedo elements that are based on isotope-separated $Mg_2B_4O_7$:Tm powder, binder and protective cover material. These thin-layer dosimeters are less sensitive than the comparatively thick LiF chips and have a smaller figure of merit (response relative to ^{137}Cs gammas) but show promise to perform very well as

laser-heatable albedo dosimeters. The known fading problems of the original $Mg_2B_4O_7$:TLD material developed by Prokic (7) has been reduced by improved fabrication processes. We have reasons to believe that, with appropriate pre-annealing and data processing, fading will be no more than around 10% in 90 days at room temperature. Controlled long-time fading tests are presently under way to confirm early indications to that effect.

Thin-layer dosimeters behind proton radiators were believed to be suitable fast neutron dosimeters if the TLD layer thickness is comparable to the range of the knock-on protons. With support from the Department of Energy we investigated this concept in detail with the result that even under the most favorable experimental conditions, the figure of merit will not exceed 5 to 10%. This is also true for bulk dosimeters which consist of fine-grain luminescence material embedded in polymers of high hydrogen content and are read with a non-heating optical stimulation beam. The cause of this limitation is rooted in the spatial distribution of a given tissue dose. Knock-on protons deposit their energy via secondary electrons in channels of a few micrometers diameter and length and very high energy density but low total specific TL yield per rem. Gammas affect a much larger volume of the dosimeter and generate on average a rather uniform excitation of low energy density and high specific TL yield. Laser stimulation (laser heating as well as optical stimulation) reads the total active volume and discriminates between neutron and gamma doses by measuring the small difference in luminescence signals between proton-radiator covered and bare dosimeters.

A significant increase in the figure of merit is possible if laser stimulation can be achieved with high spatial resolution (8). Then, in theory, one is able to sort out the small volume elements excited by a knock-on proton and discard those excited only by the gamma background radiation. This concept is known as the "proton counter" and may be viewed as the TLD equivalent of track etch and the bubble dosimeters. However, the convenience and speed of reading such a dosimeter has a price: an inherent gamma sensitivity and technical complexity.

A detailed study of theoretically expected figures of merit for thin layers composed of very small grains of $CaSO_4$:Dy as a function of proton radiator thickness, TLD layer thickness and neutron energy revealed the exciting potential of the TLD proton counter concept and yielded the experimental parameters that must be met by a practical system. The TLD proton counter can in principle take the form of a two-dimensional array of small (less than 30 micrometer diameter) single TLD phosphor grains of uniform shape and size. These are sequentially heated by a tightly focused CO_2 laser beam. The signal consists of the TL emission from each grain in the form of a few photons. Single photon counting is required and proton "hits" can in principle be registered as the number of grains yielding a photon count above a predetermined threshold. This threshold is a function of inherent background and the dose due to any gamma contributions in the radiation field. Both must be established independently for each neutron dose measurement. In practice, such an array is all but impossible to fabricate.

Instead, we have manufactured thin continuous layers of 1 cm x 1 cm area using $CaSO_4$:Dy TLD powder of grain size less than 20 micrometer and 4-8 Mg/cm^2 thickness. These layers appear very uniform, but nevertheless exhibit statistical sensitivity variations on the volume scale determined by the 30 micrometer laser beam diameter. The proton counter must be read by a highly stable scanning laser

beam. This is achieved by rotating special optics in place of that producing the uniform square beam for conventional laser TLD (Fig. 1) and moving the detector on an x-y stage. In this way the beam is scanned across its surface with slight overlap of the rows. Photons are collected in thirty 0.5 ms time intervals per 30 micrometer scan distance. The data are processed by searching for the maximum photon counts from 30 out of 60 sequential total time length time intervals, discarding the rest. A total of 12,000 of these scans are searched (corresponding to an area of 9 mm^2). They are compiled as distributions of the kind shown in Fig. 8. As can be seen, the distribution due to background noise broadens with increasing gamma dose and neutron-generated knock-on protons enhance the tail of the distribution with relatively small effects on the means.

These examples indicate that the detailed shapes of the photon distributions are indeed determined by the magnitudes of the neutron-gamma doses absorbed from a mixed radiation field. However, it turned out to be a nontrivial task to reliably de-convolute these distributions because, due to a lack of certain essential features of our experimental test bed, we have not yet achieved the required reproducibility of the data and a sufficiently low noise background. It also became clear that the analysis of photon distributions alone does not fully utilize the information content of the measured spatial "dose image." Proprietary novel detectors are also under consideration.

We are hopeful the development of the device will somehow continue at a level commensurate with the technical challenge it poses. We are fully aware of the fact that significant work and technical improvements or breakthroughs are still required to reduce the concept to practice, but remain convinced of its viability.

(a) The results summarized in this paper are due to the dedicated effort of the entire technical staff of IST, Inc. Contributions by W. Tetzlaff, S. Jones, C. Bloomsburg, J. Hegland, J. Hoelscher, B. Rogers, A. Kelley, J. Hoffman, J. Sweet and J. Thompson are gratefully acknowledged.

The work was supported by the Department of Energy (Contract No. DE-ACO384ER80165), the National Institutes of Health (Grants Nos. 5 R4CA44242B and 8 R3CA47644B) and by the Naval Surface Warfare Center (Contract No. N60921-88-C-0057).

REFERENCES

1. P. Braunlich, M. Brown, J. Gasiot, and J.-P. Fillard; Proceedings of the Ninth Workshop on Personnel Neutron Dosimetry, June 24-25, 1982, Las Vegas, Nevada (CONF-820668 and PNL-SA-10714).

2. C. D. Bloomsburg, P. F. Braunlich, J. E. Hegland, J. W. Hoelscher, and W. Tetzlaff; Radiat. Prot. Dosim. **34**, 365-368 (1990).

3. Y. Yasuno, H. Tutsui, and T. Yamashita; Jpn. J. Appl. Phys. **21,** 967 (1982).

4. Development of a 2-D dose mapping system is also pursued by the group of Prof. J. Gasiot at CEM, USTL, Montpellier, France.

5. P. Braunlich, S. C. Jones, and W. Tetzlaff; Radiat. Prot. Dosim. **6,** 103-107 (1984).

6. S. C. Jones, J. E. Hegland, J. E. Hoffman, and P. Braunlich; Radiat. Prot. Dosim. **34,** 279-282 (1990).

7. M. Prokic; Nucl. Instrm. Methods **175,** 38-85 (1980).

8. P. Braunlich and W. Tetzlaff; Radiat. Prot. Dosim. **33,** 327-330 (1990); "Radiation Dosimetry by Counting Differentially Ionized Sample Areas from Heavy Charged Particle Events," U.S. Patent No. 5,015,855, May 14, 1991.

TABLE 1. Photon Energy Response and ^{137}Cs Gamma Dose Range Response. The standard deviation of ten 75 mrem ^{137}Cs exposures was 1.7%.

Energy (KeV)	Deep Dose Response	Shallow Dose Response
1200	0.90	0.90
662	1.00	1.00
120	1.08	1.09
64	0.94	0.96
59 *	0.69	0.77
42	1.01	1.01
32	1.02	1.02
21	1.00	1.05
17 *	1.15	0.93
15	0.99	1.15

* Monoenergetic photons: 59 keV ^{241}Am photons and 17 keV K-fluorescence x-rays.

Dose (rem)	Response (rem)	
	Mean	Std Dev
0.001	.000	<.0005
0.003	.002	<.0005
0.01	.009	<.0005
0.03	.029	<.0005
0.75	.071	0.002
0.1	.101	0.002
0.3	.301	0.004
1.0	1.00	0.019
3.0	2.82	0.043
10.0	9.05	0.261

TABLE 2. Characteristics of Albedo Neutron Response with Laser Heating.
(a) Neutron reporducibility with LiF for bare ^{252}Cf with 1:1 neutron:gamma dose ratio.
(b) Neutron energy response with LiF.
(c) Comparison of MgB_4O_7:Tm and LiF.

Dose (rem)	Response (rem)	
	Mean	Std Dev
0.003	.003	0.001
0.010	.010	0.001
0.030	.028	0.001
0.075	.073	0.002
0.10	.096	0.003
0.30	.278	0.003
1.0	.950	0.029
3.0	2.68	0.18
10.0	9.27	0.91
500.0	538.	33.6

(a)

Source	Energy (MeV)	Response
Fission:		
Pu-Be	4	0.65
Bare ^{252}Cf	2	1.02
D_2O moderated ^{252}Cf	1	8.1
Mono-energetic:	15	0.14
	1	0.9
	0.5	1.75
	0.1	8.2

(b)

Dosimeter	D_2O moderated ^{252}Cf	Bare ^{252}Cf
LiF chips (>015" thick)	9.17	1.14
MgB_4O_7:Tm (thin layer)	5.61	0.72
Ratio: MgB_4O_7:Tm/LiF	0.6	0.6

(c)

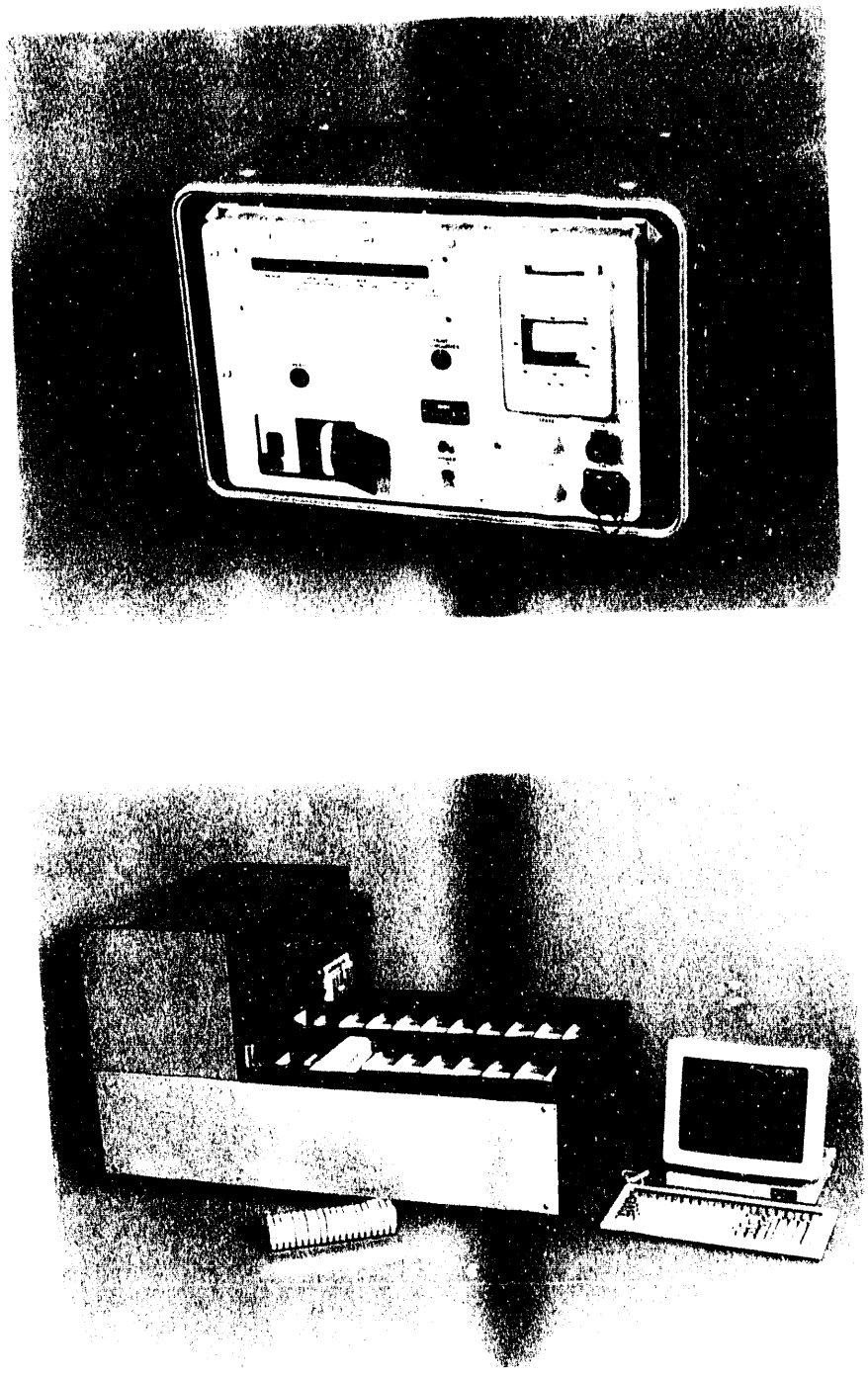

FIGURE 1. Desktop semi-automated (top) and automated laser-TLD readers.

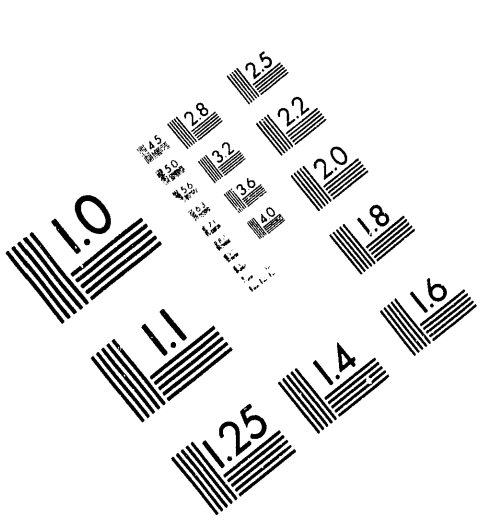

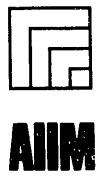

Association for Information and Image Management
1100 Wayne Avenue, Suite 1100
Silver Spring, Maryland 20910
301/587-8202

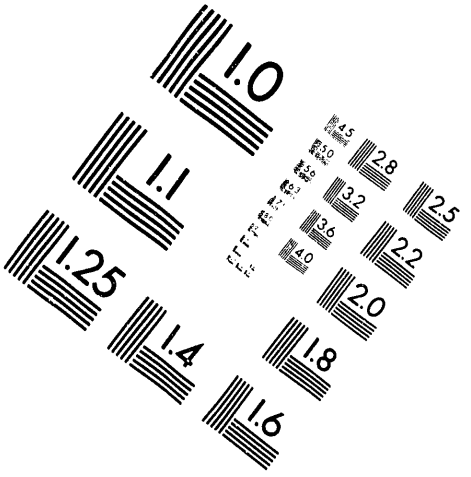

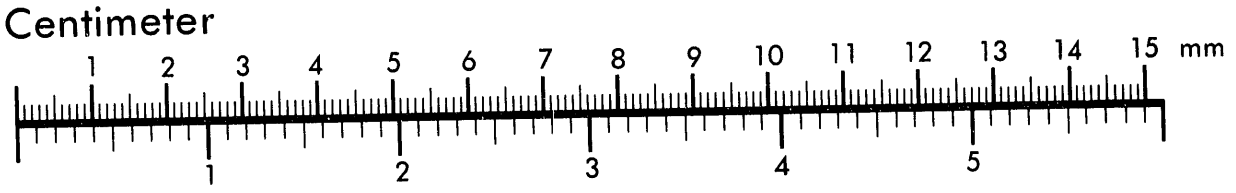

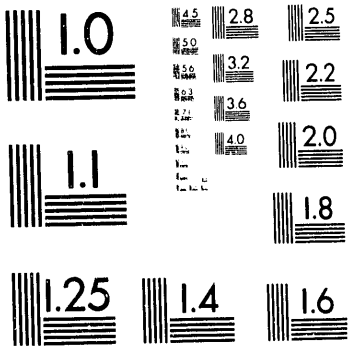

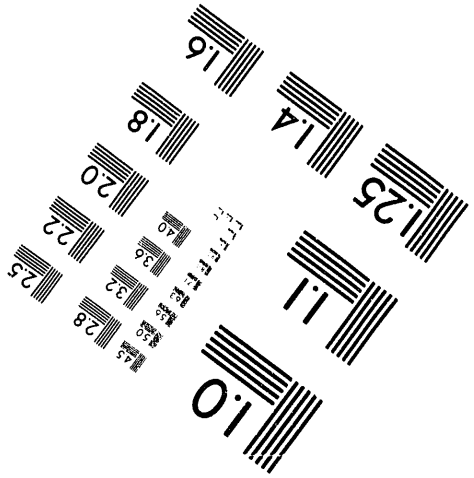

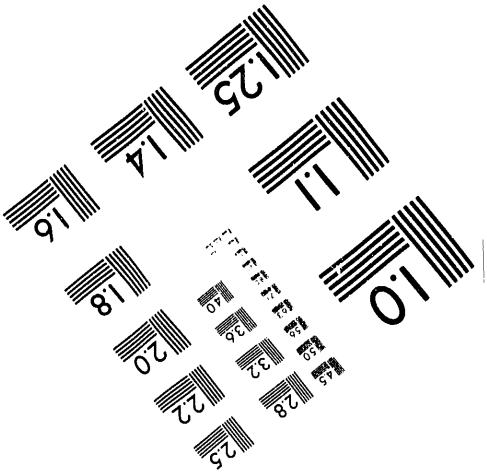

MANUFACTURED TO AIIM STANDARDS
BY APPLIED IMAGE, INC.

2 of 2

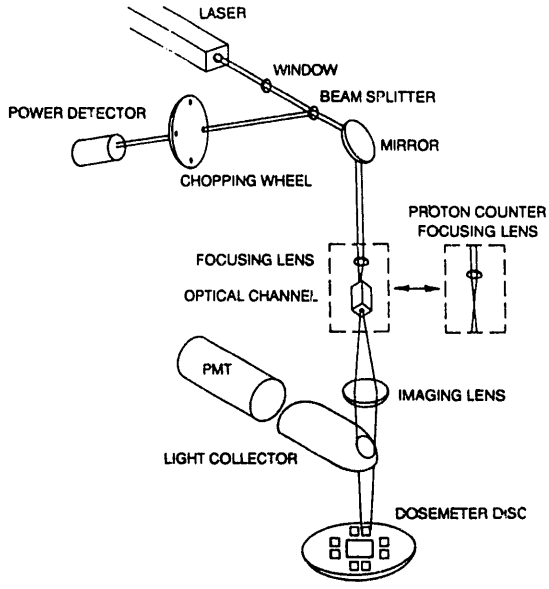

FIGURE 2. Schematic of laser-TLD reader optics

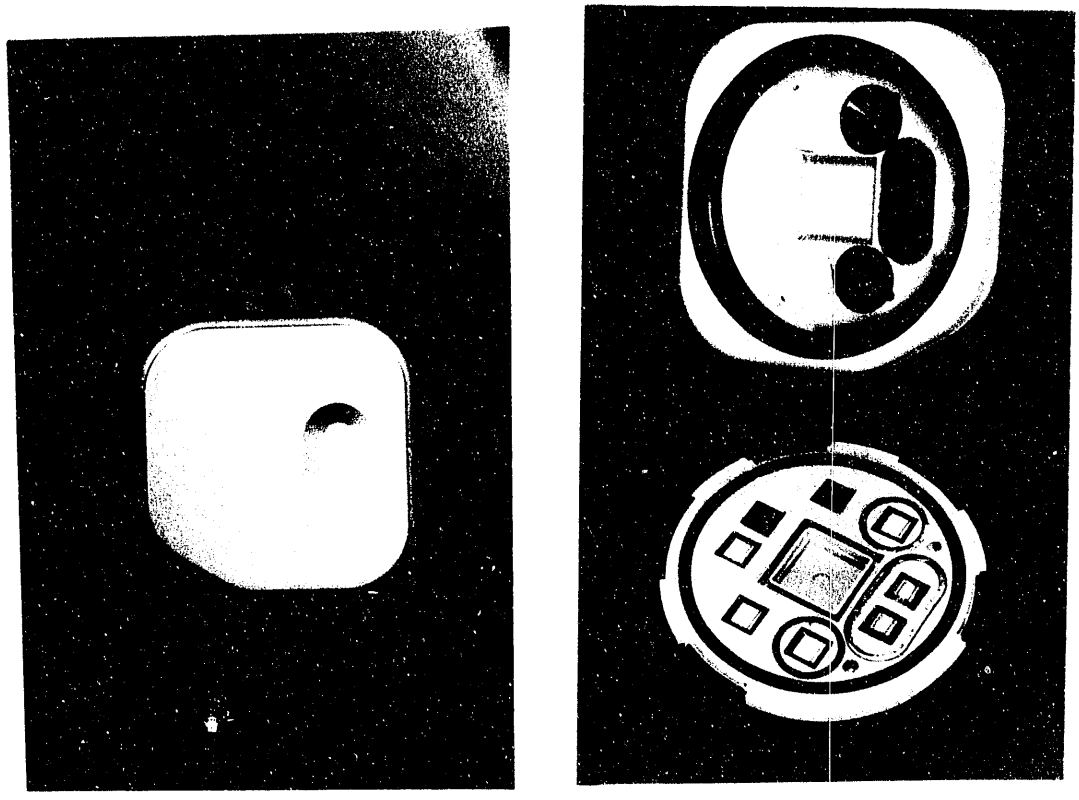

FIGURE 3. Closed and opened laser-TLD badge for personnel dosimetry.

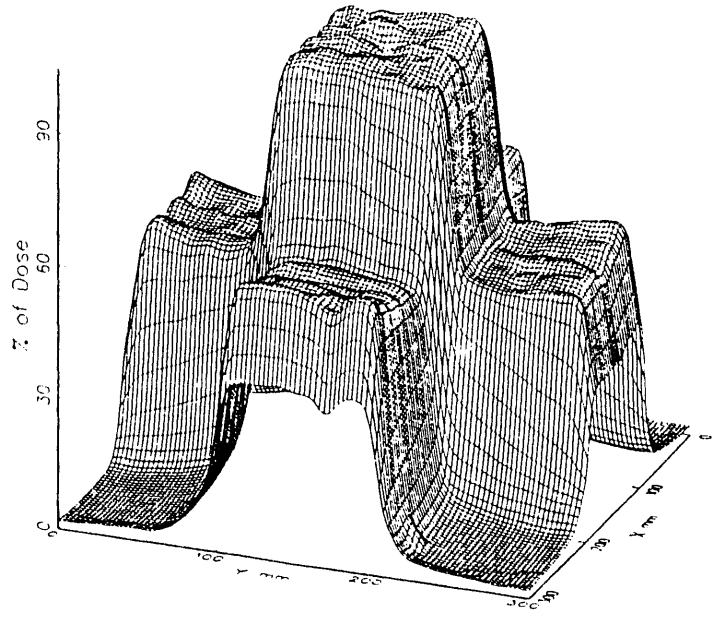

FIGURE 4. 3-D view of electron therapy beam dose distribution, measured in cross section. Beam parameters: 12 MeV electrons, 10 cm x 10 cm area. Dose: 100 cGy at center (x = y = 150 mm) Phantom: PMMA Beam axis perpendicular to x-y plane.

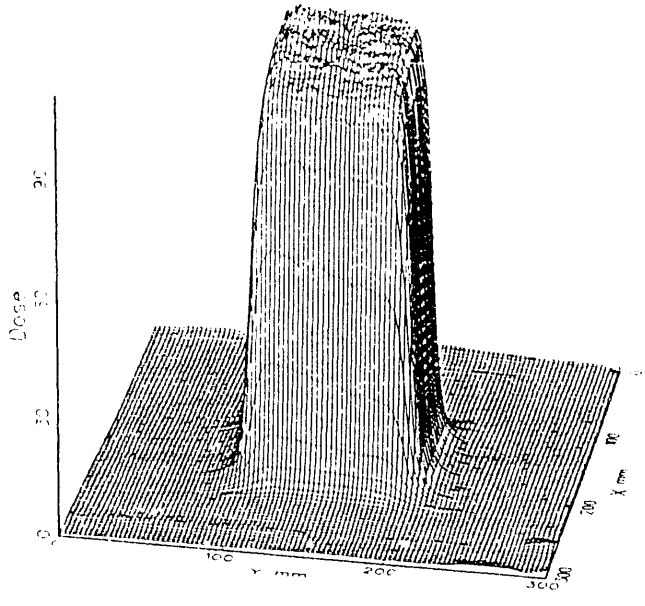

FIGURE 5. 3-D view of resultant dose distribution from two opposed pairs (4 exposures total) of 6 MV x-ray beams. Each beam is 10 cm x 10 cm, with axis parallel to x-y plane. Dose: 450 cGy at center Phantom: Solid Water™

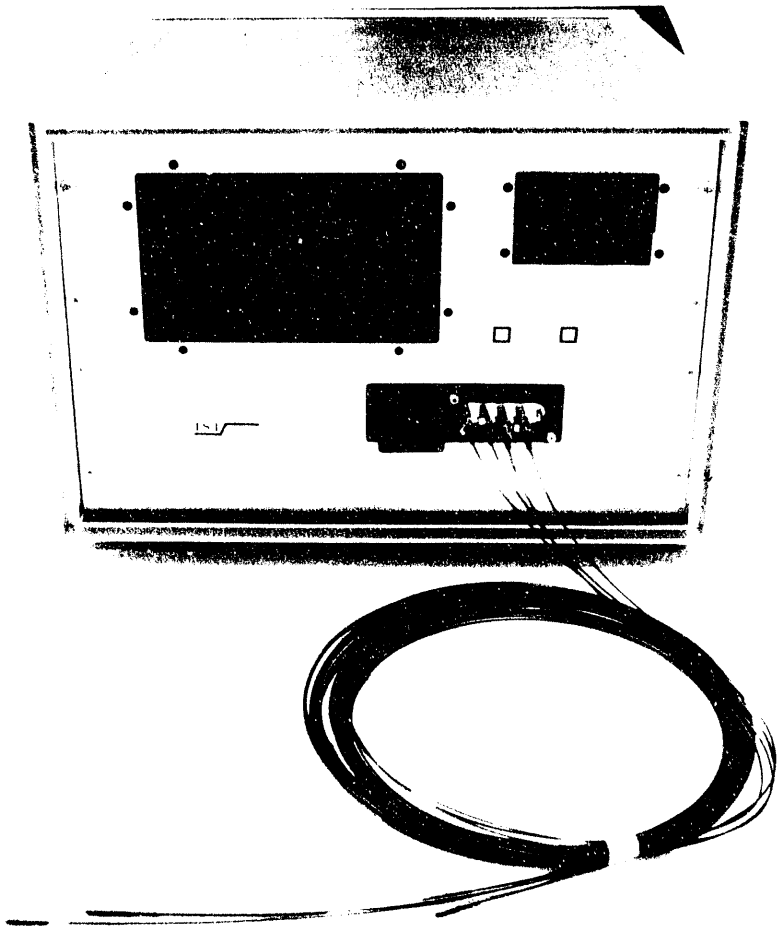

FIGURE 6. Laser-TLD fiber-optic probe reader

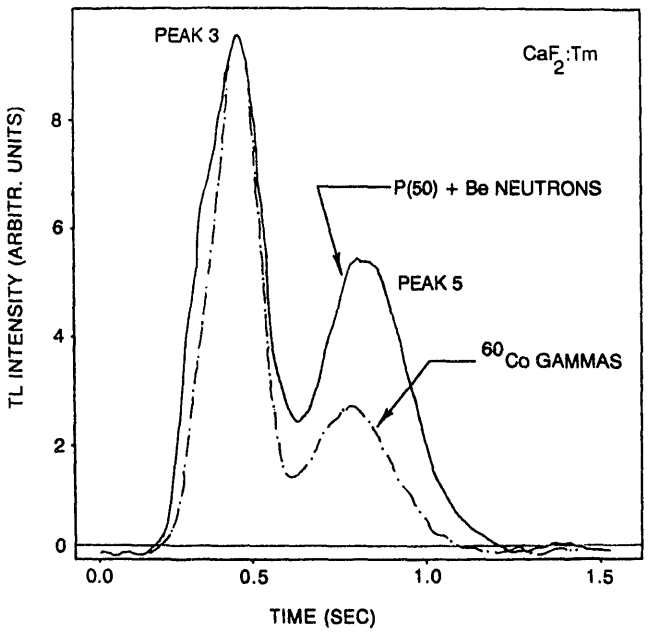

FIGURE 7. Glow curve of CaF_2:Tm probe irradiated with ^{60}Co gammas (0.86Gy) and p(50MeV) + Be generated neutrons (2.0Gy). The relative sensitivity difference of peak 5 for gamma and high-LET radiation provides neutron/gamma discrimination. Gamma contamination contributes 11% of the total dose delivered by the neutron beam.

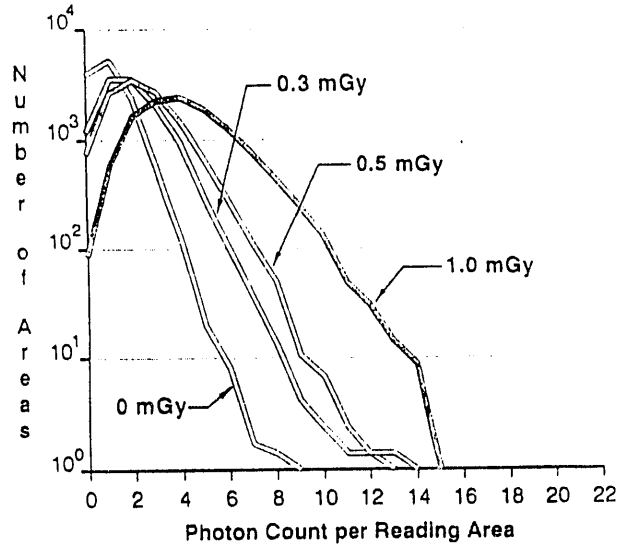

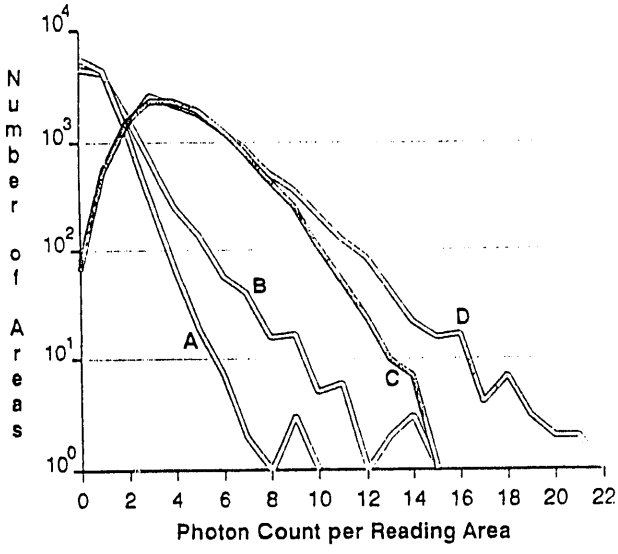

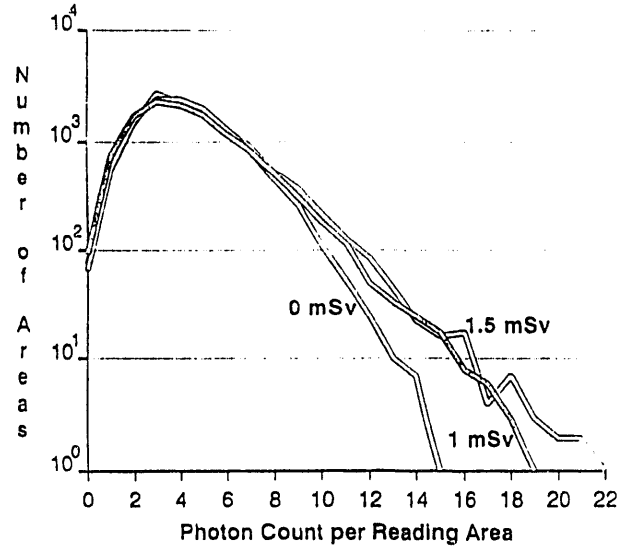

Top: Gammas only.
Bottom left: **A** zero dose distribution; **B** 1.5 mSv + 0 mGy; **C** 0 mSv + mGy, **D** 1.5 mSv + mGy.
Bottom right: Neutron doses plus 1 mGy gamma dose.

FIGURE 8. Photon count distributions compiled from 12,000 reading areas (covering an active proton counter surface of 9 mm^2) mixed ^{137}Cs gamma and Pu-Be neutron doses.

SUPERHEATED DROP, "BUBBLE", DOSIMETERS*

M. J. Harper,[1] T. L. Johnson,[2] C. R. Jones,[3] H. F. Kerschner,[4]
K. W. Lindler,[1] M. E. Nelson,[1] J. L. Rabovsky,[3] N. Rao,[3] G. K. Riel,[5]
and R. B. Schwartz[6]

[1]U.S. Naval Academy, Annapolis, MD 21401
[2]U.S. Naval Research Laboratory, Washington, DC 20375
[3]U.S. Dept. of Energy, Washington, DC 20545
[4]USN, MSC, Washington, DC 20372-5120
[5]NAVSWC, White Oak, MD 20903-5000
[6]National Institute of Standards and Technology, Gaithersburg, MD 20899

INTRODUCTION

Superheated Drop Dosimeters (SDD) offer a sensitive, immediate measure of the neutron dose equivalent, but their dynamic range is limited and their response varies with temperature, pressure, and vibration. They contain thousands of superheated liquid drops in a stabilizing matrix. High linear energy transfer (LET) radiation triggers vaporization of the drops into visible bubbles. If the matrix is a liquid, the bubbles slowly rise, and the number present indicates the dose rate. Dose may be measured by displacement of the matrix, or by counting the sounds of vaporization. If the matrix is a gel, the bubbles are fixed, and their number is proportional to the dose equivalent. Our research has focused on modeling and elimination of the environmental response, extension of the dynamic range, and tests and evaluations of prototype devices.

THERMODYNAMICS OF BUBBLE FORMATION

Bubble dosimeters work because the superheated drops are vaporized by a small energy input. However, that energy must be deposited within a very small volume. Vaporizing this "critical volume" produces a "critical bubble" of the minimum size which will grow until the entire liquid drop becomes a vapor bubble. To illustrate the relative sizes of the drops and bubbles, imagine that the critical liquid volume were the size of the Earth, then the critical vapor bubble would be four Earth diameters; the liquid drop diameter would be the size of Earth's orbit, and when vaporized the bubble would fill Jupiter's orbit.

Bubbles smaller than the critical bubble will collapse. Figure 1 illustrates the process of vapor initiation. The proton carries most of the energy, but only the recoil ion has sufficient stopping power (energy deposited per unit length, dE/dX) to produce a critical bubble. The variation of the dE/dX required with temperature is shown in Figure 2. We have verified the predicted inhibition temperatures, below which no bubble can be formed, for: Freon-12™, Freon-114™, and Isobutane at 10, 20, and 15°C, respectively.

Earlier studies accounted for only a few percent of the energy of bubble formation, and required a large, temperature dependent, efficiency factor [Ap 85]. Later studies were more complete [Lo 88]. Our model, as shown in Table 1, needs no efficiency factor. The threshold energies, determined by the thermodynamic work required to produce a critical bubble, are 16, 707, and 60 keV, at 20, 25, and 23°C for Freon-12™, Freon-114™, and Isobutane, respectively.

The stopping power must be sufficient to deposit the threshold energy in the critical drop. Thus, gamma-rays can produce no bubbles in SD neutron detectors. We computed dE/dX by Ziegler's TRIM-90 code, which includes electronic as well as nuclear effects and produces the energy spectrum of the recoil ions. We select only that part of the spectrum exceeding the threshold energy to compute the response shown in Figures 3 and 4.

Most SDD response is to neutron scattering, but SDDs based on Freon-12™ have a 16 keV threshold and measure low energy and thermal neutrons by the (n,p) reaction illustrated in Figure 1, giving the response shown in Figure 2. This may account for the low energy response observed in BD-100 but not in other SDDS. See Figure 5 [Sc 90].

THE TEMPERATURE PROBLEM

A superheated drop's vapor pressure is resisted by the surface tension of the surrounding medium. As temperature rises, so does the vapor pressure, while the surface tension falls. The fall in threshold energy with increasing temperature gives an apparent rise in sensitivity, as shown in Figure 6. We apply a temperature correction to the sensitivity, but this is not exact, as the apparent change of sensitivity with temperature depends on the neutron energy spectrum.

Devices which apply a compensating pressure that increases with temperature work, as seen in Figure 7. However, they add size, cost, and complexity to a small, inexpensive, simple system.

Keeping the temperature constant is the best solution. Many radiation work environments are air conditioned. For the others, we are building a thermoelectric heating and cooling system. See Figure 8.

The Thermoelectric Heat Pump

A heat pump transfers more heat than the power required to drive it, resulting in a coefficient of performance (COP) greater than one. Power requirements were determined for a BD-100R dosimeter and unit couple with the properties shown in Table 2. The voltage required for the maximum COP varies with temperature. Selecting three fixed voltages provides a good compromise between complexity and efficiency. For cooling the unit should switch from 0.01 to 0.04 volts when the temperature rises above 84°F, see Figure 9. The required cooling and battery power are shown in Figure 10. For heating, the unit should switch from 0.01 to 0.02 volts when the temperature falls below 50°F. The COP and power requirements for heating are shown in Figures 11 and 12. Cooling requires three unit couples, while

heating requires two. A 9 ounce 8 cubic inch Ni-Cd battery could power the dosimeter for various periods, depending on the temperature:

28 days, if the temperature is 60 or 70°F.
A week, at 50 or 80°F
At the limiting temperatures; 32°F, 34 hours, and 118°F, 8 hours.

DEVICES TESTED

Bubble Technology Industries [1]

BD-100R: The superheated drops are retained in a polymer and counted either by eye or a video system. Bubbles can be re-compressed for re-use by applying external pressure. The material can be made in special shapes, for example, an extremity monitor. Our tests involved the test tube shape, a half inch in diameter and 3 inches long (Figure 13) [Ri 88-1].

BDS-SPECTROMETER: This comprises six threshold detectors. A set of thirty six tubes containing three each of six different compositions with neutron energy thresholds nominally from 10 to 10,000 keV [Ing 88].

Apfel Enterprises Inc. [2]

Active Personnel Neutron Dosimeter (APND): The saturated drops are contained in a liquid, and the resulting sound is acoustically counted, Figure 14. Cartridges of active material are replaced when sensitivity declines.

Area/Spectrum Monitor (A/SM): Two channel versions of the APND. Cartridges are available with different neutron energy thresholds to aid in spectrum analysis. These were produced for NSWC to monitor the dose and to estimate energy dependent errors in our personnel dosimeter [Ri 88-2].

Pen Type: The drops and matrix are in a small syringe, and the dose is read from the displacement. Since the bubbles take about a half hour to rise from the matrix, the number of visible bubbles is a measure of the dose rate. This prototype device, produced for NSWC, led to a displacement device using the standard APFEL™ cartridge, and to a "Neutrometer" available in various sensitivity ranges.

RESPONSE VS DOSE AND TIME

BD-100R: In a reusability test, dosimeters maintained their sensitivity for 40 days, made up of 24 dose and recharge cycles, Figure 15. The total dose delivered was nearly 400 mrem.

In a simulated 68 day issue cycle, they retained 85% of their initial average sensitivity, but began to loose repeatability between day 19 and day 34, Figure 16. They were then recharged, but not all bubbles could be cleared. The average sensitivity, measured on the 72nd day, was 60% of the initial sensitivity, but the spread in results had doubled [Ga 91]. This cannot be called bad, as they are designed for daily reading and recharging. These tests include the nominal 100 and 1500 kev Threshold tubes from the spectrometer set, because they are used in a "Combination Dosimeter" with an albedo TLD (Liu, 89).

APFEL™ A/S Monitor and APND: Results of a 100 day, 165 mrem test are shown in Figures 17 and 18. The test included a transcontinental flight while activated. Efficiency fell to 85%, as one would predict from the dose delivered. Efficiency corrected for dose did not change with time.

DYNAMIC RANGE

The range from the lower limit of detection to the maximum dose is proportional to the maximum number of bubbles that may be counted. SDDs contain thousands of sensitive drops instead of billions of sensitive atoms, so effects that are small in ordinary dosimeters, such as change in sensitivity with dose and limitations on dynamic range become important.

BD-100R: Gel matrices retain the bubbles, so the dynamic range is limited by the maximum number of stored bubbles which may be counted. Visually, accuracy is lost between 40 and 100 bubbles. A simple video system saturates at about 300 bubbles. We expect to count 1,000 bubbles with a three dimensional video system which uses artificial intelligence to recognize bubbles and reject other images.

APFEL™ A/S Monitor and APND: The matrix determines the dynamic range of the dosimeter. Liquid matrices allow the bubbles to leave, so they can have a good dynamic range, but their life ends when too few drops remain to provide the required sensitivity:

@ 80% of initial efficiency - 6,000 Counts
@ 50% of initial efficiency - 15,000 Counts

LOST DATA AND LARGE DOSES

In all SDD systems, the dose may be read by determining the number of drops, or sensitivity remaining in a dosimeter. The equation of Figure 17 shows that dose may be calculated, given the initial and final number of drops (N_0 and N), or the initial and final sensitivity (k*No and k*N). Dose equals the negative log of either ratio. Table 3 and Figure 19 show the results of this calculation. The error in the dose depends on the repeatability of the dosimeter, the fraction of drops remaining (F), and whether F is determined by sensitivity (S) or by N, since sensitivity is less precisely known than number of drops. There is a fixed error and a proportional error. The error approaches the repeatability, typically 20% for BTI™ and 5% for APFEL™, at large doses.

OPERATIONAL TESTS IN AN AIR CONDITIONED WORK ENVIRONMENT [Ri 91]

Procedure

We followed the ISO standard [ISO 78] for testing personnel dosimeters, and we compared the bubble system's response with: LiF TLD albedo neutron dosimeters, CR-39 neutron track dosimeters, Bonner multi-sphere spectrometers, remmeters, a NE213™ neutron spectrometer, a tissue equivalent proportional counter (TEPC), and an TLD Area Monitor [Ri 88-3].

BTI™ BD-100R and BDS-SPECTROMETER: Thirty BD-100R tubes and 2 spectrometer sets (thirty six tubes each) were used for three cycles: clear, read, expose, and read, for a total exposure time of 50 hours.

APFEL™: Five monitors using the standard cartridge and six prototype pen devices were exposed continuously for eighty hours, and read nine times during the exposure.

Reproducibility (Repeatability)

The standard deviation (SD) divided by the mean of repeated tests was less than 20% for the BD-100R @ 18%, the BDS 1500 @ 12%, and the APND and A/SM Monitors @ 6%. The BDS 100 keV is marginal at 24%. The dose was too low for valid tests of the PEN and BDS-10000. The other BDS tubes exceeded 40%.

Batch Uniformity

This is the probable error in using a single efficiency for a batch of detectors. The BD-100R, at 46%, requires individual calibration. The acceptable devices are: The BDS-100 @ 15%, the BDS 1500 @ 12%, and the APND and A/SM @ 4%.

Lower Limit of Detection (LLD)

The LLD equals 1.96 times the SD divided by the square root of the number of detectors in the test. The LLD, in mrem was: BD-100R, 1.2; BDS-100, 1.7; BDS-1500, 1.2; APND & A/SM, 0.5.

Comparison with other Devices

All of the dose equivalent devices (APND, A/S Monitor, Pen, BD-100R, BDS-100, TLD Area Monitor, SNOOPY, BMS, TEPC, and NE-213 read were between 0.7 and 0.4 mrem/Hr. This is better than one would expect, since each is calibrated in a different way. NE 213 and the TEPC read about 0.4 mrem/Hr, as may be expected, since the spectrum is rich in low energy neutrons which they do not measure. The CR-39 read about 0.25 for the same reason. The LiF albedo dosimeters read low because they are calibrated with D_2O moderated Cf^{252}, and the spectrum is also rich in fast neutrons. The energy correction for this spectrum raised their reading to 0.5 mrem/Hr.

COMPARISONS @ 14 MeV

BD-100R dosimeters were compared with calculations, scintillation spectrometers, tissue equivalent proportional counters, remmeters, neutron track and albedo dosimeters. The systems had various calibrations, as shown in Table 4. For comparison, the response to Cf-252 was measured in the same room. Taking the MCNP calculation as the standard, the BD-10OR response was the most correct.

THE NAVY SDD PROGRAM

The program is aimed toward devices which may provide a small spectrometer, DT 648 energy correction, an area monitor, and a neutron dose equivalent dosimeter to complement the laser heated TLD. The state of the program may be compared favorably to TLDs in their first decade.

PRACTICAL APPLICATIONS

Do SD dosimeters have any utility? Obviously YES, because they are being used as self reading dosimeters at nuclear reactors, to map accelerator beams, as diagnostic tools for experimental neutron generators, and in space. However, they are too fragile to be relied on as a primary dosimeter in routine use.

Properly used, they can be our most accurate measurement of dose equivalent. Some applications for a small, accurate, dose equivalent (or threshold) detector with immediate readout are:

Man-rem reduction - to learn which operations produce the major doses
Albedo Dosimeter energy correction, as in the Combination Dosimeter
Measuring small Neutron doses in intense Gamma-ray fields
Mapping dose distributions in beams or phantoms
Self monitoring and/or daily monitoring
Remote sites which have no reader for conventional dosimeters

CONCLUSIONS

SDD dosimeters can supplement more conventional dosimeters in tasks requiring small size, dose equivalent response, or immediate results.

APFEL™: The Active Personnel Neutron Dosimeter and Area/Spectrum Monitors are precise and sensitive, but since they incorporate an anti-coincidence circuit to eliminate acoustical noise, a dead time counter will be required before they can be used for personnel protection.

BTI™: The BD-100R meets the 20% criteria, provided that each tube is individually calibrated. Of the BDS spectrometer set, only the 100 and 15OO keV compositions gave consistent results. They are candidates for energy correction of the albedo dosimeter.

* This work was supported by the BUMED R&D command, and Naval Sea Systems Commands 04R and 06GN. The DOE supports the Combination Dosimeter, and the program has been a cooperative effort with the Naval Research Lab, Nevada Test Site, U.S. Air Force, and U.S. Army Combat Systems Test Directorate. Field operations were aided by the Trident Refit Facility (Bangor), Puget Sound Naval Shipyard, and two U.S. Naval Vessels. Free labor was provided by students at George Town University, the University of Maryland, and the U.S. Naval Academy.

REFERENCES

Ap 85: R.E. Apfel, C.S. Roy, and Y.C. Lo "Prediction of the Minimum Neutron Energy to Nucleate Vapor Bubbles in Superheated Liquids" Physical Review A, 31, 5 May 1985 3194-3198.

Ga 91: George B. Garrott "Fading Characteristics of Superheated Liquid Drop (Bubble) Neutron Detectors" MS Thesis In Preparation, Georgetown University, Dept. of Radiation Science.

Ing 88: Ing, H. and Tremblay, K. "To develop a set of variable lower-energy threshold bubble neutron detectors for use as a spectrometer" BTI, Chalk River, Ontario, Canada KOJ IJO, February 29, 1988.

ISO 78: ISO Standard 4071-1978 (E), International Organization for Standardization, Geneva, Switzerland.

Liu 89: J. C. Liu, C. S. Sims, and J. W. Poston *The Development, Characterization, and Performance Evaluation of a New Combination Type Personnel Neutron Dosimeter* ORNL Report 6593.

Lo 88: Lo, Y. and Apfel, R. "Prediction and experimental confirmation of the response function for neutron detection using superheated drops" Physical Review A, Vol. 38 No. 10 p. 5260-5266, Nov. 15 1988.

Pe 87: C.A. Perks, R.T. Devine, K.G. Harrison, R.J. Goodenough, J.B. Hunt, T.L. Johnson, G.K. Riel, and R.B. Schwartz "Neutron Dosimetry Studies Using the new Chalk River Bubble Damage Detector" Sixth Symposium on Neutron Dosimetry Neuherberg, October 1987.

Ri 88-1: G. Riel, "The Effect of Temperature on the Response of the Chalk River Bubble-Damage Neutron Detector" in *Second Conference on Radiation Protection and Dosimetry* ORNL/TM-10971; 31 October-3 November 88.

Ri 88-2: G. Riel, N. Rao, R. Devine, T. Johnson, and R. Schwartz, "Super Heated Drop Neutron TLD Area/Spectrum Monitor" ibid.

Ri 88-3: G. Riel, et al. *Dose Equivalent LiF TLD Neutron and Photon TLD Area Monitor* NSWC TR 88-234.

Ri 91: G. K. Riel, N. Rao, H.F. Kerschner, and M.E. Nelson "Superheated Drop, "Bubble", Neutron Dosimeter Performance in a Work Environment" IEEE Transactions on Nuclear Science, Number 23 (April 1991).

Sc 90: R. B. Schwartz, and J. B. Hunt "Measurement of the Energy Response of Superheated Drop Neutron Detectors" Radiation Protection Dosimetry V. 34 #1/4 pp377-380 (1990).

[1] Bubble Technology Industries, HY 17, Chalk River, Ontario, CANADA, KOJ 1JO.

[2] APFEL Enterprises Inc. 25 Science Park, New Haven, CT, USA, 06511.

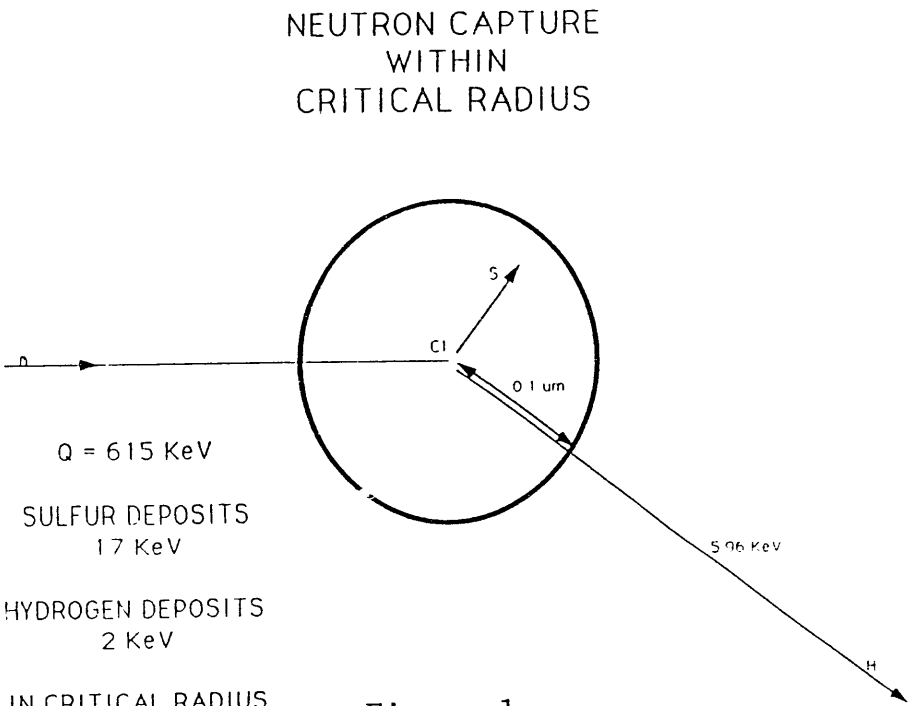

Figure 1

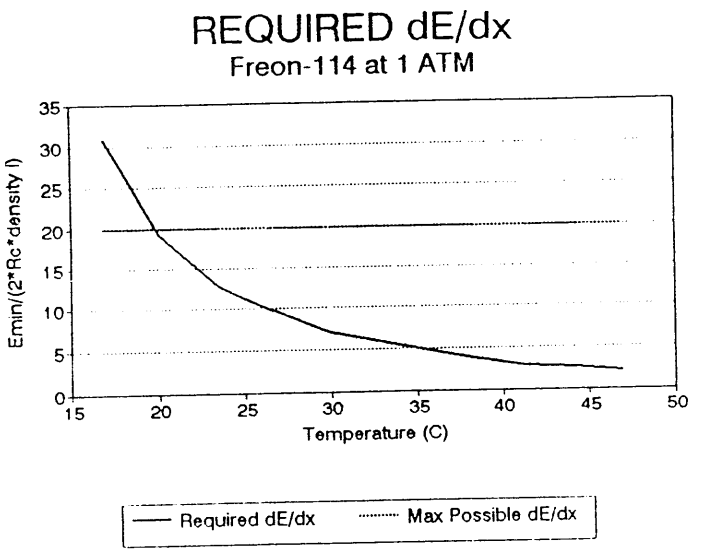

Figure 2

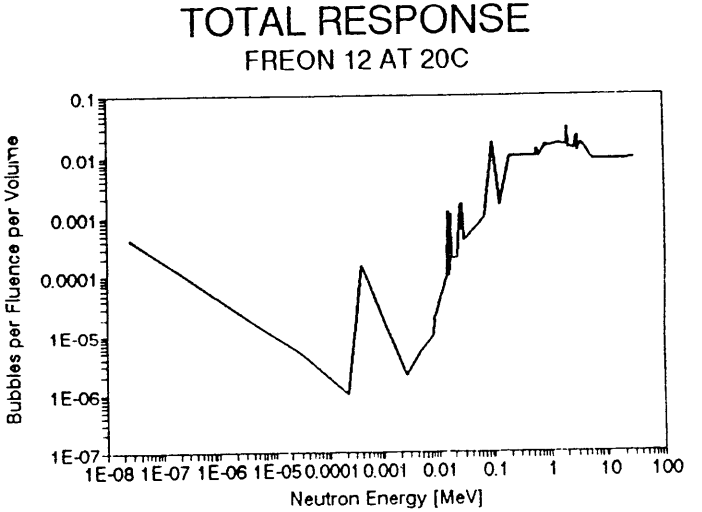

Figure 3

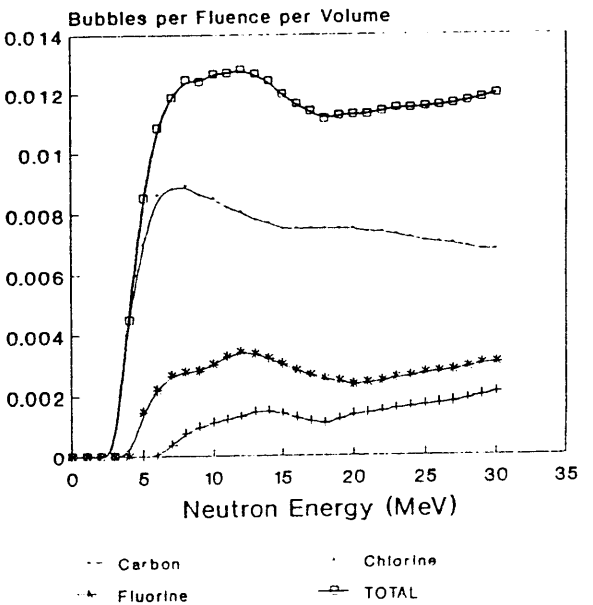

Figure 4

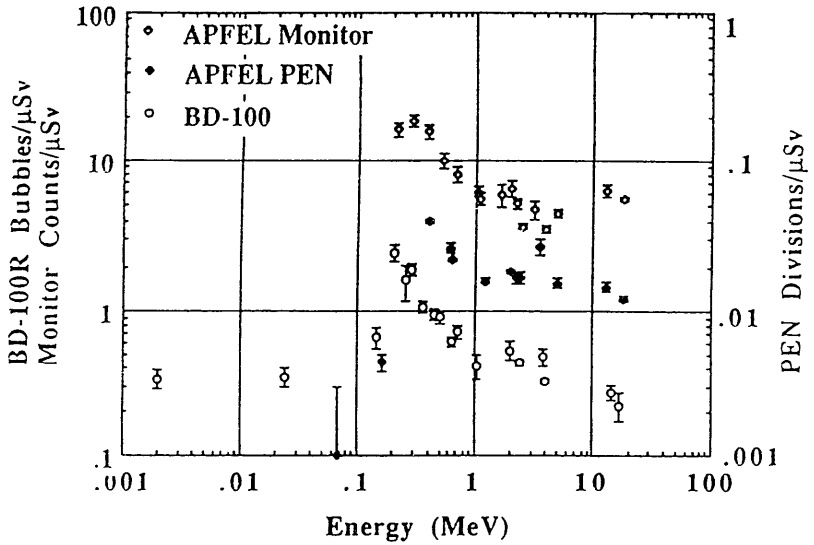

Figure 5

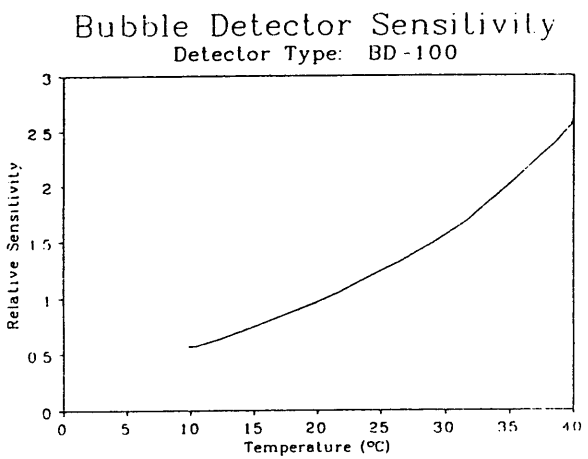

Figure 6

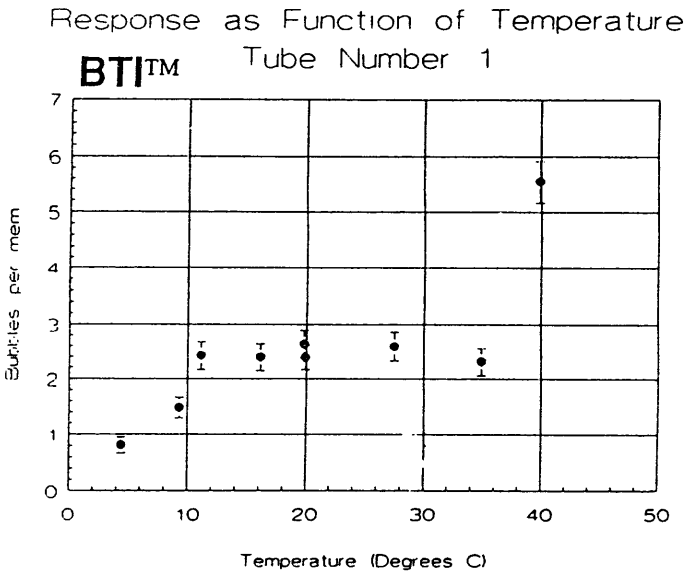

Figure 7

Bubble Dosimeter
With Thermoelectric Heat Pump

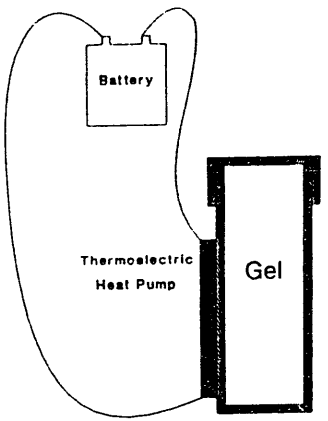

Figure 8

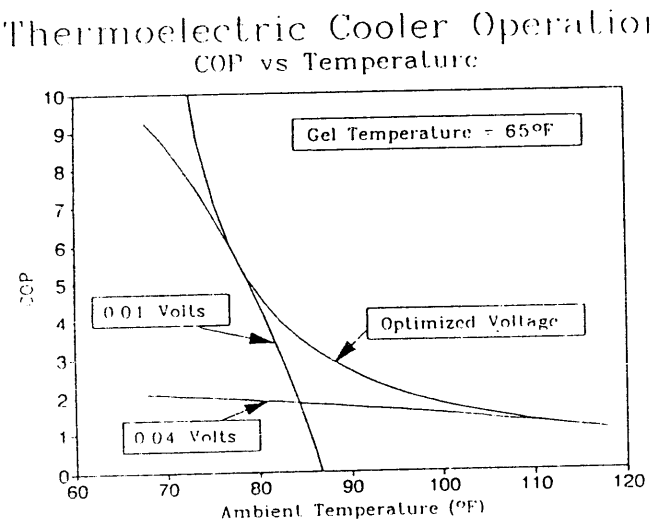

Figure 9

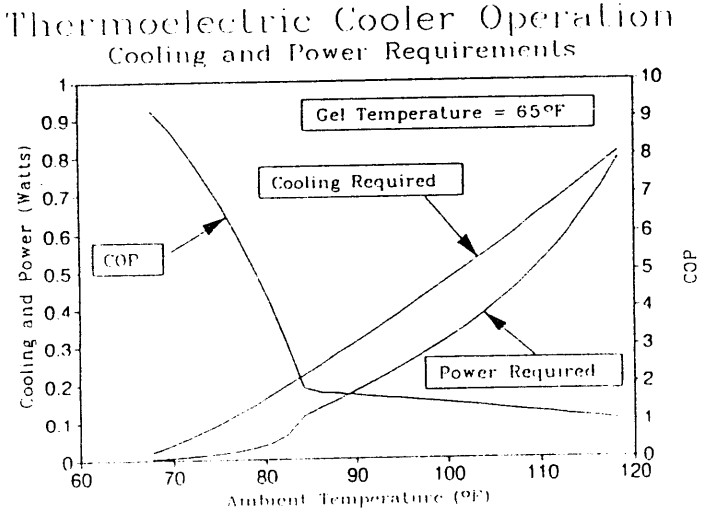

Figure 10

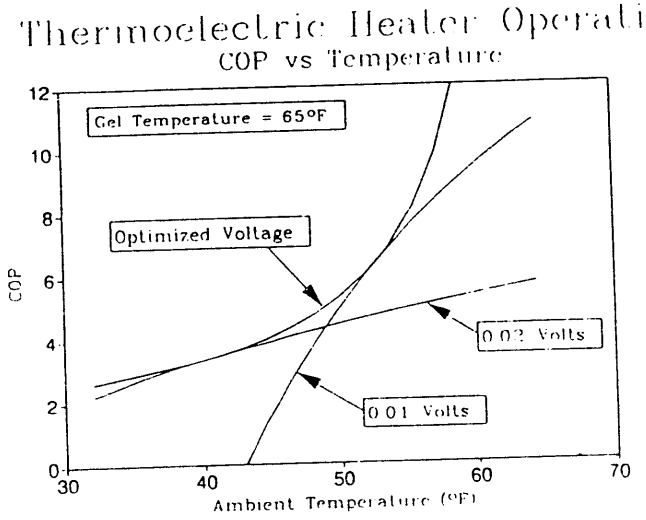

Figure 11

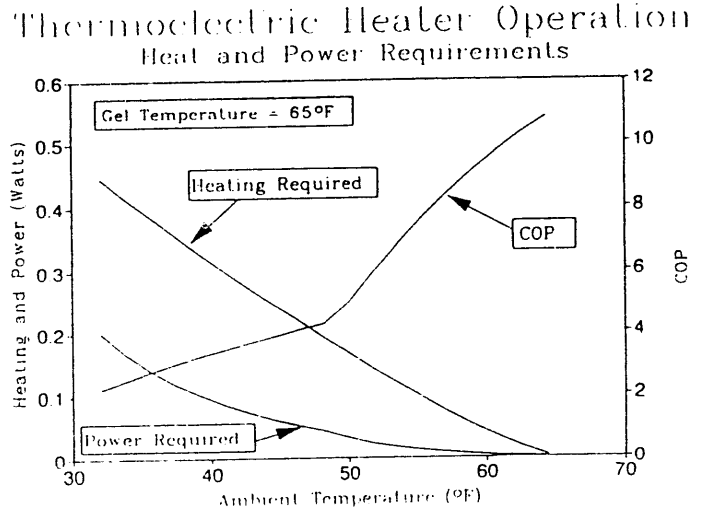

Figure 12

BD-100R Bubble Dosimeter

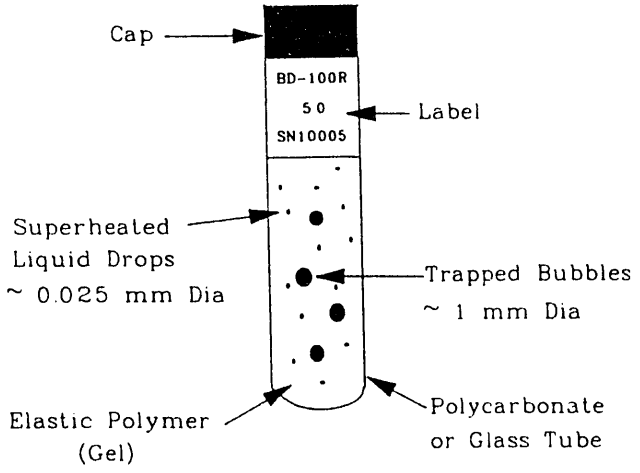

Figure 13

APFEL™ Liquid Matrix

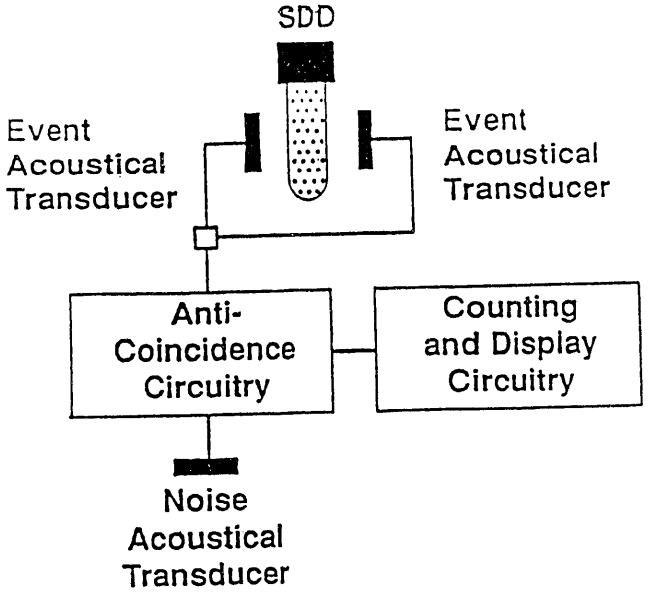

Figure 2. Block Diagram of APD/SDD

FOOTNOTE:

D. R. SISK ET AL IEEE 1989 NSS

"NEUTRON DOSIMETRY BASED ON SUPERHEATED MATERIALS"

Figure 14

Figure 15

BTI™ BD-100-R Response VS Time

(Test spans 40 days)

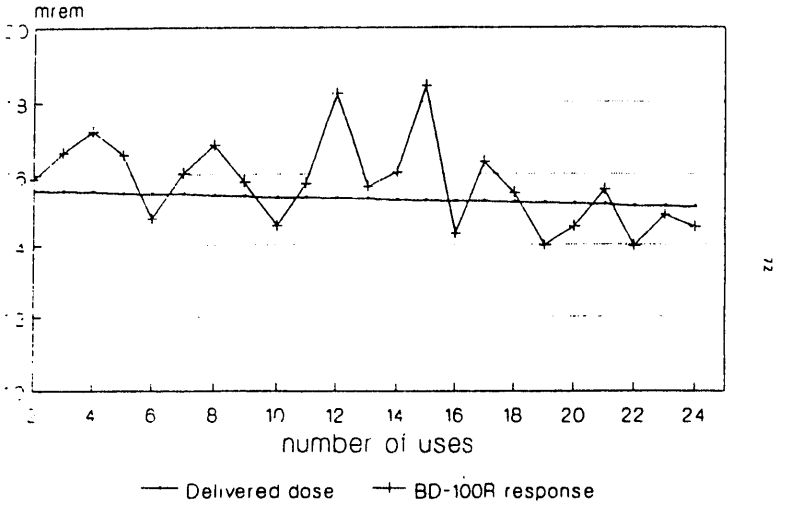

Figure 16

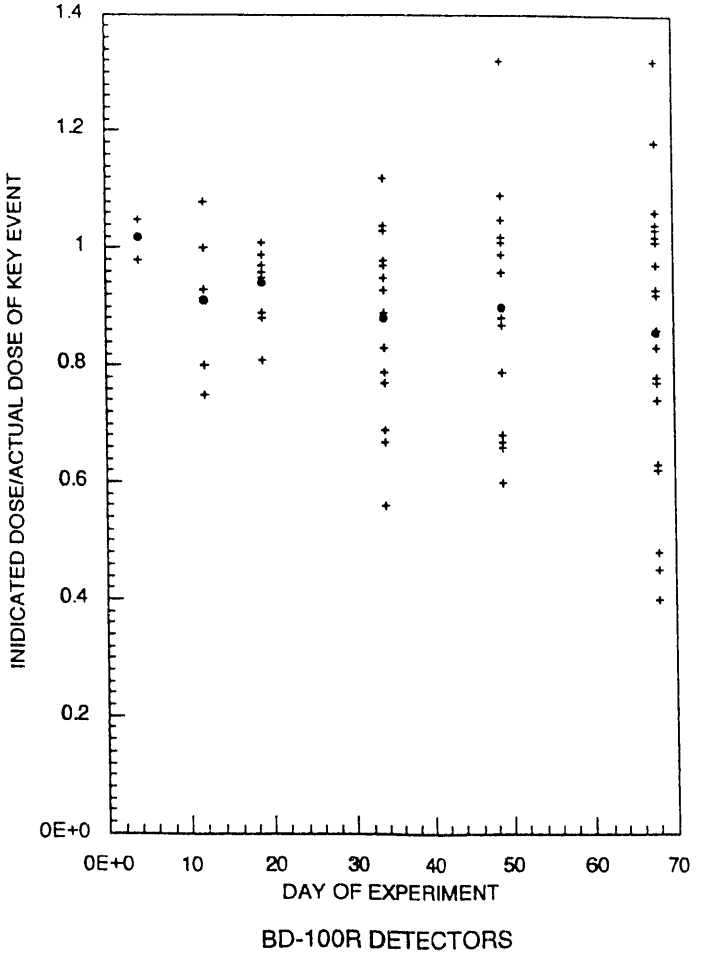

Apfel™ Efficiency VS Dose

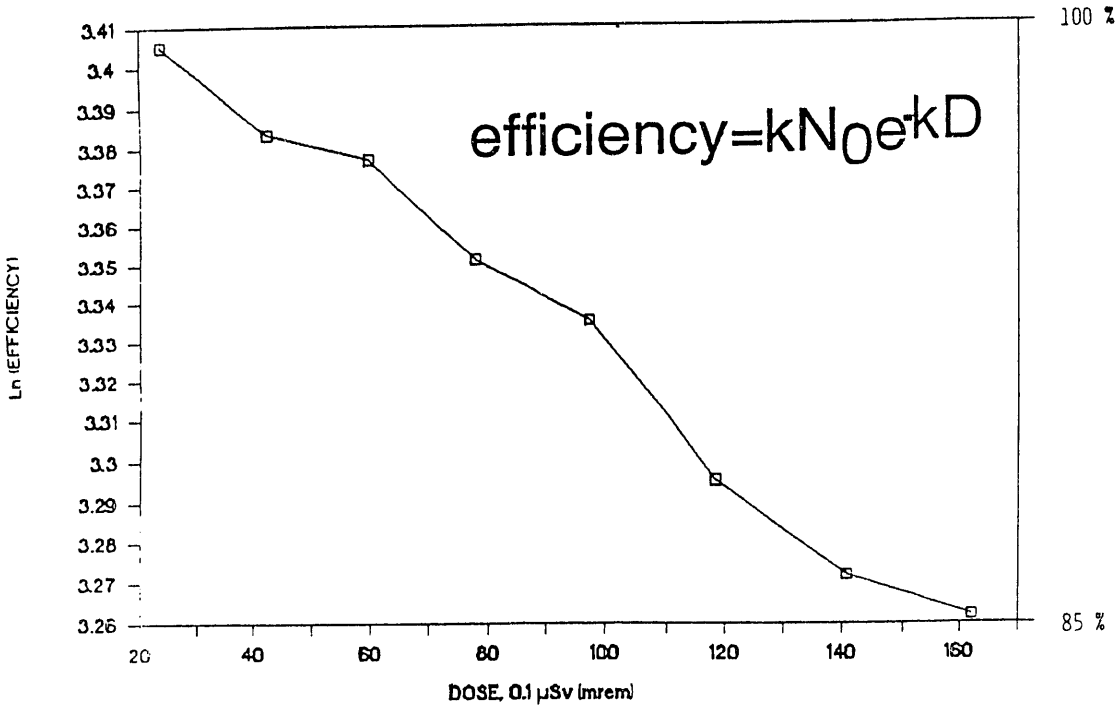

Figure 17

Apfel™ A/S Monitor Efficiency VS Time

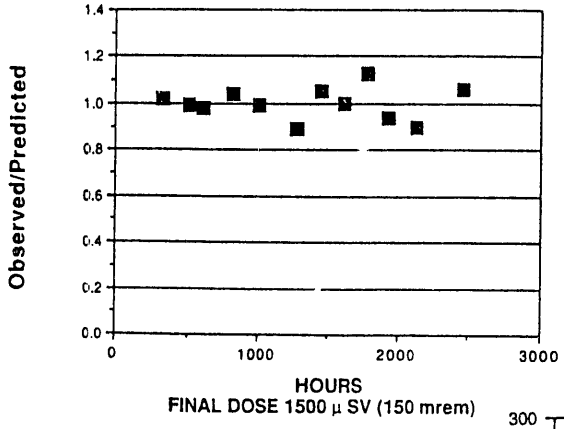

Figure 18

Figure 19

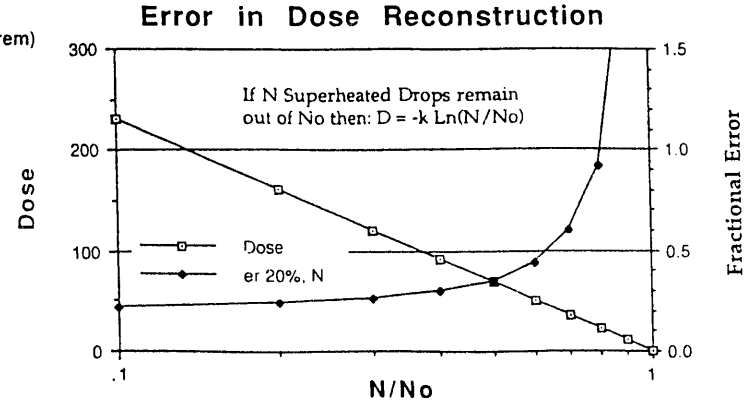

TABLE 1

EVALUATION OF BUBBLE FORMATION ENERGY FOR TYPICAL NEUTRON BUBBLE DOSIMETER LIQUIDS				
Theory: Minimum energy required to form bubble of critical radius (r_c) is provided by charged recoil particles from neutron interactions [Seitz, Phys. Fluids, 1,2 (1958)]				
Liquid		Freon-12®	Freon-114®	Isobutane
Chemical Formula		CCl_2F_2	$C_2Cl_2F_4$	C_4H_{10}
Boiling Point	°C	-29.8	3.8	-11.8
Temperature	°C	20	25	23
Saturated Vapor Pressure	atm	5.6	2.1	3.3
Pressure Drop $P_k - P_1 = \left(1 - \frac{v_1}{v_v}\right)(P_\infty - P_1)$	atm	4.5	1.1	2.3
Surface Tension (σ)	dyn/cm	9.7	12.0	11.2
Radius of Critical Bubble $R_c = 2\frac{\sigma}{P_\infty - P_1}$	cm x 10^{-6}	4.28	21.6	9.75
Minimum Reversible Work (Gibbs)	kev	0.46	14.6	2.78
Surface Free Energy $W_{s_1} = 4\pi r_c^2 \sigma$	kev	1.39	44	8.33
$W_{s_2} = -4\pi r_c^2 T \frac{d\sigma}{dT}$	kev	5.15	109	23
Vaporization Energy $W_v = \frac{4}{3}\pi^3 \rho_v h_{fg}$	kev	9.35	527	27
Expansion Energy $W_e = \frac{4}{3}\pi r_c^3 P_1$	kev	0.21	27	2.5
Total Bubble Formation Energy $W_g = W_{s_1} + W_{s_2} + W_v + W_\theta$	kev	16	707	60

TABLE 2. Properties of the P and N type materials used for the thermoelectric heat pump.

	P-Type	N-Type
Seeback Coefficient	0.0002	-0.00016 V/K
Resistivity	0.001	0.00105 Ω cm
Figure of Merit	0.0034	0.002 1/K
Thermal Conductivity	0.0118	0.0122 W/cm
Cross Sectional Area	0.993	K
Length	1.000	1.000 cm^2
		1.000 cm

TABLE 3

ERROR IN DOSE RECONSTRUCTION

N = # of Superheated Drops
S = Sensitivity, Bubbles/mrem
S = kN, So k = So/No
F at Dose D = N/No = S/So
So: D = - In(F)/k ± SQRT (err k^2 + (err F/D/k)^2)

Error in dose depends on the repeatability of the dosimeter, the fraction of drops remaining (F), and if F is determined by N or by S.

ERROR IN K=		20%	20%	5%	5%
ERROR IN F=		20%	28%	5%	7%
F		D±by	D±by	D±by	D±by
D,mrem					
1.00	0.00	(N/No)	(S/So)	(N/No)	(S/So)
0.90	10.54	191%	269%	48%	67%
0.80	22.31	92%	128%	23%	32%
0.70	35.67	60%	82%	15%	20%
0.60	51.08	44%	59%	11%	15%
0.50	69.31	35%	45%	9%	11%
0.40	91.63	30%	37%	7%	9%
0.30	120.40	26%	31%	6%	8%
0.20	160.94	24%	27%	6%	7%
0.10	230.26	22%	23%	5%	6%

TABLE 4

RELATIVE DETECTOR RESPONSE

Cd COVERED, NORMALIZED TO MCNP

DETECTOR	TYPE	14 MeV	Cf-252	CALIBRATION
MCNP	CALCULATION	1.00	1.00	FOILS
TEPC	PROPORTIONAL COUNTER	1.43	1.05	- - -
NE-213	SPECTROMETER	0.65	1.66	- - -
AN/PDR-70	REM METER	0.55	1.06	Pu-Be
BD-100R	BUBBLE DOSIMETER	1.14	1.30	Am-Be
CR-39	TRACK DOSIMETER	1.14	1.39	Cf-252
LiF TLD	PHANTOM	- - -	- - -	- - -
LiF TLD	AREA MONITOR	0.58	0.95	Cf-252
LiF TLD	LARGE LUCITE	0.16	0.53	D2O-Cf
LiF TLD	SMALL LUCITE	0.16	0.45	D2O-Cf
LiF TLD	NONE	0.02	0.03	D2O-Cf

U.S. NAVAL ACADEMY
TRIDENT SCHOLAR PROGRAM
ENS Michael Wilson
ADVISOR: PROF. M. Nelson

DOSIMETERS FOR MEASURING NEUTRON DOSE EQUIVALENT: NEW APPROACHES

M. Moscovitch

Department of Radiation Medicine
Georgetown University School of Medicine
3800 Reservoir Rd., N.W.
Washington, DC 20007-2197

ABSTRACT

Continued advancement in electronic dosimetry and recent success in developing new high-sensitivity thermoluminescent (TL) materials provide novel and exciting possibilities for developing improved neutron dosimeters.

INTRODUCTION

Development of electronic personnel dosimeters for photons is underway in several laboratories. These dosimeters, based on silicon detectors, are capable of covering a wide photon energy range (17 keV to 7.0 MeV). The possibility of expanding this concept and developing a *multi-element personnel beta-gamma-neutron microelectronic dosimeter* is discussed. The second part of this paper deals with recent improvements in neutron thermoluminescent dosimetry (TLD) including the new Harshaw albedo TLD and the potential application of high-sensitivity thermoluminescent materials to neutron dosimetry.

BETA-GAMMA-NEUTRON ELECTRONIC PERSONNEL DOSIMETRY

Electronic personnel dosimeters for photon and beta fields typically consist of two major components, one or more silicon diodes, and the signal processing circuit. Ionizing radiation interacting with the diode produces electron-hole pairs which are separated by the detector's internal electric field, resulting in charge pulses. These pulses are amplified, counted and stored for further processing and dose calculation. An electronic dosimeter using a pair of PIN silicon photodiodes has been developed recently[1] at the National Radiation Protection Board in England. There are obvious advantages to electronic dosimetry: real time dose indication, use of off-the-shelf components, no need for a reader and the ability to transfer the dose information to a central computer using a modem. This concept might be expanded to enable dosimetry in photon-beta-neutron mixed fields by combining PIN photon-beta dosimeters with dynamic random access memories (DRAM), the latter acting as the neutron sensitive element. In a DRAM, binary information is stored as a charge on small cells (miniature capacitors). Neutron-induced heavy charged particles can cause a random error to appear by generating a sufficient concentration of electrons in the vicinity of the cell to change the amount of charge stored, causing a bit

flip (a change of "1" to "0"). Assuming that the W value in silicon is 3.6 eV, it can be shown[2] that 10^5-10^6 electrons typically are needed to cause a bit flip, which corresponds to energy in the range of 360 keV-3.6 MeV. Considering the fact that typical cell dimensions are on the order of a few μm, it is expected that the sensitivity to low LET radiation, including gamma, will be negligible.

Recent feasibility studies[3] using 64 K memory chips (Apple II microcomputer) have demonstrated that thermal neutron dose levels as low as 25 μSv could be detected. A possible configuration of a multi-element personnel electronic dosimeter might consist of two photodiodes for photon-beta monitoring and two DRAM memory chips, one covered by polyethylene and the other by ^{6}LiF for fast and thermal neutron monitoring respectively. However, before such a multi-element dosimeter can be considered for practical use, its response has to be characterized and *dose calculation algorithms*[4] need to be developed. Furthermore, the effectiveness of the dosimeter-algorithm combination needs to be tested at dose levels and neutron energies and with radiation types typical of routine field use.

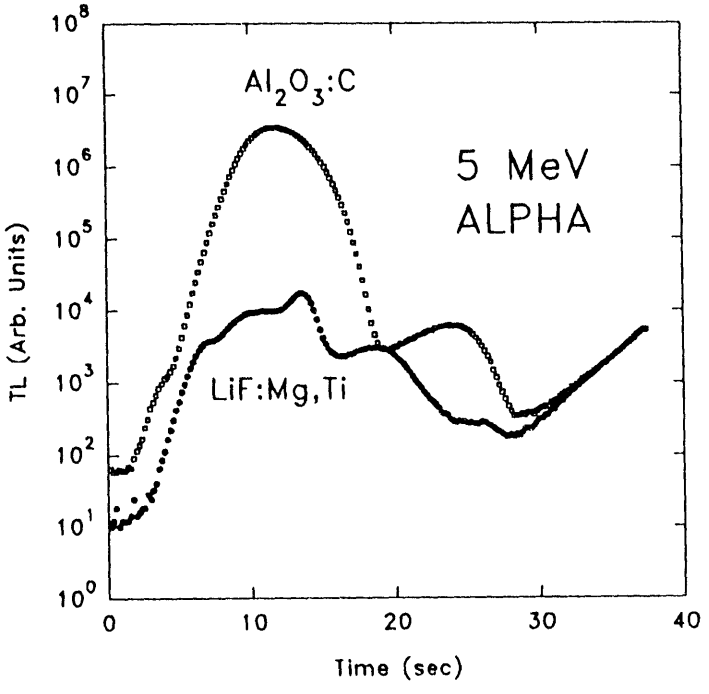

FIGURE 1. Glow curves for LiF:Mg, Ti and Al_2O_3:C for 5 MeV α-particle irradiation. Note the high temperature peak of the Al_2O_3:C glow curve.

IMPROVED NEUTRON THERMOLUMINESCENT DOSIMETRY

Although both albedo and direct proton recoil TL neutron dosimeters are known to have serious limitations, their small size, wide dose range, and the availability of automatic commercial TLD readers make it worth investigating their full potential.

A new type of albedo multi-element TLD[5] was recently developed. The dosimeter consists of four LiF:Mg,Ti paired TLD-600 and TLD-700 chips. One pair is filtered with plastic and the other with cadmium, to enable fast neutron discrimination in the presence of a thermal neutron field. The contribution to the TL signal of the incident photons and electrons, as well as the contribution of the cadmium capture gamma rays and the small contribution of the incident fast neutrons, are treated as noise and subtracted out, taking advantage of the symmetry of the dosimeter. This dosimeter has passed, by a large margin, all the neutron test categories of the Department of Energy Laboratory Accreditation Program (DOELAP).

The new high-sensitivity[6]TL materials LiF:Cu,Mg,P and Al_2O_3:C, 25 and 60 times more sensitive than TLD-100 respectively, are both excellent candidates for improved proton recoil direct neutron dosimetry. To determine whether Al_2O_3:C could be the basis of the useful "direct" neutron dosimeter, we have recorded glow curves following 5 MeV α-particle irradiation. The results shown in Figure 1 demonstrate that for α-particle irradiation, Al_2O_3:C maintains its high sensitivity relative to LiF:Mg,Ti (TLD-700). By taking advantage of the high sensitivity of the new materials and reducing their thickness, it can be expected that their neutron-to-gamma response ratio can be improved, while remaining sufficient sensitivity to enable low dose dosimetry. However, both experimental and theoretical work is needed to investigate the fast neutron response of different combinations of high-sensitivity thin TLDs with hydrogen-containing radiators.

REFERENCES

1. Marshall T. O., D. T. Bartlett, P.H. Burgess, C. S. Cranston, D. J. Higginbottom, and K. W. Sutton. 1990. Electronic Personal Dosimeter. *Radiat. Prot. Dosim.* 34:93-97.

2. Haque, A.K.M.M. and M. H. Ali. 1990. Modeling of Alpha Particle Induced Soft Errors in Dynamic Random Access Memories (DRAM). *Radiat. Prot. Dosim.* 31:101-105.

3. Haque, A.K.M.M. and M. H. Ali. 1989. Neutron Dosimetry Employing Soft Errors in Dynamic Random Access Memories. *Phys. Med. Biol.* 34:1195-1202.

4. Moscovitch, M. 1991. Effective Algorithms. *Radiat. Prot. Dosim.* 35:147-148.

5. Moscovitch, M., K. J. Velbeck, and J. D. Chamberlain. 1990. "Personnel Neutron Dosimetry Via a Symmetric Multi-Element Thermoluminescent Dosimeter." In Proc. 35th Annual Meeting of the Health Physics Society, Anaheim CA, June 24-28, Abstract THPM-D13.

6. Lucas, A.C. 1991. Hypersensitive Dosemeters. *Radiat. Prot. Dosim.* 35:219.

ACKNOWLEDGMENTS

The author wishes to thank Dr. S. Doremus for proposing the α-particle irradiation experiment and Nicki Dean for editorial assistance.

NEUTRON SPECTROMETRY: METHODS DEVELOPMENT AND CRITICAL APPLICATIONS

F. Hajnal

INTRODUCTION

Since the inception of multisphere neutron spectrometers (Bramblett et al. 1960), EML scientists have been involved in the development of these spectrometers (O'Brien et al. 1965), various applications in radiation protection (Weinstein 1970), the development of unfolding codes (Sanna and O'Brien 1971), and the calculation of their response functions (Sanna 1973). These traditions continue at EML, and we have what one might call the state-of-the-art instrumentation and data analysis techniques.

The essence of the Bonner sphere method is to expose the detectors to neutron radiation fields and take successive counts with thicker and thicker moderators surrounding a neutron capture detector. For example, for a given medium energy of neutrons the count rate increases and then drops as the moderator thickness increases. The spectral shape may be inferred from the relative responses of the detector in the variously-sized moderating spheres. This kind of spectrometer has been used extensively in radiation protection practice to determine neutron spectral distributions around particle accelerators (Awschalom 1966), nuclear power stations (Hajnal et al. 1979), and other nuclear facilities (Awschalom and Sanna 1985), as well as in cosmic ray neutron research (Hajnal et al. 1971, Nakamura et al. 1987). This spectrometer system has proven to be very useful since it is simple, portable, has an isotropic response and covers a wide energy range (Cross and Ing 1987). The data can be unfolded and interpreted fairly easily using one of the EML-developed unfolding codes.

Dose equivalent values derived form Bonner sphere neutron spectral measurements are important for regulatory purposes, for epidemiological studies and also for the determination of the "stay" time of experimenters and maintenance personnel in neutron radiation fields. At EML, neutron spectrometry is carried out on an occasional basis, usually to answer specific research requirements or questions at EML and other facilities.

THE BONNER SPHERE SPECTROMETER

The primary EML Bonner sphere spectrometer system consists of 12 (twelve) moderated polyethylene spheres equipped with boron-trifluoride proportional counters. The spectrometers are usable either in parallel or in the independent mode. The spectrometer response functions were calculated at ORNL (Maerker et al. 1971, Burgart et al. 1972), using different numerical methods (such as those incorporated in the ANISN and MORSE codes), different evaluated neutron cross section sets, and different energy binning. The calculated detector response functions are considered sufficiently accurate since the results obtained using different cross section sets and transport codes differ by only a few percent for the entire energy region. The Bonner sphere spectrometer calibrations, whenever possible,

are performed with the National Institute of Science and Technology (NIST) monoenergetic neutron beams, and the normalization of the overall response functions determined using Cf-252 spontaneous fission neutron sources. At EML, Cf-252 calibrations are performed in an open air calibration facility, where the air and ground scattering contribution in the worst case amounts to only 3% at 1 m source-to-detector separation (Hajnal 1970; Hunt 1984).

Data Analysis - Unfolding

The result of a set of measurements with Bonner spheres is a set of 12 count rates for the 12 detector configurations. A mathematical method known as unfolding is used to obtain a neutron spectrum form these data. This is accomplished using a computer code based on the TWOGO code, which was developed at EML (Hajnal 1981). The unfolding code provides a reasonable estimate of neutron fluence rate vs. energy, i.e., a neutron spectrum. The code also provides an estimate of the shape, called trial vector, of the neutron spectrum and the unfolding is performed iteratively as the code adjusts the spectrum to fit and be consistent with the data. Estimates of the relative errors of individual counts may be used as weight factors during

Several indices are computed with the TWOGO program that serve to measure the goodness of fit of the unfolding process. These indices are based on determining the degree of agreement between data obtained by observation; i.e., count rates due to neutrons for each of the detector configurations, and synthetic counts or estimates of these same parameters obtained by folding together the response matrix and the spectrum obtained by the unfolding process.

A solution can be called exact, approximate, or appropriate. Exact solutions may have zero errors, and might look reasonable. However, they may have unphysical characteristics, such as oscillations. Usually, the unfolded data should not be expected to have too good a fit, at least not better than the error of the input data. Appropriate solutions can be obtained from good measurements, and considerable experience is needed to obtain a reasonable spectral solution.

Accomplishments:

The researchers at the Radiation Physics Division of EML are recognized authorities on neutron spectral measurements, unfolding and error analysis. As a result of this they are frequently invited to either participate in important neutron spectral measurements at DOE facilities or to provide reference neutron spectral measurements in other contexts.

Three examples of such neutron spectral measurements are the following:

- The first was to assist the DOE-sponsored research group in the reassessment of the population radiation doses form the explosion of "Little Boy' at Hiroshima. A replica of the bomb was built and operated as a critical assembly at the Los Alamos National Laboratory for a period of time. The EML measurements (Hajnal and Griffith 1985), the only spectral measurements at distances greater than two meters from the core, were performed in different directions at distances of 2

to 570 meters from the assembly, which was mounted outdoors at a height of four meters. The evaluated dose-equivalent values agree well with the calculated dose-equivalent values for the actual Little-Boy in dry and humid air.

- The second set of measurements were at the now-decommissioned HPRR at ORNL. Since its startup the Health Physics Research Reactor, HPRR, provided reference spectra for many "Nuclear Accident Dosimetry Intercomparison Studies," and for "Personnel Dosimetry Intercomparison Studies." Many scientists from national laboratories in the USA and abroad participated in these studies to test dosimeters and to verify their own calibration procedures. In late 1985 a request was made by the Oak Ridge National Laboratory to perform measurements of the neutron energy spectra produced by the HPRR. These measurements were necessary to experimentally verify calculated reference spectral and dose data used to provide facility users with exposure conditions and spectral characteristics.

- The third, also at ORNL at the HFIR and TRU facilities, was conducted in January-March 1989, to provide ORNL with several reliable, good-quality neutron spectra to establish benchmark reference locations for dosimetric purposes. The High Flux Isotope Reactor (HFIR) and Transuranic Processing Plant (TRU) provide large quantities of transuranic elements for research purposes. The irradiated targets are highly radioactive and many of them decay via spontaneous nuclear fission, accompanied by a copious number of neutrons. At that time reference neutron spectral measurements were also performed at a new ORNL calibration laboratory (Liu et al. 1990).

Other important neutron spectral measurements and field characterizations:

1. Measurement of the Neutron Radiation Fields at the Princeton Tokamak Fusion Test Reactor (TFTR)

The Tokamak Fusion Test Reactor (TFTR), located at the Princeton University Plasma Physics Laboratory, was built for the purpose of studying plasma physics in a large tokamak (tokamak is doughnut in Russian), to gain engineering experience and to demonstrate that significant amounts of energy will be released in deuterium-tritium (D-T) reactions. Since the TFTR project started in the late 1970s, the TFTR has operated in the deuterium-deuterium (D-D) mode, producing record numbers of neutrons and plasma temperatures up to 400 million degrees C. In the early 1990s a D-D breakeven (breakeven: input energy output energy), followed by D-T installation and D-T breakeven, should occur.

During the D-D operations two reactions occur: one producing 3-He and a neutron which releases 3.3 MeV energy and the other producing tritium and a proton which releases 4.0 MeV energy. Some of the produced tritium will burn up, and the reaction produces 4-He and a neutron and releases 17.6 MeV energy. In all cases the released energy will be partitioned off among the products.

The purposes of the recent experiments were to provide reference radiation field quantities at designated locations around the TFTR for experimental, regulatory and calculational purposes and to

provide consultation with respect to the TFTR shielding. The crucial sites are at the boundary of the TFTR reactor, and the nearest is at 176 meters from the TFTR center. The TFTR general radiation protection design objective for normal operations as agreed upon by DOE is to limit the dose equivalent at the laboratory property line from all sources and pathways to 0.1 mSv/yr (Hajnal et al. 1991).

In the experiments, conducted in October 1990, Bonner sphere neutron spectrometers were used on the outside of the shielding very near the wails. Activation foils were positioned on the inside of the shielding at the same heights and locations, and also at 125-meter distance from the center and 50 meters from the nearest boundary line. The experimental setup, procedures, data analyses, and results have been reported, and an EML report is in preparation. Preliminary analyses for the property line for both D-D and D-T operations producing 5E+20 neutrons per year show that the design of the TFTR shielding is sufficient to meet regulatory requirements.

These studies will continue in order to experimentally characterize the radiation fields of future fusion reactors, both neutron and gamma, to benchmark shielding calculations, and to quantitatively determine the ratio of D-D to D-T reactions, which is important in breakeven studies.

2. Sea-Level Cosmic-Ray Neutron Spectral Measurements

The annual absorbed cosmic-ray neutron dose and annual effective dose equivalent were evaluated from neutron spectral measurements at EML in 1971. Sea-level cosmic-ray neutrons contribute about 10% to the total cosmic-ray dose equivalent rate, using QF = 10, and this contribution increases rapidly with altitude. Therefore it is prudent to know the cosmic ray neutron dose and dose-equivalent values with reasonable accuracy.

The EML neutron spectrometer system is well suited for these kinds of measurements, and we commenced new cosmic-ray neutron spectral measurements in 1986. The new unfolding method was used to analyze the data, and to obtain dose and dose-equivalent rates. The 1986 neutron flux density of 0.0078 n/cm$^{\sim}$/s compares favorably with the 1970 flux density of 0.0082 n/cm$^{\sim}$/s. The dose equivalent rate 1986 was 0.0572 μSv/y and 1970 was 0.0718 μSv/y (Hajnal 1989). The 1970 measurements were performed near solar maximum, i.e., when the cosmic-ray flux was near its lowest intensity, and the 1986 measurements were during solar minimum, i.e., when the cosmic-ray flux was near its highest intensity. These intensity changes are reflected by the corresponding neutron flux and dose equivalent values.

The precise knowledge of the cosmic-ray neutron spectrum is also important in special experimental situations. For example the APR, Aberdeen Army Pulse Reactor, is used to validate the Hiroshima does reevaluation calculations at large, $\sim$400 to 2500 m, distances from the reactor. The measurements were corrected for the sea-level cosmic-ray neutron contribution. An analogous correction was made for the Princeton data (see above).

3. High-Altitude Cosmic Ray Neutrons: Probable Source for the High-Energy Protons of the Earth's Radiation Belts

Several high-altitude cosmic-ray neutron measurements were performed by the NASA Ames Laboratory in the mid- to late-1970s using airplanes flying at about 13 km altitude along constant geomagnetic latitudes of 20, 44, and 51 degrees north. Bonner spheres and manganese, gold and aluminum foils were used in the measurements. In addition, large moderated BF-3 counters served as normalizing instruments.

Data analyses performed at that time did not provide complete and unambiguous spectral information and field intensities. recently, using out new unfolding methods and codes, and Bonner-sphere response function extensions to higher energies, "new" neutron spectral intensities were obtained, which show progressive hardening of neutron spectra as a function of increasing geomagnetic latitude, with substantial fluence increases in the energy region from 10 MeV to 10 GeV (Hajnal and Wilson 1991).

For example, we found that the total neutron fluences at 20 and 51 degrees magnetic north are in the ratio of 1 to 5.2 and the 10 MeV to 10 GeV fluence ratio is 1 to 18.

The magnitude of these ratios is quite remarkable. From the new results, the derived absolute neutron energy distribution is of the correct strength and shape for the albedo neutrons to be the main source of the high-energy protons trapped in the Earth's inner radiation belt. In addition, the results, depending on the extrapolation scheme used, indicate that the neutron dose equivalent rate may be as high as 0.1 mSv/h near the geomagnetic north pole and thus a significant contributor to the radiation exposures of pilots, flight attendants and aircraft passengers. We have started to compare our results with Monte-Carlo and analytical calculations, and to calculate the albedo neutron flux necessary to determine the source term for the radiation belt protons. A collaboration with several laboratories in the United States and in Europe to study the properties and dose contribution of these neutrons is currently being developed.

4. Neutron Spectroscopy. Significant Technology Transfers at EMR

Given this experience, EML scientists are able to design and conduct new kinds of radiation spectroscopic measurements, data analyses, data reduction and interpretations, which are relevant to the safety of the work place in the complex nuclear fuel cycle. Such developments later are transferred to the nuclear industry. Examples of this technology transfer are the adoption of EML neutron spectroscopy methodology, including unfolding, data reduction and interpretation skills, by Rocky Flats, Lawrence Livermore National Laboratory, South Carolina Power and Light Co., John Hopkins University, and Rensselaer Polytechnic Institute, among others.

REFERENCES

Awschalom, M. 1966. "Use of the Multisphere Neutron Detector for Dosimetry of Mixed Radiation Fields." Symposium on Neutron Monitoring for Radiological Protection, Vienna, 29 Aug-2 Sept, 1966, IAEA/SM76/16,1966, SAME AS PPAD-596-E.

Awschalom, M. and R. S. Sanna. 1985. "Application of Bonner Sphere Detectors in Neutron Field Dosimetry." *Radiat. Prot. Dosim.* 10:89.

Bramblett, R. L., R. I. Ewing, and T. W. Bonner. 1960. A New Type of Neutron Spectrometer. *Nucl. Instr. Meth.* 9:1.

Burgart, C. E. and M. B. Emmett. 1972. Monte Carlo Calculations of the Response Functions of Bonner Ball Neutron Detectors. ORNL-TM-3739, Oak Ridge National Laboratory, Oak Ridge, Tennessee.

Cross, W. G. and I. Ing. 1987. Neutron Spectrometry. In "The Dosimetry of Ionizing Radiation," Volume 11 (K. R. Kase, B. E. Bjarngard, and F. A. Attix, eds.), pp. 91-169, Academic Press, Orlando, FL.

Hajnal, F. 1981. An Iterative Nonlinear Unfolding Code: TWOGO. Report Number EML-391. U.S. Department of Energy, Environmental Measurements Laboratory, New York.

Hajnal, F. 1989. Sea-Level Cosmic-Ray Neutron Measurements. Environmental Measurements Laboratory Annual Report - Calendar Year 1988. Report EML-520, pp. 47-49, Environmental Measurements Laboratory, New York.

Hajnal, F. and R. V. Griffith. 1985. Least Squares Unfolding and Error Analysis of Bonner Sphere Neutron Measurements: Application to PWR and 'Little Boy' Critical Assembly Measurements. Proceedings of the 5th Symposium on Neutron Dosimetry, EUR 9762 EN, pp. 415-426, CEC, Luxemburg.

Hajnal, F., J. E. McLaughlin, and R. Oeschler. 1970. "Technique for Determining Moderated-Neutron Instrument Characteristics." US AEC, HASL-222.

Hajnal, F., J. E. McLaughlin, M. S. Weinstein, and K. O'Brien. 1971. 1970 Sea-Level Cosmic-Ray Neutron Measurements. USAEC Report HASL-241.

Hajnal, F., R. S. Sanna, R. M. Ryan, and E. H. Donnelly. 1979. "Stray Neutron Fields in the Contaminant of PWRs." IAEA-SM-242/24.

Hajnal, F., N. Azziz, K. Decker, P. Goldhagen, G. Klemic, K. Miller, S. Sanderson, R. Sanna, P. Shebell, K. W. Hill, and H. K Hill. "Measurement of the Neutron Radiation Fields at the Princeton

Tokamak Fusion Test Reactor (TFTR)." A paper submitted for presentation at the Seventh Symposium on Neutron Dosimetry, 14-18 October 1991 in Berlin, Germany.

Hajnal, F. and J. W. Wilson. "High-Altitude Cosmic Ray Neutrons: Probable Source for the High-Energy Protons of the Earth's Radiation Belts." A paper submitted for presentation at the Seventh Symposium on Neutron Dosimetry, 14-18 October 1991 in Berlin, Germany.

Hunt, J. B. 1984. "The Calibration of Neutron Sensitive Spherical Devices." *Radiat. Prot. Dosim.* 8:239.

Liu, J. C., F. Hajnal, C. S. Sims, and J. Kuiper. 1990. Neutron Spectral Measurements at ORNL. *Radiat. Prot. Dosim.* 30, 169-178.

Maerker, R. E., I. R. Williams, F. R. Mynatt, and N. M. Greene. 1971. Response Functions for Bonner BaH Neutron Detectors. ORNL-TM-3451, Oak Ridge National Laboratory, Oak Ridge, Tennessee.

Nakamura, I., Y. Uwamino, T. Ohkubo, and H. Hara. 1987. Altitude Variation of Cosmic Ray Neutrons. *Health Phys.* 53:509.

O'Brien, K., R. S. Sanna, and J. E. McLaughlin. 1965. "Inference of Accelerator Stray Neutron Spectra from Various Measurements." Proceedings of the USAEC First Symposium on Accelerator Radiation Dosimetry and Experience, held at Brookhaven National Laboratory, Upton, N.Y., November 3-5, 1965, CONF-651109.

Sanna, R. S. 1973. "Thirty One Group Response Matrices for the Multisphere Spectrometer, Over the Energy Range Thermal to 400 MeV." HASL-267.

Sanna, R. S. and K. O'Brien. 1971. "Monte Carlo Unfolding of Neutron Spectra." NIMS 91:573.

Weinstein, M. S., J. E. McLaughlin, and K. O'Brien. 1970. "Neutron Dose Equivalents from Multisphere Accelerator Shield Leakage Spectra." HASL-223.

Also an invited paper will be presented at the 1991 Winter American Nuclear Society Meeting in San Francisco, CA, November 10-15, 1991.

FIELD NEUTRON SPECTROMETER USING ^{3}He, TEPC, AND MULTISPHERE DETECTORS*

L. W. Brackenbush

Pacific Northwest Laboratory
Richland, Washington

INTRODUCTION

Since the last DOE Neutron Dosimetry Workshop, there have been a number of changes in radiation protection standards proposed by national and international advisory bodies. These changes include: increasing quality factors for neutrons by a factor of two, defining quality factors as a function of lineal energy rather than linear energy transfer (see ICRU-40; Joint Task Group 1986), and adoption of effective dose equivalent methodologies. In order to determine the effects of these proposed changes, it is necessary to know the neutron energy spectrum in the work place. In response to the possible adoption of these proposals, the Department of Energy (DOE) initiated a program to develop practical neutron spectrometry systems for use by health physicists. One part of this program was the development of a truly portable, battery operated liquid scintillator spectrometer using proprietary electronics developed at Lawrence Livermore National Laboratory (LLNL); this instrument will be described in the following paper. The second part was the development at PNL of a simple transportable spectrometer based on commercially available electronics. This "field neutron spectrometer" described in this paper is intended to be used over a range of neutron energies extending from thermal to 20 MeV.

The purpose of this work was to develop a simple-to-use neutron spectrometer system to measure neutron energy spectra, determine quality factors, and dose equivalent rates. It was intended to be transportable for use by health physicists in DOE facilities. The system was to be thoroughly tested by performing actual measurements in the work place, primarily at plutonium processing facilities where most neutron exposers occur. Some of these measurements are described in the workshop proceedings by J. J. Fix at Hanford and K. McMahan at Oak Ridge.

FIELD NEUTRON SPECTROMETER

About 15 years ago, PNL staff started making neutron energy spectrum measurements at commercial nuclear power plants and several DOE production facilities. This involved moving about 600 pounds of NIM bin electronics and multichannel analyzers; it was not very portable. This has been replaced using the field neutron spectrometer shown in Figure 1. A complete description of the system, including construction details, operating instructions, and the results of laboratory and field tests are included in PNL-6620, Vol. 2, Personnel Neutron Dose Assessment Upgrade, Volume 2: Field Neutron

* Work supported by the U.S. Department of Energy under Contract DE-AC06-76RLO 1830.

Spectrometer for Health Physics Applications (L. W. Brackenbush et al. 1988) and PNL-6620, Vol. 3, Field Neutron Spectrometer with Multisphere Detectors (L. W. Brackenbush, R. I. Scherpelz 1990). The field neutron spectrometer concept is based on a commercially available multichannel analyzer with four input ports mounted in a suitcase, as shown in the figure. The data collection and analysis is controlled by a lap top personal computer mounted in the suitcase. Although a number of personal computers may be adequate, the PNL system uses a Grid computer with a gas plasma display. This computer has proven dependability with over four years use in harsh operating environments, including inside containment of commercial nuclear power plants at temperatures in excess of 130 °F (54 °C).

A number of different neutron detectors can be used with the field neutron spectrometer system, including ^{3}He proportional counters, tissue equivalent proportional counters (TEPCs), and multisphere or Bonner sphere detectors. The these detectors were selected for ease of use and ease of data analysis in the field. The necessary ancillary electronics can be built into the base of the detectors or it can be included in mini-NIM bins using commercially available preamps, amplifiers, and high voltage supplies.

The ^{3}He proportional counter was selected because of it successful use in measuring the low energy neutrons in commercial nuclear power plants, in which almost all of the neutrons have energies below 1 MeV. The ^{3}He proportional counter is self-calibrating by exposing the detector to thermal neutrons and observing the 764 keV peak produced by ^{3}He(n,p)T reactions. Using this peak as a reference, a simple "stripping" program called HESTRIP calculates the incident neutron energy spectrum from response functions for each type of proportional counter used. Typically, 1-inch diameter tubes with less than 5 psi ^{3}He in argon at 1 atmosphere are used for low energy spectra below 1 MeV. Larger tubes with higher pressures are used for higher neutron energies. It was recommended that a 2.5-inch diameter proportional counter containing several atmospheres of ^{3}He be used for measuring fission neutron spectra below 5 MeV. However, field tests have demonstrated that the high pressure proportional counters have gamma-neutron separation problems. It is necessary to use pulse-shape discrimination techniques to separate neutron events from gamma ray events. The additional circuit complexity and problems associated with accurately determining the neutron response function with the pulse shape discriminator makes this type of detector useful only for neutrons with energies below about 3 MeV. It has been used successfully for plutonium tetrafluoride source measurements (average energy of 1.4 MeV), but it cannot be used for higher energy sources, such at plutonium-beryllium with an average neutron energy of 4.5 MeV.

The second type of detector used in the field neutron spectrometer is the tissue equivalent proportional counter (TEPC). At the present time, the 5-inch diameter spherical tissue equivalent proportional counters manufactured by Far West Technology, Goleta, California are used in the PNL system with a low noise preamplifier and amplifier developed at PNL attached to the base of the detector. The TEPC detector does not actually determine the incident neutron energy spectrum, but measures the pattern of microscopic energy depositions in a tissue-like site about one or two micrometers in diameter. The TEPC directly measures the absorbed neutron dose as a function of lineal energy. If neutron quality factors are redefined in terms of lineal energy as suggested in ICRU Report 40 (Joint Task Group 1986), the TEPC can be used to directly determine neutron quality factors and dose equivalents. From the

pattern of energy deposition and appropriate algorithms, it is possible to determine neutron quality factors as presently defined. Thus, it is possible to use the TEPC to determine neutron quality factors and dose equivalent rates over a wide range of neutron energies from thermal to over 20 MeV. Details of the algorithms used are given in a companion paper in this proceedings.

The third type of detector used is the multisphere or Bonner sphere detector (Bramblet, Ewing and Bonner 1960). The basic idea for the multisphere spectrometer is quite simple. A thermal neutron detector is positioned at the center of moderating spheres of various sizes. The PNL version uses a ^{6}LiI scintillator detector; thermal neutrons produce a distinct peak from the ^{6}Li(n,α) reaction which can be discriminated from gamma interactions in the scintillator. The larger spheres moderate fast neutrons to thermal energies, where they are detected. Low energy neutrons are moderated and absorbed before they can reach the detector. The smaller spheres are too small to thermalize fast neutrons, but can easily thermalize lower energy neutrons. Thus, the energy of the incident neutrons can be determined by knowing the detector response as a function of energy.

In the PNL multisphere detector is patterned after one developed at LLNL by R. V. Griffith and coworkers. It consists of a 1/2-inch long by 1/2-inch diameter ^{6}LiI scintillator coupled to a 1/2-inch diameter photomultiplier. The moderators consist of 3-inch and 5-inch diameter polyethylene spheres covered with cadmium to suppress thermal neutron response and 8-inch, 10-inch, and 12-inch diameter polyethylene spheres, and bare and cadmium covered detectors. From the count rate measured by these 7 detector/moderator configurations, it is possible to unfold the incident neutron energy spectrum using a code called SPUNIT developed at PNL (Brackenbush and Scherpelz 1983). The SPUNIT code provides an approximate neutron energy spectrum in 26 logarithmic energy bins extending from thermal energies to 20 MeV. From the measured spectrum, it is possible to calculate neutron quality factors and dose equivalent rates using published conversion factors. Details of the how the multisphere detector and analysis code are integrated into the field spectrometer are given in PNL-6620 Vol. 3, "Field Neutron Spectrometer with Multisphere Detectors" (Brackenbush and Scherpelz 1990).

ACCURACY OF THE FIELD NEUTRON SPECTROMETER

The accuracy of the field neutron spectrometer was verified by exposing the various detectors in known dose equivalent rates using ^{252}Cf sources with calibrations directly traceable to the National Institute of Standards and Technology (NIST). Each of the detectors used is self-calibrating, so the exposures to known dose equivalents is a check on the accuracy of the response functions, conversion algorithms, and computer codes used to determine the quality factors and dose equivalent rates using the fluence-to-dose equivalent conversion factors given in DOE Order 5480.11. The results of these measurements are given in Table 1 for the TEPC and multisphere detectors. The dose rates from these NIST calibrated sources are too high for the ^{3}He detector to function; pulse pile-up makes it impossible to separate neutron and gamma events on the basis of pulse height.

Two different TEPCs were used and exposures ranged from 25 mrem to 700 mrem at the PNL calibrations laboratory. Exposures were made with both bare and D_2O moderated ^{252}Cf neutron sources.

For the bare ^{252}Cf source, the TEPCs determined the neutron dose equivalent within about 5% of the delivered dose; for the D_2O moderated ^{252}Cf neutron source, the TEPCs determined the dose equivalent within about 13%. The multisphere spectrometer determined the delivered dose equivalent within 5% for the bare ^{252}Cf source. In general, the TEPC and multisphere spectrometers are judged to be accurate within 15% for bare and moderated fission sources, which is adequate for most health physics applications. The accuracy of the ^{3}He detector depends upon the particular tube used and the energy range for the measurement.

FIELD TESTING

As mention previously, the field neutron spectrometer has been tested by performing measurements in the work place. Some of these measurements are included in this proceedings in papers by J. J. Fix and K. McMahan. After extensive field testing several problem areas were identified. First of all, present detectors are not sensitive enough for quick measurements at low dose rates below about 0.1 mrem/h. A 10-inch diameter polyethylene sphere was calibrated to be an accurate rem meter for use for quick measurements at low dose rates. Second, the ^{3}He counter is not useful for neutron energies above about 2 to 3 MeV; higher fill pressures to increase sensitivity cause gamma pile-up problems. Third, commercial TEPCs have gain shift problems from outgassing of volatile components from the tissue equivalent plastic. Each TEPC detector should be refilled and checked by exposure to a calibrated neutron source prior to use in the field. Some measurements were interrupted by power transients; this problem was easily corrected by adding an uninteruptable power supply and filter. Finally, the computer code used in the field spectrometer is somewhat inflexible; a more versatile data collection/analysis capability is desirable. The existing computer only allows one to use a high pressure ^{3}He detector on port 1, a low pressure ^{3}He detector on port 2, a 5-inch diameter spherical TEPC on port 3, and the 1/2-inch ^{6}LiI multisphere detector on port 4. It would be beneficial to add a proton recoil counter system using three or four spherical counters, or a liquid scintillator detector to the field spectrometer.

CONCLUSIONS

The field neutron spectrometer system does have several distinct advantages. First, the technology for the "suitcase" analysis unit was transferred to industry, and the unit is available commercially from Paulus Engineering Co. at Oak Ridge, Tennessee at a moderate cost. Second, the modular design has easily exchanged parts. Third, it is easily transported in a 50 pound suitcase unit, including the Grid lap top personal computer. The suitcase is 7-inches by 18-inches by 24-inches. The existing system accepts high pressure ^{3}He proportional counters on data port 1, low pressure ^{3}He detectors on port 2, 5-inch diameter spherical TEPCs on port 3, and multisphere detectors or a 10-inch sphere calibrated as a rem meter on port 4. Finally, the spectrometer determines neutron energy spectra, absorbed neutron dose, quality factors, and dose equivalent rates calculated from the measured energy spectra or absorbed dose. The spectrometer can be easily set up in about 10 minutes in work locations, and is easy to use by following the instructions given on menu screens. The unit automatically stores the ray data and analyzed results automatically on hard disk every 30 minutes, so that data will not be lost.

The data can be further analyzed in the laboratory later if desired. Details of construction, testing, and operation of the field spectrometer can be found in PNL-6620, Volumes 2 and 3 (Brackenbush et al. 1988, Brackenbush and Scherpelz 1990).

In the future, several improvements are suggested. First, a highly collimated neutron detector is to be added to the spectrometer to allow measurements of the direction and the energy spectrum of incident neutrons. This information will be necessary to determine effective dose equivalent. Second, the large "suitcase" unit can be replaced by a much smaller, lightweight unit developed at PNL for NASA for use aboard the space shuttle. This unit includes 256 channel multichannel analyzers, a high voltage power supply, low-noise preamplifier, and spectrometry grade amplifier. The entire system is small enough to be mounted on the end of the detectors and powered by small batteries. Computer programs already exist for transferring the data to a notebook computer for analysis and permanent storage. This system would make a completely portable neutron and gamma spectrometer for use in the work place. If produced in sufficient quantity, the miniature battery powered multichannel analyzers could be produced very inexpensively.

REFERENCES

Brackenbush, L. W. and R. I. Scherpelz. 1983. SPUNIT, A Computer Code for Multisphere Unfolding. PNL-SA-11645, Pacific Northwest Laboratory, Richland, Washington.

Brackenbush, L. W., W. D. Reece, and J. E. Tanner. 1984. Neutron Dosimetry at Commercial Nuclear Plants, Final Report of Subtask C: ^{3}He Neutron Spectrometer. NUREG/CR-3610, U. S. Nuclear Regulatory Commission, Washington, D.C.

Brackenbush, L. W., W. D. Reece, S. D. Miller, G. W. R. Endres, J. S. Durham, R. I. Scherpelz, and P. L. Tomeraasen. 1988. Personnel Neutron Dosimetry Upgrade Volume 2: Field Neutron Spectrometer for Health Physics Applications. PNL-6620 Vol. 2, Pacific Northwest Laboratory, Richland, Washington.

Brackenbush, L. W. and R. I. Scherpelz. 1990. Personnel Neutron Dose Assessment Upgrade Volume 3: Field Neutron Spectrometer with Multisphere Detectors. PNL-6620 Vol. 3, Pacific Northwest laboratory, Richland, Washington.

Bramblett, R. L., R. I. Ewing, and T. W. Bonner. 1960. "A New Type of Neutron Spectrometer," Nuclear Instruments and Methods 9:1-12.

Joint Task Group of the ICRU and ICRP. 1986. The Quality Factor in Radiation Protection. ICRU Report No. 40, International Commission on Radiation Units and Measurements Publications, Bethesda, Maryland.

TABLE 1. Accuracy of Field Neutron Spectrometer System Exposed to Calibrated Bare and D_2O Moderated ^{252}Cf Neutron Sources in the PNL Calibration Laboratory

Detector	Percent Error
TEPC with Bare ^{252}Cf Source	
TEPC s/n 501	+1.9%
	+5.6%
TEPC s/n 504	-2.4%
	+3.6%
TEPC with D_2O Moderated Source	
TEPC s/n 501	+13.2%
	+11.7%
TEPC s/n 504	-3.8%
	+10.1%
Multisphere with Bare ^{252}Cf Source	
^{6}LiI detector s/n PE648	-4.4%

FIGURE 1. The Field Neutron Spectrometer with the Analysis Module in the Center, TEPC Detector on the Left, and ^{3}He

USING TISSUE EQUIVALENT PROPORTIONAL COUNTERS TO DETERMINE DOSE EQUIVALENT*

L. W. Brackenbush

Pacific Northwest Laboratory
Richland, Washington

INTRODUCTION

Tissue equivalent proportional counters (TEPCs) have been used in the laboratory for over 30 years to determine neutron dose in mixed radiation fields, but they are seldom used by operational health physicists. But a number of TEPC-based instruments are being developed in Europe and in the United States. The purpose of this paper is: to introduce operational health physicists to tissue equivalent proportional counters, to examine some of the algorithms used to convert data from TEPCs into dose equivalent, to examine how TEPC measurements meet the requirements of DOE Order 5480.11 (DOE 1988) and 10CFR20, and to examine some of the TEPC-based instruments that are available.

Many operational health physicists are not familiar with the concept of microdosimetry and the specialized terms that are used in analyzing the data from TEPCs, so a brief discussion is included. At present, quality factors are defined in terms of linear energy transfer, but TEPCs measure lineal energy. The differences between the two concepts can be explained by examining Figure 1, where a 1 MeV proton strikes a hydrogen atom in tissue to produce a recoil proton. In Figure 1, the dots represent ionizations produced along the track of the recoil proton and its secondary particles (delta rays or recoil electrons). There are two identical spheres drawn along the path of the recoil proton. On the left, there is little energy deposited in the volume; on the right, there is a large energy deposit in the same volume. The variation in energy deposit on a microscopic scale is the basis for the concept of lineal energy.

Lineal energy, y, is defined as the energy imparted to a volume divided by the mean track length in that volume. It is a microscopic quantity that can be measured by a TEPC. It is a stochastic quantity-i.e., it has a distribution of values that depend on where radiation interactions occur.

Linear energy transfer, LET or L, is defined as the linear rate of energy loss along the path of the charged particle, dE/dx. LET is a macroscopic quantity which is the average of many measurements. For a given energy of the charged particle, LET has a single value. Often LET is not measured, but is calculated from stopping power formulas.

* Work supported by the U.S. Department of Energy under Contract DE-AC06-76RLO 1830.

TISSUE EQUIVALENT PROPORTIONAL COUNTERS

Tissue equivalent proportional counters are hollow spheres or cylinders of A-150 tissue equivalent (TE) plastic filled with tissue equivalent gas. The gas pressure in the cavity is so low that the gas cavity has the same mass stopping power as a 1 or 2 micrometer sphere of solid tissue at unit density. Typically, a neutron strikes the TE plastic and knocks out a recoil proton, which traverses the gas cavity. The energy deposited in the cavity is roughly proportional to the charge deposited and measured by the proportional counter.

Figure 2 shows the spectrum of pulses from a spherical TEPC recorded by a multichannel analyzer. The lower curve is the spectrum recorded for gamma rays, which deposit energies less than about 15 kev/μm. The middle curve shows the spectrum recorded for 1.4 MeV neutrons, which generally deposit energies above 15 keV/μm. Thus, fast neutrons and gamma rays can be separated on the basis of pulse height. The top curve shows the absorbed dose distribution obtained by multiplying the counts per channel by the channel number or energy deposited in the TEPC. Notice that the point of inflection from proton recoils always occurs at about 150 keV/μm, regardless of the incident neutron energy. This "proton drop point" can be used to calibrate the counter.

The absorbed dose, D, can be determined from a spectrum of pulse heights measured by the TEPC using the formula:

$$D = (c/m) \sum N(e)\, e$$

where e is the energy deposited in the counter (or channel number)
N(e) is the number of events of energy e (or counts per channel)
m is the mass of the gas in the sensitive volume of the counter
c is a constant of proportionality relating the energy deposited or channel number.

The dose equivalent, H, is found from the definition:

$$H = \int Q(L)\, D(L)\, dL$$

where Q(L) is the quality factor defined as a function of linear energy transfer and D is the absorbed dose. The problem is how to convert from lineal energy distributions, which are measured by the TEPC, to linear energy transfer distributions.

About 20 years ago, Albrecht Kellerer (1969) derived a simple equation to relate lineal energy and LET. For spherical detectors, the first moment of the dose distribution in LET is approximately 8/9ths of the first moment of the lineal energy distribution:

$$L = (8/9)\, y_D$$

where L is the first moment of the dose distribution in LET

y_D is the first moment of the dose distribution in lineal energy measured by the TEPC.

One can simply substitute (8/9) y_D for L and evaluate the dose equivalent for spherical detectors using existing quality factors defined as a function of linear energy transfer.

Another way of looking at dose equivalent is to use the quality factor as an empirical conversion factor to relate dose measured by the TEPC to the "official" dose equivalent. The graph in Figure 3 shows the quality factor from ICRU Report 20 (ICRU 1971) as a function of the first moment of the dose distribution from a spherical TEPC exposed to monoenergetic neutrons. If one only examines proton recoil events with lineal energies below about 150 keV/μm, there is a simple linear relationship between the average event size in the dose distribution measured by the TEPC and the quality factor. This is the empirical algorithm that was used to determine neutron dose equivalent in the first version of the total dose meter developed at PNL. Additional information on quality factor algorithms can be found in a paper by Brackenbush et al. (1985).

DOSE EQUIVALENT CALCULATED FROM SPECTRAL MEASUREMENTS

The dose equivalent determined from TEPC measurements, as outlined above, is not necessarily the same as the dose equivalent obtained from neutron energy spectrum measurements. Let's examine how the TEPC measurement compares with the "official" or "conventional" dose equivalent calculated from the neutron energy spectrum and the fluence-to-dose equivalent conversion factors listed in DOE Order 5480.11 (DOE 1988). A comparison of the two methods is outlined in Figure 4.

The conventional dose equivalent is based on the Monte Carlo computer calculations of Auxier, Snyder, and Jones (1968) made at Oak Ridge National Laboratory almost 30 years ago. They considered a parallel beam of monoenergetic neutrons normally incident on a cylindrical phantom 30 cm in diameter and 60 cm high composed of soft tissue. The computer code calculated the highest value of dose equivalent at any depth in the phantom. In the case of the TEPC measurements, neutrons from all directions are measured at a depth corresponding to the wall thickness of the counter.

The conventional dose equivalent is calculated by measuring the neutron fluence as a function of the incident neutron energy, multiplying by fluence-to-dose equivalent conversion factors for each energy (interpolated from the Monte Carlo calculations of Auxier et al. 1968), and summing the results together. The dose equivalent from the TEPC is the product of the absorbed dose measured by the TEPC multiplied by an average or effective quality factor determined by an appropriate algorithm. Activation gamma rays from H(n,γ)D reactions are included as part of the conventional neutron dose equivalent, even though a gamma dosimeter will measure some of these activation gammas and include them as part of the incident gamma dose. In the TEPC measurement, it is impossible to determine the origin of gamma rays (from incident gamma rays or neutron activation reactions inside the TEPC) so activation gamma rays are considered as part of the gamma dose.

In conventional dose equivalent, one uses interpolated values for the conversion factors, which are calculated at only a few neutron energies. In the TEPC measurement, one includes the contributions

from neutron-alpha resonances, which produce high quality factors and contribute significantly to dose equivalent in the region of 4-5 MeV and 15-18 MeV. These resonances in neutron cross sections are ignored in the Monte Carlo calculations.

In the conventional method, one sums together the maximum dose equivalent value for each neutron energy, even though the maxima occur at different depths in tissue and are not strictly additive. In the TEPC measurement, one measures the dose at a depth of the wall thickness.

As a result, the conventional method provides a conservative value for the dose equivalent, which is impossible to measure physically. Figure 5 shows the percent of dose equivalent from heavy charged particles only (i.e., excluding gamma activation reactions) as a function of the incident neutron energy. These data are taken from the calculations of Auxier et al. used for the conversion factors listed in DOE Order 5480.11 (DOE 1988) or 10 CFR 20. The value shown in the graph is the ratio of the dose equivalent on the surface (excluding gamma activation reactions) compared to the maximum dose equivalent at any depth in the phantom. At energies above about 100 keV, the TEPC can accurately estimate dose equivalent, assuming that the quality factor algorithm is accurate. For neutron energies below about 10 keV, the TEPC can only measure about 60% of the conventional dose equivalent, because activation gamma rays from neutron capture reactions in tissue are excluded in the neutron dose measured by the TEPC. Forty percent error in this energy range may seem excessive, but one must consider that moderator-based instruments such as a Snoopy or rem ball will overestimate dose equivalent by a factor of 3 or 4 in this energy region (see Lesiecki and Cosak 1984). In most DOE plutonium production facilities, the major contribution to dose equivalent originates from neutrons with energies above 10 keV, so the TEPC measurement can be quite accurate. Generally, dose equivalents from TEPC measurements on bare or lightly moderated fission sources are accurate within 15%, as shown by the data in Table 1 of the paper on the field neutron spectrometer (Brackenbush 1991).

It is possible to almost match the dose equivalent conversion factor as a function of energy by including a shall amount of ^{3}He gas in the counter fill gas (Phiet 1989). The cross section of ^{3}He has about the same energy dependence as H(n,γ)D reactions in tissue. The He(n,p)T reaction produces charged particles (protons and tritons) that are included as part of the neutron dose measured by the TEPC.

TEPC-BASED INSTRUMENTS

There are a number of instruments that have been recently been developed that use tissue equivalent proportional counters as radiation detectors. A number of survey instruments have been developed as part of an extensive effort funded by the Commission of European Communities. These instruments have been described in a special issue of the journal Radiation Protection Dosimetry, Volume 10, devoted to a European neutron dosimetry workshop. Special intercomparisons have also been performed at the PTB in Germany to show the accuracy of these instruments when exposed to monoenergetic neutrons from accelerators and filtered beams from reactors (Schuhmacher et al. 1985; Dietze et al. 1986; Alberts et al. 1988).

Since the last DOE neutron dosimetry workshop, there have been a number of TEPC-based instruments developed. The first really practical, portable instrument to determine dose equivalent was developed by W. Quam and co-workers at EG&G/Santa Barbara Laboratories. This instrument used three cylindrical TEPCs filled with methane to determine the absorbed neutron dose; it is about the size of a portable hand-held radio.

The Pacific Northwest Laboratory has developed a variety of small instruments that use a single cylindrical tissue equivalent proportional counter to measure the absorbed dose and determine dose equivalent in mixed radiation fields, including neutrons, gamma rays, and heavy charged particles. The first instrument developed at PNL was the total dose meter, which used a single cylindrical tissue equivalent proportional counter to measure both neutron and gamma rays and display the total dose equivalent on a LCD display. This instrument was sensitive to shock, and the electronic circuitry was not sensitive enough to measure all of the lower energy gamma events.

Improved versions of instruments based on the total dose meter concept are shown in Figure 6. The instrument on the left is an improved version of the total dose meter developed for DOE. This instrument uses surface mount technology to reduce the size of the electronic circuits. In this instrument, the TEPC and the preamplifier and amplifier are contained in a copper tube 1.1-inches (28 mm) in diameter to isolate the detector from the rest of the electronics; this considerably reduces the cross-talk and increases the sensitivity to gamma events, which are 10 to 1000 times smaller than neutron events in the TEPC.

The instrument in the middle of the photograph in Figure 6 is the TEPC spectrometer developed at PNL for the National Aeronautics and Space Administration (NASA) for use aboard the space shuttle (Brackenbush, Braby, and Anderson 1989). It uses a single cylindrical TEPC to measure the absorbed dose and record the TEPC event spectra in 16 pseudologarithmic channels. The absorbed doe is read out to memory and displayed on a LCD display every minute for the duration of the flight. This instrument has been used on space shuttle missions STS31 and STS40 to determine the absorbed dose to the astronauts from protons, gamma rays, and cosmic rays. The event spectra are recorded periodically to record differences in the spectra and dose rate as a function of position of the space craft. Doses in the South Atlantic anomaly are generally 100 times higher than the rest of the orbit, and the quality factors are lower due to the trapped protons. Improved versions of the instrument are under development that have lower noise electronics and two 64 channel analog-to-digital converters to record the event spectrum in 32 logarithmic channels.

The instrument on the right is the aircraft total dose meter developed by Battelle to record the dose to passengers and flight crew aboard aircraft. As shown in the photograph, the instrument has a detachable probe containing a cylindrical TEPC with built-in preamplifier and amplifier. It also contains a 256 kbyte memory to periodically record the TEPC event spectra. A microprocessor in the instrument calculates and displays the accumulated dose equivalent on a liquid crystal display shown on the end of the instrument. All of these instruments are battery powered, and can function for several days, depending on the size of the battery pack.

Although not shown in the photograph, an improved instrument with a linear multichannel analyzer (MCA) has also been developed at PNL. One version contains a 256 channel multichannel analyzer that can record over 200 individual spectra in memory. These units can be used to record both the neutron and gamma event spectra from TEPCs. The MCAs are significantly smaller, lighter, and require less power than any existing commercially available MCA, and they are relatively inexpensive to build. Obviously, these MCAs were originally developed for personnel dosimetry and can be used for personnel or area monitors for any type of ionizing radiation. They can also be used for gamma spectrometry and environmental monitoring. Because of their small size, they can even be put down wells to monitor gamma emitters in ground water.

The precision of that can be obtained from these TEPC-based instruments is shown in Table 1. In this table, the instruments were exposed to 2 to 30 mrem gamma from a ^{137}Cs source and fast neutrons from a ^{252}Cf source. Ten to twenty identical measurements were recorded, and the results are presented in Table 1. For gamma rays, the measured dose equivalent was within 3% of the delivered dose equivalent, with a coefficient of variation of 3%. For fast neutrons, the results are more erratic because of the small delivered doses. In the worst case the measured neutron dose equivalent was 9% lower than the delivered dose equivalent, with a coefficient of variation of 14%.

CONCLUSIONS

In conclusion, TEPCs can accurately measure absorbed dose and determine dose equivalent over a wide range of neutron energies. They are quite accurate for fast neutrons, usually within 15%. They offer several distinct advantages over other types of neutron dosimeters:

- They are self-calibrating using the proton edge or internal alpha sources.
- They are an absolute dosimeter in the sense that they measure the energy deposited in a tissue-like material; they do not require exposure to a NIST-calibrated source.
- Quality factors can be determined from the pattern of energy deposition from the TEPC.
- They cover a wide range of neutron energies. The upper energy limit is determined by the wall thickness of the TE plastic required for electronic equilibrium. The problem at low neutron energies is one of definition, where activation gamma rays are included in the neutron dose equivalent in conventional dose equivalent conversion factors.

A variety of instruments have been designed using tissue equivalent proportional counters as the radiation detector. The Commission of European Communities has coordinated the development of several survey meters using TEPCs. The results of intercomparisons are reported in studies at the PTB in Germany. Several different instruments have been developed at PNL using a single cylindrical TEPC detector. Even at low doses, these instruments are surprisingly accurate. In general, the dose equivalent measured by TEPC-based instruments are usually within 15% of the delivered dose. The accuracy has been

confirmed by exposures to bare and D_2O moderated ^{252}Cf sources with calibrations directly traceable to the National Institute of Standards and Technology.

Finally, the technology developed can be applied to a number of other areas, including:

- personnel and area monitoring for mixed radiations
- space and aircraft dosimetry for neutrons, gamma rays and cosmic rays
- environmental monitoring, including neutron and gamma energy spectrum measurements.

REFERENCES

Alberts, W. G., E. Dietz, S Guldbakke, H. Kluge, and H. Schuhmacher. 1988. Radiation Protection Instruments Based on Tissue Equivalent Proportional Counters: Part II of an International Intercomparison. PTB-FMRB-117, Physicalisch Technische Bundesanstalt, Braunschweig, Germany.

Auxier, J. A., W. S. Snyder, and T. D. Jones. 1968. "Neutron Interactions and Penetrations in Tissue." In Radiation Dosimetry, Vol. 1, eds. F. W. Attix and W. C. Roesch, Academic Press, New York, pp. 289-312.

Brackenbush, L. W., L. A. Braby, and G. A. Anderson. 1989. "Characterizing the energy Deposition Events Produced by Trapped Protons in Low Earth Orbit." Radiation Protection Dosimetry. 29(1-2)119-121.

Brackenbush, L. W., J. C. McDonald, G. W. R. Endres, and W. Quam. 1985. 'Mixed Field Dose Equivalent Measuring Instruments." Radiation Protection Dosimetry. 10(1-4)307-318.

Dietze, G., S. Guldbakke, H. Kluge and Th. Schmitz. 1986. Intercomparison of Radiation Protection Instruments Based on Microdosimetric Principles. PTB-ND-29, Physicalisch Technische Bundesanstalt, Braunschweig, Germany.

Kellerer, A. M. 1969. "Analysis of Patterns of Energy Deposition." In Proceedings of the Second Symposium on Microdosimetry, Stresa, Italy, pp. 107-134. Office of the Official Publications of the European Communities, Luxembourg.

Lesiecki, H. and M. Cosack. 1984. Responses of Neutron Dose Equivalent Survey Meters. Physicalisch Technische Bundesanstalt, Braunschweig, Germany.

Phiet. 1985.

Schuhmacher, H., W. G. Alberts, H. G. Menzel, and G. Bühler. 1985. Dosimetry of Low-Energy Neutrons Using Low-Pressure Proportional Counters. Physicalisch Technische Bundesanstalt, Braunschweig, Germany.

U.S. Department of Energy. 1988. Radiation Protection for Occupational Workers. DOE Order 5480.11, U.S. Department of Energy, Washington, D.C.

TABLE 1. Precision of Total Dose Meter Instruments

	Ratio of Measured/Delivered Dose Equivalent	
	^{137}Cs	Bare ^{252}Cf
DOE s/n 201	1.03 ± 0.03	1.06 ± 0.11
NASA s/n 102	0.98 ± 0.01	1.02 ± 0.02
BNW Aircraft s/n 301	0.99 ± 0.03	0.91 ± 0.14

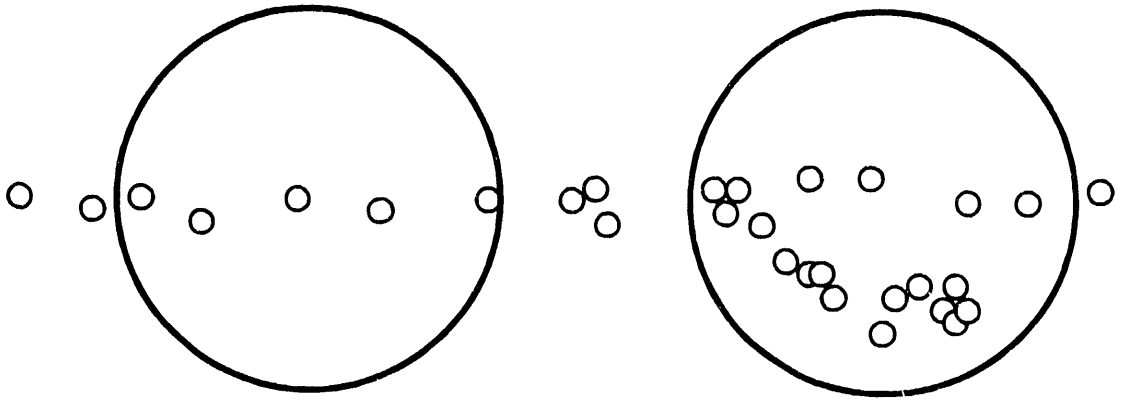

Small energy deposit

Large energy deposit

Path of recoil proton with constant linear energy transfer

Lineal Energy, y

$y = \varepsilon / \bar{\ell}$

Microscopic quantity which can be experimentally measured by TEPC

Stochastic quantity

Linear Energy Transfer, L

$L = dE / dx$

Macroscopic quantity-

average of many measurements or calculated value

FIGURE 1. Ionization Produced Along the Path of a Recoil Proton Produced by a Neutron Interaction in Tissue

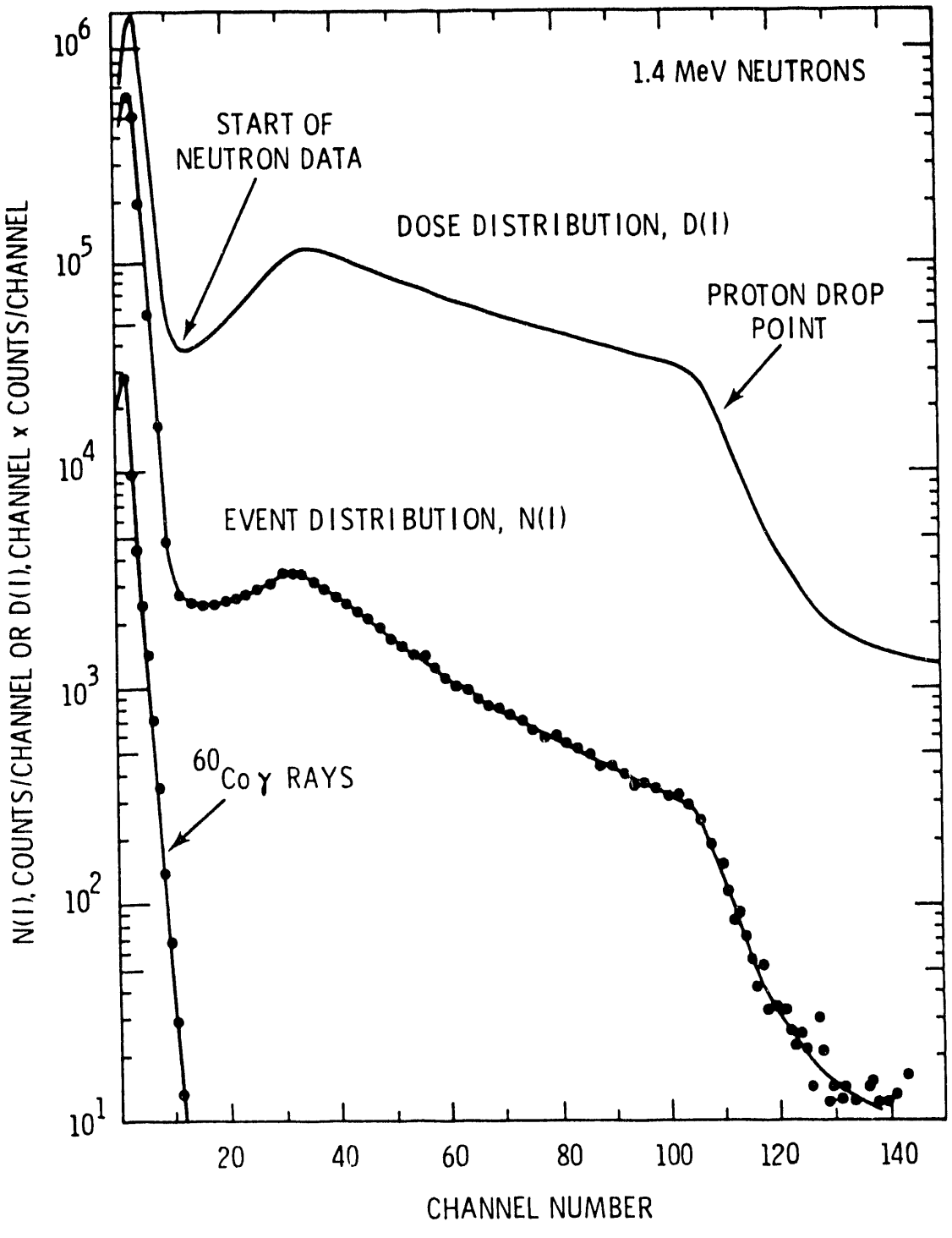

FIGURE 2. Event Spectrum and Absorbed Dose Distribution Produced by a TEPC Operated with a 1-μm Equivalent Diameter

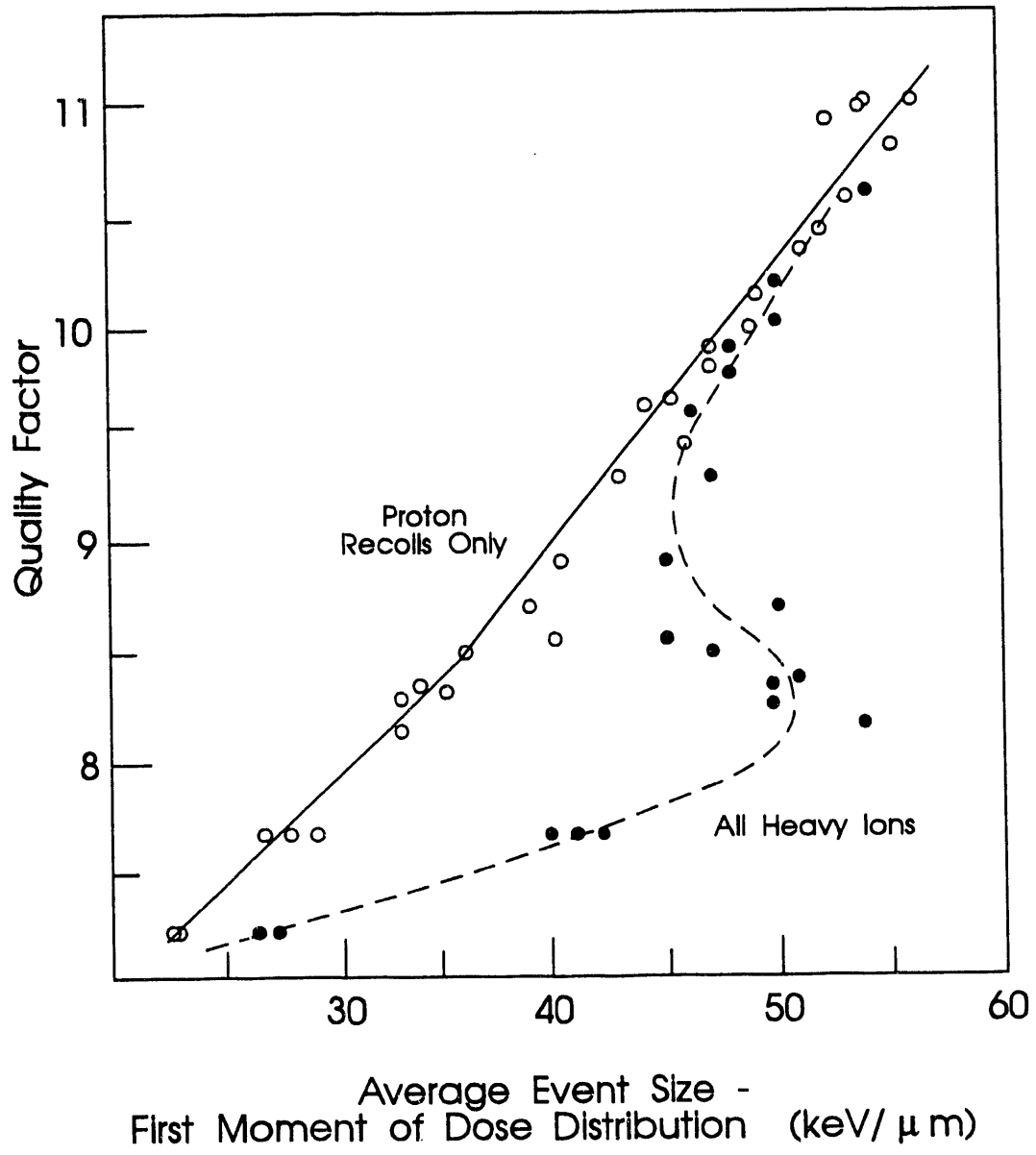

FIGURE 3. Empirical Neutron Quality Factor Obtained by Exposing Spherical TEPCs to Monoenergetic Neutrons

From Conversion Factors

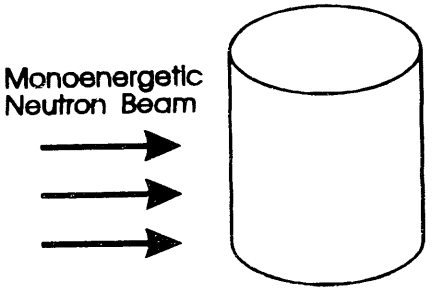

$$H = \sum C(E)\ \varphi(E)$$

Calculated Value

H(n,γ) included in neutron dose

Interpolated C(E) values for Different neutron energies

H_{max} at different depths for each neutron energy

Conservative estimate

From TEPC Measurements

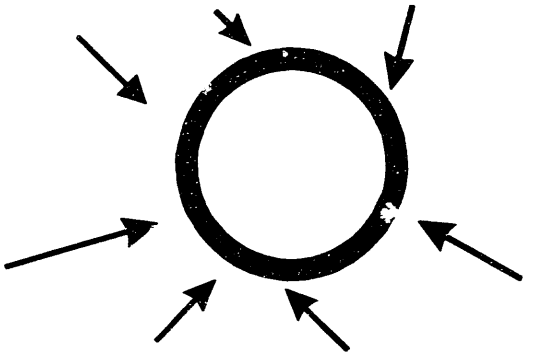

$$H = \bar{Q}\ D$$

Point in space measurement (kerma)

H(n, γ) included in gamma dose

Neutron recoils measured

Measured at single depth (thickness of wall)

FIGURE 4. Comparison of Methods of Determining Dose Equivalent from Fluence-to-Dose Equivalent Conversion Factors and Measurements Made with a TEPC

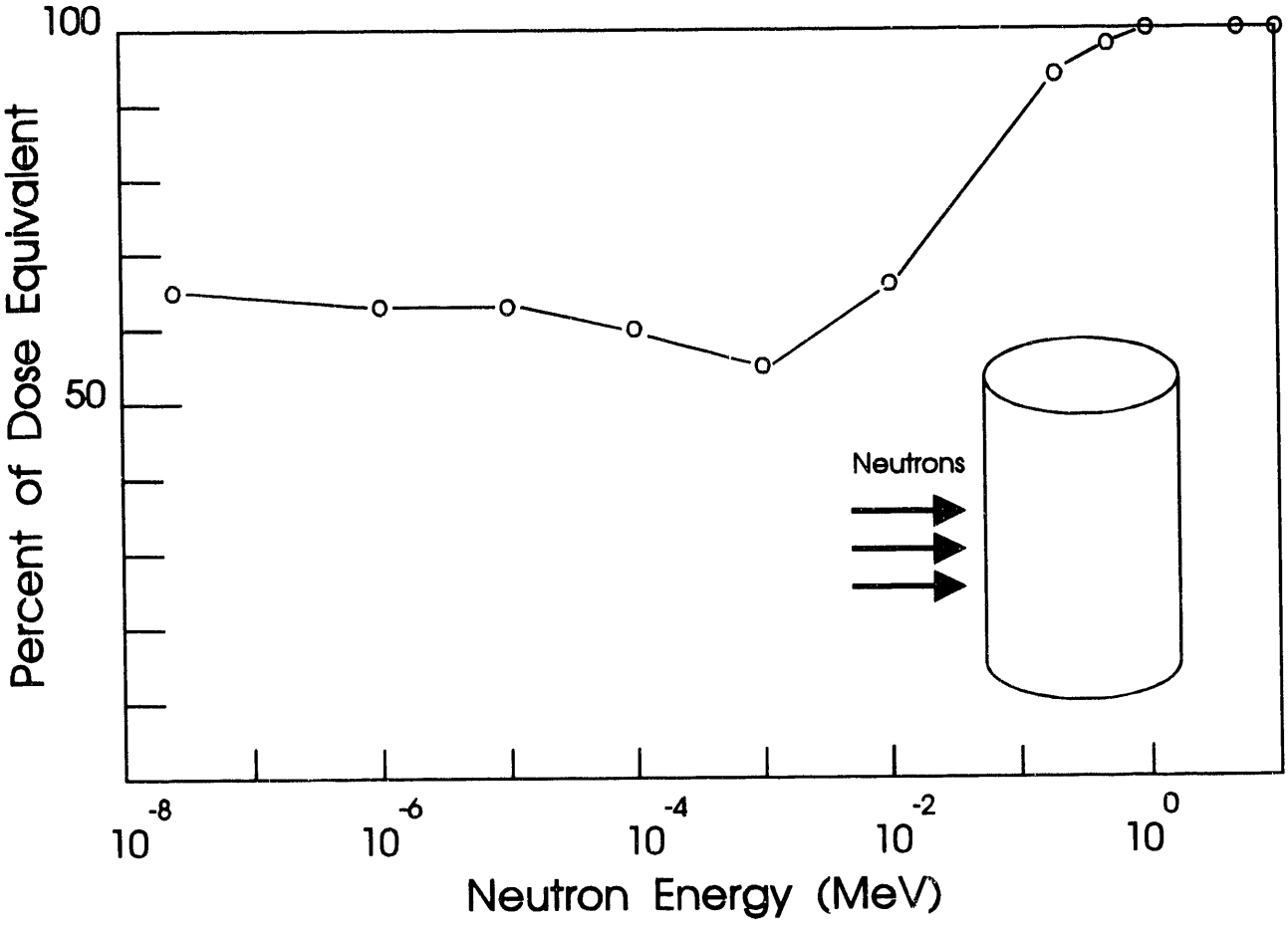

FIGURE 5. Percent of Neutron Dose Equivalent Produced by Charged Particles on the Surface of a Cylindrical Phantom

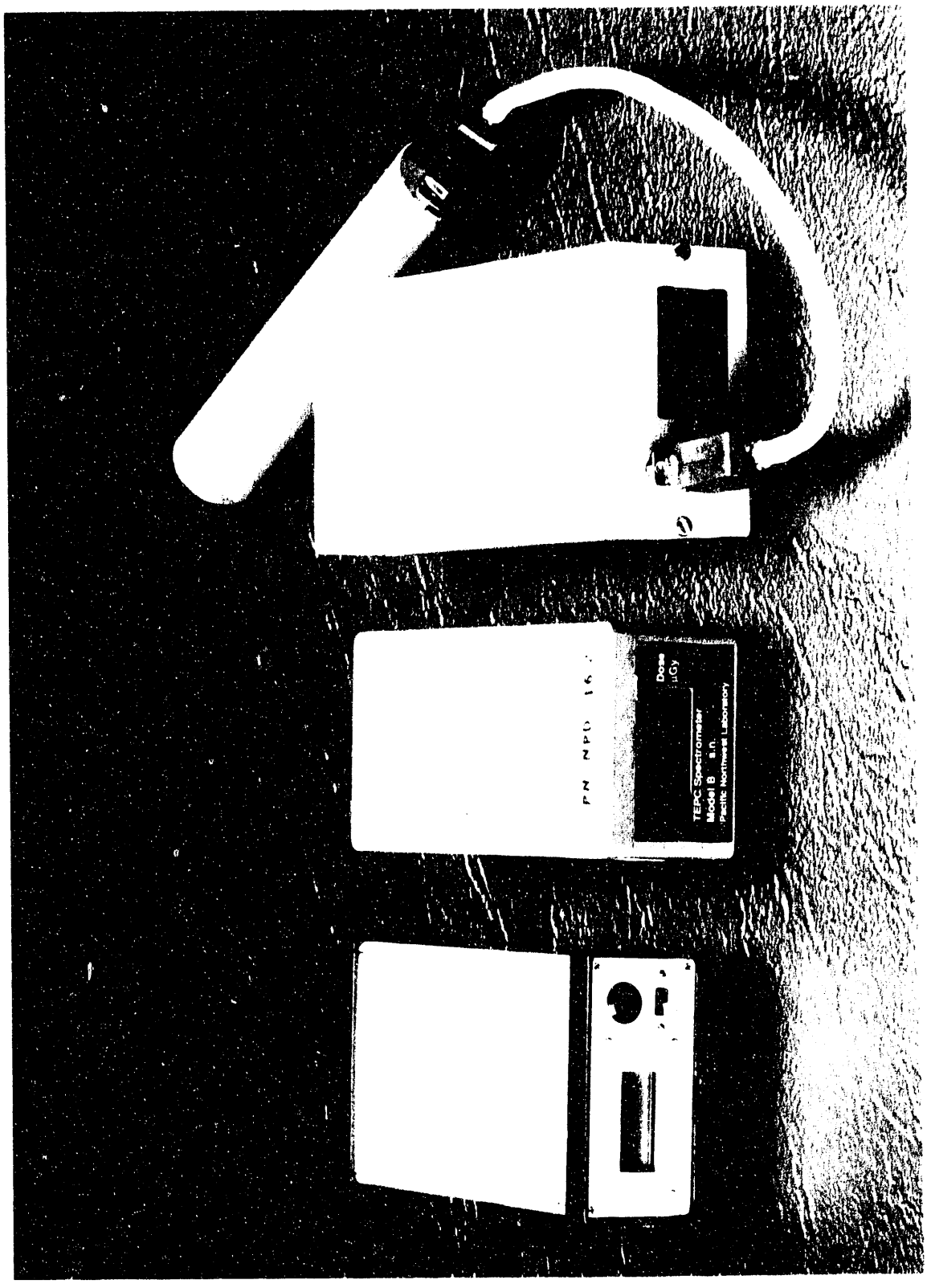

FIGURE 6. Photograph of Three Instruments Using TEPC Detectors Developed at the Pacific Northwest Laboratory

A PORTABLE 0.5- TO 16-MeV NEUTRON SPECTROMETER USING A LIQUID SCINTILLATOR[a]

J. C. Clark and J. H. Thorngate

Lawrence Livermore National Laboratory
7000 East Ave., L-386
Livermore, CA 94550

We have been developing a portable neutron spectrometer based on a liquid scintillator detector that is capable of measuring fast neutron spectra in the range of 0.5 to 16 MeV. These spectral data are needed for the calibration of neutron dosimeters and calculation of fluence-to-dose conversion factors. Recent development of low-power integrated circuits and the availability of powerful low-cost computers combine to make possible the development of a truly portable instrument. The complete spectrometer will consist of the spectrometer head, which is described in this report, a separate battery pack, and a lap-top computer with the appropriate interface to the spectrometer head.

The overall functional block diagram of the spectrometer head is shown in Fig. 1. The front end consists of an NE213 liquid scintillator and photomultiplier tube (PMT) coupled with a light pipe. The light pipe is necessary to equalize the effects of neutrons interacting in different parts of the scintillator. The PMT delivers a high-impedance charge pulse in response to the scintillator light pulse. The PMT gain is kept low so that the power consumption of its high-voltage bias is low. The pre-amp integrates the charge pulse with a 50-μs time constant and presents the resultant voltage to the shaping amplifier.

A neutron spectrometer has to separate out signals produced by neutrons from those produced by gammas. The light produced in the scintillator decays with a combination of fast (5 ns) and slow (150 ns) time components. Signals produced by gamma rays occur primarily in the fast component and can be rejected with a pulse-shape discriminator. Neutrons release recoil protons that produce light about equally in the fast and slow components. The neutron spectrum is obtained by pulse-height analysis of the slow component. The technique for discrimination used in this spectrometer is to take the pre-amp signal and add an inverted delayed version of the original signal to it. A 1-μs delay is necessary to allow full integration of the slow component. In this case, the fall of the resultant pulse is the same as the rise, except for some degradation introduced by the delay line. This pulse is fed to two RC differentiators, which give signals that pass through zero at 15 and 85 percent of the fall of this composite pulse. A time-to-amplitude converter triggered by the 15- and 85-percent zero crossings then gives a signal that is a measure of the rise time of the original pulse. The rise time of a compact 1-μs delay line degrades the signal such that the 85-percent point for the gammas and neutrons were 42 and 165 ns, respectively. This difference still allows a comparator to be adjusted so that it triggers only for neutron input signals;

(a) Work was performed under the auspices of the U.S. Department of Energy by the Lawrence Livermore National Laboratory under Contract W-7405-Eng-48, and supported by PNL through MPO 006705-A-G2.

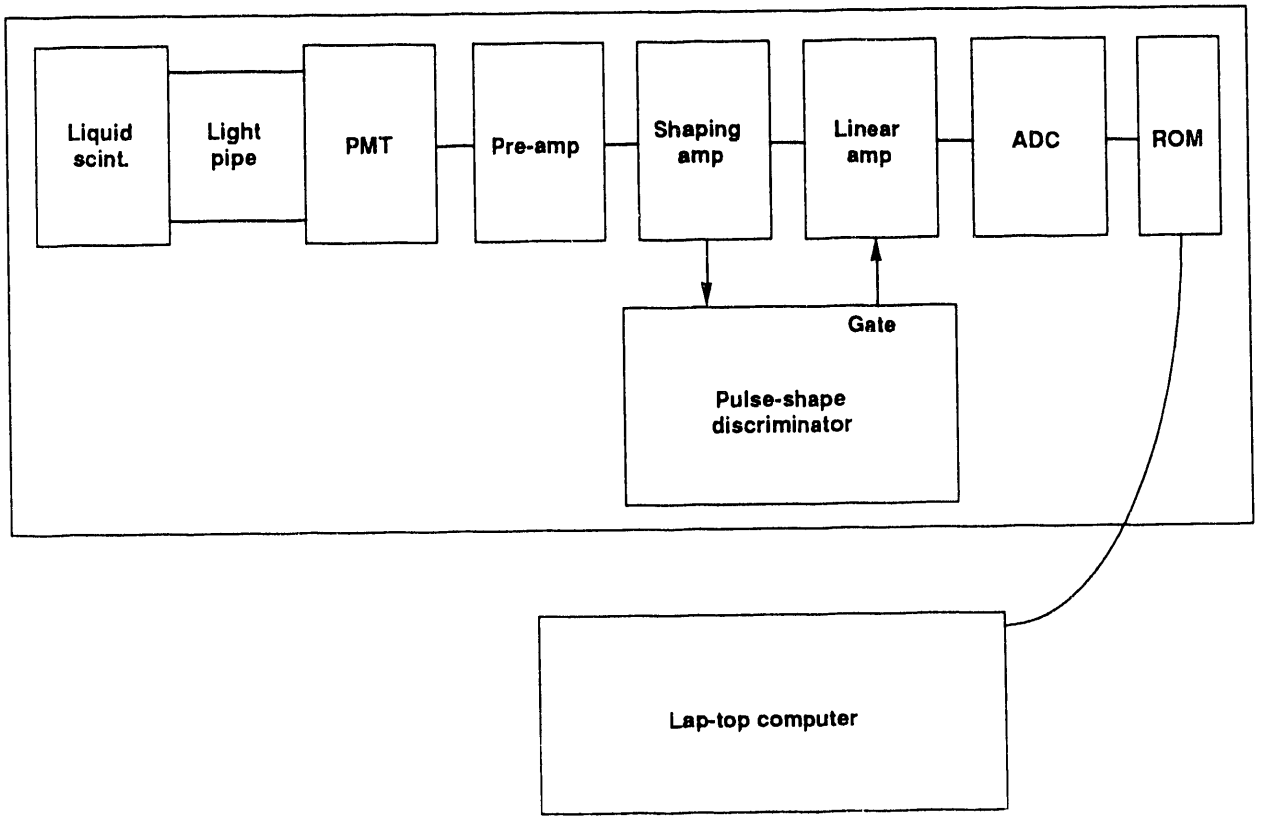

FIGURE 1. Functional block diagram of the portable neutron spectrometer.

this is the gate for the linear amplifier. The pulse-shape discriminator circuit used here was chosen to have mostly passive components so as to keep power consumption less than 1 W.

The shaping amplifier, pulse-shape discriminator, and linear amplifier were built and tested. A pulser with neutron-like signals was used to test the circuit, and discrimination was possible over a dynamic range greater than 200 to 1. This dynamic range is sufficient to allow the spectra to be displayed in 0.1-MeV energy bins over the range of the spectrometer from 0.5 To 16 MeV.

The spectrometer will require a 12-bit analog-to-digital converter (adc) with differential nonlinearity (dnl) of less than 3 percent. The 12-bit digitization will allow eight channels in the narrowest energy bin, and no interpolation of the data will be required. A variety of low-power 12-bit successive approximation digitizers are now available. They have fast conversion time, but poor DNL, and are usually specified as lease significant bit. In spectroscopic applications, this is a DNL of 50

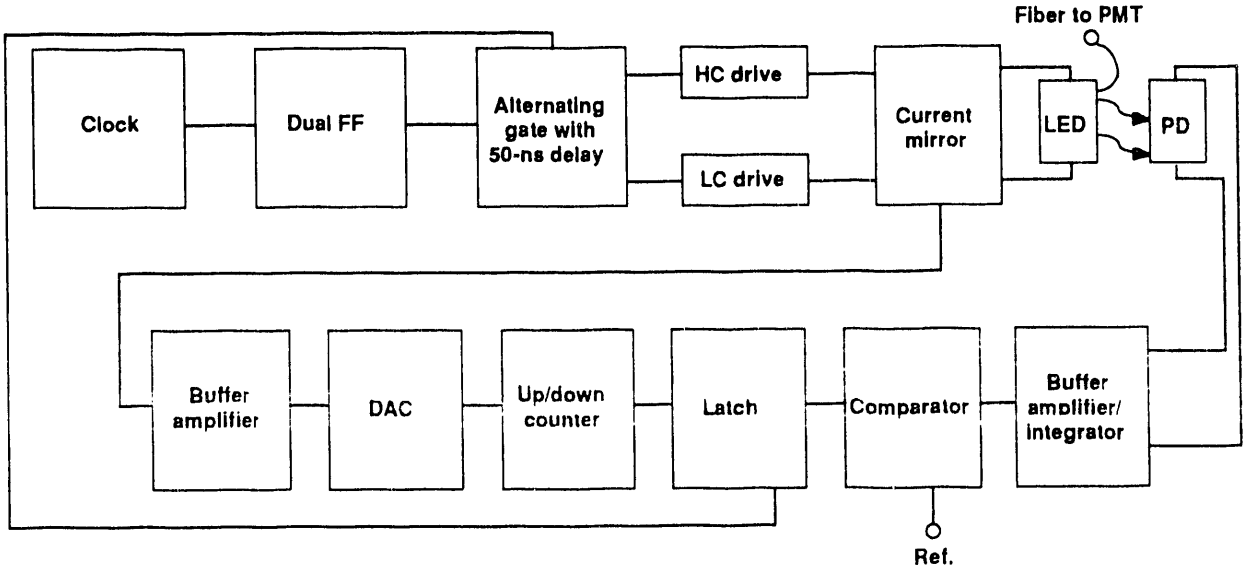

FIGURE 2. Stable light pulser for calibrating and stabilizing a neutron spectrometer.

percent or greater. There are techniques of bin-width averaging that can improve the effective DNL to less than 1 percent. We expect to develop a 12-bit ADC with up/down sliding scale averaging that will provide the required DNL, and we are now in the process of designing this circuit.

A unique element of this spectrometer is a stable light pulser that is used to set the gain of the detector system. The system gain is automatically adjusted by varying the PMT high voltage in response to the low-repetition-rate light pulser. This compensates for changes in the gain of the PMT with temperature and maintains the energy calibration of the instrument. A functional block diagram of the stable light pulser is shown in Fig. 2. The circuit begins with a clock operating at 100 Hz. A 50-ns delay circuit together with logic circuits are used to generate a 50-ns pulse that alternately drives a high and low current to a current mirror; thus, stabilization occurs at two different light pulses. The current mirror pulses a green light-emitting diode that is used to provide a light pulse directly to the PMT. This light pulse is stabilized using a photodiode that is referenced to a stable voltage. The stabilized photodiode pulse is used to vary the voltage drive to the current mirror to keep the light pulse constant.

The mechanical and electrical design of the spectrometer has been developed using a three-dimensional CAD system. Figure 3 shows the spectrometer head. The cover is made of 4-in. square pipe, and the overall length will be about 15 in.

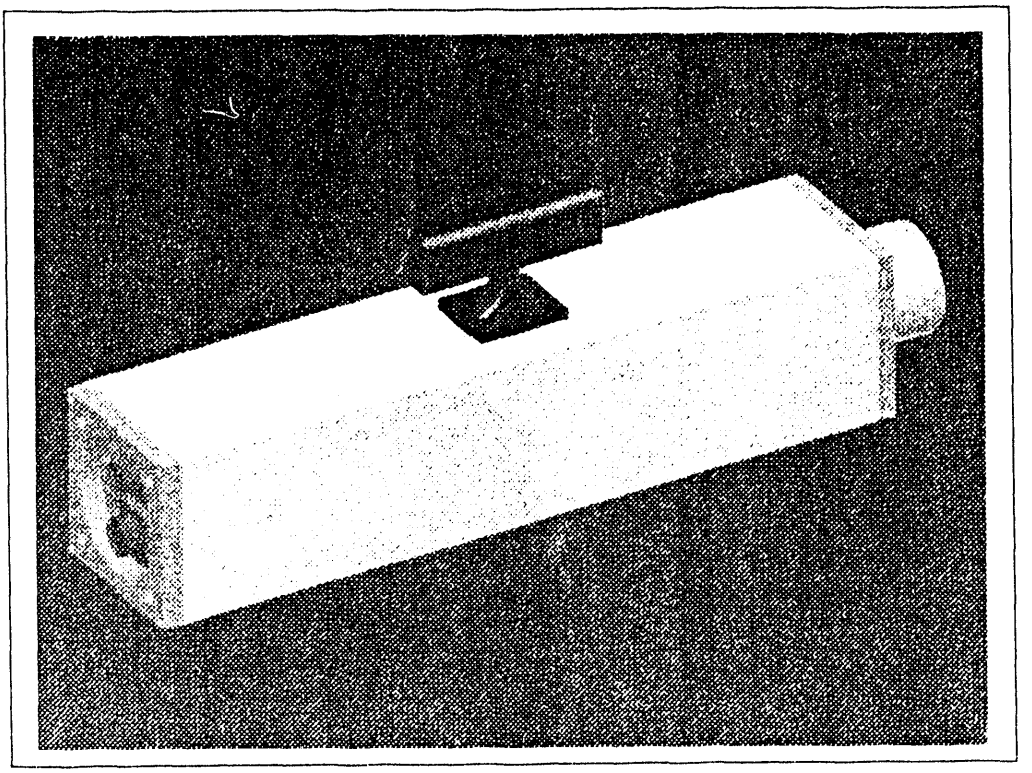

FIGURE 3. CAD image of the portable neutron spectrometer head.

THE UTILIZATION OF BUBBLE DETECTOR TECHNOLOGY IN THE DEVELOPMENT OF A COMBINATION AREA NEUTRON SPECTROMETER (CANS)[a]

M. A. Buckner and C. S. Sims

Oak Ridge National Laboratory
P.O. Box 2008
Oak Ridge, Tennessee 37831-6379

INTRODUCTION

Spectrum, spectrum who has the spectrum? This must be the cry of every health physicist who has ever attempted to characterize his neutron environment. Since God created them, He is the only one who knows for sure what they are. And until He chooses to "publish" them, differences in opinion will surely continue to prevail! Therefore, our job as health physicists is to keep tweaking our methods until our knowledge of the spectrum corresponds analogically with His knowledge. Then, and only then will we have the true answer!

The Dosimetry Applications Research Group (DOSAR) at the Oak Ridge National Laboratory (ORNL) is considering various applications of a relatively new technology built upon the bubble chamber concept of Glaser[1], the superheated liquid droplet or bubble detector (BD). One such application involves the spectrometric capabilities made possible with the combined technologies of BD and thermoluminescent dosimeters (TLD).

The doctoral dissertation of C. J. Liu heralded the first amalgamation of the two technologies, combining the BD-100R, BDS-1500 and Harshaw TLD-albedo dosimeter in the Combination Personnel Neutron Dosimeter or CPND[2,3,4]. The performance of the CPND was evaluated in several radioisotopic neutron fields and *in situ* working environments at ORNL. The CPND demonstrated that obtaining a four energy interval (EI) neutron spectrum as well as the total neutron dose equivalent was possible in a compact and relatively inexpensive package. Since its inception, aspects of the CPND have been modified, resulting in improved spectral and dosimetric accuracy. The bottom line is a total neutron dose equivalent performance within 11% of reference value for the *in situ* measurements and within 2% for the radioisotopic measurements[5].

COMBINATION AREA NEUTRON SPECTROMETER (CANS)

The information gleaned from these improvements lead us to believe that superior spectral resolution and, consequently, improved neutron dose equivalent accuracy could be realized through: 1) modification of the TLD component eliminating the need for a phantom, providing greater thermal

---

(a) Research sponsored by the Office of Health, U.S. Department of Energy under Contract NO. DE-AC05-840R21400 with Martin Marietta Energy Systems, Inc.

neutron measuring accuracy and simulating a 4n geometry, 2) inclusion of an additional BD to obtain better spectral resolution in the 0.01 to I MeV region and 3) determination of the effect temperature has on the shape of the energy response, R(E), and how to best correct for it.

The TLD component of CANS was redesigned to capitalize on the detection of thermal and slow or epi-Cd neutrons without using a phantom. This is possible because the BD components measure the higher energy neutrons. A Harshaw card was used (two teflon-sandwiched TLD-600/700 paired elements in an Al substrate) with one pair sandwiched between Cd filters and the other backed by a Cd filter. The paired TLD-700 is used to subtract the incident photon contribution and the Cd capture gammas from the TLD-600 response. The Cd-sandwiched TLD-600 responds to incident epi-Cd neutrons (> 0.414 eV) and the Cd-backed TLD-600 to incident thermal and epi-Cd neutrons. The difference in the two provides an accurate measure of the incident thermal fluence. By placing two of these units back-to-back, a 4n geometry is simulated (Figure 2).

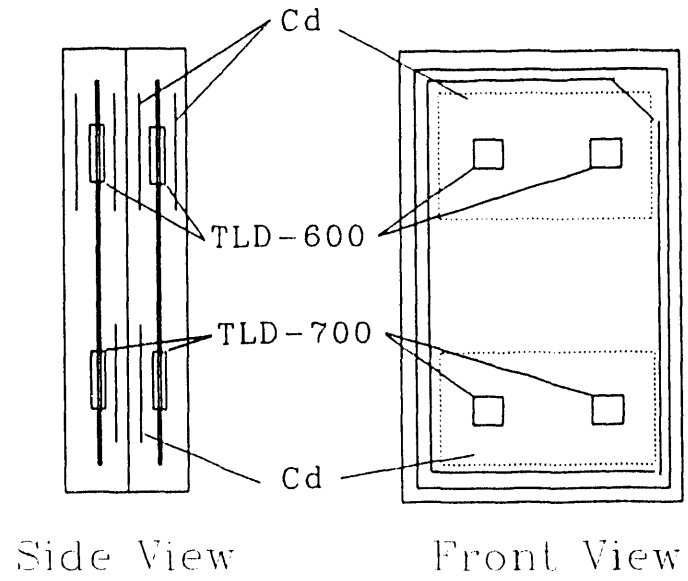

FIGURE 1. Description of the modified TLD component of CANS.

The region of greatest change in the fluence-to-dose equivalent conversion factor as defined by the International Commission on Radiological Protection in Publication 21 is between about 0.01 Mev and 1 Mev[6]. Improving the accuracy of the fluence measurements in this region will spawn a subsequent improvement in the total neutron dose equivalent accuracy. Since the BD-10OR and BDS-1500 possess respective thresholds at about 0.1 and 1 MeV, adding a BD with a threshold at about 0.01 MeV (BDS-10) sub-divided this region into upper and lower segments, thereby improving the spectral resolution in this region. BDs possessing thresholds other than these are also being reinvestigated.

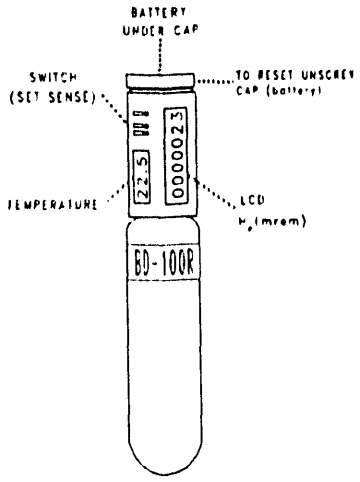

FIGURE 2. Real-time temperature corrected neutron dosimeter using a BD-IOOR and miniature ARAP.

Due to its use of a superheated liquid, the BD detector will always inherently possess a degree of temperature dependence. Efforts are currently underway to conduct another set of monoenergetic neutron irradiations at Columbia Universities Radiation Accelerator Research Facility (RARAF) in New York. The experiment will focus on determining how temperature affects a BDs R(E) by irradiating BDs with monoenergetic neutrons at various controlled temperatures. This knowledge, once acquired, will allow us to make inherently more accurate measurements of neutron spectra by redefining the BD R(E)s to reflect what they are at the irradiation temperature, instead of applying a gross temperature correction factor to the integrated response which ignores the change in R(E) caused by temperature.

The future of BD research at ORNL is questionable at best considering the cuts in DOE research funding experienced across the board. The hoped-for short and long range goals include 1) a more in-depth characterization of the BD R(E)s, including theoretical modeling and temperature related effects, 2) extensive field testing and 3) further development of Alternative Real-time Acoustical Processing (ARAP), the acoustical detection of bubbles formed in the BTI BDs which promises to make "real-time" applications of the BTI detector a reality. With ARAP we hope to 1) increase the dynamic range of BDs, 2) improve accuracy, 3) provide "real-time" measurement capabilities and 4) provide on-line temperature correction using a thermistor and micro-processor. Figures 2 and 3 depict an artist's conception of these real-time devices.

CONCLUDING REMARKS

The compact and relatively inexpensive CANS should provide neutron spectral capabilities heretofore available only via complex set-ups and time-consuming, painstaking calculations. Some of its strong points include the measurement of neutron fluence and the need for only a single algorithm, with a single solution, regardless of the spectra. Because fluence, a real quantity, is the foundation of dose

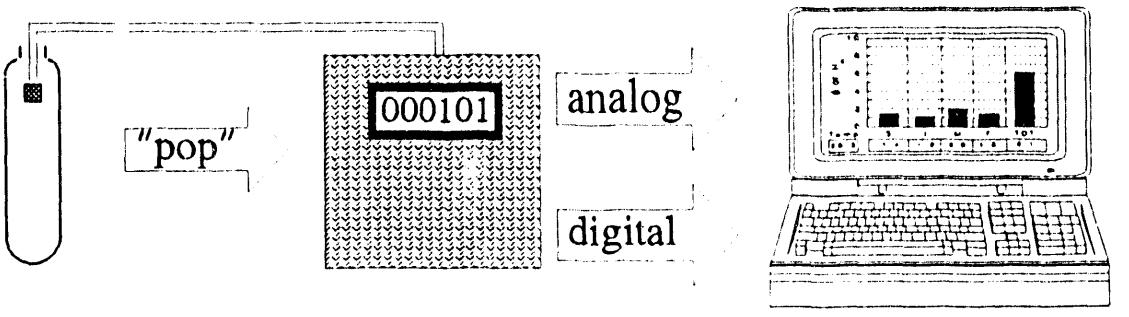

A. B. C.

Figure 3. Real-time spectrometry: A) "pop" detected by a microphone; B) counted by simple circuitry and displayed; C) multiple detector signals come to a laptop with signal processing board, recorded, pr and spectral results displayed graphically.

equivalent determination, the results of CANS should endure the winds of change accompanying the definition of dose equivalent and its consorted conversion conventions. It is also hoped that personnel applications may be realized in a miniature version of CANS, the Personal Neutron Dosemeter/Spectrometer (PENDOSE).

REFERENCES

1. Glaser, D. A. *Some Effects of Ionizing Radiation on the Formation of Bubbles in Liquids*. Phys. Rev. **87**, 665 (1952).

2. Liu, J. C. *The Development, Characterization, and Performance Evaluation of a New Combination Type Personnel Neutron Dosimeter*. Ph.D. Dissertation, Texas A&M University, College Station, Texas (1989) [Also Oak Ridge National Laboratory, Oak Ridge, Tennessee 37831, ORNL-6593 (1989)].

3. Liu, J. C. and Sims, C. S. *Characterization of the Harshaw Albedo TLD and the Bubble Detectors BD-IOOR and BDS-1500*. Radiat. Prot. Dosim 1), 21-32 (1990).

4. Liu, J. C. and Sims, C. S. *Performance Evaluation of a New Combination Personnel Neutron Dosimeter*. Radiat. Prot. Dosim. 32(1), 33-43 (1990).

5. Buckner, M. A., Sims, C. S. and Miller, L. F. *Improving Neutron Dosimetry Using Bubble Detector Technology*. To be published as ORNL TM-11916 (in draft).

6. International Commission on Radiological Protection. *Data for Protection Against Ionizing Radiation for Extemal Sources*. (Oxford: Pergamon Press) ICRP Publication 21 (1973).

NEUTRON FLUENCE TO DOSE CONVERSION FACTORS: WHICH ONE(S)?

N. E. Hertel

Nuclear Engineering Program, Mechanical Engineering Department
The University of Texas at Austin
Austin, TX 77812

For 30 years, the concept of dose equivalent has been employed in the field of radiation protection. The quest for improved, less conservative dose limitations systems have necessitated improvements in fluence-to-dose conversion factors. These conversion factors relate neutron fluence to personnel dose for shielding specialists and operational health physicists, while serving as the neutron-energy dependent response function which must be reproduced by personnel dosimetry systems and radiation survey instrumentation. These factors must of necessity be derived from computations. Not surprisingly, the complexity of such computations and representations of the human body have kept pace with continuing advancements in digital computers.

The earliest computations of neutron dose conversion factors used 30 cm thick semi-infinite slab phantoms. This phantom was followed a 60-cm-by-30-cm-diameter cylindrical representation of the human body, which was followed by the 30-cm-diameter ICRU sphere.[1] Currently anthropomorphic phantoms, containing organs and tissues similar to the MIRD-V phantom,[2] are in use. All computations of dose-equivalent conversion factors for neutrons below 20 MeV have been based on the computation of kerma in the phantom.

In 1977, the International Commission on Radiological Protection (ICRP) released ICRP Publication 26[3] which introduced a risk-based dose limitation system. This system requires the computation of mean dose equivalent in organs/tissues, H_T, and the weighted summation of these dose equivalents into a quantity known as the effective dose equivalent, H_E. A single set of H_E/ϕ values are used for both male and female workers regardless of variations in body mass. These conversion factors as found in ICRP Publication 51[4] are being incorporated into the revision of the ANSI 6.1.1.[5] The older version of ANSI 6.1.1 was based upon maximum dose equivalent values computed in the cylindrical phantom.[6] In ICRP Publication 26, it was noted that for external exposures, the required organ/tissue doses needed to compute the effective dose equivalent might not be available in practice. In such a case, the shallow dose equivalent and the deep dose equivalent indices can be used as secondary limitation quantities. The reader is referred to International Commission on Radiation Units and Measurements (ICRU) Report 25[7] for further information on these quantities.

In 1985, the ICRU introduced operational dose equivalent quantities for use in the measurement of dose due to external radiation sources, see ICRU Report 39.[8] These quantities were further clarified in ICRU Report 43.[9] These quantities were deemed necessary since H_E is essentially unmeasurable and, therefore, must be determined at locations in suitable surrogate receptors. Two sets of quantities were introduced. The first set of quantities, ambient dose equivalent and directional dose equivalent, were

intended for use in environmental and area monitoring. While the second set, Individual Dose Equivalent (Penetrating) and Individual Dose Equivalent (Superficial), were to be used in personnel monitoring. Ambient dose equivalent is defined below and the reader is referred to ICRU Report 39 for the definition of the other quantities. The first two quantities are based on the ICRU sphere, while the second two are intended to have the same response as a dosimeter on the surface of an individual's body.

The ambient dose equivalent, $H^*(d)$, at a point in a radiation field, is the dose equivalent that would be produced by the corresponding aligned and expanded field, in the ICRU sphere at a depth, d, on the radius opposing the direction of the aligned field.[8] An aligned and expanded field is a field in which the fluence and its energy distribution have the same values throughout the volume of interest as in the actual field at the point of reference, but the fluence is unidirectional. The recommended value for d is 10 mm. This quantity usually is an upper bound to the ICRP Publication 26 dose equivalent quantities. A plot of the energy dependences of the effective dose equivalent, ambient dose equivalent, and deep dose equivalent is shown in Figure 1. Exceptions to this statement are observed for several organ dose equivalents, for example see Figure 2.

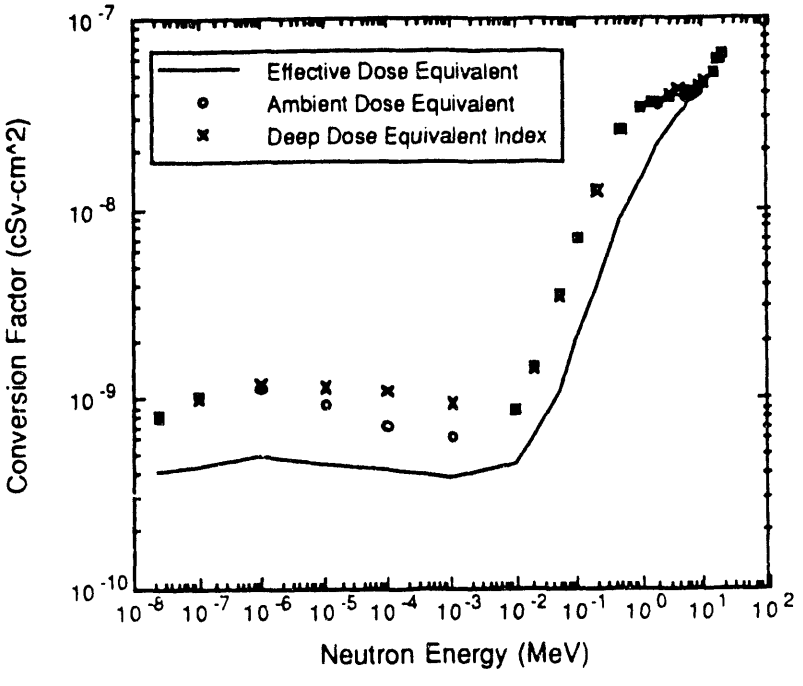

FIGURE 1. Effective Dose Equivalent, Deep Dose Equivalent, and Ambient Dose Equivalent Conversion Factors as a Function of Energy

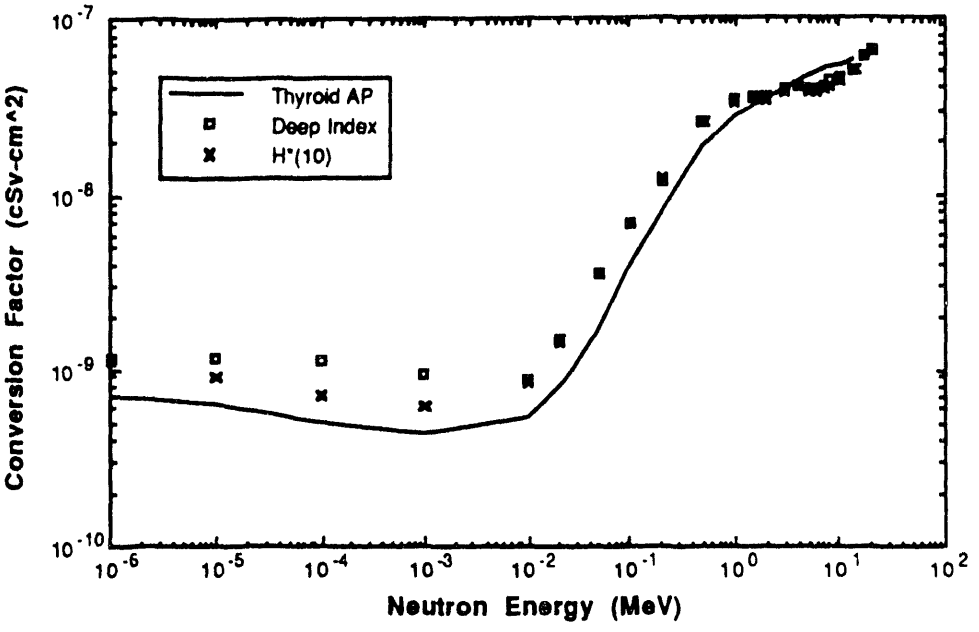

FIGURE 2. Thyroid Dose Equivalent, Deep Dose Equivalent, and Ambient Dose Equivalent Conversion Factors as a Function of Energy. Notice that the ambient dose equivalent does not overestimate the thyroid dose at all energies.

A difficulty arises in the use of these operational quantities in that different materials and geometrical configurations are employed in calibration. Should the limitation quantities be related to these intermediate operational units, which themselves are then related to calibration quantities; or should some calibration dose equivalents be related directly to the limitation quantities? This was addressed recently in Reference 10 and it was demonstrated that standard calibration setups/sources can be related to the operational quantities. However, this approach would lead to a cumbersome dosimetry protocol.

The evolution of dose equivalent quantities in all likelihood will continue. The end result may be a set of conversion factors for each individual worker based on his/her unique physique. There is also a need to develop neutron dose equivalent conversion factors above 10 MeV since none of the quantities introduced since ~ 1975 have been calculated for these energies.

REFERENCES

1. International Commission on Radiation Units and Measurements, "Radiation Quantities and Units," ICRU Report 33, 1978.

2. W.S. Snyder and G.G. Warner, MIRD Pamphlet No. 5, Revised: Estimates of Specific Absorbed Fractions for Photon Sources Uniformly Distributed in Various Organs of a Heterogeneous Phantom, Society of Nuclear Medicine, N.Y.

3. International Commission on Radiological Protection, "Recommendations of the ICRP," ICRP Publication 26, 1977.

4. International Commission on Radiological Protection, "Data for Use in Protection Against External Radiation," ICRP Publication 51, 1987.

5. American National Standards Institute, Inc., "American National Standard Neutron and Gamma-Ray Flux-to-Dose-Rate Factors," ANSI/ANS-6.1.1-1977 (N666), 1977.

6. National Council on Radiation Protection and Measurements, "Protection Against Neutron Radiation," NCRP Report No. 38, 1971.

7. International Commission on Radiation Units and Measurements, "Conceptual Basis for the Determination of Dose Equivalent," ICRU Report No. 25, 1976.

8. International Commission on Radiation Units and Measurements, "Determination of Dose Equivalents Resulting from External Radiation Sources," ICRU Report 39, 1985.

9. International Commission on Radiation Units and Measurements, "Determination of Dose Equivalents from External Radiation Sources - Part 2," ICRU Report 43, 1988.

10. N.E. Hertel and J.C. McDonald, "Calibration of Neutron Personnel Dosemeters in Terms of the ICRU Operational Quantities," Radiat. Prot. Dosim. (in press).

CURRENT DOE STUDIES ON EFFECTIVE NEUTRON DOSE EQUIVALENT[a]

J. E. Tanner

Pacific Northwest Laboratory
Richland, Washington

INTRODUCTION

The effective dose equivalent is defined as the sum of the weighted dose equivalents to specific organs and tissues. This can be shown by the following equation:

$$H_E = \sum_T W_T H_T$$

where H_E = Effective Dose Equivalent
W_T = Weighting Factor for a Specific Organ or Tissue (T)
H_T = Dose Equivalent for a Specific Organ or Tissue (T).

This methodology to determine an effective dose equivalent to the entire body accounts for the different radiosensitivities of various organs and tissues and reduces the large amount of conservatism inherent in the old neutron fluence-to-dose-equivalent conversion factors based on the cylindrical phantom. The same methodology is to be applied to uniform and nonuniform exposures and internal and external exposures, thus standardizing the way exposures are evaluated.

The concept of effective dose equivalent was introduced in 1977 in the International Commission on Radiological Protection (ICRP) Publication 26, Recommendations of the ICRP. ICRP 26 presented tissue weighting factors based on the absolute risk coefficients for the induction of a fatal malignant disease (see Table 1). In 1988, ICRP came out with Publication 51 which presented actual data on calculations of organ dose equivalents and the effective dose equivalent for uniform incident neutron fields from 1 eV up to 13.5 MeV. The International Commission on Radiation Units and Measurements (ICRU) sphere quantities were also presented for the same neutron energies and fields. The ICRU published it's Report 43 in 1988 entitled Determination of Dose Equivalents from External Radiation Sources - Part 2. This report presented data correlating the ICRU Report 39 operational quantities to organ dose equivalents and effective dose equivalent for neutrons and photons.

(a)Work performed for the Office of Health, Assistant Secretary for Environment, Safety and Health, U.S. Department of Energy under Contract DE-AC06-76RLO 1830.

TABLE 1. ICRP 26 Weighting Factors to Determine Effective Dose Equivalent

Tissue	Risk (rem^{-1})	W_T
Gonads	40×10^{-6}	0.25
Breast	25×10^{-6}	0.15
Red Bone Marrow	20×10^{-6}	0.12
Lung	20×10^{-6}	0.12
Bone Surfaces	5×10^{-6}	0.03
Thyroid	5×10^{-6}	0.03
Remainder	50×10^{-6}	0.30
Total	165×10^{-6}	1.00

Based on the many recommendations issued by the ICRP and the National Council on Radiation Protection and Measurements (NCRP), President Reagan, in January 1987, signed the "Radiation Protection Guidance to Federal Agencies for Occupational Exposure; Approval of Environmental Protection Agency Recommendations" which adopted the ICRP 26 methodology. DOE Order 5480.11, which was effective as of January 1, 1989, dealt with radiation protection for occupational workers and stated that the effective dose equivalent was to be evaluated for internal exposures and nonuniform external exposures. However, the order stated that for uniform external exposures a weighting factor of one could be applied.

The main objective of this work is to develop a dosimeter system for evaluating the effective neutron dose equivalent at DOE facilities from external sources based on detailed calculations of the angular and energy dependence of the organ dose equivalents and the effective dose equivalent. The results of the calculations will be used to determine dosimeter response criteria and design a prototype dosimeter system.

CALCULATIONAL MODEL

Organ dose equivalent and effective dose equivalent calculations were performed at Pacific Northwest Laboratory (PNL) using the Monte Carlo radiation transport code, MCNP Version 3B, developed at Los Alamos National Laboratory. MCNP is a general purpose Monte Carlo code for neutron and photon transport. A new version of MCNP, Version 4, also incorporates beta transport but this version has not been implemented for this work yet. The advantages of using MCNP include the use of continuous energy cross-section data, the complex three-dimensional modeling capability, the built-in geometry plotting for extensive debugging, the elaborate choice of tallies, and the user-defined output structure. The nuclear cross-section data from the Evaluated Nuclear Data File B-V (ENDF/B-V) was used with MCNP.

The mathematical anthropomorphic phantoms used to calculate organ dose equivalents were based on the MIRD-V phantom. The MIRD phantom is reference man size with both male and female organs, thus a separate male phantom was developed from the MIRD phantom to include only the male organs. The female phantom was modeled after the German developed phantom, EVA, also a MIRD-based phantom. However, the shape of the breasts was modified to be more realistic. The male and female phantoms, as drawn by MCNP, are shown in Figure 1.

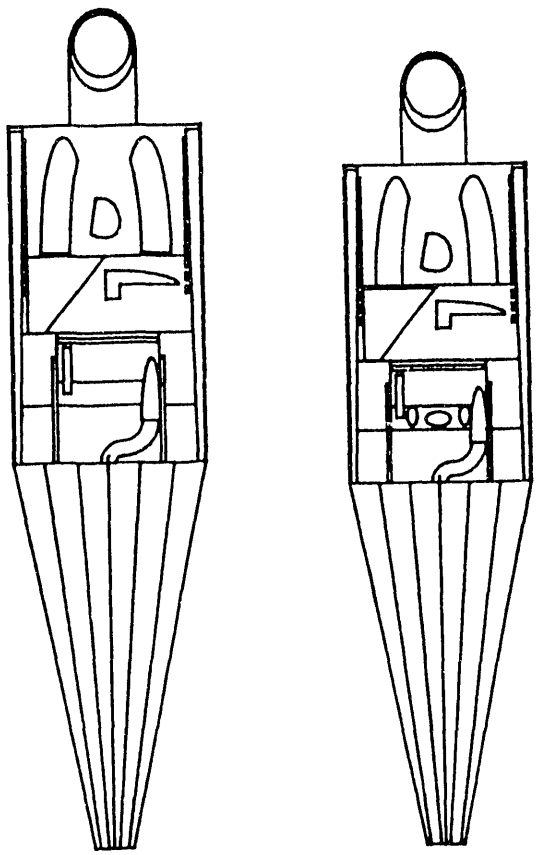

FIGURE 1. The Male and Female Phantoms, as Drawn by MCNP

The output from a single MCNP calculation consisted of neutron fluences and secondary gamma fluences averaged over the volumes of twenty individual organs, the lens of the eye, and the surface of the torso. The neutron fluences were broken down into 96 energy groups to match the kerma factors of Caswell and Coyne (1980). The photon fluences were given in 27 energy groups to allow the conversion to absorbed dose using the energy absorption coefficients of Hubbell (1982). To manipulate the large amount of data generated, a post-processing code, KOOKIE, was written at PNL to read in the output file from the MCNP calculations. For each organ and each energy group, KOOKIE converts the fluence to absorbed dose using the appropriate factor for either tissue, bone, bone marrow, or lung, and converts the neutron absorbed dose to neutron dose equivalent using the energy dependent quality factor (Cross and Ing 1984). Kookie then sums over all energies, adds the neutron dose equivalent and secondary

photon dose for each organ, and, finally, combines the organ dose equivalents with the appropriate weighting factors to determine the effective dose equivalent. The user has a choice of using the organ weighting factors from ICRP Publication 26, the sex specific weighting factors (ICRP 1977), or the new tissue weighting factors from ICRP Publication 60.

An initial set of calculations was performed for the standard uniform irradiation geometries. These geometries were the anterior-posterior (AP), the posterior-anterior (PA), and lateral (LAT) broad parallel beams and an isotropic (ISO) field. The LAT beam was incident on the phantoms right side. The results of these calculations are shown in Figure 2 along with the traditional conversion factors taken from ANSI/ANS-6.1.1 (1977). As seen in the figure, the effective dose equivalent is always lower than the dose equivalent based on the cylindrical phantom and in most cases the effective dose equivalent is lower by a factor of two or more. The statistical errors associated with the Monte Carlo calculations were less than 10% for the individual organs and less than 5% for the effective dose equivalent. The PNL results are also compared to other sets of data from ICRP 51 (Figure 3) and R. A. Hollnagel at PTB (Figure 4). These initial results provide the basis for further development and verification of this calculational technique.

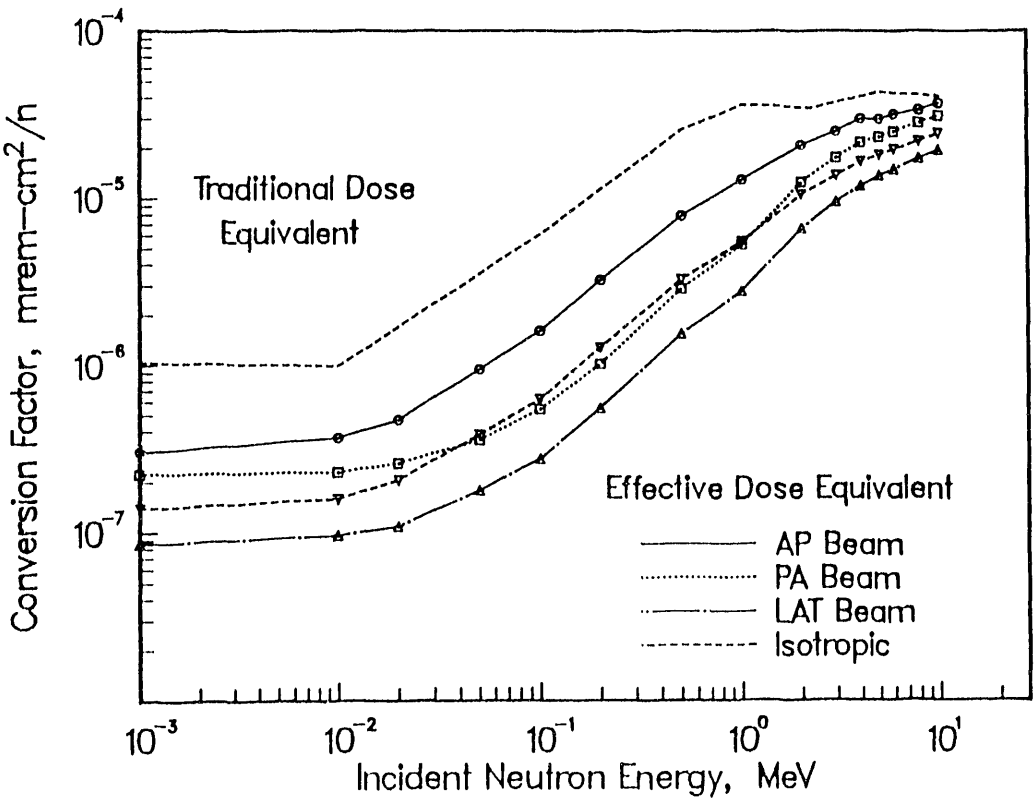

FIGURE 2. Comparison of Effective and Traditional Dose Equivalent Conversion Factors

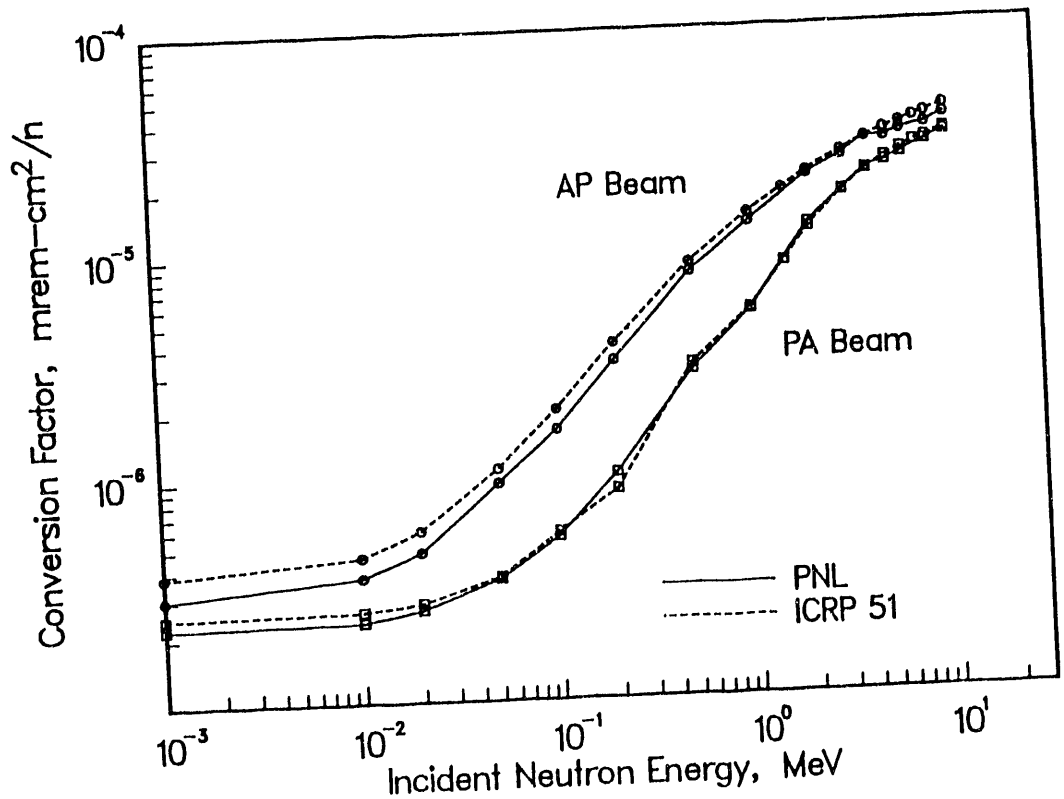

FIGURE 3. Comparison of ICRP 51 and PNL Effective Dose Equivalent Conversion Factors

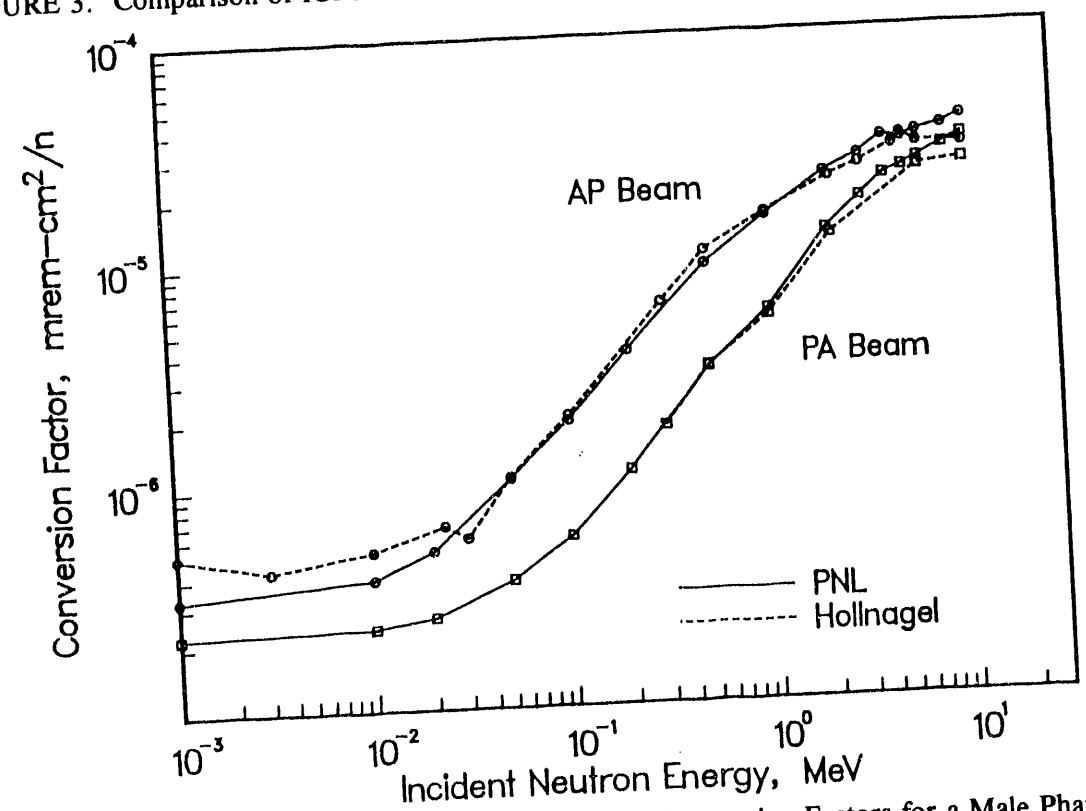

FIGURE 4. Comparison of Effective Dose Equivalent Conversion Factors for a Male Phantom

VERIFICATION MEASUREMENTS

To verify the calculational model, several sets of measurements were performed using a RANDO Average-Man phantom and the neutron and gamma sources at the PNL Low-Scatter Facility. The RANDO phantom consists of 1-in. slices with 5 mm diameter holes drilled on a 3 cm x 3 cm grid and is composed of Alderson Muscle. For the first set of measurements, the phantom was loaded with thermoluminescent (TL) chips and exposed to a ^{60}Co source. These measurements were conducted first to gain confidence and experience since it was believed the gamma measurements would be more straightforward than the neutron measurements. The second set of measurements consisted of partially loading the phantom with TL chips and CR-39 samples and exposing the phantom to a bare ^{252}Cf source and a D_2O-moderated ^{252}Cf source. The third and final set of measurements used a 1/2-in. tissue equivalent proportional counter (TEPC) at a few select locations inside the phantom exposed to bare and moderated ^{252}Cf. Figures 5 and 6 show the TL chips and the CR-39 samples and Figure 7 shows the experimental setup for the D_2O-moderated ^{252}Cf source.

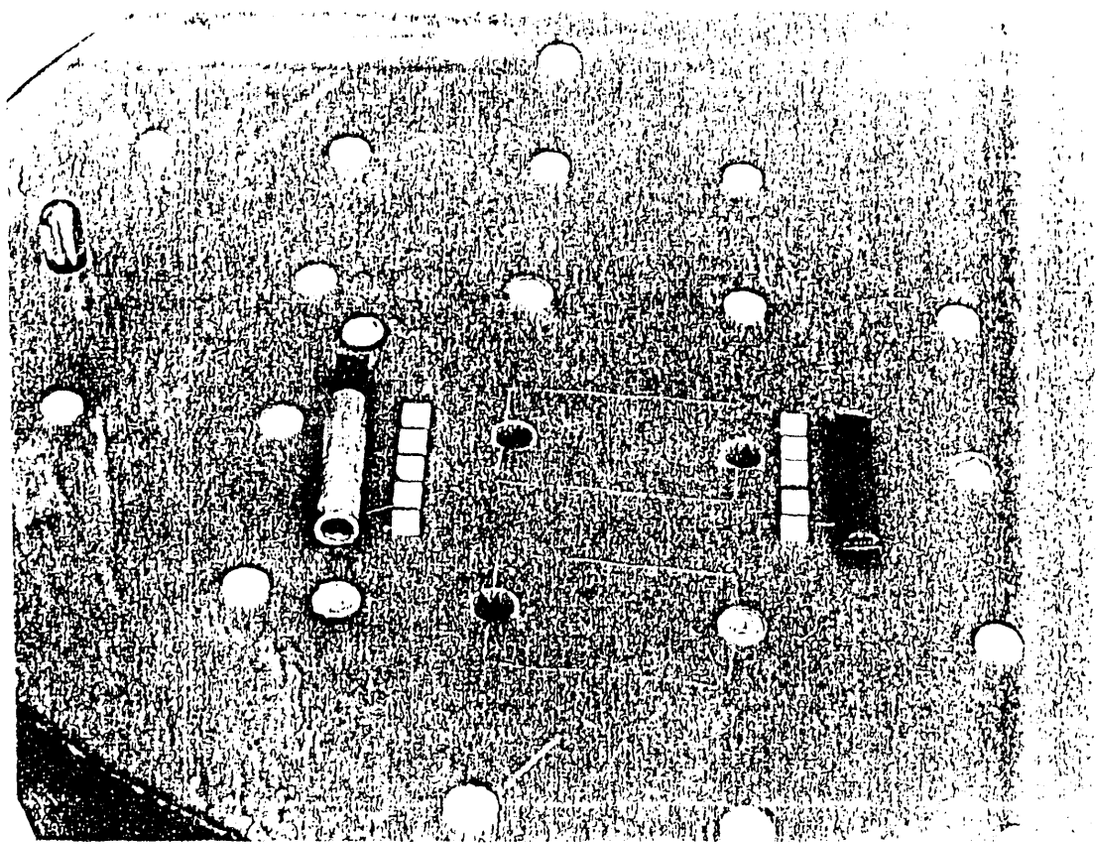

FIGURE 5.

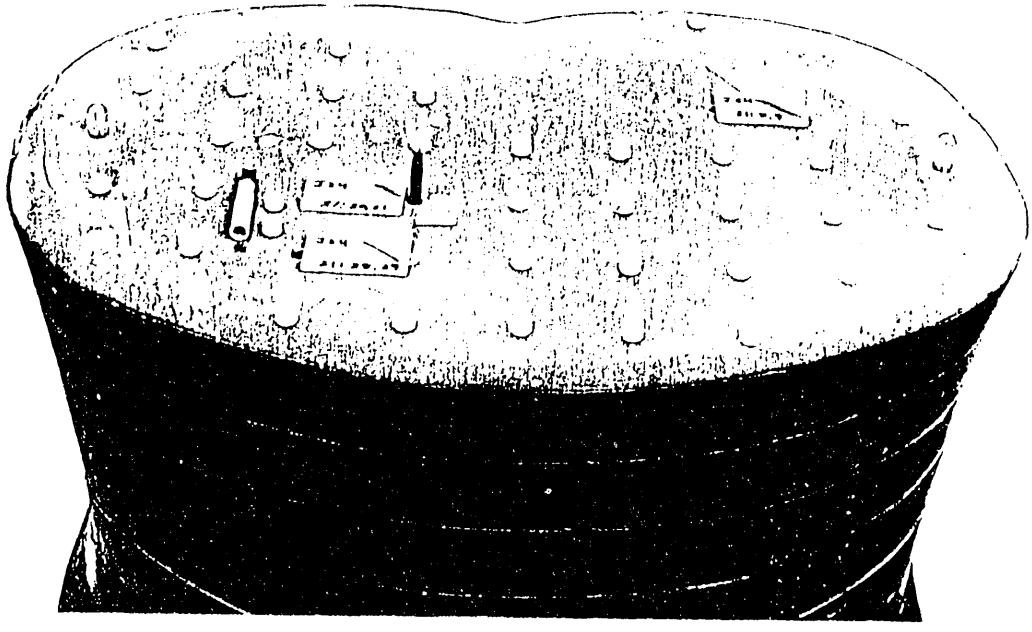

FIGURE 6.

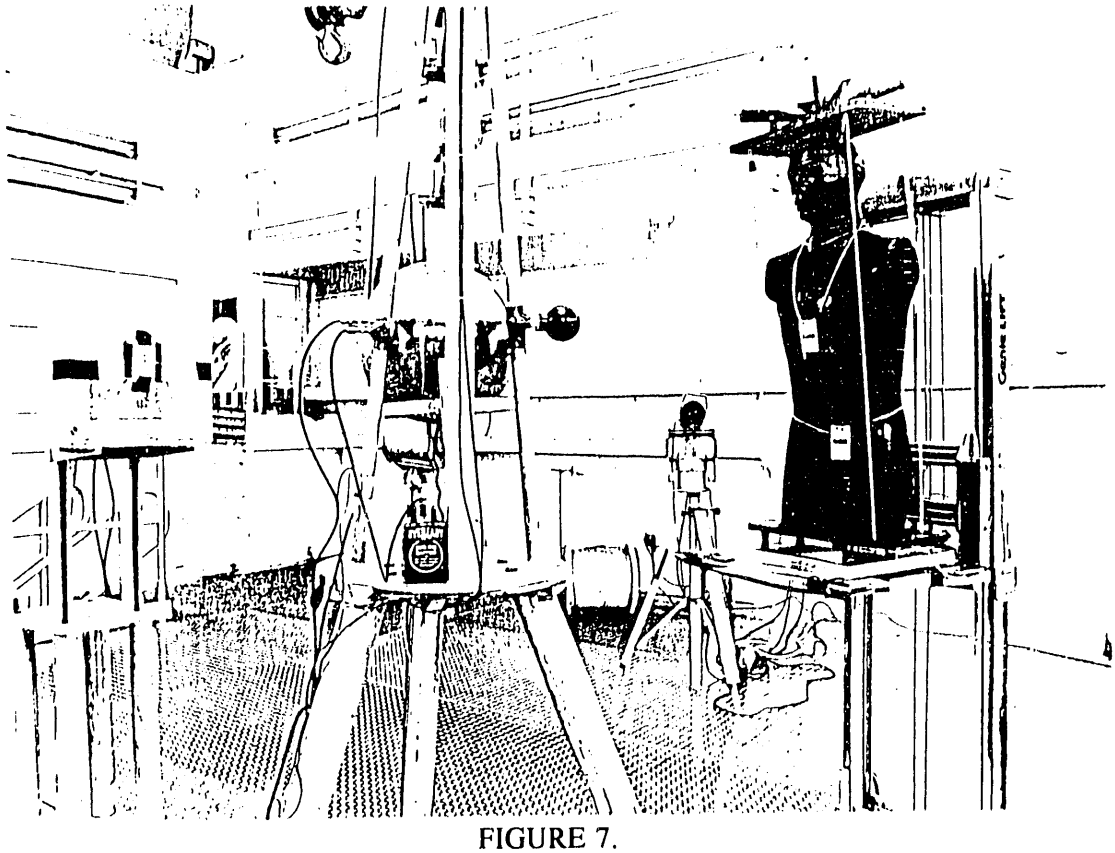

FIGURE 7.

The gamma measurements were performed using ^{7}LiF chips sealed inside a plastic capsule to hold them in place. These capsules were placed in holes that corresponded to locations of organs. In some instances one hole represented the location of a single organ, other organs, such as the lungs, consisted of a great many holes. When the total number of holes encompassed by an organ was very large, capsules were not place in every hole but rather scattered throughout the organ. The phantom was exposed at 1 meter for 10 hours to a 2-curie ^{60}Co source. The same setup was modeled for the calculations by using a gamma point source at 1 meter from the front of the phantom with an energy distribution of 50% 1.173 MeV and 50% 1.332 MeV. The results of the organ dose measurements and calculations for a male phantom are presented in Table 2.

TABLE 2. Organ Doses for ^{60}Co Exposure

Organ	Calculated/Measured
Liver	1.04
Stomach	1.11
Pancreas	1.04
Kidneys	0.99
Spleen	1.13
Small Intestine	1.00
Upper Large	1.08
Lower Large	1.11
Lung	1.14
Adrenals	1.18
Thyroid	1.09
Testes	1.00
Brain	1.03
Thymus	1.24
Heart	1.14
Skin	1.01
Red Bone Marrow	1.00

The overall agreement between the measurements and the calculations was better than 10% on the average. The largest differences occurred for the small organs, the adrenals and the thymus, where the uncertainty in the Monte Carlo calculations was largest due to their small volumes.

Initially, neutron measurements were made in the RANDO phantom using a combination of ^{6}LiF and ^{7}LiF chips inside the holes and CR-39 track etch detectors (TEDs) placed horizontally between the phantom slices. A measurement location consisted of a set of chips inside a plain plastic capsule in one hole, another set of chips inside a cadmium-covered capsule in an adjacent hole, and a piece of CR-39 placed between the two holes above the slice that the chips were in. Due to the complexity of the setup and analysis of the measurements, only a few organs were selected for comparison. The results of the

measurements and calculations for the thyroid, heart, liver, and kidneys are shown in Table 3 for the bare ^{252}Cf exposure. Table 4 shows the results for the D_2O moderated ^{252}Cf exposure. The results varied significantly due to the difficulty in calibrating the TL chip response for the correct neutron energies and the angular dependence and energy threshold of the CR-39.

Based on the poor correlations obtained with the TLDs and the TEDs in the phantom, it was decided to try and use a 1/2-in. TEPC to obtain a direct measurement of the absorbed dose within the phantom to compare with a calculation of the same. The TEPC used was a 1/2-in. diameter tissue-equivalent (TE) sphere enclosed in a cylindrical aluminum housing at the end of a long stem. The sphere was filled with propane TE gas at a pressure of 33.4 torr to simulate 1 micron of tissue. To avoid drilling large holes in the RANDO phantom to accommodate the TEPC, a 1-in. thick slab of polyethylene in the shape of a typical phantom torso slice was substituted for an actual slice in the phantom. The polyethylene slice had a 3/4-in. hole drilled through from the back of the torso to the middle of the slice. The TEPC was inserted from the back into the phantom in this way and the center of the TEPC's active volume was in the center of the slice.

TABLE 3. Organ Doses for Bare ^{252}Cf (mrem)[a]

Organ	TEDs	TLDs	Calculated
Thyroid	96.0	424.0	355.5
Heart	69.3	569.4	237.5
Liver	88.0	350.6	226.4
Kidneys	36.0	236.6	59.9

(a) Reference dose of 500 mrem delivered to front of phantom.

TABLE 4. Organ Doses for D_2O Moderated ^{252}Cf (mrem)[a]

Organ	TEDs	TLDs	Calculated
Thyroid	171.0	398.0	483.6
Heart	137.0	178.2	365.0
Liver	136.5	153.7	327.4
Kidneys	32.0	61.0	88.5

(a) Reference dose of 750 mrem delivered to front of phantom.

Measurements were attempted with the substitute slice at three different elevations within the phantom torso to approximate three separate possible organ locations. The outer shape and size of the slices changes with elevation, however, the front of the substitute slice was always lined up flush with the front

of the rest of the torso and the distances from the center of the detector to the front of the torso and to the source were carefully measured and recorded. The measurements were performed at slice 11, 21, and 31 with the phantom exposed to both bare and D_2O moderated ^{252}Cf.

For the purpose of comparing the calculated absorbed dose to the measured absorbed dose, the male mathematical phantom was modified to include a model of the TEPC inside the phantom in place of tissue/organ material. The phantom composition was also changed from ICRP tissue to Alderson Muscle and the legs were chopped off several inches below the torso to match the actual physical phantom. Instead of calculating organ averaged fluences, a calculation of the energy deposited in the active volume of the detector was performed to compare to the absorbed dose measured by the TEPC. The results of the TEPC measurements and calculations are compared in Table 5.

TABLE 5. Absorbed Doses for Bare and D_2O Moderated ^{252}Cf (mrad/hr)

	Bare		D_2O Moderated	
Location	Measured	Calculated	Measured	Calculated
Slice 11	94.1	110.7	23.3	26.0
Slice 21	108.6	126.9	26.2	29.4
Slice 31	100.9	108.0	19.9	21.8

The measured and calculated absorbed doses in the phantom agreed within 15% which is within the level of agreement (20%) required for a reliable system for conducting further evaluations of effective dose equivalent and developing a dosimeter system to determine EDE.

RESULTS OF CALCULATIONS

To determine the dependence of effective dose equivalent on incident neutron energy and angle, further calculations were undertaken for a multitude of angles and energies. The angles of the different broad parallel beams modeled can be described by the polar angle, phi(ø), and the azimuthal angle, theta(θ). Figure 8 shows the coordinate system used in the phantom calculations and Table 6 lists all the energies and angles that data were generated for. The phantom itself is centered with the origin at the bottom center of the torso and the z-axis directed upward toward the head. The x-axis is directed toward the phantom's left and the y-axis is directed toward the posterior side of the phantom. Theta was only varied from 0 to 180 degrees since it can be shown that the effective dose equivalent is symmetric with respect to the y-axis. Calculations for phi were limited to the five values shown due to time constraints. The Monte Carlo transport calculations, especially the ones for phi=45 degrees and phi=135 degrees, took up to several weeks worth of computer time for each run.

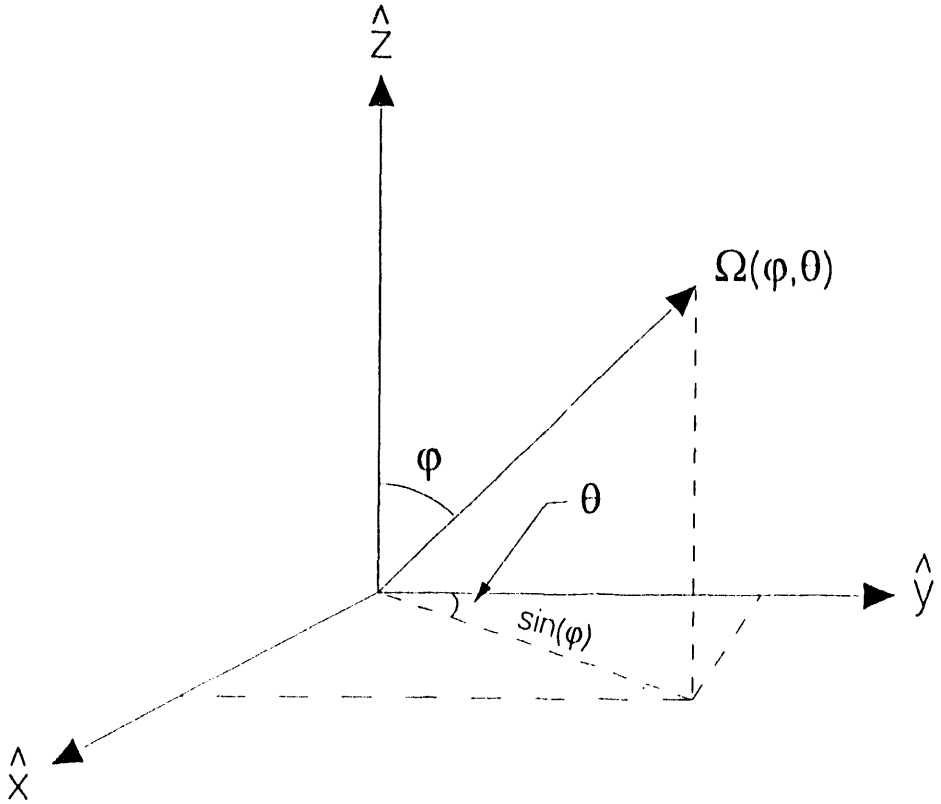

FIGURE 8. The Spherical Coordinate System Used in the Effective Dose Equivalent Calculations

TABLE 6. Values of energy and angle for extended calculations of effective dose equivalent

Phantoms	Energy (MeV)	Phi	Theta
Male	0.001	0[(a)]	0
Female	0.01	45	40
	0.02	90	60
	0.05	135	75
	0.10	180[(a)]	90
	0.20		105
	0.50		120
	1.00		140
	2.00		180
	3.00		
	4.00		
	5.00		
	6.00		
	8.00		
	10.00		

(a) No variation in theta for phi

For each combination of phi and theta, the organ dose equivalents were calculated for monoenergetic broad parallel beams incident on the phantom for each of the fifteen energies shown in Table 6. Altogether, 435 different cases were set up and run. Figure 9 shows the effective dose equivalent per unit incident fluence versus energy for theta=90 to 180 degrees at phi=90 degrees. These curves are very similar in shape to the curves in Figure 2. For reference purposes, the AP beam from the earlier calculations is the same as the beam with phi=90 and theta=180 and the LAT beam is the same as the beam with phi=90 and theta=90. As expected, the effective dose equivalent decreases as theta rotates from the front to the side. All results presented here are for the male phantom.

Figure 10 shows the effective dose equivalent versus theta with phi fixed at 90 degrees for several incident neutron energies. As one would expect, the effective dose equivalent decreases with increasing theta from theta=0 (PA) to theta=90 (LAT), then increases with increasing theta from theta=90 (LAT) to theta=180 (AP). Also, a beam incident on the top of the phantom (phi=0) results in a lower effective dose equivalent than any beam incident perpendicular to the z-axis (phi=90). The effective dose equivalent goes up with increasing energy for all incident angles.

Another approach to viewing the effective dose equivalent's dependence on angle of incidence is shown in Figure 11. In this figure, the effective dose equivalent for 1 MeV neutrons is shown on a linear scale normalized to an AP beam. The effective dose equivalent displays a cosine distribution with the angle theta much like a dosimeter response. However, the front and back have different absolute magnitudes.

To study the significance of incident neutron energy in more detail, the effective dose equivalent was estimated for a fission spectrum moderated with 10 cm of polyethylene. The effective dose equivalent conversion factors for the AP beam were folded in with the energy dependent fluences given in IAEA Technical Report 180. Figure 12 shows the fractional and cumulative effective dose equivalent as a function of incident neutron energy. It can be seen that incident neutrons below 500 KeV contribute less than 1% of the total effective dose equivalent. The largest contribution to the effective dose equivalent comes from the fraction of neutrons with energies between 2 MeV and 4 MeV incident on the body.

The calculations have only been completed for the male phantom. Calculations for the female phantom will probably take well into fiscal year 1992. However, it is expected that the results for the female phantom will exhibit the same trends as the male phantom.

NEW DEVELOPMENTS

Developments in recent years of new risk estimates associated with exposure to ionizing radiation have lead to the publication of new recommendations by the ICRP (ICRP 1990). The new recommendations extend the concepts introduced in ICRP Publication 26 and keep the basic framework of using an assessment of total detriment to determine exposure limits for both workers and the public. Although the biological data has not changed significantly for deterministic (non-stochastic) effects and hereditary defects, the newly revised data on cancer induction has resulted in major changes to the overall values

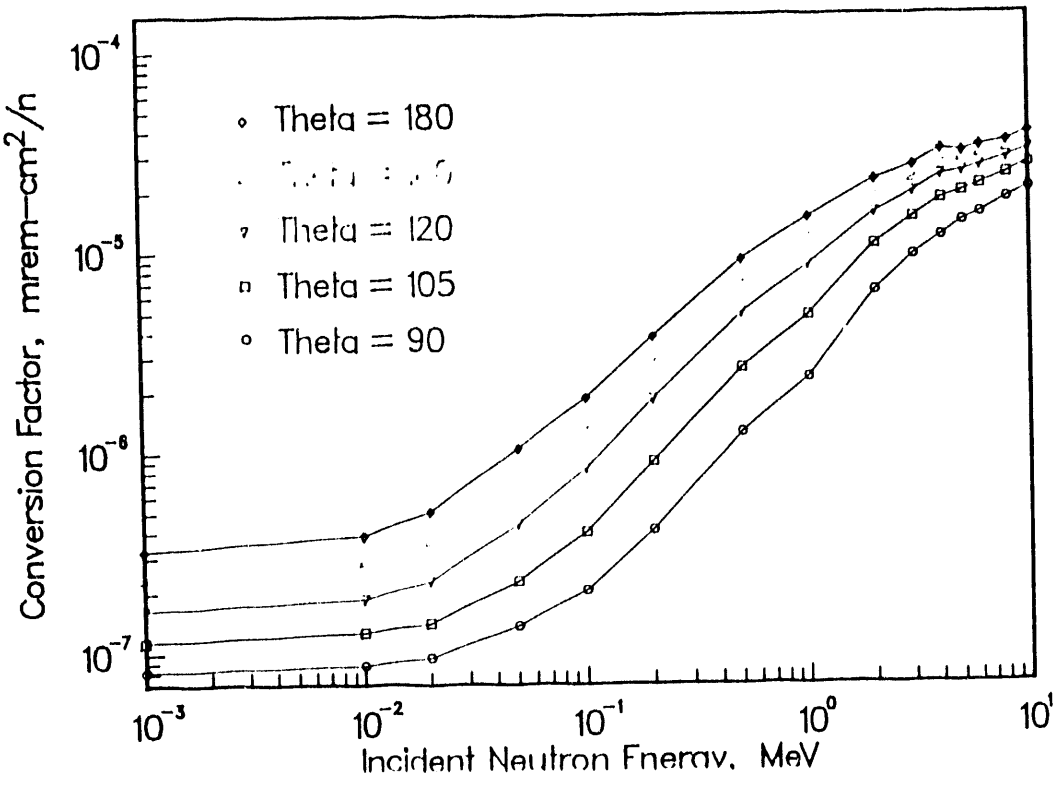

FIGURE 9. Effective Dose Equivalent vs. Energy and Angle of Incidence

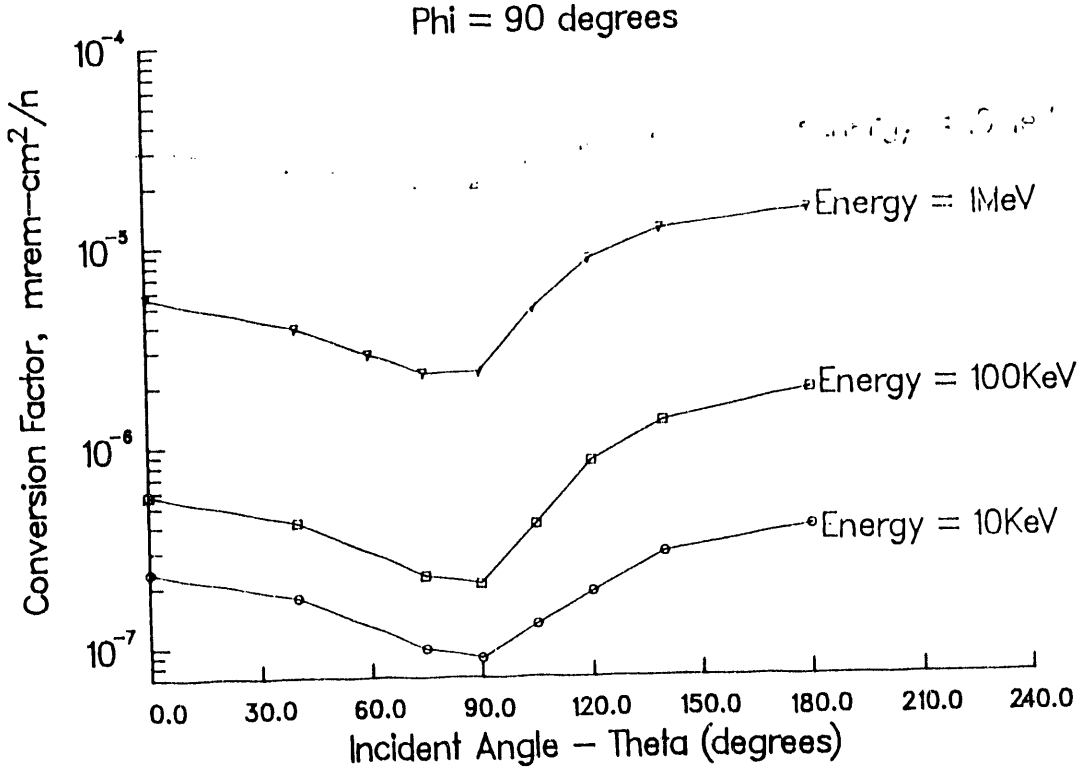

FIGURE 10. Effective Dose Equivalent vs. Energy and Angle of Incidence

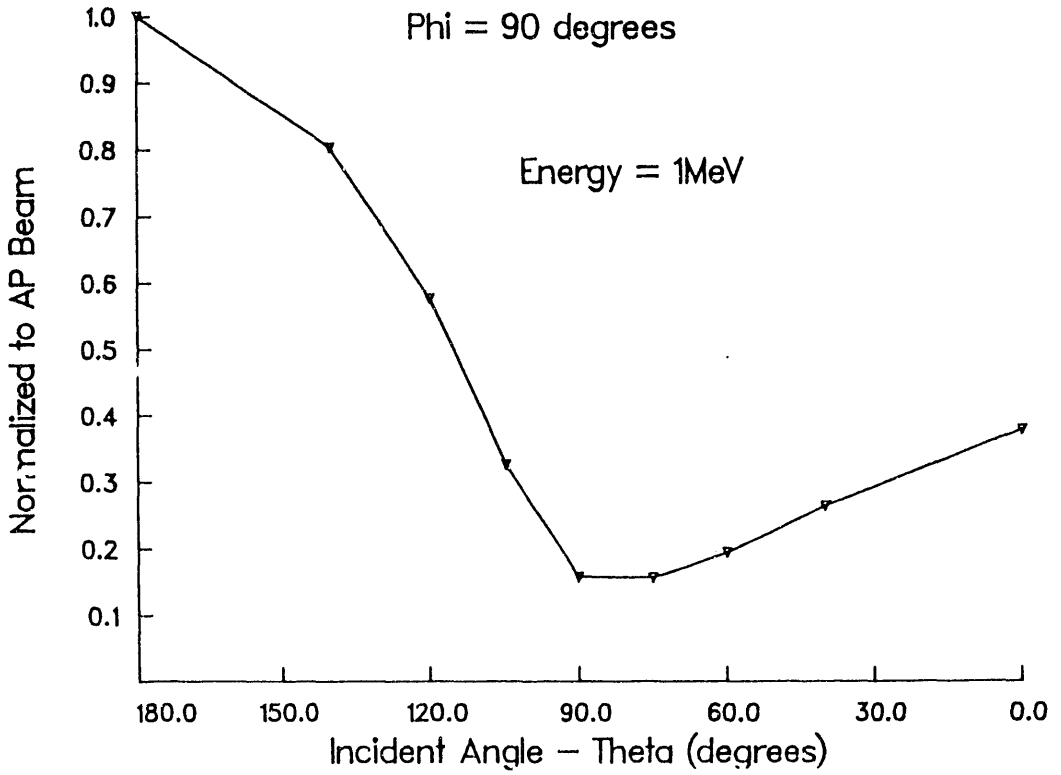

FIGURE 11. Effective Dose Equivalent vs. Energy and Angle of Incidence

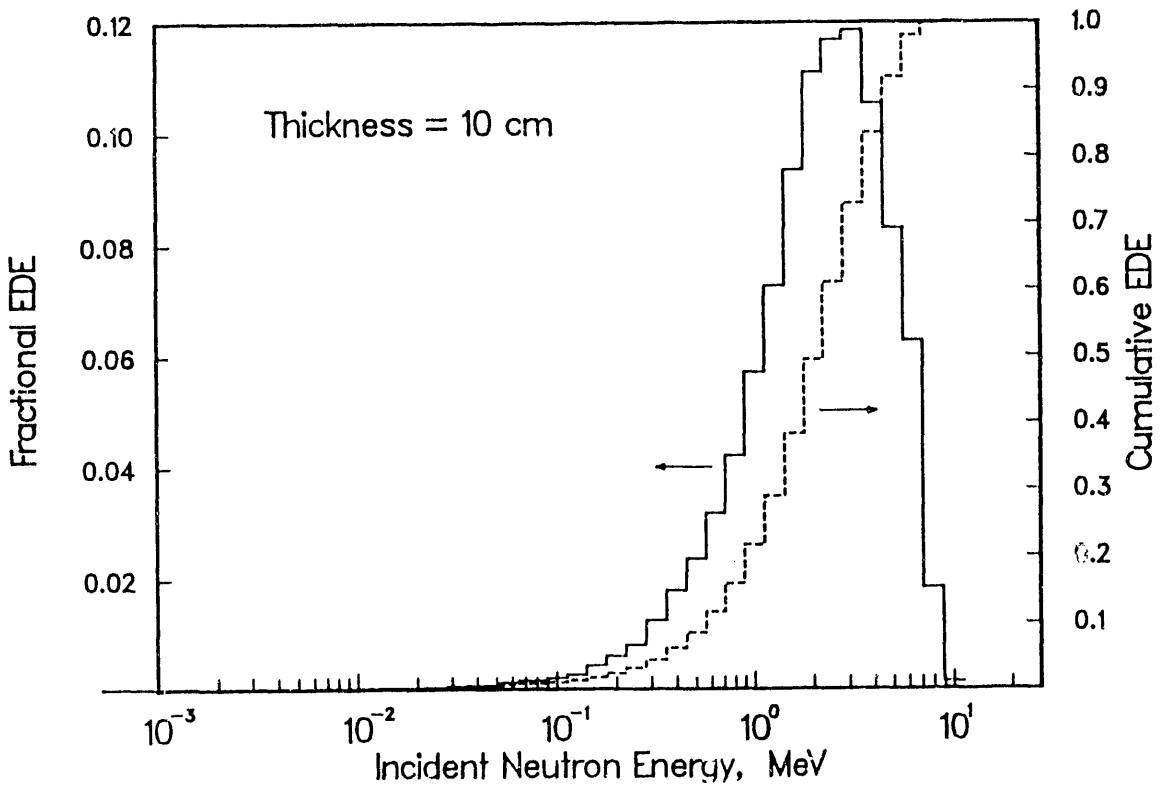

FIGURE 12. Differential Effective Dose Equivalent for Fission Neutrons Through Polyethylene

of risk applied in the new recommendations. The new tissue weighting factors now include not only the risk from cancer mortality but also expected loss of life, the morbidity of non-fatal cancers, and the hereditary defects for all future generations. The quality factors for neutrons have also been revised and are now a function of the neutron energy incident on the body, not at the point of interest within the body. The quality factor is now called the radiation weighting factor and the effective dose equivalent is given the shorter name of effective dose.

The graphs in Figures 13 and 14 compare the traditional dose equivalent, the effective dose equivalent (ICRP 1977), and the effective dose (ICRP 1990) for neutrons. The traditional dose equivalent curve is based on the neutron-flux-to-dose-equivalent factors in ANSI/ANS-6.1.1 which in turn are based on the 1968 calculations of the maximum dose equivalent in the Auxier-Snyder cylindrical phantom. The ICRP 26 curve showing the effective dose equivalent per unit fluence is based on PNL's Monte Carlo transport calculations, Cross and Ing quality factors and the ICRP 26 tissue weighting factors. The ICRP 60 curve shows the effective dose per unit fluence and is based on the same transport calculations as the ICRP 26 results except that the organ doses were multiplied by the radiation weighting factors and tissue weighting factors given in ICRP Publication 60. Table 7 shows the differences in the tissue weighting factors between ICRP Publication 26 and 60.

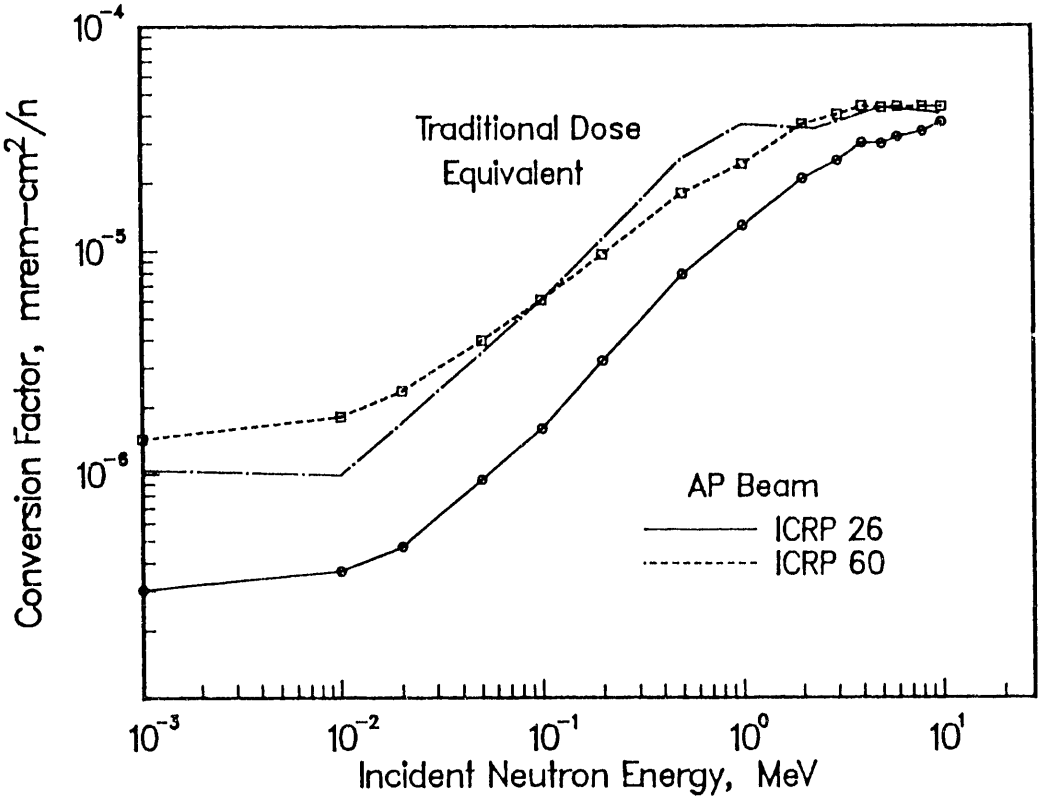

FIGURE 13. Comparison of ICRP 26 and ICRP 60 Weighting Factors

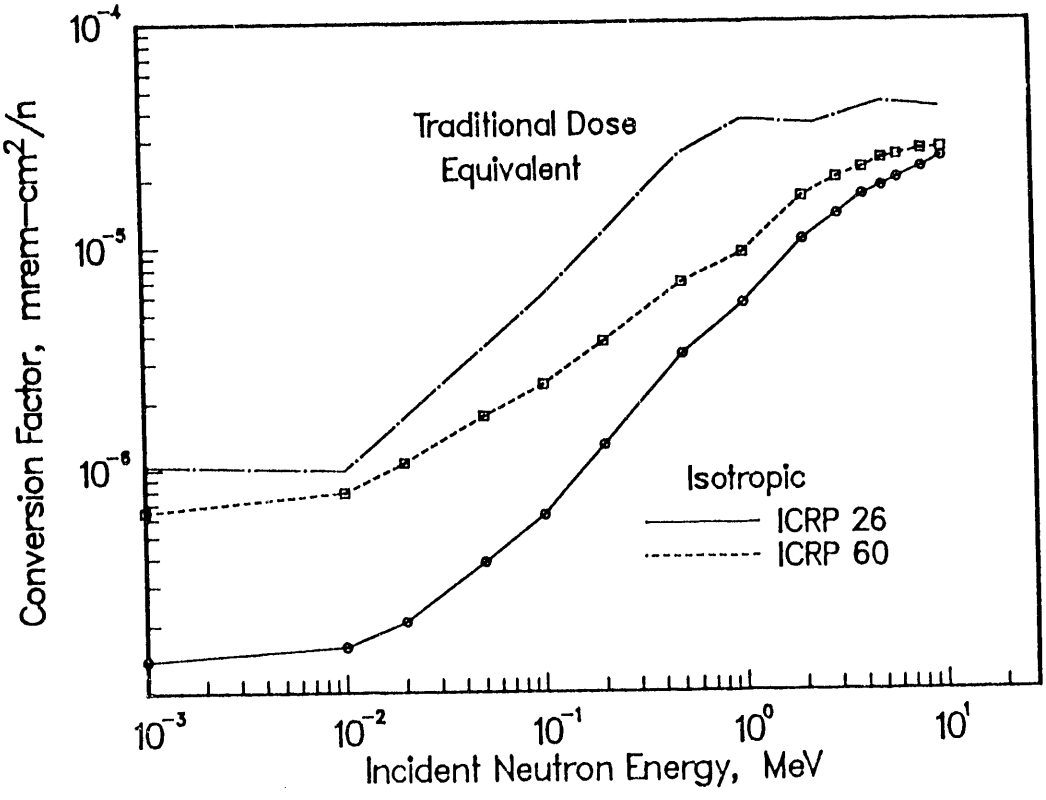

FIGURE 14. Comparison of ICRP and ICRP 60 Weighting Factors

TABLE 7. Tissue Weighting Factors

Tissue or Organ	ICRP 26	ICRP 60
Gonads	0.25	0.20
Red bone marrow	0.12	0.12
Colon		0.12
Lung	0.12	0.12
Stomach		0.12
Bladder		0.05
Breast	0.15	0.05
Liver		0.05
Oesophagus		0.05
Thyroid	0.03	0.05
Skin		0.01
Bone surface	0.03	0.01
Remainder	0.30	0.05

For the determination of the effective dose equivalent (ICRP 26), a fixed remainder was used consisting of the liver, the small intestine, the upper large intestine, the lower large intestine, and the stomach which were each given a weighting factor of 0.06. For the ICRP 60 effective dose, the colon was interpreted to be the lower large intestine, the thymus dose was substituted for the oesophagus dose, and the remainder was split between all the remaining internal organs. In the case of the doses to the gonads and the lungs, the female and male calculated doses were averaged (ICRP 51) and the values for the breast are based solely on the female phantom calculations. All other organ doses used in the estimates are based on the male phantom calculations.

An important difference between the effective dose equivalent and the effective dose is the conversion of the absorbed dose to dose equivalent or equivalent dose. For the calculation of the effective dose equivalent, the neutron energy spectrum over the organ or tissue volume of interest was used to multiply the absorbed dose by the energy dependent quality factors. These quality factors are based on the charged particle dose resulting from first interactions of monoenergetic neutrons in tissue. To determine the effective dose, the absorbed doses for all the organs were multiplied by the single radiation weighting factor for the monoenergetic neutrons incident on the surface of the phantom for each computer run. The radiation weighting factors are given in Table A-2 in ICRP Publication 60 and have values of 5, 10, or 20 depending on the neutron energy. To afford consistency in calculations, a smooth fit of the values is provided in Publication 60 and is shown by the following relationship:

$$w_R = 5 + 17e^{-(\ln(2E))2/6}$$

where E is the neutron energy in MeV. This relationship was used in determining the value of the radiation weighting factor to use for each set of phantom calculations.

During the Monte Carlo calculations, the incident neutrons were transported through the phantom as well as the secondary photons produced by the neutrons in the tissue. Each calculation resulted in separate neutron and photon absorbed doses for each organ. In the calculation of the effective dose equivalent, the photon dose was added after the neutron dose had been converted to neutron dose equivalent to determine the total organ dose equivalent. For the effective dose, the total absorbed dose to the organ from neutrons and neutron-induced photons was multiplied by the radiation weighting factor to determine organ equivalent doses. At low neutron energies, the gamma dose dominates, contributing up to 85% to the total below 10 keV. Therefore, the change from quality factor to radiation weighting factor has very little impact at the lower energies.

CONCLUSIONS

The data base of organ fluences as a function of incident neutron energy and angle is detailed enough to provide estimates of organ dose equivalents and effective dose equivalent regardless of changes in quality factors and weighting factors. The time-consuming radiation transport calculations will not have to be repeated. The only modifications would occur in the post-processing code, KOOKIE, which can include any set of conversion factors or weighting factors.

As complicated a concept as effective dose equivalent is and as difficult as it might seem to estimate organ dose equivalents, thereby estimating effective dose equivalent, several dosimeters positioned at strategic locations on the body with a very coarse energy discrimination could provide an adequate estimation of the effective dose equivalent for the neutron fields typically found in DOE facilities.

Future work will entail developing response criteria for a dosimeter system to evaluate the effective neutron dose equivalent and then designing a dosimeter system that will meet that criteria. Once a dosimeter system has been developed, a prototype will be field tested at representative locations in work areas at DOE sites where workers receive significant occupational exposures.

REFERENCES

American Nuclear Society. Neutron and Gamma-Ray Flux-to-Dose-Rate Factors. ANSI/ANS-6.1.1. 1977.

Caswell, R. S., and J. J. Coyne. Kerma Factors for Neutron Energies Below 30 MeV. 1980. Radiation Research, Vol. 83, 217-254.

Cross, W. G., and H. Ing. Quality Factors for Monoenergetic Neutrons. 1984. Radiation Research, Vol. 99, 1-19.

Golikov, V. Y., and V. V. Nikitin. Estimation of the Mean Organ Doses and the Effective Dose Equivalent from RANDO Phantom Measurements. 1989. Health Physics, Vol. 56, No. 1., 111-115.

Hollnagel, R. A. Effective Dose Equivalent and Organ Doses for Neutrons from Thermal to 14 MeV. 1990. Radiation Protection Dosimetry, Vol. 30, No. 3, 149-159.

Hubbell, J. H. Photon Mass Attenuation and Energy-Absorption Coefficients from 1 keV to 20 MeV. 1982. Int. J. Appl. Radiat. Isot., Vol. 33, 1269-1290.

Huda, W., and G. A. Sandison. Estimation of Mean Organ Doses in Diagnostic Radiology from RANDO Phantom Measurements. 1984. Health Physics, Vol. 47, No. 3, 463-467.

International Atomic Energy Agency. Compendium of Neutron Spectra in Criticality Accident Dosimetry. Technical Reports Series No. 180. IAEA, Vienna, 1978.

International Commission on Radiological Protection, Publication 26. Recommendations of the International Commission on Radiological Protection. Pergamon Press. 1977.

International Commission on Radiological Protection, Publication 27. Problems Involved in Developing an Index of Harm. Pergamon Press. 1977.

International Commission on Radiological Protection, Publication 51. Data for Use in Protection Against External Radiation. Pergamon Press. 1987.

International Commission on Radiological Protection, Publication 60. 1990 Recommendations of the International Commission on Radiological Protection. Pergamon Press. 1990.

Kramer, R., M. Zankl, G. Williams, and G. Drexler. The Calculation of Dose from External Photon Exposures using Reference Human Phantoms and Monte Carlo Methods. Part I: The Male (Adam) and Female (Eva) Adult Mathematical Phantoms. GSF-Bericht S-885. December 1982.

MCNP - A General Monte Carlo Code for Neutron and Photon Transport. Version 3A. LA-6396-M, Revision 2. September 1986, MCNP3B Newsletter July 1988.

Medical Internal Radiation Dose (MIRD) Pamphlet No. 5, Revised January 1978. Estimates of Specific Absorbed Fractions for Photon Sources Uniformly Distributed in Various Organs of a Heterogeneous Phantom.

DATE
FILMED
8/11/93
END